





Universitat Autònoma de Barcelona

**ADVERTIMENT.** L'accés als continguts d'aquesta tesi queda condicionat a l'acceptació de les condicions d'ús establertes per la següent llicència Creative Commons:  [http://cat.creativecommons.org/?page\\_id=184](http://cat.creativecommons.org/?page_id=184)

**ADVERTENCIA.** El acceso a los contenidos de esta tesis queda condicionado a la aceptación de las condiciones de uso establecidas por la siguiente licencia Creative Commons:  <http://es.creativecommons.org/blog/licencias/>

**WARNING.** The access to the contents of this doctoral thesis it is limited to the acceptance of the use conditions set by the following Creative Commons license:  <https://creativecommons.org/licenses/?lang=en>



PhD thesis

**Unveiling the role of FAIM in the retina:**

Characterization of the neurodegenerative and functional alterations of a FAIM knockout mouse model and associated molecular mechanisms

**Anna M. Sirés**

Doctorat en Neurociències

Institut de Neurociències

Universitat Autònoma de Barcelona

**Setembre del 2022**





## **Unveiling the role of FAIM in the retina:**

Characterization of the neurodegenerative and functional alterations of a FAIM knockout mouse model and associated molecular mechanisms

Memòria de tesi doctoral presentada per Anna Martínez Sirés per optar al grau de Doctora en Neurociències per la Universitat Autònoma de Barcelona.

Aquest treball ha estat realitzat al grup de Senyalització Cel·lular i Apoptosi de l'Institut de Recerca de Vall d'Hebron (VHIR), i al Departament de Bioquímica i Biologia Molecular i Institut de Neurociències de la Universitat Autònoma de Barcelona (UAB), sota la direcció dels doctors Joan X. Comella i Montse Solé.

El treball ha estat parcialment finançat per les següents entitats: Ministerio de Ciencia e Innovación (SAF2016-80236-R i PID2019-107286RB-I00), CIBERNED (CB06/05/1104), i la Generalitat de Catalunya (2017SGR996).

Doctoranda

Director

Directora

Anna Martínez Sirés

Joan X. Comella

Montse Solé

**Setembre del 2022**



*A la meva família,  
Al Roger,*



# Acknowledgments

*“Alone we go faster but together we go  
further.”*





# Agraïments

Són les 21:08 d'un dijous. Un dia tan bo com qualsevol altre per començar a escriure el fragment a la vegada menys científic i més llegit d'una tesi doctoral. A menys de dues setmanes d'entregar-la i quan l'estrès ja és difícil d'amagar, el que sí que resulta fàcil és pensar (i distreure'm) en com he arribat fins aquí: gràcies a la gent que m'envolta i m'ha recolzat durant aquests anys.

Començaré els meus agraïments pels meus mestres de cerimònia, el Joan i la Montse. Joan, ha set un plaer i un honor poder estar tots aquests anys sota la teva tutela. Gràcies per veure el meu potencial, per donar-nos la ploma de Dumbo al començar i la motivació quan no la trobàvem, i per haver-nos posat entre les cordes quan calia. Gràcies també pels debats tan enriquidors (que espero que no s'acabin), i pel teu respecte en les meves opinions. Per últim, gràcies per haver-nos cuidat quan més ho necessitàvem i per ser un referent. Espero que haguem fet retrocedir una mica la foscor.

Montse, gràcies per apostar per nosaltres en un moment tan decisiu i complicat, per reviuire el grup amb la teva energia i pel teu compromís amb nosaltres. Gràcies per la teva sinceritat tant per les coses bones com dolentes, que m'ha fet superar-me cada dia més. Gràcies fer la recerca fàcil, per la llibertat de deixar-me fer, però sempre amb la mà estesa. Gràcies per creure en mi i per la teva paciència. Això hagués set molt diferent sense tu.

Gràcies Quim, per alleugerir-nos la feina sempre que has pogut, per ser l'enciclopèdia del lab i per tot el que fas "entre bambolines", que potser no veiem però apreciem molt. Gràcies també Victor per acollir-nos al pitjor moment i per exprimir-nos el cervell amb les teves preguntes tan incisives, vas ser tot un revulsiu quan vam arribar a la UAB. Gràcies també als

membres de la meva comissió de seguiment, Pepe Rodríguez, Ramon Trullàs i Xavier Xifró, per donar-me l'empenta durant el primer any a lluitar pel que jo volia fer i per les paraules sempre tan bones que heu tingut per mi. Muchas gracias a Cati, Enrique y Pedro por acogerme en vuestro laboratorio. El paso por vuestro grupo marcó un antes y después en el curso de mi tesis. Gracias a Mateo, por explicarme con tanta paciencia cómo funcionaba el ERG y por los buenos ratos que pasamos en experimentos que en condiciones normales habría aborrecido.

Gràcies també a totes aquelles persones que han fet el dia a dia de la recerca més fàcil. Als zeladors del VHIR, Tau i Ray, per sempre tenir un somriure i unes paraules. A les coordinadores del laboratori, Anna i Helena, per tenir material sempre a punt. A la Marta Valeri, per totes les hores dedicades a ajudar-me a què les immunos sortissin perfectes. A la Susanna i a la Cris per batallar cada problema de la UAB. A la Patri, per les teves paraules sempre tan càlides. A las renalas: Mònica i Mònica, Jazz, Irene, Contxi i Edu, gràcies per sempre estar disposades a uns riures, un cafè i una bona sessió de cotilleo. A les estudiants que heu passat pel grup, AnnaBaby, Ana, Álvaro i Marina, i tots els demés, gràcies per l'aire fresc que porteu al lab, tot i que no entenc com podeu ser del 2000 i ser uns bebès, però ahora tenir permís de conduir.

Volia aturar-me un moment per donar-los-hi les gràcies, no sé ben bé com, als meus ratolinets. Estarem eternament en deute amb vosaltres.

A big thank you to Alexandra Elbakyan, creator of sci-hub. Sadly (but luckily) today's science would not be possible without you.

Mai una mudança ha set tan interminable, però el que ens esperava a l'arribar ha pagat la pena amb escreix. Moltíssimes gràcies Laura (LMEH) per acollir-nos com ho vas fer, per ajudar-nos en absolutament tot i deixar-nos el lab

sencer quan no trobàvem ni una trista pinta de western. Gràcies pels moments al cehpe, per les nostres sortides esportives i per lligar-me els cordons quan més ho necessitava. Never forget. Gràcies Montse per ser tan extremadament cuki. Per posar-nos sempre un somriure a la cara amb la teva manera de ser, per aguantar les nostres rucades quan ens passem el dia fent el tonto i riure per absolutament tot. Gràcies per donar aquesta brillantor a la UAB. Gràcies Laura (LMAH), no només aguantar-nos, sinó per sumar-te a aser la ablasió i estar disposada sempre a unas risas. Sabem que deixem la UAB en bones mans. Gràcies Mireia, per la teva serenor i saber estar, però també per obrir-te a nosaltres i deixar que t'infectem una mica de la nostra tonteria. Gràcies per tota l'ajuda amb el primer paper, i gràcies per sempre estar disposada a ajudar.

Sense cap mena de dubte, el millor que m'ha aportat el VHIR és la gent que hi he conegut i les amistats de per vida que hi he fet. Elena, gracias, gracias y mil gracias. Por todo lo científico, pero por encima de todo por lo personal. Por descubrirnos tu otro yo y que nuestra tontasi3n se matchee completamente. Por todas las risas, todos los filtros, los tatuajes, los shalalalalá, los unicornios, los Coatxel-la, por inventarnos la mejor canci3n de reguet3n, por el yoga, por los dibujitos, por aprender raps conmigo y por tupelorubiotucarawapa, por los momentos al sol, por los infinitos consejos y por querernos y cuidarnos tanto.

Isa, qué habríamos hecho sin ti. La voz de la raz3n, nuestro Pepito Grillo. Gracias por ayudarme a seguir en el cauce correcto y aplanarme el camino, por enseñarme lo que es la resiliencia. Gracias por tus mil pasteles y dulces, por habernos permitido ser tus conejillos de india y probar todas tus creaciones. Por ser la “repostera, instagrammer, influencer” del grupo y

postear las bravas. Gracias por desmelenarte cuando lo necesitábamos y por cuidarnos tantísimo.

Amiga. Vesina. Fren. Rachela. Que ya está. Que lo hemos (casi) conseguido. Mano a mano, juntas y revueltas. Realmente no creo que hubiese sido posible sin ti. Gracias por ser el Zipi de mi Zape, el Pin de mi Pon y el Pili de mi Mili (*disclaimer*: no sé ni quién son). Gracias por compartir un diccionario conmigo, por reír juntas y llorar juntas, por confiar siempre en mí, por estar *in* a cualquier plan, por todas las cervezas, por Barberá sity best sity, por ser mi amiga, por ser imprescindible. Gracias. Bupasión.

Gràcies Laura i David, per tots els moments nascuts al VHIR però sobretot per tots els que han vingut després. Gràcies per ser sempre un glopada d'aire fresc, per totes les barbacoes, per tots els bars que el David ens ha donat a conèixer a la cantonada de casa seva, per ser víctimes d'un tiroteig de balins a casa la Laura, pels riures, pels cotilleos, per poder parlar de tot sense pèls a la llengua, per tots els plans frustrats perquè sou ben cars de veure i per tots els plans que han de venir. I gràcies a tots els membres de Sticker's life, Lucía, Amparo, Dani i Jaume, per completar i fer rodó aquest grupet que m'estimo tant.

Gràcies a tots els que han set des d'abans d'arribar aquí. Gràcies als meus Mitocondris i a la meva Chupipandi, que tot i no veure-us tan com voldria sempre us porto amb mi.

Gràcies Adrià per estar just a l'altre costat, per ser-hi sempre tot i que hi siguis cansat, per mantenir Dinsnosaure ple de videoclips i dades aleatòries només per parlar una estona, per ser una constant a les nostres vides. Gràcies a la Marina i la Mariàngels, les meves nenes, les meves butiful frens. Les que m'estimen quasi tant com jo les estimo a elles, les que hi són sempre i no

fallen mai. Gràcies per estar sempre pendents, per totes les vegades que ens hem vist i per totes les que no, quan finalment el doctorat ha pogut amb mi. Gràcies per venir a mi quan jo no podia, i pel vostre suport al final de la tesi. Sou un tresor.

Gràcies a tota la meva família. Per totes les Mones, tots els Nadals, tots els Alcoletges i tots els Paddocks. Gràcies Toïto i Evi pel vostre carinyo i els vostres ànims. Gràcies als meus Angelitos de la guarda, que m'estimen i em cuiden des d'allà on siguin.

Gràcies a la meva segona família. Gràcies Elvira i Pere per cuidar-me tant, per tots els tapers que ens han salvat la vida i per fer-ho tot sempre tan fàcil amb vosaltres. Gràcies als meus cunyis, a l'Anna, l'Oriol, la Lorena i el Xavi. Per sempre trobar moments per veure'ns, per tots els dinars, sopars i sobretauls amb gintònics i Haribos, les barbacoes i futures pizzes. I no em podia oblidar de bebesito Blai, gràcies per omplir d'amor les nostres vides. Gràcies a tots per ser tan meravellosos i fer-me sentir com a casa.

Gràcies a la meva família. Als que m'ho han donat tot, als que m'han donat ales i han set directament responsables que jo pugui ser on sóc, escrivint això ara mateix. Al meu pare, perquè no calen tantes paraules per saber qui t'estima, per saber que sempre hi ets i hi seràs i que sempre sortiràs al balcó a dir-nos adeu, nevi o plogui. A la meva mare, per totes les trucades, tots els missatges, totes els "holacukiquefas", per escoltar-me, per donar-me energia i contagiar-me la teva fortalesa, per estimar-me i cuidar-me tant sense exigir res a canvi, pels teus "seny i rauxa" i els "tú puedes nena", pel teu amor incondicional i per no defallir mai amb mi. A la meva germana i la meva *cheerleader* particular, la Paula. Per creure sempre en mi sense condicions, sense cap dubte, per ser la meva confident i per celebrar amb mi cada petita

victòria com si fos un campionat. Per ser sempre a l'altre costat del telèfon tot i estar a l'altra punta del món, i tenir sempre un espai per mi tot i que tinguis les 24h ocupades. Per totes les gambes amb te i pels "take my". Sóc molt afortunada de tenir-vos com a família, aquesta tesi és també vostra.

I finalment, però indubtablement no per menys important, gràcies al meu Roger. Al meu bonic, la meva sort, qui m'entén quan ni jo mateixa m'entenc, qui remou cel i terra per mi, qui m'acompanya a fer passes cel·lulars a les 12 de la nit perquè la UAB de nit és terrorífica i em construeix el material de laboratori que necessito i no existeix. Qui ha set la meva roca en els meus pitjors moments i m'ha suportat quan era insuportable, qui em senyala el nord quan jo no veig dos passos més enllà i qui m'assegura que tot anirà bé. I al final sempre tens raó. Els moments més durs els he pogut superar gràcies a què passés el que passés, cada dia tornava a tu, i els moments més bonics sempre han set més bonics quan per fi els podia compartir amb tu. Gràcies per creure sempre en mi quan jo no hi creia i per ser casa. Aquesta tesi també és teva.

Són les 12:23h del dia de l'entrega de la tesi. No és un dia com qualsevol altre per acabar d'escriure'n el fragment més emotiu. A falta de minuts de finalment començar a tancar aquesta etapa, només puc sentir-me afortunada, estimada i orgullosa. Gràcies a tots.

# Abstract

*“The stars don’t look bigger, but they do look brighter.”*

Sally Rice (1951-2012)





# Abstract

Fas Apoptotic Inhibitory Molecule protein (FAIM) was first described as a death-receptor antagonist and an apoptosis regulator. However, new roles like ubiquitin modulation and prevention of protein aggregation have been described over the past years. The *Faim* gene encodes two isoforms, namely FAIM-short (FAIM-S) and FAIM-long (FAIM-L), and both isoforms hold significant neuronal functions. Although FAIM-S is ubiquitously expressed, it is specifically involved in neuronal roles like neurite outgrowth. However, it does not protect neurons from apoptosis. FAIM-L, on the other hand, is exclusively expressed in neurons and it does confer protection against apoptosis. Moreover, FAIM-L is also involved in non-apoptotic functions, such as synaptic plasticity. Interestingly, FAIM-L protein levels are downregulated in patients and mouse models of Alzheimer's disease before the onset of neurodegeneration, and *Faim* gene levels are decreased in mouse models of retinal degeneration. Surprisingly, preliminary bioinformatic data determined how the expression of *Faim* is greatly enriched in the retina among every other tissue and is heavily correlated with phototransduction. However, to this date few studies had addressed the role of FAIM *in vivo* in the central nervous system, yet alone the retina.

To study a possible implication of FAIM in the retina we explored histologically and functionally this tissue in *Faim* knockout (*Faim* KO) mice at different ages. Here, we describe that a *Faim* depletion in mice leads to retinal neurodegeneration and malfunction, and that *Faim* KO retinas present accumulation of ubiquitin aggregates from early ages, gliosis and vascular leakage, alterations that are exacerbated with age. Together with these results, we also found a decrease in the functional activity of photoreceptor,

bipolar and retinal ganglion cells in electroretinogram analyses in comparison to wildtype mice.

Surprisingly, we also found that Faim KO mice present a delay in dark adaptation, which can be caused by a detrimental function or localization of proteins involved in this mechanism, like Arrestin-1. In here, we report that Arrestin-1 translocation through photoreceptor segments upon light reception is impaired in Faim KO mice. Moreover, the redistribution mechanism of Arrestin-1 translocation could rely on Arrestin-1 ubiquitination, a post-translational modification that is significantly reduced in the presence of FAIM *in vitro*, indicating that FAIM regulation of dark adaptation could be dependent on its role on Arrestin-1 translocation.

These results suggest that FAIM is an important player in the maintenance of proteostasis and correct phototransduction in the retina, as we unravel novel functions for FAIM in this previously unexplored tissue.

In summary, in the present thesis we describe how the absence of FAIM leads to histopathological alterations that are probably responsible for the functional deficits we found, namely the dark adaptation delay from early ages, and the decreased activity of retinal cells at late ages. Remarkably, the alterations we report are also features of multiple inherited and age-related retinal diseases, such as retinitis pigmentosa, diabetic retinopathy and age-related macular degeneration. Therefore, this supports the notion that further research on FAIM in the retina could be a turning point to unveil the molecular mechanisms of these diseases.

## Resum

Fas Apoptotic Inhibitory Molecule (FAIM) va ser descrita per primer cop com un antagonista de receptors de mort i un regulador de l'apoptosi. Tot i això, durant els últims anys se li ha atribuït nous rols com la modulació de la ubiquitinació i la prevenció de l'agregació proteica. El gen de Faim codifica per dues isoformes FAIM-short (FAIM-S) i FAIM-long (FAIM-L), i les dues tenen funcions neuronals rellevants. Tot i que FAIM-S s'expressa de forma ubiqua, està específicament involucrat en funcions neuronals com el creixement neurític, però no confereix protecció a les neurones davant d'estímuls apoptòtics. D'altra banda, FAIM-L s'expressa de forma exclusiva en neurones i sí que atorga protecció contra l'apoptosi. A més a més, FAIM-L també està involucrada en funcions no-apoptòtiques com la plasticitat sinàptica. De forma rellevant, s'ha descrit com els nivells proteics de FAIM-L estan reduïts en pacients i models murins de la malaltia d'Alzheimer abans de l'inici de la neurodegeneració, i l'expressió gènica de Faim està disminuïda en models murins de neurodegeneració retiniana. Curiosament, dades preliminars obtinguts amb eines bioinformàtics van determinar que l'expressió de Faim està particularment enriquida a la retina abans que qualsevol altre teixit, i com correlaciona de forma significativa amb gens de fototransducció. Tot i això, fins el dia d'avui pocs estudis han adreçat el rol de Faim *in vivo* al sistema nerviós central, i cap s'ha centrat en la retina.

Per tal d'estudiar una possible implicació de FAIM a la retina vam explorar-la de forma histològica i funcional en ratolins knockout per a Faim (Faim KO) a diferents edats. En la present tesis descrivim com una depleció de Faim genera una neurodegeneració retiniana i un mal funcionament de la retina, i com les retines Faim KO presenten acumulació d'agregats

d'ubiquitina des d'edats primerenques, gliosis i vessament vascular, alteracions que empitjoren amb l'edat. A més d'aquests resultats, també vam trobar una reducció en l'activitat funcional de cèl·lules fotoreceptores, bipolars i ganglionars de la retina en anàlisis d'electrorretinografia en comparació amb animals silvestres.

Sorprenentment, també vam trobar els ratolins Faim KO pateixen un greu retard en l'adaptació a la foscor, la qual pot ser causada per una funció o localització alterada de les proteïnes involucrades en aquest mecanisme com l'Arrestina-1. En aquesta tesi, reportem com la translocació de l'Arrestina-1 a través dels segments dels fotoreceptors arran d'un estímul lumínic és deficient en animals Faim KO. A més a més, el mecanisme de redistribució de l'Arrestina podria ser dependent d'ubiquitinació. Aquesta modificació posttransduccional està significativament reduïda en la presència de FAIM *in vitro*, indicant que la regulació de l'adaptació a la foscor de FAIM podria ser a través del seu rol en el mecanisme de translocació de l'Arrestina-1.

Aquests resultats suggereixen que FAIM és important pel manteniment de la proteostasis i del correcte funcionament de la retina, i d'aquesta manera revelem noves funcions de Faim en un teixit en el qual no havia set explorat. En conclusió, en aquesta tesi descrivim com l'absència de FAIM comporta unes alteracions histopatològiques que probablement són responsables pels dèficits funcionals que hi hem trobat, tals com el retard en l'adaptació a la foscor des d'edats primerenques i la disminució en activitat elèctrica de les cèl·lules de la retina a edats avançades. Aquestes alteracions són característiques de malalties de la retina genètiques o causades per l'edat, tals com la retinosis pigmentària, la retinopatia diabètica i la degeneració macular associada a l'edat. Així doncs, la investigació de FAIM en la retina podria ser decisiva per desemmascarar els mecanismes moleculars d'aquestes malalties.

# Table of contents

*“A ship in port is safe, but that’s not what  
ships are built for.”*

Grace Hopper (1906-1992)



# Table of contents

<b>Abbreviations .....</b>	<b>5</b>
<b>Introduction.....</b>	<b>11</b>
<b>1.1. The retina .....</b>	<b>11</b>
1.1.1. History of the retina.....	11
1.1.2. Macroscopic structure .....	15
1.1.3. Microscopic structure.....	16
1.1.4. Retinal neurodegeneration.....	31
<b>1.2. Apoptosis and apoptotic modulators.....</b>	<b>43</b>
1.2.1. XIAP .....	45
1.2.2. FAIM.....	47
<b>1.3. Ubiquitin .....</b>	<b>54</b>
1.3.1. Ubiquitin-proteasome system.....	57
1.3.2. Nonproteolytic cellular functions of ubiquitin .....	59
1.3.3. Ubiquitin in the retina .....	61
<b>Hypothesis and Aims.....</b>	<b>67</b>
<b>Materials and methods.....</b>	<b>71</b>
<b>2.1. In vivo animal procedures.....</b>	<b>71</b>
2.1.1. Animal care .....	71
2.1.2. Optical tomography coherence.....	72
2.1.3. Electroretinography .....	72
2.1.4. Light exposure protocol .....	75
2.1.5. Light damage protocol .....	76
2.1.6. Measurement of retinal vessel leakage.....	77
<b>2.2. Ex vivo analyses.....</b>	<b>77</b>
2.2.1. Tissue collection and processing.....	77
2.2.2. Histology and retinal morphometry analysis.....	78
2.2.3. Immunohistochemistry and quantification .....	79
2.2.4. Immunofluorescence and quantification .....	81
2.2.5. TUNEL assay .....	84
2.2.6. Western blotting .....	85
2.2.7. RNA isolation and qRT-PCR.....	87
<b>2.3. Bioinformatic analyses.....</b>	<b>89</b>
2.3.1. RNA-sequencing and analysis.....	89
2.3.2. Bioinformatic tools.....	90
<b>2.4. In vitro analyses .....</b>	<b>92</b>
2.4.1. Cell culture conditions .....	92



2.4.2. Cell transfection and ubiquitin assay.....	93
<b>2.5. Statistical analyses .....</b>	<b>94</b>
<b>Results.....</b>	<b>99</b>
<b>Chapter One.....</b>	<b>103</b>
4.1.2. Rationale .....	103
4.1.4. <i>Faim</i> <sup>-/-</sup> mice show photoreceptor death at 18 months.....	104
4.1.5. <i>Xiap</i> and <i>Tnf-α</i> mRNA expression is increased in <i>Faim</i> <sup>-/-</sup> retinas .....	109
4.1.6. Ubiquitin complexes accumulate in <i>Faim</i> <sup>-/-</sup> retinas.....	110
4.1.7. <i>Faim</i> <sup>-/-</sup> retinas present chronic reactive gliosis .....	112
4.1.8. BRB homeostasis is disrupted in <i>Faim</i> <sup>-/-</sup> retinas .....	115
4.1.9. Edn2/Egf2 neuroprotective pathway could be activated in <i>Faim</i> <sup>-/-</sup> retinas ....	119
4.1.10. Discussion.....	122
<b>Chapter Two .....</b>	<b>131</b>
4.2.1. Rationale .....	131
4.2.2. Loss of FAIM leads to age-related rod photoreceptor and retinal ganglion cell defects	133
4.2.3. Faim depletion causes a delayed dark adaptation.....	140
4.2.4. Light-dependent Arrestin-1 translocation is delayed in Faim KO mice .....	143
4.2.5. Both FAIM isoforms prevent Arrestin-1 ubiquitination <i>in vitro</i> .....	145
4.2.6. Photoreceptors in Faim KO mice are more sensitive after light damage .....	147
4.2.7. Discussion .....	153
<b>Global discussion .....</b>	<b>163</b>
5.1. Faim throughout the years.....	163
5.2. Photoreceptor stress and ubiquitin aggregates in Faim KO mice .....	165
5.3. Neurodegeneration in Faim KO mice resembles the phenotype of several inherited and age-related retinal diseases.....	170
5.4. FAIM in ageing and senescence.....	176
5.5. Summarizing our results: FAIM in the retina.....	179
<b>Conclusions.....</b>	<b>185</b>
<b>References.....</b>	<b>189</b>
<b>Annex.....</b>	<b>251</b>

# Abbreviations

*“It’s not enough what I did in the past – there  
is also the future.”*

Rita Levi-Montalcini (1909-2012)



# Abbreviations

<b>adCSNB</b>	Autosomal dominant CSNB
<b>ADRP</b>	Autosomal dominant retinitis pigmentosa
<b>arCSNB</b>	Autosomal recessive CSNB
<b>BIR</b>	Baculoviral IAP repeat
<b>BRB</b>	Blood-retinal barrier
<b>cGMP</b>	Cyclic guanosine monophosphate
<b>c-IAP</b>	Cellular inhibitor of apoptosis
<b>CNG</b>	Cyclic nucleotide-gated
<b>CNS</b>	Central nervous system
<b>CSNB</b>	Congenital stationary night blindness
<b>DCP</b>	Deep capillary plexus
<b>DISC</b>	Death-inducing signaling complex
<b>DR</b>	Diabetic retinopathy
<b>DUB</b>	Deubiquitinating enzymes
<b>Edn2</b>	Endothelin-2
<b>EDNRB</b>	Endothelin receptor type B
<b>ER</b>	Endoplasmic reticulum
<b>ERG</b>	Electroretinogram
<b>FADD</b>	Fas associated via death domain
<b>FAIM</b>	Fas apoptotic inhibitory molecule
<b>FAIM-L</b>	FAIM-long
<b>FAIM-S</b>	FAIM-short
<b>FGF2</b>	Fibroblast growth factor 2
<b>GCAPS</b>	Guanylyl cyclase-activating protein
<b>GCL</b>	Ganglion cell layer
<b>GFAP</b>	Glial fibrillary acidic protein
<b>GluRs</b>	AMPA or kainite ionotropic glutamate receptors

<b>GMP</b>	Guanosine monophosphate
<b>GNAT1</b>	G Protein Subunit Alpha Transducin 1
<b>GRK1</b>	G protein-coupled rhodopsin kinase 1
<b>IAP</b>	Inhibitor of Apoptosis
<b>iBRB</b>	Inner blood-retinal barrier
<b>ICP</b>	Intermediate capillary plexus
<b>IL-1<math>\beta</math></b>	Interleukin-1 $\beta$
<b>INL</b>	Inner nuclear layer
<b>IPL</b>	Inner plexiform layer
<b>IS</b>	Inner segment
<b>KO</b>	Knockout
<b>LTD</b>	long-term synaptic depression
<b>NVU</b>	Neurovascular unit
<b>oBRB</b>	Outer blood-retinal barrier
<b>ONL</b>	Outer nuclear layer
<b>OPL</b>	Outer plexiform layer
<b>OS</b>	Outer segment
<b>PCD</b>	Programmed cell death
<b>PDE6</b>	Phosphodiesterase 6
<b>PDE6B</b>	Phosphodiesterase 6 subunit B
<b>PhR*</b>	Activated and phosphorylated rhodopsin
<b>R*</b>	Activated rhodopsin
<b>retGC-1</b>	Retinal guanylyl cyclase-1
<b>RGC</b>	Retinal ganglion cell
<b>RP</b>	Retinitis pigmentosa
<b>RPE</b>	Retinal pigment epithelium
<b>SAG</b>	S-arrestin
<b>SVP</b>	Superficial vascular plexus
<b>TNFR</b>	TNF receptor
<b>UBA</b>	Ubiquitin binding domain
<b>UPR</b>	Unfolded protein response
<b>UPS</b>	Ubiquitin proteasome system
<b>XIAP</b>	X-linked inhibitor of apoptosis

# Introduction

*“Nothing in life is to be feared, it is only to be understood. Now is the time to understand more, so that we may fear less.”*

Marie Curie (1867-1934)



# Introduction

## 1.1. The retina

### 1.1.1. History of the retina

Philosophers have argued over the course of humanity about the concept of reality. Throughout history, the knowledge we have built about our surroundings has relied primarily on our sensory systems: sight, hearing, touch, taste, and smell. However, in these tumultuous times we have learned that everyone can have their own perception of reality when presented with the same evidence.

In “The Problems of Philosophy” (Russell 1912), Bertrand Russell gives us a great example about these conflictive concepts when he talks about an object as simple as a table:

*“To the eye it is oblong, brown, and shiny, to the touch it is smooth and cool and hard; when I tap it, it gives out a wooden sound. Anyone else who sees and feels and hears the table will agree with this description.”*

However,

*“Although I believe that the table is “really” of the same colour all over, the parts that reflect the light look much brighter than the other parts, and some parts look white because of reflected light.” [...] “If several people are looking at the table at the same moment, no two of them will see exactly the same distribution of colours, because no two can see it from exactly the same point of view, and any change in the point of view makes some change in the way the light is reflected.”*



Current science relies on the principle that any idea, at any time, can (and should) be scrutinized with the goal of being refuted or further accepted. Historically, many scientists and philosophers have pursued the answers on how we perceive and actually “see” reality, which have led them to enunciate their own refutable theories.

In the fourth century b.C., Plato enunciated the very first emission theory of vision. He wrote that eyes emanated a substance akin to the light of everyday life, like a flashlight, that flowed in a stream smooth and dense, illuminating objects with its rays. This idea was also followed by Galen of Pergamon (129-216 b.C.), who was considered the greatest physician of the Roman Empire (**Figure 1**). Aristotle disagreed with this thought, anticipating the more actual theory of intromission vision: he speculated that the eye receives light rays rather than emitting them, theoretically exploring the principle that would later be developed.

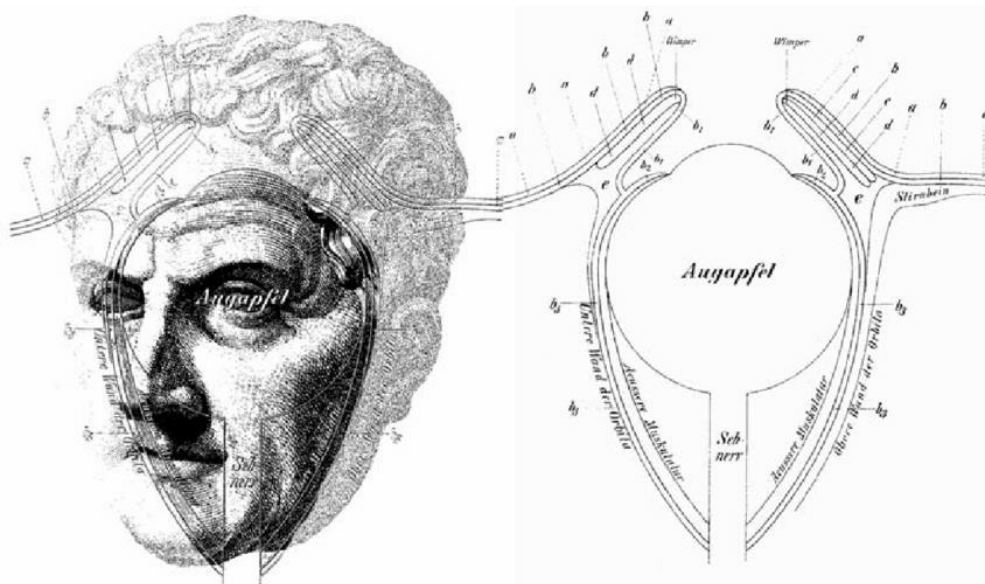


**Figure 1.** Portrait of Claudius Galen (left) and a diagram of the eye based on a description given by Galen from Magnus 1901 (right).

Many personalities like Chinese philosopher Mo-Ti (400 b.C.), physicist Alhazen (965-1040), and even Leonardo Da Vinci (1452-1519) flirted with the retinal image theory long before Johannes Kepler coined the term “*camera obscura*” in the early 17<sup>th</sup> century. They described how the eye behaves like this device: a darkened room with a small hole at one side, through which the light penetrates and creates an inverted image of the objects from the outside (**Figure 2**).

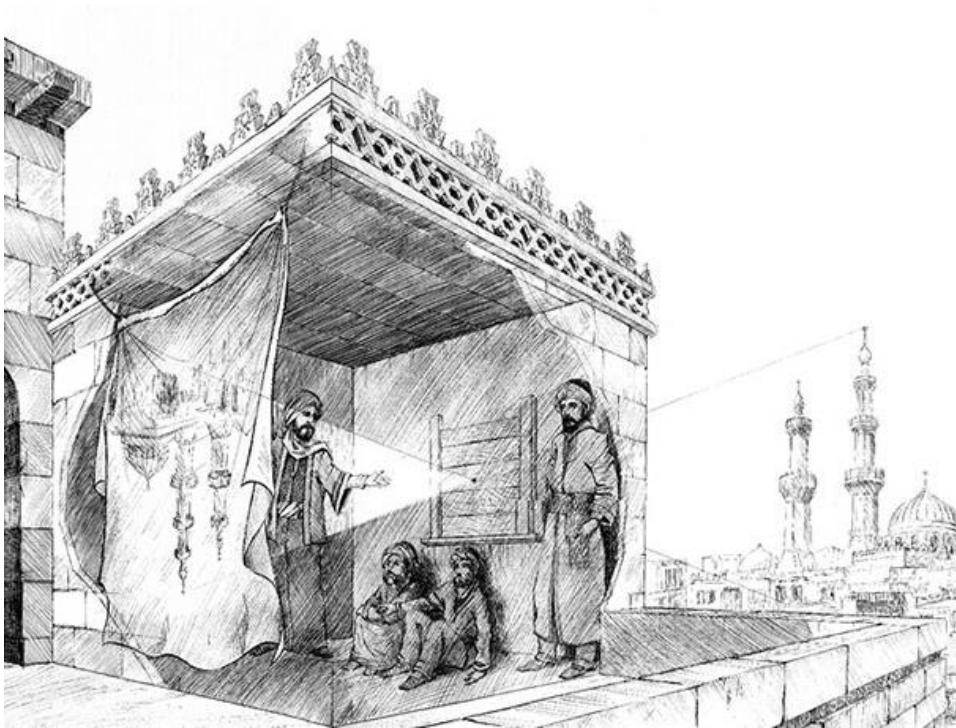


**Figure 2.** Illustration of what is thought to be the first camera obscura, as an experiment carried out by Alhazen (965-1040).

Although this theory explained phenomena that otherwise would have been impossible (such as central visual acuity, visual field, and dark adaptation), it was not promptly accepted. Even in Kepler’s times, Galen intromission theory was still largely accepted. Following the Greek’s physician research, it was thought that the image itself needed to arrive to the brain to be perceived.

By applying Kepler's theory, they thought that image would be lost in its passage from the retina to the brain.

To connect both ideas, René Descartes (1596-1650) resolved that there was a sensory projection from the eye to the brain. He pointed out that the "code" which symbolizes sensations in the brain does not have to resemble the sensation itself. Henceforth, he enunciated the visual perception theory, in which images are formed in the retina and coded into impulses that are carried by the optic nerve to the brain (**Figure 3**).

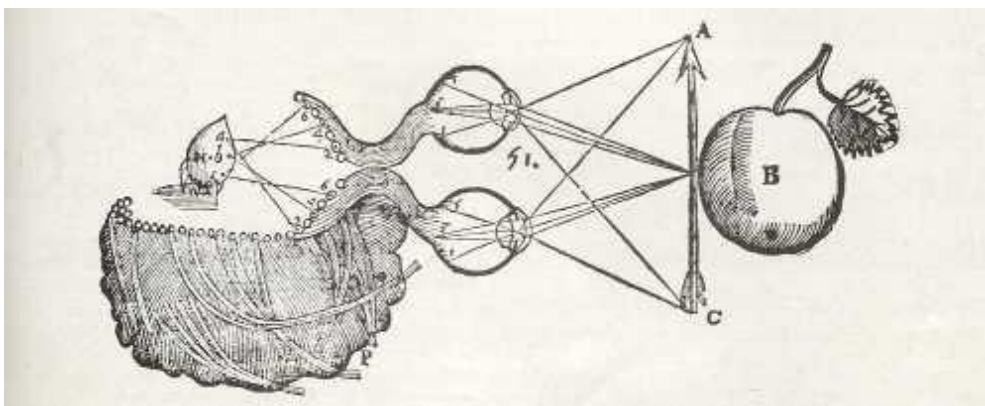


**Figure 3.** Diagram of the optic chiasm by René Descartes (Descartes 1664).

It is safe to admit that scientific knowledge of the visual system has enormously evolved since then, but they laid the foundation in which current scientists would develop today's science. Certainly, the eye acts as a *camera obscura*, in which images are inverted because of the great curvature of the lens surface and its resulting refractive power. As the image is inverted by the lens, the superior half of each eye's visual field is projected onto the inferior half of each eye's retina. Also, the temporal (left) hemifield of the left eye is projected onto the nasal (right) half of the left eye's retina; and the nasal (left) hemifield of right eye is projected onto the temporal (right) half of the right's

eye retina. When light rays reach the retina, it transforms light energy into electrical signals that are carried through to the brain the optic nerve, where visual information is reoriented and processed.

### 1.1.2. Macroscopic structure

The anatomy of the vertebrate retina can be described both macroscopically and microscopically. The macroscopic structure of the retina is comprised by four different structures in humans: optic disk, macula, fovea and ora serrata; while mice are lacking the macula and fovea (Murali et al. 2019) (**Figure 4**).

The optic disk is located in the very center of the retina. It is a circular region where visual information from the retina is transmitted through axons that form the optic nerve. This area lacks photosensible cells, meaning that it is not sensible to light stimulation. Because of this, the field of vision associated to this specific zone is invisible, which gives it the name of blind point or “*punctum caecum*”. Visual information relative to this point is achieved by surrounding detail and information from the other eye.

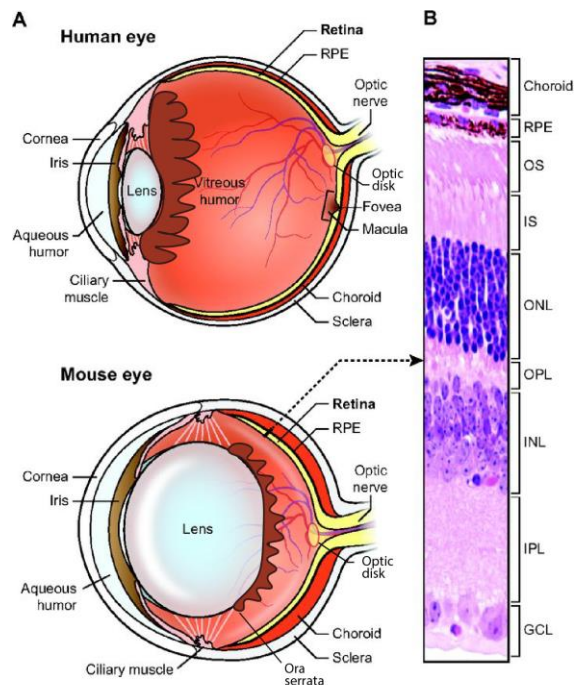


**Figure 4.** Comparison of the human and mouse eye. RPE: retinal pigment epithelium, OS: outer segment, IS: inner segment, ONL: outer nuclear layer, OPL: outer plexiform layer, INL: inner nuclear layer, IPL: inner plexiform layer, GCL: ganglion cell layer. Modified from (Veleri et al. 2015)

The macula is the area responsible for central light since it houses the maximum density of cone photoreceptors. The fovea is located in a pit within the center of the macula, and it provides the maximum visual acuity in humans. Neither rats nor mice have a macula, and do not have an area of high cone density.

Finally, the ora serrata is the scalloped and peripheral termination of the sensory retina and forms a junction between the choroid and the ciliary body.

### 1.1.3. Microscopic structure

Ramon y Cajal was the first to describe the microscopical retinal structure. He set the basis on which scientists would come to build our current knowledge of the microscopic retina when he described its different cell types and how they interconnect with each other (Ramón y Cajal 1891) (**Figure 5**).

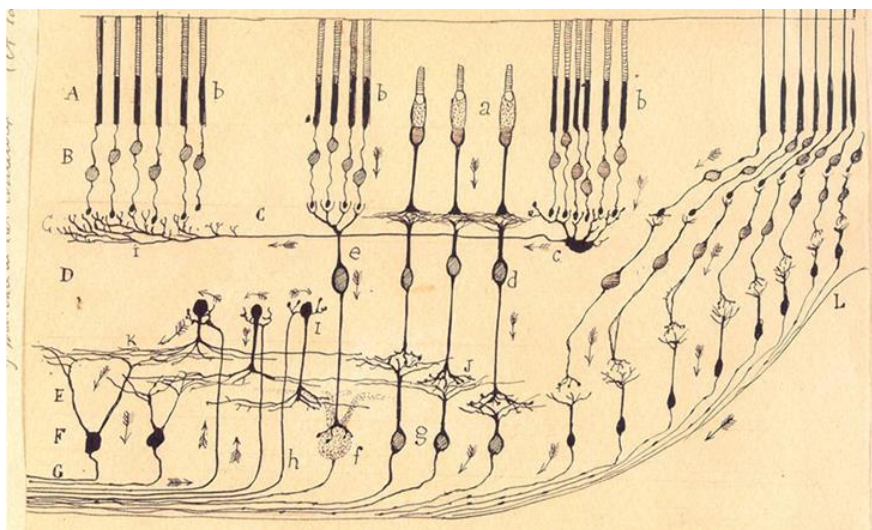


**Figure 5.** Ramon y Cajal drawing of retinal microscopic structure representing retinal structures and cells (1901). For instance, A: photoreceptor segments, B: outer nuclear layer, C: outer plexiform layer, D: inner nuclear layer, E: inner plexiform layer, F: ganglion cell layer, G: retinal nerve fibers. a-b: cone and rods photoreceptors c: horizontal cells, d-e: cone and rod bipolar cells, f-g: retinal ganglion cells, i: amacrine cells.

The retina is comprised by up to ten different layers, and it can be arranged in two different categories: nuclear layers and plexiform layers (**Figure 6**). The nuclear layers consist of the outer nuclear layer (ONL) where rod and cone photoreceptors are found; the inner nuclear layer (INL) that houses bipolar, amacrine and horizontal cells; and the ganglion cell layer (GCL), which contains the Retinal Ganglion Cells (RGCs). The outer and inner plexiform layers (OPL and IPL) are layers of neuronal synapses. In the OPL, photoreceptors synapse with bipolar and horizontal cells, and in the IPL, bipolar and amacrine cells synapse with RGCs.

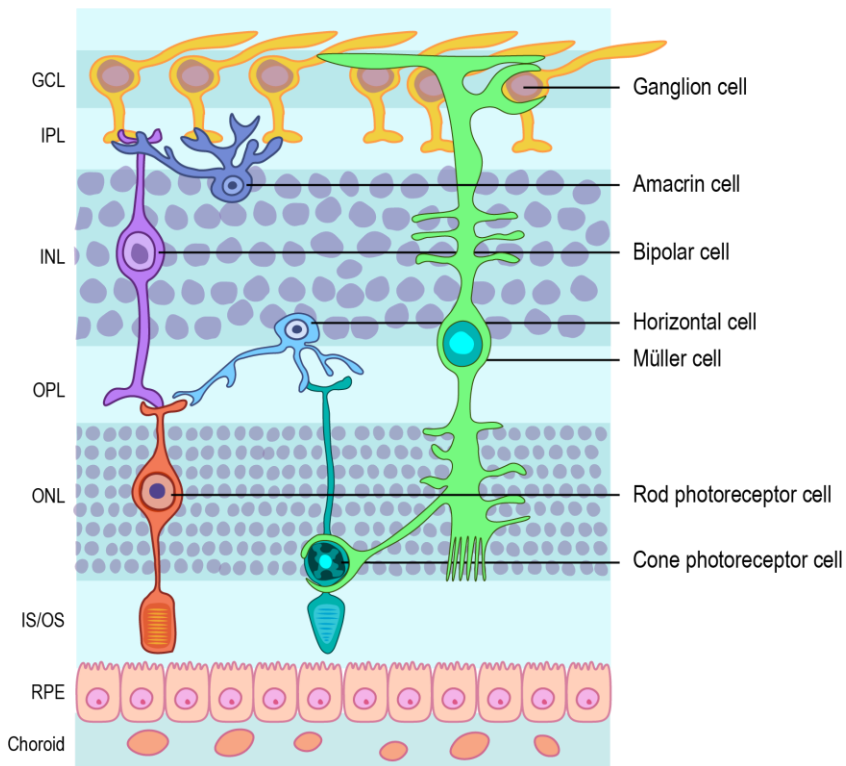


**Figure 6.** The microscopic structure of the neuroretina. In the left, the different layers are described: ganglion cell layer (GCL), inner plexiform layer (IPL), inner nuclear layer (INL), outer plexiform layer (OPL), outer nuclear layer (ONL), inner and outer segments (IS and OS), retinal pigment epithelium (RPE). In the right, the different cell types, and its anatomical correspondence in the retina.

The whole structure of the neural retina is sustained by the retinal pigment epithelium (RPE), which is found in the outermost zone and separated from the choroid by the Bruch membrane. It is constituted of cuboidal cells that synthesize melanin, which absorbs light that passes through the retina and protects it against reflected light. It also oversees trophic support and protects photoreceptors from oxidative stress.

### 1.1.3.1. Photoreceptors

Photoreceptor cells are highly specialized neurons. There are two types of photoreceptor cells: cones and rods, and they are composed of five compartments: outer segment (OS), inner segment (IS), soma, axon and synaptic terminal (**Figure 7**).

Rods account for approximately 97% of retinal photoreceptors in human and mice. In humans, there is an average of 120 million rods and 6 million cones.

Rods are found along the periphery and its density increases in central retina before reaching the fovea, where cones peak in density and become the most abundant photoreceptors. Since mice lack a fovea, rod/cone ratios are preserved throughout the retina (Volland et al. 2015).

Rods and cones differ vastly in its intrinsic properties despite its major

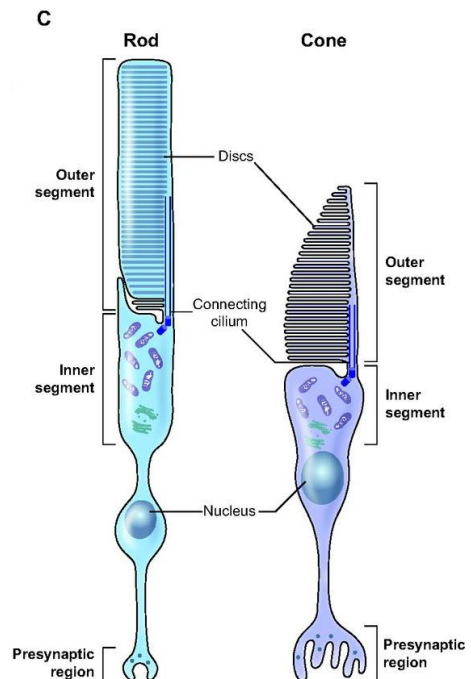


**Figure 7.** Anatomy of rod (left) and cone (right) photoreceptors. Figure from (Veleri et al. 2015).

similarities. Both photoreceptor cells are heavily conserved in evolution, but cones are even older than rods. Along with gene duplication and modification of cone pigments to produce rod pigments, molecular and anatomical changes came through. Rods are exceptionally sensitive to light and can act as light detectors even in extremely low levels of luminance, but become very easily saturated in bright light. On the other hand, cones exhibit adaptive properties that allow them to detect motion and luminance changes when photon flux is less limiting (Morshedian and Fain 2017).

The OS is an elaborate primary cilium in which phototransduction takes place by capturing photons and converting them into electrical signals (Yildiz and Khanna 2012). The OS of cones is formed by invaginations of the plasma membrane that form membranous disks, and are connected to a ciliary membrane, which stems from the connecting cilium (W. J. Spencer et al. 2020). Rod's disks, on the other hand, are not connected to the ciliary membrane and remain enclosed inside the outer segment (see **Figure 7**). These disks house the proteins necessary for phototransduction, and its composition varies between rods and cones (Morshedian and Fain 2017). Rods OSs only express rhodopsin visual pigment, whereas cones can express different pigments depending on its spectral sensitivity. Human cones can be divided into red, green and blue-sensing cones, while mice only express two kinds of opsins: S and M, which detect blue/UV and green light, respectively (Terakita 2005).

The OS development is similar to common cilia. When photoreceptors exit the cell cycle, centrioles are moved to the apical end of the IS, where the mother centriole becomes the basal body. As it matures it is capped by the ciliary vesicle, which separates the IS from the OS (Ishikawa and Marshall 2011; JN et al. 2013; Sedmak and Wolfrum 2011).



The RPE, which is adjacent to the OS, is regularly renewing the ends of the OS by phagocytosis (Mazzoni, Safa, and Finnemann 2014). This takes a high maintenance of energetic demands, such as protein and lipid synthesis and subsequent vesicular trafficking from the IS to the OS through the ciliary vesicle.

Most of the housekeeping functions of photoreceptors take place in the IS, where organelles such as the Golgi, ER and mitochondria are localized (Szikra and Križaj 2007) (see **Figure 7**).

The nuclei of rod and cone photoreceptor comprises the ONL, and is separated from the IS by the external limiting membrane. Finally, terminals of photoreceptors are localized in the OPL, which is majorly formed by inner fibers of rods and cones and a narrower inner band of synapses between photoreceptors and INL cells.

#### **1.1.3.1.1. Phototransduction**

Phototransduction is the process in which light is converted into electrical signals in the retina, specifically in the OS of photoreceptors.

This light-induced electrical activity of the retina can be captured and measured, allowing the electroretinogram (ERG) recordings. In dark-adapted subjects (scotopic conditions), ERG records the activity of rod-mediated responses and mixed (rod-cone) mediated responses, and in light-adapted subjects (photopic conditions), ERG records the activity of cone-mediated responses (further described in Materials and Methods section).

In the dark, photoreceptors remain significantly more depolarized than most neurons (-35 mV vs -60 mV) and release the neurotransmitter glutamate (Tessier-Lavigne 2020). This constant depolarization is caused by the flow of

positively charged sodium ( $\text{Na}^{+2}$ ) and calcium ( $\text{Ca}^{+2}$ ) ions into photoreceptor cells through sodium ion channels that are activated by free cyclic guanosine monophosphate (cGMP) (Krizaj and Copenhagen 2002). In most sensory systems, reception of the adequate stimulus causes the cell membrane of neurons to depolarize, stimulating an action potential and triggering the release of a neurotransmitter onto the synapsing neurons. Like bipolar cells, photoreceptors do not fire action potentials, but rather use graded potentials and a variation on the levels of neurotransmitter release (Purves et al. 2001).

Light activation of rhodopsin drives the phototransduction cascade that initiates vision, which is the main function of the retina. It is originated by photoexcitation of the visual pigments located in the OS of photoreceptors and is finished with phototransduction termination. This process can be subdivided into three different steps: 1) Activation state, 2) Rhodopsin deactivation and light adaptation, and 3) PDE deactivation and GMP synthesis (Y. Fu and Yau 2007; Kawamura and Tachibanaki 2010; Lyubarsky, Nikonov, and Pugh 1996).

### 1) Activation state

OS disks are studded with rhodopsin, a pigment-containing sensory protein that converts light into an electrical signal. When light enters the retina, the 11-cis-retinal molecule that is embedded in rhodopsin isomerizes to all-trans-retinal, enabling activated rhodopsin ( $\text{R}^*$ ) to activate multiple Transducin- $\alpha$  molecules (**Figure 8**) (Kono, Goletz, and Crouch 2008; Melia et al. 1997; Cohen, Oprian, and Robinson 1992). Its activation, in turn, activates phosphodiesterase 6 (PDE6), which hydrolyzes cyclic-GMP (cGMP) into GMP. cGMP is required for the opening of cyclic nucleotide-gated (CNG) channels, which are strictly ligand-gated. The reduction of free cGMP levels

by PDE6 causes the closing of CNG channels, and a drop in intracellular levels of  $\text{Ca}^{+2}$ , which culminates in photoreceptor hyperpolarization and the inhibition of glutamate release (Krizaj and Copenhagen 2002). This starts an electrical current flow through the retina, in which the signal passes to bipolar and horizontal cells and eventually reaches RGCs, that form the optic nerve that will reach the optic chiasm through the optic canal.

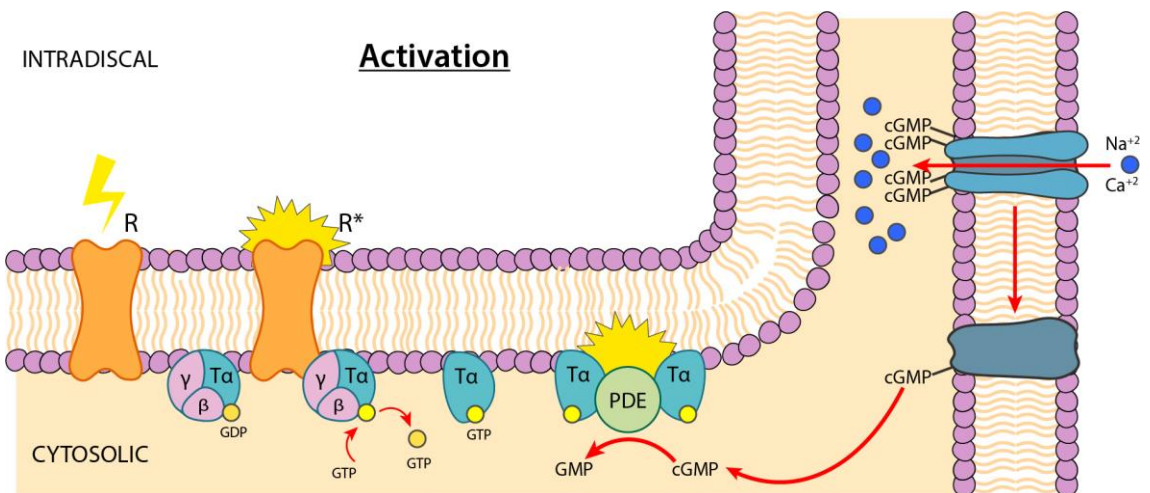


**Figure 8.** Rhodopsin activation in phototransduction after light absorption. Rhodopsin (R) absorbs a photon (lightning symbol) and becomes activated ( $\text{R}^*$ ).  $\text{R}^*$  interacts with and activates Transducin- $\alpha$ , which binds PDE, resulting in the closing of ionic channels through the depletion of cGMP levels.

## 2) Rhodopsin deactivation and light adaptation

This amplified response and its consequent electrical activity remain sustained if rhodopsin is catalytically active, therefore its deactivation is necessary to restore the darkness equilibrium (Mendez et al. 2000).

Light adaptation is the process that the retina uses to avoid saturation if light persists. In this process, the retina has to quickly adapt to background illumination to distinguish objects and to adjust to various levels of light. To

achieve this, photoreceptors need to be deactivated in a timely manner to be able to absorb subsequent photons.

Termination of the phototransduction cascade relays in two simultaneous conditions: 1) the deactivation of rhodopsin, Transducin- $\alpha$  and PDE6, and 2) the reestablishment of free cGMP levels (**Figure 9**).

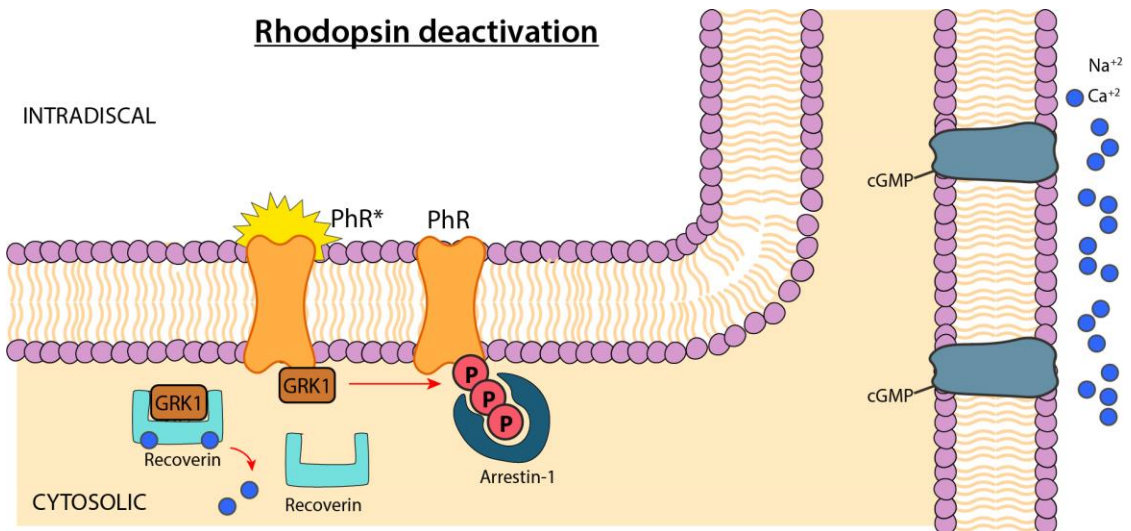


**Figure 9.** Rhodopsin deactivation via a two-step mechanism. First, Recoverin frees GRK1 due to the low levels of Ca<sup>2+</sup> and GRK1 phosphorylates rhodopsin (PhR\*), and second, Arrestin-1 binds activated and phosphorylated rhodopsin, rendering it inactive (PhR).

The drop in Ca<sup>2+</sup> is detected by recoverin, a calcium-sensor protein, which stops sequestering G protein-coupled rhodopsin kinase 1 (GRK1) (J. Chen et al. 1995; Kawamura 1993). As its very name implies, GRK1 phosphorylates activated rhodopsin (PhR\*), which is the first step towards its deactivation. This phosphorylation prepares PhR\* for the high-affinity binding of visual arrestin, the second step on rhodopsin deactivation. This interaction enables rhodopsin to exchange bleached all-trans retinal to 11-cis retinal, allowing

rhodopsin to become activated again and to absorb another photon, and it effectively shuts off further signaling by blocking its ability to bind and activate Transducin- $\alpha$ .

### 3) PDE deactivation and GMP synthesis

Once rhodopsin uncouples Transducin- $\alpha$ , it reassembles to its heterotrimeric inactive complex. PDE6 remains inactivated and cGMP hydrolysis is reduced (Figure 10).

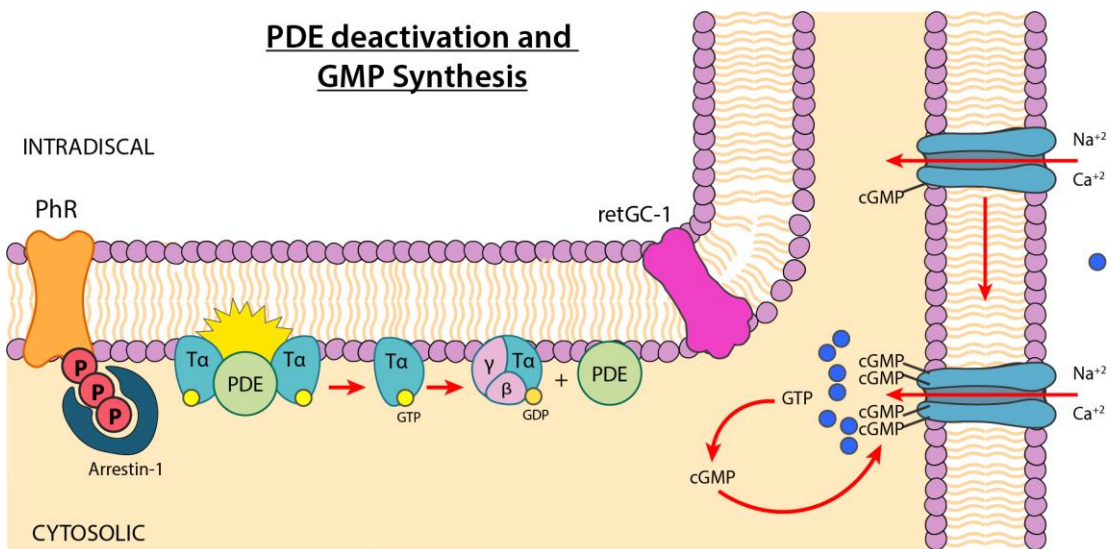


**Figure 10.** PDE deactivation and GMP synthesis. After rhodopsin deactivation and the consequent liberation of Transducin- $\alpha$ , PDE becomes inactive. retGC-1 synthesises cGMP, activating and opening ion channels.

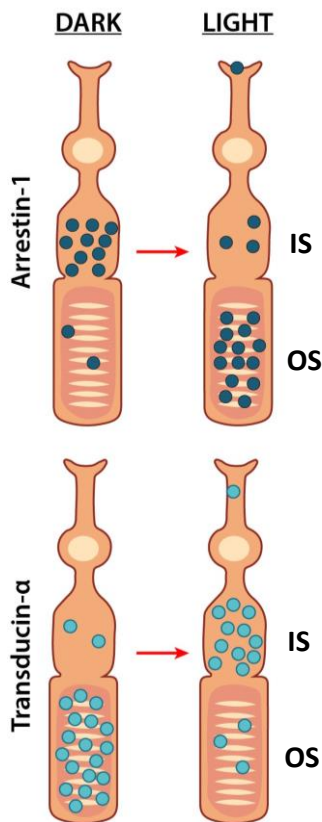
As the intracellular levels of  $\text{Ca}^{+2}$  reduce, guanylyl cyclase-activating proteins (GCAPS) dissociate from it and are able to activate retinal guanylyl cyclase-1 (retGC-1) (Lyubarsky, Nikonov, and Pugh 1996). This promotes cGMP synthesis, which in turn activates the CNG-channels thanks to the calcium sensor protein calmodulin (T. Y. Chen and Yau 1994).

### 1.1.3.1.2. Dark adaptation

Dark adaptation is the opposite process to light adaptation. This mechanism allows to increase visual sensitivity following a drop in luminance levels. After being exposed to a bright light in a sunny day, and coming indoors into a dark room, we can barely see anything. However, as time passes by, the retina gradually adapts and allows us to detect our surroundings. Both rods and cones have crucial roles in dark. As rods are much more sensitive than cones, they saturate easily in bright light and are slower. Cones, on the other hand, can adapt faster, but they are not as reliable in dimly lit conditions (Weiss 2020). As of this, the first moments of dark adaptation reflect cone function, but rods take over once enough time has passed to adapt to darkness.

To achieve dark adaptation rhodopsin needs to be dephosphorylated and bind a new 11-cis-retinal, which can only be done after stable rhodopsin inactivation by GRK1 and Arrestin-1 (Frederiksen et al. 2016; Weiss 2020; Bayburt et al. 2011). Visual function has to respond to a wide range of light intensities, and it needs to maintain high sensitivity. To achieve effective photoreceptor vision, photoresponse termination must be attained in a timely manner. This process will cause an electrical response decay after photoresponse is blocked, allowing photoreceptors to become activated again and recover its sensitivity in dimly-lit conditions.

As mentioned above, Arrestin-1 has a crucial role in rhodopsin signalling quenching, and thus on dark adaptation. Upon rhodopsin phosphorylation by GRK1, Arrestin-1 binds to Rhodopsin and blocks its binding to Transducin- $\alpha$ , thus stopping the phototransduction cascade and terminating rhodopsin photoresponse (see **Figure 10**) (Bayburt et al. 2011; Frederiksen et al. 2016).



One mechanism that is thought to have an important role on the regulation of light and dark-adaptation is the light-driven redistribution of photoreceptor-segment proteins, such as Transducin- $\alpha$  and Arrestin-1. Upon light reception and after dark-adaptation, Arrestin-1 translocates from the IS to the OS, whereas Transducin- $\alpha$  moves in opposite directions (Mendez et al. 2003; Nair et al. 2005) (**Figure 11**).

**Figure 11** Representation of translocation upon light reception of Arrestin-1 and Transducin- $\alpha$  in photoreceptor segments. In dark-adapted retinas, Arrestin-1 is almost completely localized at the IS, while Transducin- $\alpha$  is localized in the OS (where Rhodopsin is bound). After light-stimulation, redistribution of both Arrestin-1 and Transducin- $\alpha$  ensues in opposite directions: Arrestin-1 translocates to the OS and Transducin- $\alpha$  to the IS.

### 1.1.3.2. Retinal bipolar cells

Bipolar cells receive inputs from a set of photoreceptor cells that comprise their receptive field. Some bipolar cells are only post-synaptic to cones, others only to rods and some are receptive to mixed rod-cone inputs (Behrens et al. 2016). Although there is a multiplicity of bipolar cells depending on their morphological characteristics, they can be physiologically classified into two categories: ON and OFF bipolar cells (Werblin and Dowling 1969).

ON bipolar cells respond to glutamate by hyperpolarization (inhibition), so after light exposure, when photoreceptors are hyperpolarized and they release less glutamate, ON bipolar cells become activated. OFF bipolar cells respond

on the exact opposite way: they activate after glutamate release from photoreceptor in dark conditions, and become hyperpolarized in the light (Feher 2012; Popova 2014) (**Figure 12**).

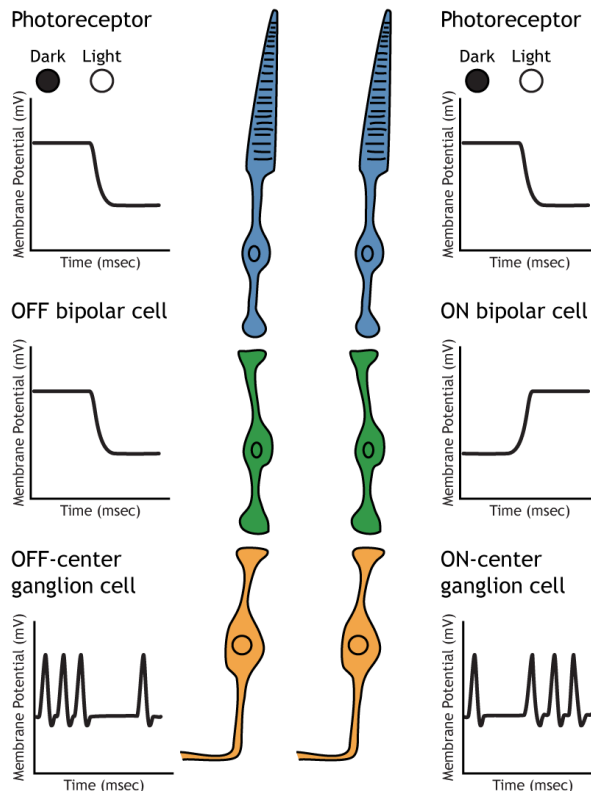


**Figure 12.** Synapses and neuron responses of photoreceptors, bipolars and ganglion cells upon illumination. At the left, OFF-bipolar cells hyperpolarize after illumination. At the right, ON-bipolar cells depolarize after illumination.

ON and OFF bipolar cells act in opposite ways in response to glutamate release from photoreceptors due to their different glutamate receptors (Hack, Peichl, and Brandstätter 1999; Popova 2014; Puller, Schubert, and Haverkamp 2011). Glutamate is excitatory for OFF bipolar receptors, so in the dark, when photoreceptors release glutamate, OFF bipolar cells depolarize and increase glutamate release onto RGCs. However, after light reception photoreceptors stop releasing glutamate, so OFF bipolar cells are



hyperpolarized. On the contrary, glutamate is inhibitory for ON bipolar cells. Hence, when photoreceptors release glutamate in dark conditions, ON bipolar cells are hyperpolarized, and upon light reception they depolarize.

Like photoreceptors, bipolar cells also do not fire action potentials, but rather respond with graded postsynaptic potentials. OFF and ON bipolar cells synapse on OFF and ON RGCs, respectively (Dong, Agey, and Hare 2004).

### **1.1.3.3. RGCs and other retinal cell types**

RGCs are responsible for transmitting the electrical signal of the phototransduction cascade out of the retina and onto the brain (Corbett and Chen 2018). Also, RGCs (along with amacrine cells) are the only retinal cell type that fires action potentials. They fire in all luminance conditions, but the relative firing rate encodes the necessary information about light.

In the INL, horizontal and amacrine cells send their processes laterally, allowing communication at the level of the photoreceptor-to-bipolar and bipolar-to-RGC synapses, respectively (see **Figure 6**) (Gallego 1971). Horizontal cells also undergo graded changes in membrane potential like photoreceptors and bipolar cells, but amacrine cells do fire action potentials. Amacrine cells send their processes laterally, following the IPL and at the level of the synapses between bipolar and RGCs.

Finally, glial population in the retina is comprised of microglia, astrocytes and Müller cells, the retinal resident macroglia (Vecino et al. 2016). Although they have a different developmental origin, they share many functions within the retina: they provide structural support and are involved in metabolism phagocytosis of neuronal debris and release of certain trophic factors (Vecino et al. 2016).

While astrocytes and microglia are responsible for synaptic pruning like in the brain (Vainchtein and Molofsky 2020; F. Li, Jiang, and Samuel 2019; X. Wang et al. 2016), Müller cells also serve as progenitors for retinal neurons. Müller cells are evenly distributed over the retina, but their nuclei are localized in the INL and their endfeet cover the entirety of the inner retina. Müller cells are involved in several responses to injury and disease, and they provide trophic and anti-oxidative support to photoreceptors (Andreas Bringmann and Wiedemann 2012). After the retina has been exposed to inflammation, injury, disease or any kind of insult, Müller cells display reactivity in the form of reactive gliosis. This response is placed to protect retinal tissue from further damage and to promote tissue repair and remodeling. This causes Müller cell hypertrophy and proliferation (Andreas Bringmann et al. 2006; Andreas Bringmann and Wiedemann 2012). Moreover, Müller cells also have a role in regulating the blood-retinal barrier (BRB), which is described in the following section.

#### **1.1.3.4. Blood-retinal barrier**

The BRB is a restrictive physiological blood-ocular barrier that regulates flow of nutrients, metabolic waste, water and ion flux and proteins out of the retina (Díaz-Coránguez, Ramos, and Antonetti 2017; Cunha-Vaz, Bernardes, and Lobo 2010). It is divided into the inner BRB (iBRB) and the outer BRB (oBRB) (**Figure 13**).

The iBRB is comprised by the unique properties of the neurovascular unit (NVU), which is a highly selective barrier that prevents toxic molecules from entering the inner retina, and is very similarly in functions the that of the blood-brain barrier (Nian et al. 2021).

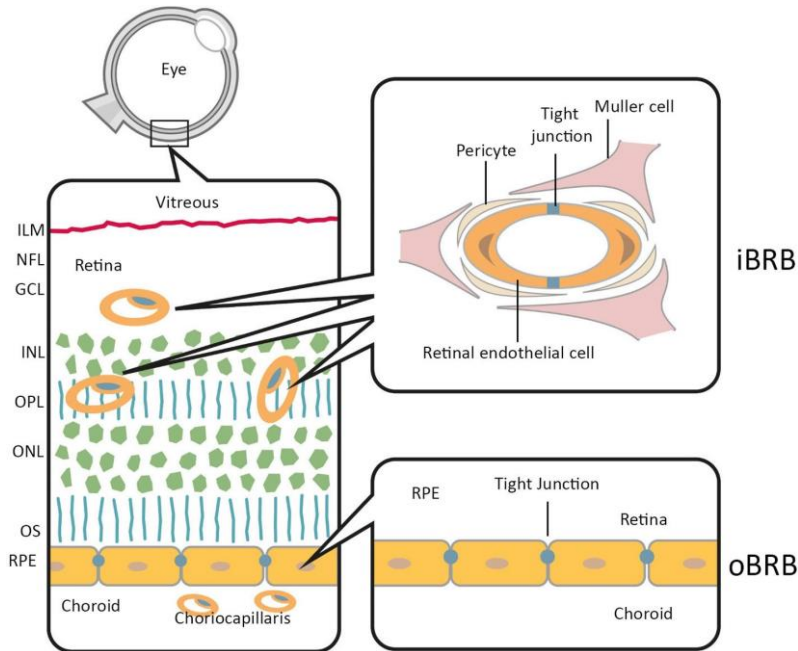


**Figure 13.** Inner (iBRB), outer (oBRB) blood-retinal barrier and the neurovascular unit (NVU), which is comprised by tight junctions from endothelial cells, pericytes, Müller cells and astrocytes (not depicted here). Figure from (Cunha-Vaz, Bernardes, and Lobo 2010).

In the retina, the NVU consists of endothelial cells and pericytes covered by multiple processes of the Müller cells, while astrocytes and microglia surround the capillaries with their long processes (Nian et al. 2021; van der Wijk et al. 2018). This retinal vasculature can also be divided into three vascular plexus: the superficial vascular plexus (SVP), the intermediate capillary plexus (ICP), and the deep capillary plexus (DCP) (Campbell et al. 2017) (**Figure 14**).

In contrast, the oBRB is formed by tight junctions between the apical lateral membranes of RPE, the Bruch's membrane and the choriocapillaris. The RPE is composed of a single layer of epithelial cells that separate the neuroretina

from the Bruch's Membrane. Beneath the latter structure the choriocapillaris are found, which form a dense vascular layer that provides metabolic support for the RPE and photoreceptor cells (Matet et al. 2020).

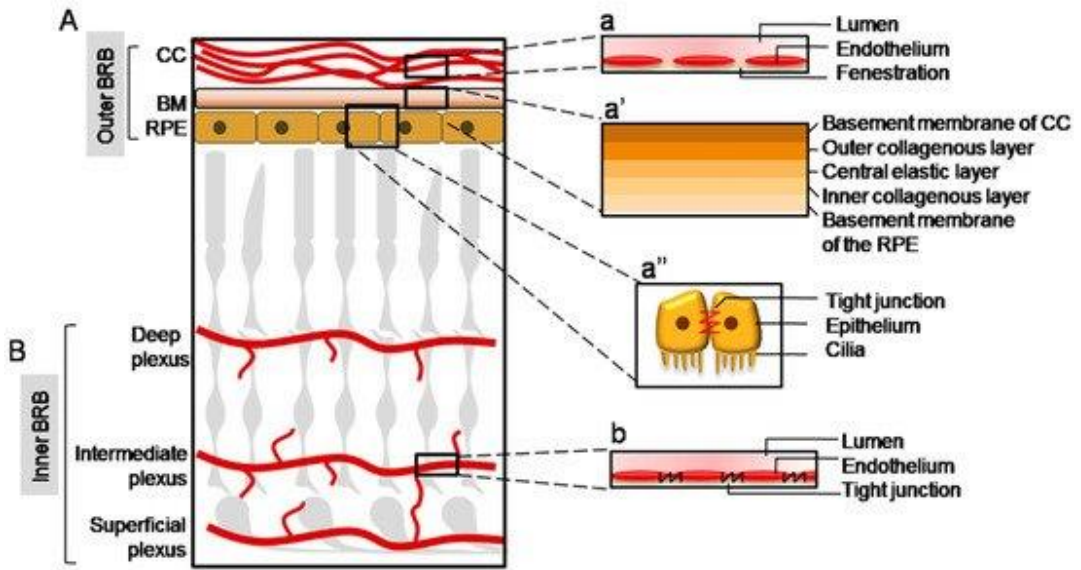


**Figure 14.** Capillary plexus of the iBRB and composition of the oBRB

Photoreceptors and the majority of OPL receive irrigation from choriocapillaris indirectly, while the inner retina (GCL, IPL, INL and a minor portion of the OPL) is supplied by the superficial and deep capillary plexuses of the iBRB. The RPE also contains tissue-specific tight junctions that regulate protein transportation and are highly selective (Díaz-Coránguez, Ramos, and Antonetti 2017). Anatomically speaking, the oBRB and RPE are crucial for the proper maintenance and integrity of photoreceptor cells.

#### 1.1.4. Retinal neurodegeneration

The retina is a highly specialized tissue with unique characteristics and mechanisms that distinguish it from the rest of the central nervous system (CNS).

Aside from this, the retina has long been considered as a window to the brain due to its intrinsic properties and great accessibility (London, Benhar, and Schwartz 2013; Criscuolo et al. 2018; Chiquita et al. 2019; Beard et al. 2020; Y. Zhang et al. 2021; Rodrigues-Neves et al. 2021). Anatomically and developmentally speaking, the retina is an extension to the CNS, and various neurodegenerative diseases manifest earlier as ocular alterations in the eye. Evidently, numerous eye diseases have been described in which retinal malfunction is the primary cause and are not subordinate to brain alterations.

#### **1.1.4.1. Retinal gliosis in diabetic retinopathy**

Diabetic retinopathy (DR) is the most common microvascular complication of diabetes, caused by high blood sugar levels that damage the retinal tissue (“Diabetic Retinopathy - NHS” n.d.). DR is the leading cause of preventable blindness in working-age population, and the duration of the disease, the type of treatment for diabetes and the degree of metabolic alterations are crucial factors for the evolution of the disease (Cheung, Mitchell, and Wong 2010; Yau et al. 2012). Epidemiology of DR in Spain has been changing due to the variation in screening programs, and its incidence has dramatically increased in the past years. Within diabetic patients, DR is present in ~16% of affected people, and the annual incidence of DR is of approximately 4% (Romero-aroca et al. 2022). This high prevalence of diabetic retinopathy is fuelled by the increase in incidence of type 2 diabetes mellitus in the adult population. Recently it has been estimated that by year 2045, 745 million people worldwide will be diabetic. In 2020, global DR prevalence was estimated around 103 million people (22.27% of the total diabetes patients), but it is projected to increase to 160.5 million by 2045 (Teo et al. 2021). This poses as a highly problematic healthcare issue, given that although nutritional and lifestyle changes can slow the disease and its complications, there are no

effective therapies that address the microvascular alterations in the retina (Mayo Clinic 2021).

DR can be subdivided into two different stages: pre-proliferative and proliferative retinopathy. In the early stages, DR is characterized by reactive gliosis, in which Müller glia become activated and overexpress GFAP, along with an impairment of astrocyte and microglial function, which release cytokines that contribute to the pro-inflammatory phenotype (Rungger-Brandle, Dosso, and Leuenberger 2000; Araszkiwicz and Zozulinska-Ziolkiewicz 2016). Proliferative DR is also measured by microaneurysms, retinal haemorrhage and intraretinal microvascular abnormalities. If severe, it can also manifest diabetic macular edema (DME) (**Figure 15**, adapted from (Duh, Sun, and Stitt 2017)).

The proliferative retinopathy occurs in a more advanced phase of the disease, when neovascularization and fibrosis develop to the retinal surface (Cheung, Mitchell, and Wong 2010).

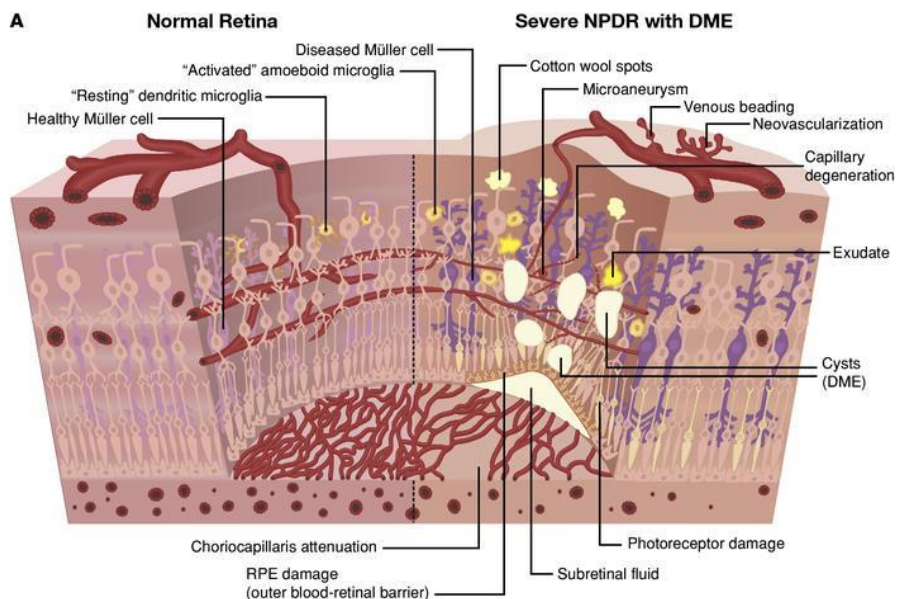


**Figure 15** Illustrated schema of the normal retina compared to non-proliferative DR with diabetic macular edema (DME). Normal retina has BRB integrity and healthy Müller glia, photoreceptors and microglia. On the other hand, DR retinas manifest multiple alterations, like vascular abnormalities (microaneurysms, capillary degeneration and neovascularization), lesions associated with vascular damage (cotton wool spots and exudate), and importantly, retinal gliosis with swelling of Müller cells, neuronal damage, activated microglia, damage in the RPE and thinning of the choriocapillaris.

- **Retinal neurodegeneration and inflammation as a cause and not a consequence of RD**

As explored above, vascular irrigation in the retina is dual: it is comprised by the retinal vasculature and the choriocapillaris. This makes the retinal oxygenation a fairly unique and complex process. This delicate balance is crucial for maintenance of retinal homeostasis, which puts the retina in particular risk against ischemic damage. The hyperglycaemia in diabetes can cause hypoxic stress, and the production of free radicals and advanced glycation end-products cause retinal gliosis and early microvascular impairment and dysfunction of the retinal neurovascular unit (NVU) (Nian et al. 2021). This can lead to pericyte loss, excitotoxicity, apoptosis of endothelial cells and the thickening of the intermitting membrane, which collectively contribute to the breakdown of the BRB (Simó and Hernández 2014).

Thus, until recently it has been described how the cell death and neuronal stress activate the astrocytes and Müller cells of the NVU, leading to reactive gliosis (Coorey et al. 2012). Nonetheless, current research also associates diabetic-derived retinal neurodegeneration as one of the main mechanisms that lead to DR, and not only a consequence of disruption of the NVU. In this

hypothesis, reactive gliosis occurs early in DR, when astrocytes and Müller cells become activated following diabetes onset. For instance, it has been shown how a Müller depletion in the rat retina leads to BRB breakdown and vascular alteration, both hallmarks of RP (Shen et al. 2010). Moreover, post-mortem samples from diabetic patients with no signs of vascular alterations display high levels of retinal gliosis (Carrasco et al. 2007; Garcia-Ramírez et al. 2009; Mendonca et al. 2020), suggesting this event precedes the vascular clinic and is an early event in DR.

Ironically, once Müller cells activate, they stop performing their physiological functions. They become hypertrophic, increase its production and release of reactive oxidative species and pro-inflammatory cytokines, finally failing to maintain the integrity of the BRB (Carpi-Santos et al. 2022), which ultimately leads to the activation of cell death pathways and retinal damage (Xi et al. 2005; Jiang et al. 2013; Han et al. 2015).

In physiological conditions, astrocytes (but not Müller cells) express glial fibrillary acidic protein (GFAP) in the GCL. During DR, however, Müller cells become gliotic and there is a massive GFAP upregulation, which is why this protein is an excellent marker of reactive gliosis in the retina (Chang et al. 2007). In addition, activated Müller cells secrete pro-inflammatory cytokines, which in turn activate the innate immune response and feed this loop of neuroinflammation (Coughlin, Feenstra, and Mohr 2017).

Several pro-inflammatory molecules like interleukin-1 $\beta$  (IL-1 $\beta$ ) and tumor necrosis factor  $\alpha$  (TNF- $\alpha$ ) participate in this loop, but interestingly there are multiple neurotrophic factors and proteins involved in endothelial regulation that feed this pro-inflammatory loop (Koleva-Georgieva, Sivkova, and Terzieva 2011; Y. Liu, Costa, and Gerhardinger 2012). Endothelin



dysregulation has been implicated in multiple disorders, including diabetes and DR (Sorrentino et al. 2018). Over the past years a number of potential markers for DR have been evaluated, and endothelin-2 (Edn2) has gained growing importance, as hyperglycaemia in DR results in increase of Edn2 presence in serum concentration (Binz et al. 2016; Rattner, A.; Nathans 2005). Interestingly, Edn2 has been linked to photoreceptor survival. After acute stress, photoreceptors express Edn2 as a pro-survival signal, which exerts its function through its receptor endothelin receptor type B (EDNRB), expressed in Müller glia. Müller glia, in return response, becomes activated and gliotic, but also secretes neuronal growth factors that provide support for photoreceptors, such as fibroblast growth factor 2 (FGF2) (Bramall et al. 2013; S. Joly et al. 2008), which stimulates photoreceptor survival via ERK1/2 activation (Kinkl, Sahel, and Hicks 2001).

- **The role of photoreceptors in DR pathophysiology**

Even though photoreceptors have been massively overlooked in DR research, accumulating evidence over the last years is linking photoreceptors in the pathogenesis of early stages of DR (**Figure 16**).

Interestingly, in a survey it was stated that the DR from patients that also suffered from retinitis pigmentosa (RP), a disease characterised by photoreceptor cell death, was less severe than those with only DR (Arden, Wolf, and Tsang 1998). Moreover, induction of diabetes in mice lacking rhodopsin (and thus, most photoreceptors), did not cause the expected decrease in density of retinal microvasculature (H. Liu et al. 2016).

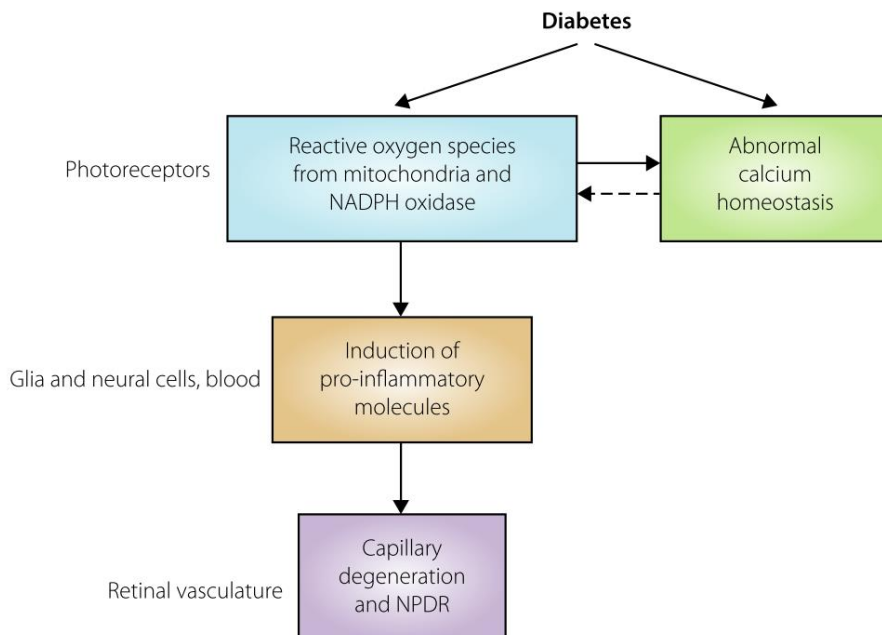


**Figure 16.** Postulated mechanism by which retinal photoreceptors contribute to the development of common vascular lesions in early DR, from (Kern and Berkowitz 2015)

All this data suggests that photoreceptors may be involved in the severity of vascular degeneration of DR (Kern and Berkowitz 2015). Different hypothesis that can cohabit have been stated that explain the deleterious effect of photoreceptors in DR: oxidative stress and hypoxia.

Photoreceptors are the most abundant cells in the retina, and these post-mitotic cells display a high metabolic rate, using more oxygen than any other cell type in the retina and the body. This makes them especially vulnerable to oxidative stress (Berkowitz et al. 2018), leading to the release of Müller cell-activating proteins like Edn2 that feed DR pro-inflammatory loop (Du et al. 2013). Additionally, multiple reports have stated that photoreceptors are the major producers of superoxide and other reactive oxygen species in the retina (Du et al. 2013). Oxidative stress is crucial for this disease, as it has been

proven that its inhibition prevents inflammation and subsequent vascular lesions of early DR. (Kowluru, Zhong, and Kanwar 2010; L and TS 2009).

Moreover, in the presence of a compromised vasculature such as that in DR, the same photoreceptor activity and high metabolic demand can make the retina more hypoxic than normal, contributing to its deterioration (**Figure 16**).

Given these considerations, photoreceptors arise as key contributors of the development of DR's pathology along with glial cells, which also have a crucial role DR prevention.

#### **1.1.4.2. Dark adaptation delay in night blindness**

Night blindness is a symptom that is presented in retinal disorders in which patients suffer from loss of night vision (nyctalopia). It is often associated with an inability to quickly dark-adapt when coming from a well-illuminated to a poorly illuminated environment.

There are multiple hereditary and environmental retinal diseases that present night blindness among other alterations, like retinitis pigmentosa (Athanasidou et al. 2018; Singhal et al. 2013), diabetic retinopathy (Shukla and Tripathy 2022), glaucoma (Orlowski, Harmening, and Wagner 2012) and vitamin A deficiency (Saari 2012; Clifford, Turnbull, and Denning 2013; Duignan et al. 2015), but there are also specific retinal diseases in which their main symptom is nyctalopia, like congenital stationary night blindness (CSNB) (Zeit 2007; Fuente García et al. 2018; Singhal et al. 2013) and Oguchi disease (Fuchs et al. 1995; Aryan et al. 2020; Zeit, Robson, and Audo 2015). Depending on the origin of the disease, night blindness is avoidable and even curable.

CSNB is a group of genetically and clinically heterogeneous retinal disorders that lead to night blindness. Aside from poor night vision, CSNB patients often complain of photophobia, and some forms may be associated with poor visual acuity, myopia, nystagmus, strabismus and fundus abnormalities (Zeitz 2007). It has been linked to at least 17 different genes that account for 360 mutations (Zeitz, Robson, and Audo 2015). These mutations mainly affect the signal processing of photoreceptors, retinoic recycling, the RPE or signal transmission via retinal bipolar cells (Zeitz 2007).

Depending on fundus results, CSNB can be classified into the following categories (Zeitz, Robson, and Audo 2015; L. Kim 2019):

➤ **Normal fundus:**

- **Riggs type**: associated with photoreceptor dysfunction, selective loss of rod function. The dim flash scotopic electroretinogram (ERG) is flat, whereas the strong flash scotopic ERG shows a decreased a- and b-wave. Photopic ERG remains normal.
- **Schubert-Bornstein type**: associated with bipolar cell dysfunction. It demonstrates normal a-wave and abnormal b-wave. Photopic ERG remains normal.

➤ **Abnormal fundus:**

- **Fundus albipunctatus and Oguchi disease**: similar full-field ERG as Riggs type, but with abnormal fundus. With prolonged dark adaptation, scotopic ERG normalizes.
  - **Fundus albipunctatus**: caused by mutations in 11-cis retinol dehydrogenase, found in the RPE and crucial to produce 11-cis-retinal.

- **Oguchi disease: caused by mutations in Grk1 and s-arrestin (SAG) genes.**

Depending on inheritance types, it can be subdivided into the following categories:

- **X-linked CSNB (xlCSNB), which can be subdivided into complete (CSNB1) and incomplete (CSNB2) (MacDonald, Hoang, and Tuupanen 2019)**
- **Autosomal recessive CSNB (arCSNB)**
- **Autosomal dominant CSNB (adCSNB)**

Common CSNB-causing mutations are linked to Rhodopsin, G Protein subunit alpha Transducin- $\alpha$  1 (GNAT1) and PDE6 subunit B (PDE6B) (Singhal et al. 2013).

Oguchi disease is a rare form of arCSNB with abnormal fundus, and it is associated to mutations in SAG and GRK1 (Fuchs et al. 1995; Yamamoto et al. 1997).

As seen above, Arrestin-1 and GRK1 (which are encoded by SAG and GRK1 genes, respectively), are crucial for photoresponse termination. Signal amplification after photon absorption persists as long as R\* remains active, hence, if this process is delayed, photoresponse is greatly prolonged and rods are incapable of proper dark adaptation, leading to night blindness. In this disorder, rods incorrectly behave as if they were light adapted and are unable to respond to light in low levels of illumination (Miyake and Shinoda 2012).

Aside from hereditary causes, night blindness is often associated to vitamin A deficiency, which is frequent in developing countries, but also found in psychiatric patients with conditions like autism, food phobia and anorexia

nervosa (Duignan et al. 2015; Velasco Cruz et al. 2005; Cooney, Johnson, and Elner 2007). 11-cis-retinal, the molecule in charge of absorbing photons in rhodopsin, is derived from vitamin A. In the dark, 11-cis-retinal is bound to opsin and makes the retinal pigment sensitive to low-intensity light. After light exposure, 11-cis-retinal is converted to all-trans-retinal and rhodopsin is recycled. If the body lacks vitamin A, the ability to see in the dark decreases, leading to night blindness (Saari 2012). As the cause of this type of night blindness is vitamin A deficiency, this disorder is reversible and can be treated with vitamin A supplements (Duignan et al. 2015; Clifford, Turnbull, and Denning 2013).

Night blindness, however, is often just a symptom of a much serious disease. For instance, retinitis pigmentosa (RP) is characterised by selective rod photoreceptor cell death, causing elevated dark adaptation thresholds that severely impact night vision, leading to nyctalopia (Kalloniatis and Fletcher 2004). Consequently, research centred in the mechanisms that cause alterations in photoresponse termination and dark adaptation is needed in order to address these disorders.

#### **1.1.4.3. Protein misfolding and retinal cell death in retinitis pigmentosa**

After glaucoma, RP is the most common form of retinal pathologies associated to visual loss in Spain (Instituto Nacional de Estadística, EDAD-2008), and the most common disease of inherited retinal dystrophies, affecting more than 1.5 million patients worldwide, with an incidence of 1 in 3000 people (O'Neal and Luther 2021). RP is the most common cause of inherited blindness, and it is characterised by the progressive neurodegeneration of photoreceptor cells (Kalloniatis and Fletcher 2004; Wright et al. 2010). As mentioned in the previous section, due to rod

photoreceptor death RP initially presents with night blindness (Singhal et al. 2013), but the disease progresses to further degeneration of photoreceptors with a more severe phenotype.

At least 150 genes have been linked to this disease, but mutations in rhodopsin, b subunit of cGMP, PDE6 and peripherin-2 are especially relevant (Athanasίου et al. 2018; Boon et al. 2008; Parmeggiani et al. 2011). There are several mechanisms by which these mutations can result in cell death, such as oxidative stress, cGMP and  $\text{Ca}^{+2}$  influx dysregulation and ER stress (Newton and Megaw 2020).

Rhodopsin mutations that affect the amino acidic sequence are responsible for autosomal dominant retinitis pigmentosa (ADRP), and account for at least 30% of this form of RP (Iannaccone et al. 2006). Rhodopsin misfolding is one of the main causes of endoplasmic reticulum (ER) stress in RP, a hallmark of the disease (Chan et al. 2016; McLaughlin et al. 2022). This is easily understandable, given that rhodopsin accounts for approximately 30% of the entire proteome of photoreceptors, and comprises 90% of the OS.

The OS renewal in photoreceptor is constant. It requires a great metabolic activity, and thus a high level of performance in protein synthesis, folding and protein trafficking is of utmost importance. If this process is disrupted by the accumulation of misfolded rhodopsin, it can trigger the unfolded-protein response (UPR), a cellular stress response (Smith and Mallucci 2016; Lenox et al. 2015), which under excessive damage can lead to cell death. For instance, P23H mutation (the most common RP-mutation in American patients) causes rhodopsin to be extremely predisposed to aggregation, becoming a target for degradation by the ubiquitin proteasome system (UPS), suggesting that UPS impairment has a greater role in the development of RP

pathophysiology than thought before (Campello et al. 2013; Illing et al. 2002).

Ultimately, the consequences on the correct folding and misfolding of proteins in photoreceptors are critical, as the UPR and UPS dysfunction can trigger apoptotic cell death if ER stress is not alleviated (S. X. Zhang et al. 2014).

## 1.2. Apoptosis and apoptotic modulators

Programmed cell death (PCD) is an evolutionary conserved mechanism in multicellular organisms. In the nervous system, apoptosis sculpts the developing brain and is essential for tissue homeostasis (Yuan and Yankner 2000). Nonetheless, apoptosis is a crucial feature of both acute CNS injury such as trauma, spinal chord injury, acute retinal ischemia; and chronic neurodegenerative diseases like Alzheimer's, Parkinson's and Huntington's disease in the brain and AMD and DR in the retina (Ekshyyan and Aw 2004; Kermer et al. 2004).

Apoptosis is characterized and distinguished from other forms of PCD by a series of specific signaling and morphological changes like cell shrinkage, chromatin condensation, DNA fragmentation and the formation of apoptotic bodies and blebbing (X. M. Hu et al. 2021; Henriquez et al. 2008; Neel et al. 2022); and it can be induced by the extrinsic pathway or the intrinsic pathway ( **Figure 17**). The extrinsic pathway is caused by inadequate conditions in the extracellular environment, which activate death receptors (DR). The intrinsic pathway of apoptosis responds to an intracellular stress and involves the mitochondria, which originates the signals that initiate the activation of caspase signaling (Elmore 2007).



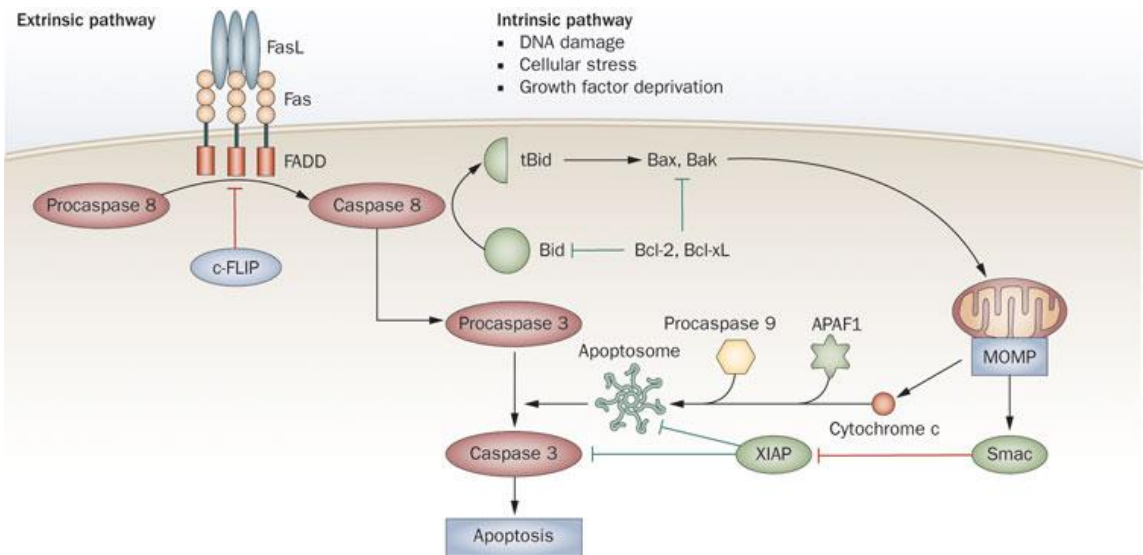


**Figure 17.** Extrinsic (left) and intrinsic (right) apoptosis mechanism, both converging in the activation of pro-caspase-3 to caspase-3, the effector caspase of apoptosis. Figure from (Ramaswamy, Deng, and Siegel 2011).

At the molecular level, apoptosis is regulated by the activation of the caspases cascade (Yuan and Yankner 2000; Taylor, Cullen, and Martin 2008). There are two types of caspases: initiator and effector. Initiator caspases contain a death-effector domain that interacts with the intracellular domains of DR like  $\text{TNF}\alpha$  and Fas receptors (Schulze-Osthoff et al. 1998; A. Yamada et al. 2017; Kaufmann, Strasser, and Jost 2011). As a result of this, caspase initiators aggregate and activate, which in turn activates the effector caspases through a specific cleavage. Immediately after, effector caspases will carry out the massive proteolysis that will lead to cell disassembly during apoptosis.

However, caspases are not only involved in apoptosis, but they can also act on non-apoptotic events when their levels are finely regulated, such as in plasticity modulation processes (Nakajima and Kuranaga 2017). In the nervous system, restricted and localized caspase activation allows for pivotal

processes in neuronal development and differentiation and essential mechanisms in synaptic processing, neurite growth and rearrangement. During apoptosis, caspases orchestrate a massive proteolysis that leads to cell death. Hence, if caspase activity is finely modulated and spatially controlled within the cell, it can be organelle-specific, which allows for terminal differentiation of some vertebrate cell types (Dehkordi, Munn, and Fearnhead 2022).

In view of its multiple functionalities, activation of caspases is tightly regulated. The enzymatic activity of caspases can be physiologically inhibited by endogenous Inhibitors of apoptosis (IAPs), an evolutionary conserved family of proteins. They are able to block effector caspases activity thanks to its binding affinity (Hunter, LaCasse, and Korneluk 2007; Holcik 2002).

IAPs active domain is the baculoviral IAP repeat (BIR) that contains roughly 80 amino acids folded around a zinc atom (H. Shin et al. 2005; Cossu et al. 2019). For instance, three members of IAPs family such as X-linked IAP (XIAP), cellular IAP1 (c-IAP1) and 2 (c-IAP2) are comprised by three BIR domains each. The third BIR domain (BIR3) selectively targets active initiator caspase-9, while the linker region between BIR1 and BIR2 inhibits effector caspase-3 and -7. As a result, XIAP, c-IAP1 and c-IAP2 inhibit both initiator caspase-9 and effector caspase-3 and -7 (Holcik 2002) (**Figure 18**).

### **1.2.1. XIAP**

XIAP is one of the most powerful and therefore studied endogenous caspase inhibitors. Aside from the three BIR domains, it contains a UBA, a ubiquitin binding domain (UBD) and a RING domain that functions as an E3 ubiquitin ligase (Tse et al. 2011).

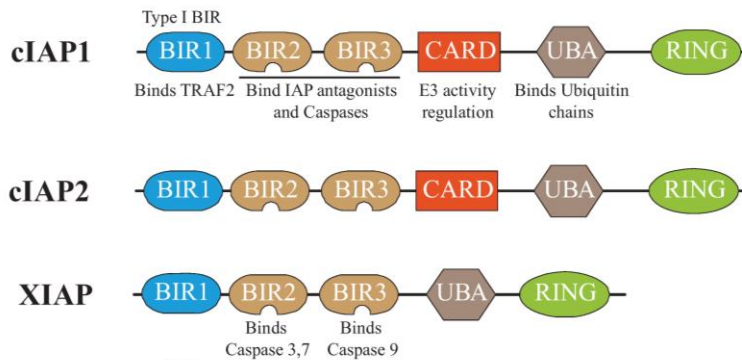


**Figure 18** Mammalian forms of IAP family proteins cIAP1, cIAP2 and XIAP, with their different domains associated to their functions. Figure adapted from (Berthelet and Dubrez 2013).

Through its RING domain, XIAP ubiquitinates a broad selection of substrates, hence interfering with many cellular activities (Tse et al. 2011). XIAP participates in many mechanisms beyond apoptosis, such as morphogenesis, cell maturation and differentiation, and neurite outgrowth (Arroba et al. 2007; Martínez-Mármol et al. 2016). Moreover, the role of XIAP in cell signalling through its E3 ubiquitin ligase activity has been largely studied. However, it has eluded to be placed in a specific receptor-initiated signalling, which would be the case for c-IAPs in TNF receptor (TNFR) signalling (Galbán and Duckett 2010; Weissman, Shabek, and Ciechanover 2011).

XIAP can be degraded through the UPS, and strikingly, is capable of autoubiquitination through its RING domain. In mammalian cells, c-IAP1 and XIAP are autoubiquitinated and degraded after induction of apoptosis in thymocytes by glucocorticoids or etoposide (Weissman, Shabek, and Ciechanover 2011), suggesting self-ubiquitination and subsequent degradation of XIAP may also be an important event in apoptosis.

As a result, XIAP needs a tight regulation, as ubiquitin-protein ligases are not exempt from UPS and its protein fate. Some time ago, our group described that the long form of Fas Apoptotic Inhibitory Molecule (FAIM-L) is able to block XIAP autoubiquitination and degradation by UPS, thus preventing caspases activation.

### 1.2.2. FAIM

In humans, the FAIM1 gene contains six exons and three putative translational start sites. FAIM1 is located in the long arm of chromosome 3 (3q22.3), and while it encodes for four different isoforms by alternative splicing (Coccia et al. 2017), it only generates two protein products: FAIM-short (FAIM-S) and FAIM-long (FAIM-L) (T. J. Schneider et al. 1999) (**Figure 19**). In mice, the *Faim* gene is located in chromosome 9 (chr9f1) and there are two known splice variants that also produce FAIM-S and FAIM-L proteins (Zhong et al. 2001).

As far as we know, neither isoform possess any characterized domain related to cell death functions (such as death domains that are common in other DR antagonists) or any recognizable effector binding motif (T. J. Schneider et al. 1999), but they both hold anti-apoptotic functions.

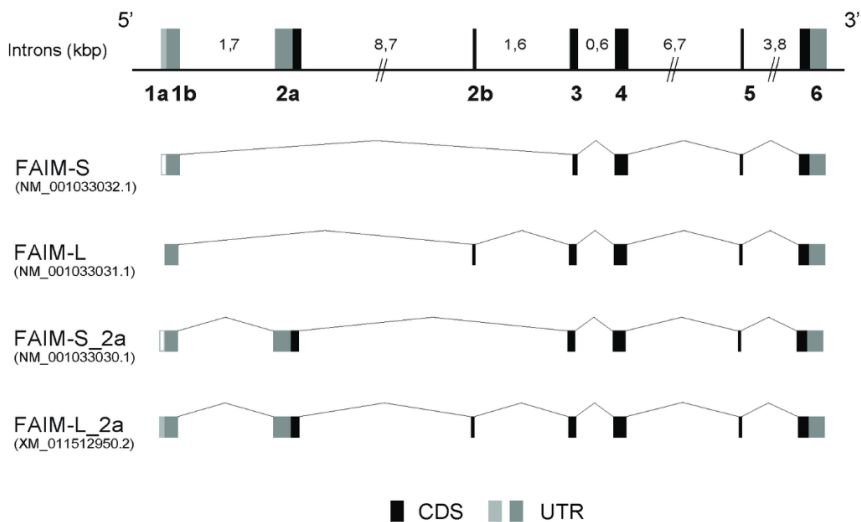


**Figure 19** Genomic representation of *FAIM* isoforms in human. From top to bottom: *FAIM-S*, *FAIM-L*, *FAIM-S\_2a*, *FAIM-L\_2a* Figure from (Coccia et al. 2017).

### 1.2.2.1. FAIM-S

FAIM-S is ubiquitously expressed throughout the organism and is highly conserved throughout evolution. It was first described as an anti-apoptotic protein in B lymphocytes (T. J. Schneider et al. 1999). Afterwards, FAIM-S was found to also inhibit apoptosis in thymocytes and hepatocytes, aside from B lymphocytes (J Huo et al. 2009).

In extrinsic apoptosis, binding of FasL to Fas triggers the trimerization of Fas and the formation of the downstream death-inducing signalling complex (DISC), which always contains Fas associated via Death Domain (FADD), a cytosolic adapter, and pro-caspase-8. Pro-caspase-8 recruitment to the DISC leads to its-self activation and autocleavage, and mature caspase-8 cleaves caspase-3, which executes apoptosis (Ashkenazi and Dixit 1998). Overexpression of FAIM-S confers protection to Fas-induced cell death (T. J. Schneider et al. 1999), and there is an increased sensitivity to Fas-triggered apoptosis in FAIM-deficient B cells (J Huo et al. 2009), where the amount of caspase-8 bound to Fas was increased upon activation of Fas. This suggests that FAIM blocks caspase-8 interaction with FADD, thus hindering the trigger of the apoptotic cascade.

Nonetheless, our group has described how these anti-apoptotic functions do not trespass to the brain. FAIM-S does not confer protection to neurons against apoptosis but holds other significant functions. In neuronal models, FAIM-S is involved in NGF-induced neurite outgrowth in an ERK- and NFkB-dependent manner (Segura et al. 2007).

NGF induces neurite outgrowth and neuronal survival in peripheral nervous systems, and it promotes the differentiation of PC12 cell line to neuron-like cells with neurite abilities (K. P. Das, Freudenrich, and Mundy 2004; R. Hu et al. 2018). When FAIM-S is overexpressed in NGF-stimulated PC12 cells, it significantly enhances neurite outgrowth. Moreover, when FAIM-S is depleted from PC12, neurite outgrowth is decreased (Segura et al. 2007).

Dr. Rothstein's group in Michigan also asserted a new FAIM-S role. In FAIM-deficient cell lines there was increased sensibility to heat and oxidative stress-induced cell death when compared to non-modified conditions. They also found that FAIM is recruited to aggregates of ubiquitinated proteins after cellular stress induction (Hiroaki Kaku and Rothstein 2020).

Interestingly, they also recently reported that both recombinant human FAIM-S and FAIM-L disaggregate and solubilize A $\beta$  fibrils in the human neuronal cell line Neuro 2A (Hiroaki Kaku et al. 2021).

#### **1.2.2.2. FAIM-L**

While FAIM-S is ubiquitously expressed throughout the organisms, FAIM-L is almost exclusively expressed in neurons (Zhong et al. 2001; Segura et al. 2007). This high tissue-specificity stems from the fact that FAIM-L alternative splicing is accomplished by nSR100, a neuron-specific splicing factor (Coccia et al. 2017).

Our group has described how both in *in vivo* and *in vitro* neuronal models, FAIM-L transcription is regulated during neuronal differentiation. In mouse brains, FAIM-L levels are relatively low at E12, with a moderate increase at E15 and a peak of expression at E18. Afterwards, FAIM-L levels are

stabilized in early postnatal stages and in adult tissue. It was also determined that FAIM-L expression levels are regulated via the MAPK/ERK signalling pathways after NGF stimulation *in vitro* (Segura et al. 2007).

FAIM-L does possess anti-apoptotic properties in the nervous system. It inhibits Fas-triggered apoptosis by two different mechanisms. Similarly to FAIM-S in non-neuronal tissues, FAIM-L binds to non-stimulated Fas receptor, blocking the recruitment of caspase-8 to the DISC complex (Segura et al. 2007). In addition, FAIM-L (but not FAIM-S) directly interacts with XIAP through the latter's BIR2 domain, hampering its auto-ubiquitination and its consequent degradation via the UPS

As a result, FAIM-L is able to maintain XIAP protein levels, conferring it the ability to inhibit effector caspases and to promote neuronal survival (Moubarak et al. 2013) (**Figure 20**).

Moreover, through regulating levels of XIAP, FAIM-L is able to inhibit the non-apoptotic functions of caspases, such as long-term synaptic depression (LTD) and neurite pruning. Thus, FAIM-L is not only a regulator in neuronal cell death but is also a crucial player for neuronal processes and physiology.

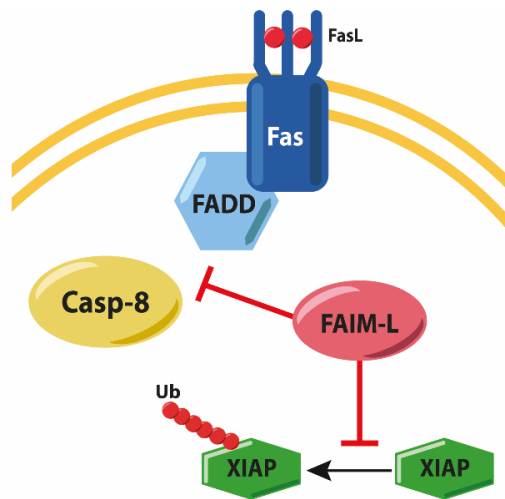


**Figure 20.** FAIM-L antiapoptotic functions: it blocks the interaction between FADD and caspase-8, hence hampering its activation, and blocks XIAP autoubiquitination, allowing it to inhibit caspase-3.

FAIM-L is also crucial in tipping the balance to the protective role of TNF $\alpha$ . This DR ligand can hold opposite roles in neurodegenerative disorders like Alzheimer's disease depending on its context (Micheau and Tschopp 2003). Under certain circumstances, TNF $\alpha$  can confer protection against amyloid beta (A $\beta$ )-induced cell death or be deleterious with its pro-inflammatory properties. Our group has shown how the ability of TNF $\alpha$  to protect neurons against A $\beta$  is lost when FAIM-L levels are reduced *in vitro* in neuronal models (P Carriba et al. 2015; Paulina Carriba and Comella 2014).

FAIM-L has also been involved in the pathophysiology of Alzheimer's disease. Remarkably, there is a decreasing reduction of its protein levels in the hippocampi of patients with Alzheimer's Disease throughout the BRAAK stages, and in an APP/PS1 mouse model of the disease (Blanchard et al. 2003) there is also a reduction in the entorhinal and hippocampal cortex before the onset of neurodegeneration (P Carriba et al. 2015).

As previously mentioned, Kaku and colleagues also showed how, along with FAIM-S, FAIM-L was able to disaggregate and solubilize already established A $\beta$  fibrils in a neuronal cell line. Along with these results, it is possible that the previous results of this group in which they reported that FAIM-S is recruited to aggregates of ubiquitinated proteins after cellular stress could be extrapolated to FAIM-L, nonetheless these experiments were only conducted having in mind the shorter isoform (Hiroaki Kaku and Rothstein 2020).

Altogether, these results support the notion that FAIM-L could contribute to the pathophysiology of Alzheimer's disease through plasticity modulation, regulating the deleterious effect of TNF $\alpha$  in neuronal cells and inhibiting apoptosis via the inhibition of XIAP degradation.



### 1.2.2.3.Faim knockout mouse models

To the best of our knowledge, there are currently two Faim knockout mouse models of both isoforms. The first one was generated by Dr. Lam's group in Singapore in 2009 (J Huo et al. 2009). After obtaining a phage clone of the cDNA for murine *faim*, a targeting vector was designed to replace the first two exons of *faim* with a neomycin-resistant gene. To generate germline transmitted chimeras, the targeting vector was transfected into E14.1 embryonic stem cells, and a homologous recombinant was injected into C57BL/6J blastocysts. These mice were raised in a mixed C57BL/6J and 129 genetic backgrounds.

Authors reported that these Faim KO mice suffer from metabolic diseases like non-hyperphagic obesity and hepatosteatosis, hyperinsulinemia, adipocyte hypertrophy, dyslipidaemia, and hyperglycaemia. They also reported that in Faim KO livers, lipogenesis was elevated. These results led them to hypothesize that FAIM could be a novel regulator of insulin signalling. The aforementioned roles of FAIM in this KO model cannot be officially attributed to either isoform because this was not specified in these studies. Nonetheless, due to the expression pattern of both isoforms it is hypothesized that these reports are linked to FAIM-S and not FAIM-L.

In 2020, Dr. Rothstein and Dr. Kaku developed another Faim KO mice (Hiroaki Kaku and Rothstein 2020). Some discrepancies were found between their model and Dr. Lam's, as they did not report any obesity in their mice. On the other hand, they found vulnerability to oxidative stress induced by menadione and arsenite in skin-derived fibroblasts. Interestingly, they also demonstrated that in liver and spleen samples from FAIM KO mice there is an accumulation of ubiquitinated protein aggregates after inducing oxidative

stress through intraperitoneal injection of menadione (vitamin K3) (Hiroaki Kaku and Rothstein 2020).

Since our group was interested in finding the neural phenotype in Faim KO mice, mainly corresponding to FAIM-L deficiency, Dr. Lam kindly provided their transgenic mice. The mouse colony was bred homozygously, and C57BL6/J OlaHsd WT mice were bought and bred separately. Surprisingly, in our hands we observed that Faim KO mice developed age-dependent seizures. However, when our group started to crossbreed Faim KO mice with C57BL/6j OlaHsd mice and maintain the colony in heterozygosity, the epileptic phenotype was completely lost. This could be due to the original strain that was used to generate these Faim KO mice, or the effect of flanking genes. Precisely, a review was published in 2011 discussing the effects of genetic background strain on epilepsy phenotypes of mice (Schauwecker 2011), and has been extensively discussed recently (Matamoros i Anglès 2019; Matamoros-Angles et al. 2022).

It is worth pointing out that the research on the present thesis was carried out using Dr. Lam's Faim KO mice, which we crossbred and maintained in heterozygosity in the C57BL/6J OlaHsd background. No epileptogenic phenotype was observed in the Faim KO mice that we used for this study and bred in these conditions.

These knockout mice are lacking the expression of the *faim* gene, meaning that are defective for both FAIM-S and FAIM-L. To study the specific role of a FAIM-L deficiency, our group has recently generated a knockout mouse model of the *FAIM-L* isoform using CRISPR-Cas9 technology. This will allow us in the future to differentiate whether FAIM-S and/or FAIM-L are

implicated in the specific phenotypes that have been reported in the nervous system and ascertain its specific role.

Remarkably, there are no reports of FAIM in other neuronal tissues such as the retina, and this was a crucial turning point for the present thesis.

### 1.3.Ubiquitin

Ubiquitin is a highly conserved and expressed peptide of 76 amino acid that has a crucial role in protein regulation (Nath and Shadan 2009). It is covalently conjugated to cellular proteins to achieve multiple and very diverse goals, such as protein degradation, protein trafficking and signal transduction (**Figure 21**) (Mukhopadhyay and Riezman 2007).

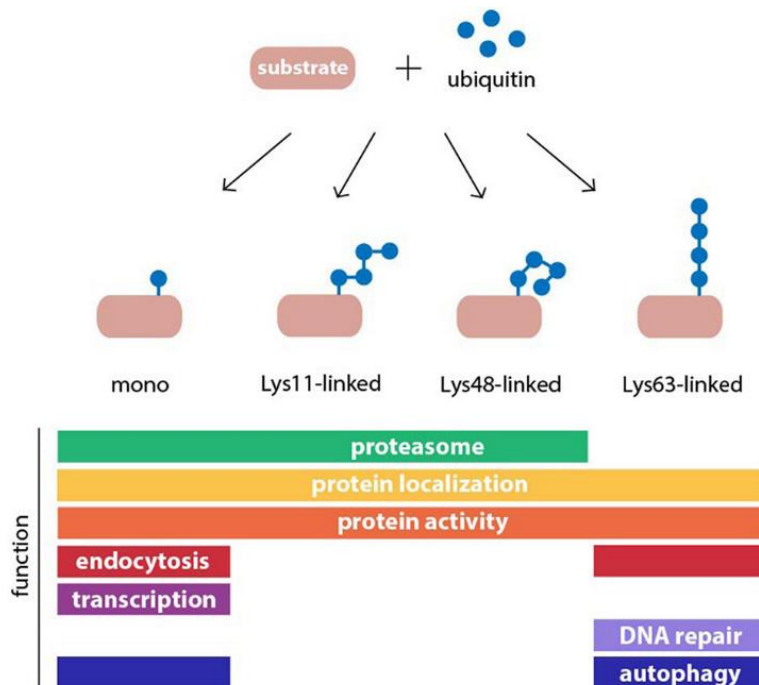


**Figure 21.** Different types of ubiquitination. Ubiquitin ligases can transfer a single ubiquitin to its target (mono) but can also elongate the ubiquitin chain through Lys residues within ubiquitin. Depending on the Lys residue, ubiquitin chains ultimately hold different roles. Figure from (Dantuma and Bott 2014)

The process in which ubiquitin is conjugated to its target proteins is called ubiquitination. This post-translational modification is catalysed by the activity of three enzymes that act sequentially: ubiquitin-activating enzyme (E1), ubiquitin-conjugating enzyme (E2), and ubiquitin ligase (E3) (Zheng and Shabek 2017). E3 ligases mainly transfer ubiquitin to lysin residues, but serine, threonine or cysteine residues can be also substrates (Zheng and Shabek 2017; Q. Yang et al. 2021).

After ATP-activation, E1 transfers ubiquitin to E2, which with the aid of substrate-specific E3 enzymes, covalently attaches ubiquitin to its target (**Figure 22**) (Hicke, Schubert, and Hill 2005). To date, eight known E1 or E1-like enzymes have been found (the two major ones being UBE1 and UBA6) (Groettrup et al. 2008), alongside ~40 E2 conjugating enzymes (Stewart et al. 2016) and at least 600 E3 ligases (Q. Yang et al. 2021), and similar numbers are found on mice (Semple et al. 2003). The obvious difference in the number of ubiquitin enzyme types is due to the high substrate affinity of E3 ligases and the versatility of E1 and E2 enzymes.

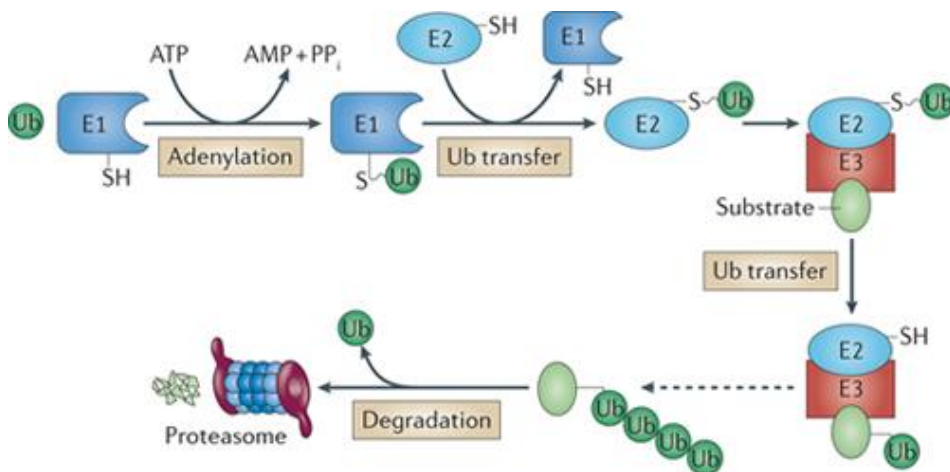


**Figure 22.** Ubiquitin transfer process from ubiquitin-activating enzymes (E1) to ubiquitin-conjugating enzymes (E2), to ubiquitin ligases (E3). After the target protein is ubiquitinated, it becomes degraded by the proteasome. Figure from (Maupin-Furlow 2011)

Long considered as a simple mediator, E2 is not a simple carrier of ubiquitin. Despite its relatively small size (only twice the ubiquitin size), this enzyme performs a great deal of roles. Among others, E2 enzymes primarily engage in two of the ubiquitination reactions: transthioylation (transfer of ubiquitin from a thioester to a thiol group) and aminolysis (transfer from a thioester to an amino group) (Stewart et al. 2016). Remarkably, E2s only interact with one E1, but with multiple E3 ligases, and most E2/E3 interactions have a weak affinity and cannot be co-purified.

E3 ligases bind to their targets either directly to their domains/surfaces or indirectly via co-factors or multi-subunit complexes that are assembled to the target protein. Then, they catalyse the formation of an isopeptide bond between the ubiquitin carboxyl terminus and a primary amino group of an acceptor (Hicke, Schubert, and Hill 2005; Dikic, Wakatsuki, and Walters 2009). In its simplest form, a single ubiquitin will be attached to a single residue (monoubiquitination), but multiple lysine residues in the target protein can be ubiquitinated at the same time (multiubiquitination). However, the most common form of ubiquitination is polyubiquitination, where the ubiquitin peptide acts as an acceptor of ubiquitin on account of its seven different lysine residues, allowing for chain elongation (Haglund and Dikic 2005; Dikic, Wakatsuki, and Walters 2009) (**Figure 23**).

As many ubiquitin lysines can serve as acceptors, the type of polyubiquitin linkage dictates the topology of the resulting chain, for instance regulating protein function and acting as signalling for many cellular processes, including development of synaptic connections and synaptic plasticity (Dantuma and Bott 2014; Hegde and Upadhyaya 2007).

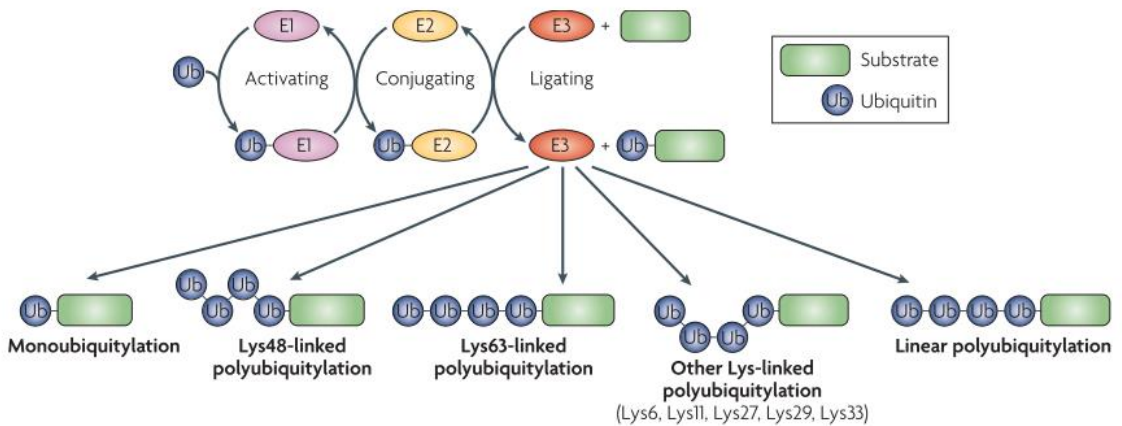


**Figure 23.** Mono and polyubiquitination and chain elongation Figure from (Dikic, Wakatsuki, and Walters 2009)

### 1.3.1. Ubiquitin-proteasome system

The UPS is one of the main cellular mechanisms for protein degradation. This process is highly specific, and it is responsible for the elimination of damaged, misfolded or obsolete proteins in both physiological and pathological environments (Dantuma and Bott 2014; Lecker, Goldberg, and Mitch 2006). The UPS has gained increasing attention and importance in the neurodegenerative field, since it is a critical regulator of protein homeostasis in eukaryotic cells and many disorders pivot around the dysfunction of this system (Ciechanover and Brundin 2003). For instance, the UPS can be triggered by ER stress and the unfolded protein response (UPR) (Flick and Kaiser 2012; Qu, Zou, and Lin 2021). As previously mentioned, the UPR response is activated to alleviate the ER stress and restore its function and E3 ubiquitin ligases can regulate ER stress both in a positive and a negative manner (Qu, Zou, and Lin 2021).

Different combinations of ubiquitin linkage lead to proteasome degradation, such as Lys48-linked ubiquitin (the canonical form) (Dikic, Wakatsuki, and Walters 2009; Manohar et al. 2019), Lys11 and Lys29 (Kravtsova-Ivantsiv and Ciechanover 2012). The 26S proteasome is a multi-protein complex that consists of a 20s core particle and a 19s regulatory particle that is capped at one or both ends. This regulatory particle prepares degradation substrates for passage through a narrow entry, which ultimately end in the catalytic centre of the core particle (Ciechanover and Brundin 2003).

The UPS needs to be highly specific towards its targets, and this is mainly achieved thanks to the high selectivity of E3 ubiquitin ligases and the regulation of deubiquitinating enzymes (DUBs). DUBs are proteases that cleave ubiquitin from another protein by reversing the isopeptide bond. Incidentally, numerous specific DUBs have been found in the retina, and some have emerged as potential candidates for retinal disorders (Esquerdo et al. 2016; Esquerdo-Barragán et al. 2019). They act in multiple functions, but mainly have a role in rescuing proteins from being degraded by the proteasome and recycling ubiquitin molecules and returning them to the intracellular pool (Ristic, Tsou, and Todi 2014) (**Figure 24**).

In recent years it has been demonstrated how ubiquitination is not only involved in protein degradation, but also has functions regarding cell cycle regulation, DNA damage, protein localization, protein interaction, apoptosis, and many others.

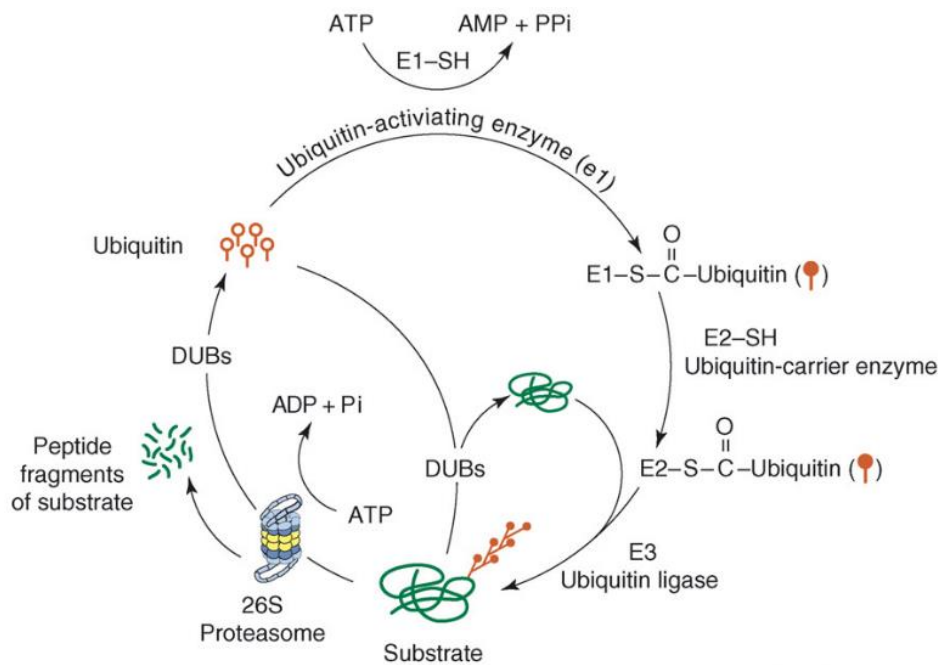


**Figure 24.** Deubiquitinase enzymes mechanism. Figure from (Hegde and Upadhy 2007)

### 1.3.2. Nonproteolytic cellular functions of ubiquitin

While proteasomal degradation is the most studied function of ubiquitin, other roles have emerged. Several proteins are able to noncovalently interact with monoubiquitinated proteins to mediate non-proteasomal functions of ubiquitin (Donaldson et al. 2003) through their UBDs.

#### A. Vesicle trafficking

Over the past years, at least nine different UBDs have been found. In those UBDs in which the dissociation constant ( $K_d$ ) of the ubiquitin interaction has been characterised, the binding goes from moderate to weak (Hicke, Schubert, and Hill 2005). In the human interactome there is a wide range of interactions that are highly specific but have low affinity, like those in vesicle



trafficking to plasma membranes. One plausible explanation for this type of interactions is the need to create a network of unstable interactions that is fluid and can undergo rapid assembly and disassembly (Praefcke et al. 2004).

Ubiquitin can regulate protein transport between membrane compartments by acting as a sorting signal on protein cargo and controlling the activity of trafficking machinery.

## **B. Protein-protein interactions**

Monoubiquitination of a protein influences the ability of a target protein to interact with other proteins, posing ubiquitin as a regulator of protein-protein interactions. There are cellular ubiquitin networks that are formed by the dynamic interactions of ubiquitinated and ubiquitin-binding proteins. Through the different UBDs that have been identified, there is a wide arrange of variety of proteins that interact directly or indirectly with Ub. These allows for weak interactions that might be important in rapid cellular processes, like recruitment of ubiquitinated proteins to early endosomes and protein translocation (Haglund and Dikic 2005).

There are proteins that act as enhancers or competitors for ubiquitin binding. For instance, p47 protein (which is involved in ER reassembly), only binds ubiquitin when it is associated with p97, one of its interacting partners. This is crucial for allowing p47 and p97 to perform their functions like transport of vesicles and homotypic membrane fusion to reassemble the ER and Golgi membrane (Meyer 2002). Moreover, protein interaction can also inhibit ubiquitin binding. Rad23 is involved in nucleotide excision repair and proteasome-dependent proteolysis of certain substrates, and it is a substrate of ubiquitination. When another molecule interacts with the UBD and ubiquitin-associating domains of Rad23, ubiquitin binding is blocked and its

consequent functions on proteasome degradation are hindered (Raasi et al. 2004).

Monoubiquitination is also linked to regulatory roles for the targeted protein, like changes in subcellular localization, conformation, receptor endocytosis and protein interactions (Haglund and Dikic 2005). There is more yet to discover about the cellular regulation of monoubiquitination, but the array of roles that has been associated to this post-translational modification is wide and has been increasing in the recent years.

### **1.3.3. Ubiquitin in the retina**

Although the UPS has been widely studied, the knowledge on its molecular composition and functions on the retina is limited (reviewed in (Campello et al. 2013)). Free ubiquitin is expressed throughout the retina, although more prominently in RGCs and the RPE, but the majority of endogenous ubiquitin is linked to its target proteins.

In the retina, the UPS has also been linked to modulation of the visual cycle. Phosducin is a regulator of Transducin- $\alpha$  that is highly expressed in photoreceptor outer segments. It binds to  $\beta\mu$  subunits of Transducin blocking the signal transmission of activated rhodopsin to Transducin- $\alpha$ , and hence it has a role in the dark and light adaptation process of the retina. Phosducin has also been reported to interact with a 26s proteasome ATPase subunit, suggesting this protein could also be modulated by ubiquitination.

Interestingly, the UPS is involved in the regulation of the phototransduction protein levels in rod outer and inner segments. The protein levels of rhodopsin in the outer segment are maintained in rods by two different processes that involve the shedding of OS tips and their phagocytosis by RPE

cells and by the novo membrane synthesis at the OS base. Hence, adequate dark adaptation and light adaptation is associated to disc-shedding patterns and is linked to the regulation of rhodopsin levels within the OS disks.

Furthermore, there is a great number of E3 ligases that have been found in the retina, but a wide range of their substrates and co-adaptors remain elusive (Campello et al. 2013). Two of the most studied E3 ligases in the retina are Parkin and Mdm2. Arrestin-1 interacts with both, which have been reported to modulate the ubiquitination of arrestin-1. (Xiufeng Song et al. 2006). Sadly, the functional properties of Arrestin-1 interactions and ubiquitination have not been fully characterised, as they have in nonvisual arrestins. Although ubiquitination of nonvisual arrestins has reported to enhance its affinity for receptors, to our best knowledge this process has not been studied in the retina (Kommaddi and Shenoy 2013).

Aside from this, the retina contains a complex formed by an E3 enzyme named cullin 3 (Cul3) Kelch-like 18 (Klh18) and its substrate-specific adaptors in rod photoreceptors. Interestingly, this complex has been shown to be important for dark adaptation (Campello et al. 2013). Cul3-Klh18 modulates rod Transducin- $\alpha$  translocation during light and dark adaptation through its interaction with uncoordinated 119 protein (UNC119), also known as Retina Gene 4 protein (RG4). This result was obtained through observing Transducin- $\alpha$  mislocalization from the outer segment to the inner segment in two different mouse models, a Klh18 KO mice, and a transgenic mice that overexpresses UNC119. As explained before, light and dark-dependent translocation of Transducin- $\alpha$  is known to modulate photosensitivity in rod photoreceptors, suggesting ubiquitination has a role in light and dark adaptation in the retina.

Considering these very diverse but also missing pieces of information, one can infer that the research on this topic has been relatively unstudied. The role of ubiquitin in the retina, aside from protein degradation, is very complex and offers multiple research possibilities, spanning from phototransduction modulation to translocation of retinal proteins.



# Hypothesis and Aims

*“Science makes people reach selflessly for truth and objectivity; it teaches people to accept reality, with wonder and admiration, not to mention the deep awe and joy that the natural order of things brings to the true scientist”*

Lise Meitner (1878-1968)



## Hypothesis and Aims

The two different isoforms of Fas Apoptotic Inhibitory Molecule, FAIM-S and FAIM-L, hold important roles throughout the organism (carried by FAIM-S) and the CNS (carried by FAIM-S and FAIM-L). In neurons, FAIM-S is involved in neuritogenesis, while FAIM-L acts as an anti-apoptotic regulator. Aside from their unique roles in neurons, both FAIM-S and FAIM-L have been reported to block ubiquitination and to prevent and dissolve protein aggregates, such as amyloid- $\beta$ , *in vitro*. Remarkably, FAIM-L role has been specifically linked to neurodegeneration in Alzheimer's disease, in which FAIM-L protein levels are decreased before the onset of neurodegenerative events.

Unexpectedly, preliminary reports showed how FAIM expression is greatly and particularly enriched in the retina among other neuronal tissues, including the brain, suggesting an important implication in this tissue. Hereby, **we hypothesized that the absence of FAIM in the retinas could be detrimental to this tissue and lead to a neurodegenerative phenotype.**

Hence, the **MAIN AIM** of this thesis was **to explore the consequences of a FAIM deficiency in the retina and to unveil new roles of FAIM linked to the retinal tissue.**

### **SPECIFIC AIMS:**

- i. To explore potential retinal alterations and neurodegenerative events due to lack of FAIM in a FAIM KO mouse model**, since FAIM has been reported to have a role in neurodegeneration and to be greatly enriched in the retina.



- ii. **To study a possible disruption in ubiquitinating events in the absence of FAIM**, since both FAIM isoforms are reported to block ubiquitination.
- iii. **To assess retinal functional activity in response to light in the absence of FAIM** by studying the specific electrical responses of photoreceptors, bipolar and retinal ganglion cells *in vivo*.
- iv. **To explore the involvement of FAIM in phototransduction at the molecular level**, given that *in silico* preliminary data suggested that FAIM was heavily associated to retinal-specific function like phototransduction.
- v. **To study whether the absence of FAIM renders the retina more sensible to light damage**, a stress that specifically damages the retina and causes neurodegeneration.

# Materials and Methods

*“The way you do science should have an  
intrinsic beauty to it”*

Elizabeth Blackburn (1948)



# Materials and methods

## 2.1. *In vivo* animal procedures

### 2.1.1. Animal care

All experimental procedures were conducted in compliance with European Union Council directives (2010/63/EU) and with the Spanish legislation for the use of laboratory animals (BOE 34/11370-421, 2013). Protocols were approved by the Ethics Committee for Animal Experimentation of the Vall d'Hebron Research Institute (VHIR) (CEEA 07/23 and 20/15) and Generalitat de Catalunya (DARP 11769 and 8594).

Homozygous Faim knockout (*Faim*<sup>-/-</sup> or Faim KO) mice were kindly provided by Dr. Lam (J Huo et al. 2009) and crossbred with C57BL/6J OlaHsd wild-type mice (WT) (Envigo, France) (IMSR Cat# JAX:000664) for at least 10 generations before using them, and no epileptic phenotype was observed.

Heterozygous mice were used to breed Faim KO mice and WT littermates for experimental procedures. Animals were bred and maintained in the animal facility at VHIR. They were housed in groups of a maximum of five animals per Tecniplast GM-500 cage (36 x 19 x 13.5 cm) under standard laboratory conditions at 22 ± 2°C, under a 12 h light/dark cycle (8 am to 8 pm) and relative humidity of 50-60%. Animals had access to water and food *ad libitum* (Teklad Global 18% Protein Rodent diet, Envigo, France). An equal number of females and males per study group was selected, and at least four animals per genotype were used for each experiment.

Genotypes were confirmed by PCR analysis. A tail snip was used for DNA extraction. The tail sample was digested in alkaline solution with Proteinase

K (0.24 Units/sample) (Qiagen, Hilden, Germany) for 120 min at 55°C. The following primers were used to perform a semiquantitative PCR: FAIM-P1-Fw 5'-GAGACTGAGACAGGAGAAGCC-3'; FAIM-P2-Fw 5'-GCTCTTCAGCAATATC-ACGGG-3' and FAIM-P3-Rev 5'-GCTCAGGTAAAGTGAAGTGCG-3'.

### **2.1.2. Optical tomography coherence**

For optical tomography coherence (OCT) analyses, a Spectralis OCT machine was used (Heidelberg Engineering GmbH ©, Germany). Mice were anesthetized intraperitoneally with a mixture of ketamine (37 mg/kg) (Ketolar® 50mg/mL, Pfizer, Madrid, Spain) and xylazine (10 mg/kg), and the eye pupils were dilated with atropine 1% (Colircusí®, Novartis Farmacéutica, S.A., Madrid, Spain). After anesthesia, the analysed eye (right eye) was covered with a contact lens, while the non-used eye was humidified with saline teardrops to avoid drying. After the mice were immobilized, the eye bottom was focused (0.5–1.5 optic dioptries) and images were captured with a high-resolution mode in two scanning modalities: radial (six radius per image) and longitudinal. For total retina, INL and ONL thickness, nine longitudinal sections separated by 50 µm were averaged per each mouse.

### **2.1.3. Electroretinography**

Retinal function was assessed by electroretinography (ERG), which measures the electrical activity of the retina in response to a light stimulus. Protocols used were previously described elsewhere (Sánchez-Cruz et al. 2021; Fernández-Sánchez et al. 2012).

Briefly, mice were dark-adapted overnight in their own cages in a separate dark room only illuminated with red light and covered with reflective black

covers. Just before ERG analyses, mice were anesthetized intraperitoneally with a mixture of ketamine (70 mg/kg) and xylazine (10 mg/kg). Mice were placed on a heating pad maintained at 37°C. Corneal surface was protected with a drop of non-irritating ionic conductive solution (contact lens solutions containing sodium chloride and 0.5% methylcellulose). Then, a golden loop electrode was placed over the cornea of the right eye. A needle reference and ground electrodes were inserted into the cheek and subcutaneously on the side of the mouse, respectively. Electrical activity of the retinal cells was measured as amplitude ( $\mu\text{V}$ ) in response to a light stimulus in a scotopic or photopic manner (see below for protocol specification) (**Figure 25**).

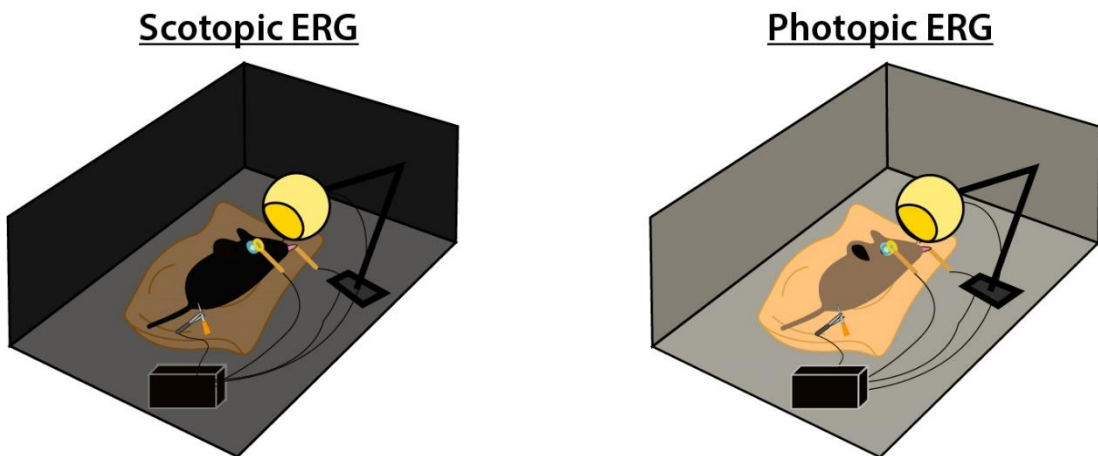


**Figure 25.** Representation of a mouse in its cage and lighting depending on ERG conditions. Left, scotopic conditions in dark-adapted mice. Right, photopic conditions in light-adapted mice.

### ➤ Scotopic and photopic ERG

After dark-adaptation overnight, mice were stimulated by flashing lights of different intensities, ranging from  $-5.0$  to  $2$  log scotopic candlepower ( $\text{cd}\cdot\text{s}/\text{m}^2$ ) in a Ganzfeld dome (Sánchez-Cruz et al. 2021). There was a pause of 15 to 120 seconds between flashes depending on light intensity to allow

photoresponse recovery. For each intensity, electrical responses after 4-60 consecutive light flashes were averaged.

Each range of light intensities allows recording currents arising from specific cell types (**Figure 26**). In dark-adapted (scotopic) ERG recordings, RGC activity is detected from -5 to -4  $\text{cd}\cdot\text{s}/\text{m}^2$ ; rod-mediated responses from -4 to -1.52  $\text{cd}\cdot\text{s}/\text{m}^2$ ; mixed rod and cone responses from -1.42 to 0.48  $\text{cd}\cdot\text{s}/\text{m}^2$ ; and oscillatory potentials are detected at 0.48  $\text{cd}\cdot\text{s}/\text{m}^2$  and at recording frequency range of 100-1000 Hz.

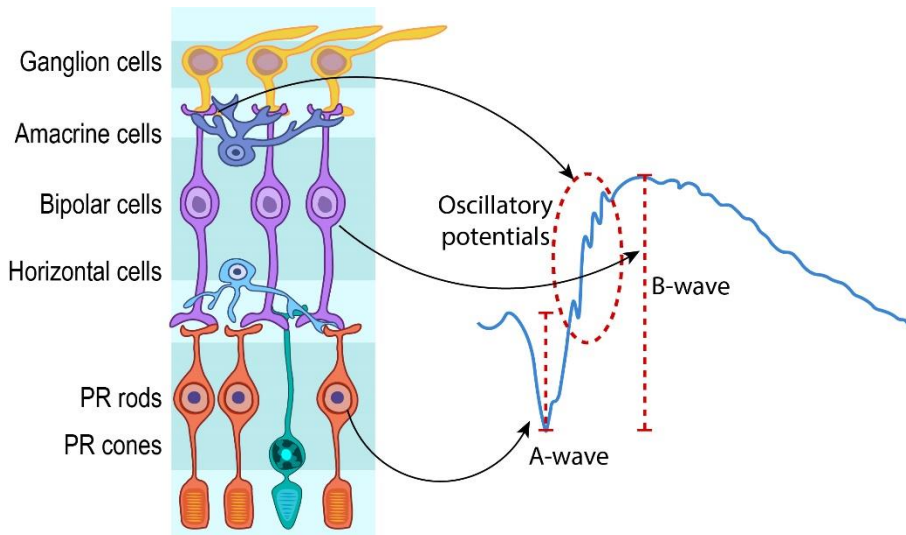


**Figure 26** Diagram representing retinal cell-specific responses on scotopic ERG.

For light-adapted (photopic) ERG recordings, a background of 30  $\text{cd}\cdot\text{s}/\text{m}^2$  was applied for five minutes to suppress rod stimulation, and from -0.52 to 1.48  $\log \text{cd}\cdot\text{s}/\text{m}^2$  cone-mediated electrical responses were recorded. Also, at 1.48  $\text{cd}\cdot\text{s}/\text{m}^2$  flicker responses were recorded (20 Hz) (**Figure 27**).



**Figure 27.** Representation of light flashes (yellow stars) in Flicker ERG.

### ➤ **Double-flash ERG for dark adaptation assessment**

For the assessment of dark adaptation, a double-flash protocol was performed (Samaranayake et al. 2020; Lyubarsky, Nikonov, and Pugh 1996). Mice were dark-adapted overnight, handled, and anesthetized as stated before ERG analyses. A first (test) flash was delivered to suppress rod circulating current. Then, a second (probe) flash was delivered to monitor the recovery of rod current. The time interval between the two flashes increased with each set, ranging from 1 to 150 seconds. The intensity of the flashes was  $2 \text{ cd}\cdot\text{s}/\text{m}^2$ , and there was a delay with each subsequent set of double-flash ranging from two to five minutes. The amplitude of response recorded in the second flash is plotted as a function of time interval between flashes (**Figure 28**).

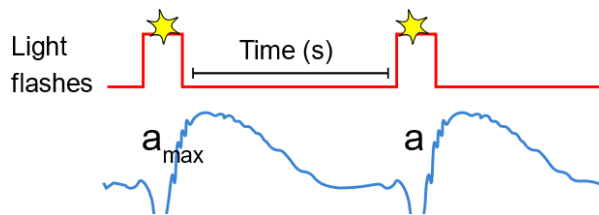


**Figure 28** Representation of double-flash protocol. Light flashes are represented by yellow stars. The first flash elicits the maximum electrical response: “ $a_{\text{max}}$ ”, while the second flash elicits “ $a$ ”.

#### **2.1.4. Light exposure protocol**

Two-month-old Faim KO and WT mice were dark-adapted overnight and exposed to bright light in a cage with LED panels (2,500 lux) for different time periods (30 seconds, 5 minutes, and 15 minutes) after their pupils were dilated with a topical drop of 1% tropicamide, a mydriatic drug. For the dark-adapted condition, mice were euthanized after overnight dark adaptation. Eyes were collected in the dark, under a dim infrared light for immunofluorescence analysis.



### 2.1.5. Light damage protocol

For light-induced retinal damage (LIRD), two-month-old Faim KO and WT mice were dark-adapted overnight and then exposed to LED light at 10,000 lux in non-reflective cages for 8 or 24h (**Figure 29**) after pupils were dilated with drops of 0.5% tropicamide and 2.5% phenylephrine hydrochloride. During light-stress, mice were allowed free access to food and water.

For ERG measurements and consequent sample collection for biochemical or immunohistological analyses, mice were kept in their cages after 8h LIRD for two weeks and dark-adapted overnight before the ERG procedure.

For RNAseq analyses, mice were immediately euthanized after 24h LIRD. Left-eye retinas were rapidly collected and submerged in 1ml of RNAlater (Thermofisher) and maintained at 4°C overnight before freezing at -20° for a maximum of 5 days. Right-eye retinas were snap-frozen in liquid nitrogen and stored at -80°C until further use.

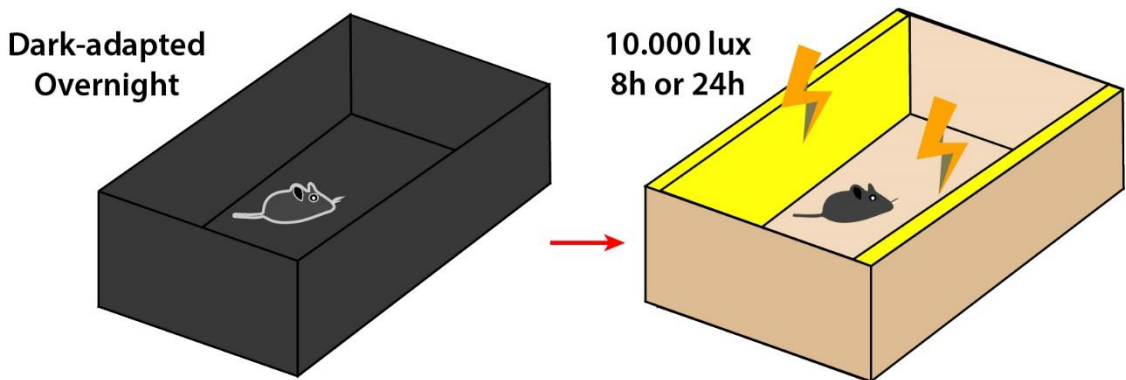


**Figure 29.** Representation of the protocol of light damage Animals are dark-adapted overnight (left), and exposed to 10,000 luxes for 8 or 24h depending on the protocol (right). After two weeks, animals were euthanized.

### **2.1.6. Measurement of retinal vessel leakage**

BRB permeability and vascular leakage were quantified using Evans Blue dye (E2129 Sigma-Aldrich), which binds irreversibly to serum albumin. Under anesthesia, five animals per group were injected intraperitoneally with a solution of Evans Blue (17 mg/kg dissolved in PBS) via the tail vein. After 2 h, mice were euthanized and eyes were enucleated and immediately immersed in 2% paraformaldehyde for 2 h. Afterwards, eyes were washed five times for 10 minutes in PBS. Retinas were dissected and flat-mounted slides for whole mounts with the vitreous side up. Images from multiple random fields of the retina were acquired under an Olympus FV1000 spectral confocal microscope and the number of extravasations per field of 60x was counted in a double-blinded manner. Extravasation intensity was measured in Fiji (Schindelin et al. 2012). A ROI was manually drawn following the outlines of the retinal vessels in each photomicrograph. Z-stack images corresponding to the SVP were selected and used to calculate maximum intensity.

## **2.2. Ex vivo analyses**

### **2.2.1. Tissue collection and processing**

Mice were euthanized by cervical dislocation and eyes were enucleated. The retina was extracted from the left eye and snap-frozen in liquid nitrogen for protein or mRNA extraction, unless stated otherwise. The right eye was fixed in 4% paraformaldehyde for 5 h, washed five times for 10 minutes in PBS and embedded in paraffin blocks. Next, 4- $\mu$ m-thick sections were cut on a microtome (Microm HM 355 S, ThermoFisher Scientific, Waltham, USA), and three or four sections were placed on one slide. Slides were stored at room temperature until analysis. Experiments were performed using samples

from 2-, 12- or 18-month-old mice, and at least four animals per group were used in each experiment.

### 2.2.2. Histology and retinal morphometry analysis

Slides were heated at 60°C for 1 h, deparaffinized in xylene, rehydrated in a graded ethanol (EtOH) series as described in **Table 1**.

**Table 1** Series of graded rehydration.

<i>Product</i>	<i>Time</i>
<i>Xylene,</i>	6 minutes
<i>Xylene/EtOH 1:1,</i>	6 minutes
<i>100% EtOH,</i>	6 minutes
<i>95% EtOH,</i>	6 minutes
<i>70% EtOH,</i>	3 min
<i>50% EtOH,</i>	3 min
<i>ddH<sub>2</sub>O</i>	3 min

Then, slides were stained with Harris hematoxylin for 8 minutes (VWR chemicals, Cat# 351945s) and rinsed with water to remove excess. They were submerged in eosin (Alfa Aesar. Karlsruhe, Alemania, Cat# B24535) immediately afterwards for one minute. Finally, slides were rehydrated oppositely as stated above (50%, 70%, 95%, 100% EtOH) for one minute each condition. After, slides were submerged in xylene for 6 minutes. Slides were fixed with DPX mounting media (VWR Chemicals, Cat# 1.005.790.500) and a coverslip was attached. Whole digital scans were taken using a NanoZoomer 2.0HT high-resolution whole-slide scanner (Hamamatsu).

The thickness of the whole retina was measured manually using the ruler tool of NanoZoomer software at 0.6 mm from both sides of the optic nerve and then averaged, as based on (Berger et al. 2014; Z. Fu et al. 2015).

To manually measure the number of rows of photoreceptor nuclei in the outer nuclear layer (ONL), we also took two segments of the retina at 0.6 mm from the optic nerve. At least 11 columns per segment were manually counted using ImageJ software and then averaged, as based on (Gosbell et al. 2006; Trachsel-Moncho et al. 2018).

The number of nuclei in the ganglion cell layer (GCL) and the inner nuclear layer (INL) was manually counted in ImageJ using 0.5 mm-wide segments (at 0.6 mm from both sides of the optic nerve).

At least four mice per group were measured for each morphometric analyses, at least three sections per animal were used, and at least four comparable segments per section were averaged. All measurements were taken in a double-blinded manner.

### **2.2.3. Immunohistochemistry and quantification**

Slides were deparaffinized and rehydrated as stated above. Antigen retrieval was achieved by immersing the slides in antigen retrieval solution (0.1M citrate buffer pH 6.0) and placing them in a pressure cooker at 150°C for 4 min. Slides were washed in PBS for 10 minutes each wash without agitation until room temperature was achieved.

Slides were individually shaken, and the surroundings of the tissue were dried with a paper towel to remove PBS excess and placed in a humidity chamber. Then, non-specific binding sites were blocked for 1 h at room temperature with PBS containing 10% NGS. After blocking, sections were

delimited with a hydrophobic pen (Dako Pen, Agilent, Cat# S2002) and incubated with 20 µl of multiubiquitin primary antibody in blocking solution (Santa Cruz Biotechnology, Cat# sc-8017, 1:2,000) overnight at 4°C (for details of antibody, see **Table 2**) in a humidity chamber.

**Table 2.** List of primary antibodies for immunohistochemistry and immunofluorescence

<i>Antibody</i>	<i>Supplier information</i>	<i>Immunogen</i>	<i>Dilution</i>
<i>Multi-ubiquitin</i>	Santa Cruz Biotechnology mouse monoclonal antibody Cat# sc-8017	UBB human, mouse, rat	1:2,000
<i>GFAP</i>	Abcam rabbit polyclonal Cat# ab7260	Full-length human recombinant GFAP expressed in bacteria and highly purified	1:2,000
<i>IL-1β</i>	Abcam rabbit polyclonal Cat# ab9722	IL1 beta mouse	1:100
<i>EDN2</i>	Biorbyt rabbit polyclonal Cat# orb445105	KLH conjugated synthetic peptide derived from human Endothelin 2	1:500
<i>Arrestin-1</i>	Rabbit polyclonal antibody provided by Dr. Ana Méndez	C10C10 epitope (residues 290-297 of bovine arrestin)	1:1,000
<i>Transducin-α</i>	Rabbit polyclonal antibody, provided by Dr. Ana Méndez	Residues 85–103	1:2,000

The following day, slides were washed three times with PBS for 10 minutes each wash, and they were incubated for 1 h at room temperature with 40 µl of HRP-conjugated antibody (listed in **Table 3**) in blocking buffer. Slides were washed three times with PBS for 10 minutes. Antibody labeling was visualized with EnVision Detection System (Dako, Agilent mouse Cat# K5007, 1:2,000) and slides were counterstained with Harris hematoxylin as stated above and mounted in DPX (255254, PanReac AppliChem, Chicago, USA). Samples without primary antibodies were used as negative controls.

Images were taken under a Nikon ECLIPSE 80i microscope at 20x and 40x in the Histology Service Unit at the Neurosciences Institute, UAB. Pictures were taken and analyzed in a double-blinded manner by two researchers.

**Table 3.** List of secondary antibodies for immunohistochemistry and immunofluorescence

<i>Antibody</i>	<i>Supplier information</i>	<i>Immunogen</i>	<i>Dilution</i>
<i>Dako REAL EnVision Detection System, Peroxidase/DAB, Rabbit/Mouse, HRP Kit</i>	Agilent mouse Cat# K5007	IgG rabbit, mouse	1:2,000
<i>Goat Anti-Rabbit IgG (H+L) Antibody, Alexa Fluor 488 Conjugated</i>	Molecular Probes rabbit polyclonal Cat# A-11008	Rabbit IgG (H+L)	1:600
<i>Goat Anti-Rabbit IgG (H+L) Antibody, Alexa Fluor 594 Conjugated</i>	Molecular Probes rabbit Cat# A-11012	Rabbit IgG (H+L)	1:600

To quantify ubiquitin immunostaining, ubiquitin-positive cells in the GCL and INL were manually counted. Measurements of ubiquitin-positive cells were averaged for the INL and GCL to obtain the number of ubiquitin-positive GCL cells in 0.6 mm segments, and the number of ubiquitin-positive INL cells in 0.4 mm segments. Four equally sized random segments across the retinal section were selected, and three retinal sections per mouse were used. All measurements were taken in a double-blinded manner.

#### **2.2.4. Immunofluorescence and quantification**

Slides were deparaffinized and rehydrated as stated above. They were then post-fixed in ice-cold methanol-acetic acid solution (95% methanol, 5% glacial acetic acid) for 1 min and washed three times with PBS for 10 minutes. Antigen retrieval was achieved by immersing the slides in antigen

retrieval solution (0.1M citrate buffer pH 6.0) and placing them in a pressure cooker at 150°C for 4 min.

After washing with PBS three times for 10 minutes, PBS excess was removed shaking slides and drying the surroundings of the tissue with a paper towel. Slides were placed in a humidity chamber and non-specific binding sites were blocked for 1 h at room temperature with PBS containing 0.2% Triton X-100 and 1% BSA. After blocking, sections were washed three times for 10 minutes in PBS and incubated with the corresponding primary antibody overnight at 4°C (see **Table 2**).

The following day, sections were washed three times for 10 minutes 3x10 in PBS and incubated for 1 h at room temperature in the dark with the fluorescent secondary antibodies (see **Table 3**).

Nuclei were stained with Hoechst 33342 at 1:10.000 in PBS for 10 minutes and washed three times for 10 minutes in PBS afterwards. Sections were mounted with Prolong™ Gold Antifade Mountant. Samples without primary antibodies were used as negative controls. Images were taken at 20x, 40x and 60x in an Olympus FV1000 spectral confocal microscope in the UAT at VHIR. Pictures were analyzed in a double-blinded manner by two researchers.

For Edn2 fluorescence intensity, regions of interest (ROI) corresponding to the inner plexiform layer (IPL) and outer plexiform layer (OPL) were manually drawn, and average intensity was measured for each ROI in ImageJ. Four photomicrographs of the retina, each separated by at least 0.6 mm, were used for each retinal section, and three retinal sections were used per mouse.

The degree of GFAP and IL-1 $\beta$  expression and immunolocalization in Results – Chapter 1, was estimated using a previously established 5-point scoring system (Anderson et al. 2008), as follows: staining only in Müller cell endfeet region or GCL (score 1); GCL plus a few proximal processes (score 2); GCL plus many processes, but not extending to ONL (score 3); GCL plus processes throughout, with some in the ONL (score 4); and GCL plus many processes to the outer margin of the ONL (score 5) (**Figure 30**).

The intensity of GFAP immunolabeling in Results – Chapter 2 was assessed as total immunofluorescence intensity of an average of 5 retinal sections per mice.

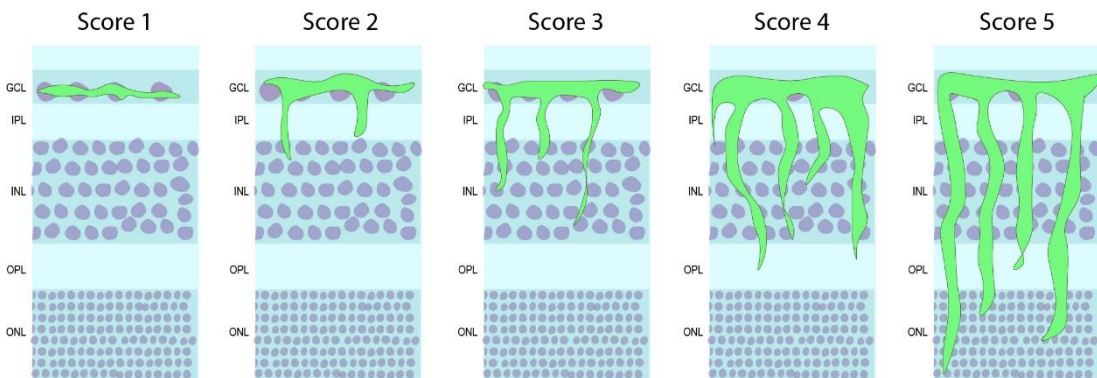


**Figure 30** Depiction of the GFAP and IL-1B scores of Müller glia, depending on the localization of its processes in the retina.

#### 2.2.4.1. Arrestin-1 and Transducin- $\alpha$ immunofluorescence

Slides were heated at 60°C for 1 h, deparaffinized in xylene and rehydrated in a graded ethanol series as stated before. Tissue sections were subjected to antigen retrieval by placing slides in a glass-staining container with antigen retrieval solution (PBS with 0.1 mg/ml proteinase K (Roche)) at room temperature for two minutes and heating slides at 70°C for 6-8 seconds individually.



Non-specific binding sites were blocked and permeabilized for 1 h at room temperature with and PBS 0.2% Triton X-100 and 5% BSA in a humidity chamber. Afterwards, blocking solution was removed by shaking the slides and the surroundings of the tissue were dried with a paper towel. Sections were individually isolated with Dako pen and incubated with the corresponding primary antibody overnight at 4°C (see **Table 2**) in a humidity chamber. The following day, slides were washed three times for 10 minutes in PBS and Dako pen was reapplied. Slides were incubated in the dark in a humidity box for 1 h at room temperature with 20 µl of the corresponding fluorescent secondary antibodies (see **Table 3**). Hoechst 33342 was used to stain the nuclei and sections were mounted with Prolong™ Gold Antifade Mountant, and slides were washed five times for 10 minutes with PBS.

Immunofluorescence signal intensities were measured and quantified using ImageJ software (National Institutes of Health NIH). Signal was quantified using Region of Interest (ROI) tool of ImageJ, which was used to outline the whole photoreceptor inner (IS) and outer segments (OS) of the retinal image in order to calculate the percentage of Arrestin-1 and Transducin- $\alpha$  signal that was located in the OS.

### **2.2.5. TUNEL assay**

Slides were deparaffinized and rehydrated as above. They were then permeabilized for 8 min in 0.1% sodium citrate containing 0.1% Triton X-100 and rinsed twice with PBS for 10 minutes. Slides were afterwards placed in a plastic jar containing 200 ml of 0.1M citrate buffer pH 6.0 and irradiated at 750W in a microwave for 1 min for antigen retrieval. Next, they were immediately cooled by adding room temperature ddH<sub>2</sub>O, and washed three times with PBS for five minutes before blocking.

Slides were immersed in Tris-HCl 0.1M pH 7.5 containing 3% BSA and 20% fetal bovine serum for 30 min at room temperature for blocking and then washed with PBS three times for 10 minutes. Excess of PBS was removed by shaking and drying with a paper towel and sections were transferred to a humidity chamber. The slides were incubated for 1 h at 37°C with 20 µl TUNEL (Terminal deoxynucleotidyl transferase dUTP Nick End Labeling) reaction mixture (11767291910 and 11767305001, TUNEL Label Mix and TUNEL Enzyme, Roche), following the manufacturer's instructions. The mixture was added individually to each retinal section. Negative controls were incubated with TUNEL reaction mixture without TUNEL enzyme. Slides were rinsed three times for five minutes with PBS and counterstained with Hoechst 33342 (0.05 µg/ml, ab228551, Abcam) for 10 min and rinsed again with PBS three times for five minutes. Finally, slides were mounted in Prolong™ Gold Antifade Mountant (P36930, Thermofisher) and 40x images were taken with Olympus FV1000 spectral confocal microscope in the High Technology Unit (UAT) at VHIR. TUNEL-positive cells in retinal sections were manually counted in a blind manner using ImageJ software. Three distinct whole retinal sections per mouse were analyzed and averaged, and at least four animals per group were used.

#### **2.2.6. Western blotting**

Retinal proteins were homogenized mechanically by pipetting the tissue up and down with different-sized pipette tips and insulin syringes with RIPA lysis buffer (150 mM NaCl, 1% IGEPAL® CA-630, 0.5% sodium deoxycholate, 0.1% SDS, and 50 mM Tris pH 8.0) containing 1x cComplete™ EDTA-free protease inhibitor cocktail (11873580001, Roche, Darmstadt, Germany). Extracts were kept ice-cold and supernatants from the homogenates were collected after centrifugation at 9300 x g for 15 min at

4°C. Protein concentration was quantified using the Modified Lowry kit (DC protein assay; Bio-Rad, Hercules, CA, USA).

Next, 20 to 40 µg of total protein was resolved by SDS-PAGE and transferred onto PVDF Immobilon-P transfer membranes (Millipore Iberica, Madrid, Spain). Membranes were blocked with Tris-buffered saline with 0.1% TWEEN®-20 and 10% non-fat dry milk for 1 h at room temperature and then probed overnight with the appropriate primary antibody (**Table 4**).

**Table 4** List of primary antibodies used for western

<i>Antibody</i>	<i>Supplier information</i>	<i>Immunogen</i>	<i>MW (kDa)</i>	<i>Dilution</i>
<i>Anti-FAIM</i>	In-house rabbit polyclonal antibody [5]	Recombinant protein corresponding to full-length rat FAIM	21, 23	1:2,000
<i>Anti-GFAP</i>	DAKO rabbit polyclonal Cat# Z0334	GFAP isolated from cow spinal cord	48, 50	1:4,000
<i>Arrestin-1</i>	Rabbit polyclonal antibody provided by Dr. Ana Méndez	C10C10 epitope (residues 290-297 of bovine arrestin)	48	1:10,000
<i>Transducin-α</i>	Rabbit polyclonal antibody, provided by Dr. Ana Méndez	Residues 85–103 of transducin-α	40	1:5,000
<i>Multiubiquitin</i>	Santa Cruz Biotechnology mouse monoclonal antibody Cat# sc-8017	UBB human, mouse, rat		1:6,000
<i>Anti-α-tubulin</i>	Sigma-Aldrich mouse monoclonal antibody Cat# T5168	B612 clone hybridoma produced by the fusion of mouse myeloma cells and splenocytes from an immunized mouse	50	1:60,000
<i>Anti-cyclophilin A</i>	Enzo Life Sciences Cat# BML-SA296	Recombinant human cyclophilin A conjugated to KLH	17	1:10,000
<i>Anti-GAPDH</i>	Enzo Life Sciences, Cat# ADI-CSA-335	Pig GAPDH, clone ID4	36	1:8,000

Blots were then incubated with the corresponding peroxidase-conjugated secondary antibodies (listed in **Table 5**) for 1 h at room temperature, developed using the EZ-ECL Enhanced Chemiluminescence Detection Kit for HRP (Biological Industries, Kibbutz Beit Haemek, Israel), and captured with Fuji X-ray films Super RX-N (Fujifilm, Tokyo, Japan). Band intensities were quantified with ImageJ software, version 1.53e (C. A. Schneider, Rasband, and Eliceiri 2012). To control equal loading, housekeeping  $\alpha$ -tubulin, actin, GAPDH or cyclophilin A (cypA) were used to normalize protein expression.

**Table 5** List of secondary antibodies used for western

<i>Antibody</i>	<i>Supplier information</i>	<i>Immunogen</i>	<i>Dilution</i>
<i>Goat anti-Rabbit IgG</i>	Sigma-Aldrich goat Cat# A0545	Purified rabbit IgG	1:20,000
<i>Rabbit anti-mouse IgG</i>	Sigma-Aldrich rabbit polyclonal antibody Cat# A9044	Purified mouse IgG	1:20,000

### 2.2.7. RNA isolation and qRT-PCR

Total RNA was isolated from mouse retinas using the RNeasy kit (Qiagen, Cat# 74004) and following the manufacturer's instructions. RNA concentration and integrity were determined using a NanoDrop spectrophotometer (ThermoFisher Scientific). A ratio of ~2 was considered acceptable for 260/280 ratio, and ~2.0-2.2 for 260/230. At least 250 ng of RNA was reverse-transcribed using the High-Capacity cDNA Reverse Transcription Kit (ThermoFisher Scientific, Cat# 4368814).

qRT-PCR was performed in 384 well-plates (ThermoFisher Scientific) using PowerUp™ SYBR™ Green Master Mix (ThermoFisher Scientific, Cat#

A25741) under standard conditions: 2 min at 50°C, 10 min at 95°C, 40 cycles of 15 s at 95°C, 1 min at 60°C, and 15 s at 95°C and followed by 15 s at 60°C and 15 s at 95°C in the 7900HT Fast Real-Time PCR System (ThermoFisher Scientific). Volumes of the reaction are detailed in **Table 6**.

**Table 6** Reactives and volumes for RT-

<i>Product</i>	<i>Volume (μl)</i>
<i>Forward primer</i>	0.25
<i>Reverse primer</i>	0.25
<i>Sybr</i>	5
<i>dH<sub>2</sub>O</i>	0.5
<i>cDNA</i>	4

Each sample was measured in triplicate, relative fold change gene expression levels were calculated with the presented formula  $2^{-(\Delta\Delta Ct)}$ , and  $\beta$ -actin (*ActB*) was used as an internal control. Each pair of primers used to perform qRT-PCR is listed in **Table 7**.

**Table 7** List of primers used for qRT-PCR (continues at the following page).

<i>Gene</i>	<i>Forward primer</i>	<i>Reverse primer</i>
<i>Gfap</i>	5'-GGCGCTCAATGCTGGCTTCA-3'	5'-TCTGCCTCCAGCCTCAGGTT-3'
<i>Tnf-α</i>	5'-CCCTCACACTCACAAACCAC-3'	5'-ACAAGGTACAACCCATCGGC-3'
<i>Xiap</i>	5'-GCACGGATCGTTACTTTTGAACA-3'	5'-GTGAAAGCACTTCACTTTATCGCC-3'
<i>Siva-1</i>	5'-AAGTCTGGTGTGGTAGGAGC-3'	5'-AGGTCCAATCAACATCTGTC-3'
<i>Fasl</i>	5'-ATCCCTCTGGAATGGGAAGA-3'	5'-CCATATCTGTCCAGTAGTGC-3'
<i>Cd11b</i>	5'-CCACACTAGCATCAAGGGCA-3'	5'-AAGAGCTTCACACTGCCACC-3'

<i>Iba-1</i>	5'-ACGAACCTCTGATGTGGTC-3'	5'-TGAGGAGGACTGGCTGACTT-3'
<i>Vcam-1</i>	5'-ACAAGTCTACATCTCTCCAGG-3'	5'-TCAGGAGCTGGTAGACCCTC-3'
<i>Icam-1</i>	5'-AAGGTGGTTCTTCTGAGCGG-3'	5'-TCCAGCCGAGGACCATACAG-3'
<i>Vegfa</i>	5'-AGCAGAAGTCCCATGAAGTGATC-3'	5'-TCAATCGGACGGCAGTAGCT-3'
<i>Mmp9</i>	5'-CGGCACGCCTTGGTGTAGCA-3'	5'-AGGCAGAGTAGGAGCGGCC-3'
<i>Edn2</i>	5'-TCATCTGGGTGAACACTGCG-3'	5'-TCGATGGCAGAAGGTAGCAC-3'
<i>Ednrb</i>	5'-TGGCTGGGGTAGCTGACTTA-3'	5'-CGGGCGATTGCATGTTACAG-3'
<i>Fgf2</i>	5'-GAAACTCTTCTGTAACACTT-3'	5'-GTCAAACATAACTCCAAGCAG-3'
<i>Actb</i>	5'-CTAAGCCAACCGTAAAAG-3'	5'-ACCAGAGGCATACAGGGACA-3'

## 2.3. Bioinformatic analyses

### 2.3.1. RNA-sequencing and analysis

Immediately after LIRD protocol (24h at 10,000 lux) or normal light exposure, mice were euthanised, eyes were enucleated, and retinas were rapidly obtained and preserved in RNAlater at 4°C overnight and frozen the following day. Total RNA was obtained using RNeasy kit following the manufacturer's instructions. RNA concentration was determined with NanoDrop spectrophotometer (ThermoFisher Scientific). RIN integrity, RNA quality assessment, library preparation and Illumina sequencing was performed in the Genomic Unit of the Centre de Regulació Genòmica (CRG) facility (Agilent Technologies).

A cDNA library for every RNA sample was made using 5-10 µg of RNA to prepare the RNA-seq library using TruSeq RNA Sample Prep Kits (Illumina). First, the RNA was isolated from the sample and traces of contaminating DNA was removed with DNase. The polyA containing mRNA

molecules were purified using poly-T oligo-attached magnetic beads. Then, the mRNA is reverse transcribed into double-stranded cDNA, and sequence adapters are added to the ends of the fragments. cDNA library was made by synthesizing the first-strand cDNA using reverse transcriptase and random primers and followed by synthesis of the second-strand cDNA using DNA polymerase I and RNase H. After construction of the libraries, paired-end sequencing on Illumina HiSeq 2000 platform was performed using the nucleotide sequences of the ends of the fragments, from now on called “reads”, and 2x100 bp reads were obtained.

The raw reads (in fastq format) were aligned with an indexed mouse reference genome (GRcm39) with Spliced Transcripts Alignment to a Reference (STAR) (Dobin et al. 2013). Transcript quantification and differential analysis of count data was performed with count-based statistical method DESeq2 (Love, Huber, and Anders 2014) in RStudio (RStudio Team 2015). Exploratory data analysis for quality assessment and to explore the relationship between the samples was made. Variance stabilizing transformation was performed with rlog and VST, and sample distances to assess similarity was calculated with VST data and plotted with principal components analysis (PCA).

### **2.3.2. Bioinformatic tools**

#### **➤ Open-source software**

Data from the Human Proteome Map (Research Resource Identifier, (M.-S. Kim et al. 2014) and Human Protein Atlas v20.0 (HPA) (Uhlén et al. 2015) were used. The former consists of LC-MS/MS data that show relative expression of the proteins of interest in fetal and adult tissues, while the latter

deploys RNA single-cell type specificity in the form of transcript expression values.

➤ **Weighted-gene co-expression network analysis (WGCNA)**

The GeneFriends tool (GeneFriends) (Raina et al. 2021) was used to generate an unsupervised mouse co-expression gene map based on 34,322 RNA-seq samples containing 31,236 genes. To this end, we calculated the distance for each possible gene paired with *Faim*. The mutual rank, which was obtained by taking a geometric average of Pearson's correlation coefficients from each pair of genes bidirectionally, was used as the threshold parameter at 1306. WebGestalt (WEB-based GENE SeT AnaLysis Toolkit) (J. Wang et al. 2013) was then used to conduct a Gene Ontology (GO) term enrichment analysis of biological processes among the resulting FAIM co-expressed genes.

The Overrepresentation Analyses (ORA) approach was used to determine the enrichment for gene sets based on some shared theme, in this case, GO terms. The False Discovery Rate (FDR), which estimates the probability that a gene set with a given enrichment score is a false-positive finding, was used to filter the results.

Differential expression analysis was executed with DESeqDataSet, which performs the estimation of size factors (controlling the differences in the sequencing depth of the samples), the estimation of dispersion values for each gene and a fitting of a generalized linear model. We had two variables to account for: the presence or absence of light damage (normal light: NL, light damage: LD), and the genotype (WT and KO). Different comparisons (contrasts) were made to assess the profile of differentially expressed genes. An adjusted p value below 10% was used to filter the results (0.1) and log<sub>2</sub> fold change, which estimates the effect size (how much the gene expression



has changed due to our studied conditions) was used to report the differences between our groups and to plot our data. Gene enrichment analysis was performed using GO terms and KEGG pathways with topGO package (Alexa and Rahnenfuhrer 2022).

## **2.4. *In vitro* analyses**

### **2.4.1. Cell culture conditions**

HEK293T cells were cultured in DMEM (ATCC Cat# CRL-3216) supplemented with 10% of heat-inactivated foetal bovine serum (FBS) (Invitrogen), 20 U/ml penicillin and 20 ug/ml streptomycin. Cells were maintained at 37°C in a 5% CO<sub>2</sub> atmosphere in a humidified incubator.

To subculture cells, medium was removed, and dissociation was performed with a 1:5 dilution of 0.25% trypsin-EDTA in PBS. Cells were incubated at 37°C until they were detached and the enzymatic effect of trypsin-EDTA was blocked with FBS-containing fresh culture media. Cells were harvested, centrifugated, counted using a hemocytometer chamber and seeded in culture dishes with fresh media. Subcultures were performed when an 80% of cell confluence was achieved.

To cryopreserve HEK293T cells, they were harvested and pelleted in PBS with centrifugation at 100g for 5 minutes. Pellets were resuspended in cryopreservation medium (10% DMSO in FBS), which is used to prevent the formation of ice crystals and cell disruption. Cells were rapidly aliquoted in cryovials and stored at -80 °C in a Mr. Frosty™ Freezing Container (Thermo Scientific, Cat# 5100-0001). The cells were then transferred to a liquid nitrogen tank in the next following days for long-term storage.

#### 2.4.2. Cell transfection and ubiquitin assay

Ubiquitylated proteins were detected using the 6xHis-ubiquitin assay for mammalian cell protocol of Tansey laboratory ([www.tanseylab.com](http://www.tanseylab.com)). Cells were seeded at a  $2.5 \times 10^6$  confluency in a P100 dish in the evening, and cells were transfected the morning after for 6 hrs with the desired expression plasmids using polyethylenimine (PEI) in DMEM without FBS. Five  $\mu\text{g}$  of 6xHis-ubiquitin plus 5 additional  $\mu\text{g}$  of Arrestin-1 (plasmid kindly provided by Dr. Vsevolod Gurevich), FAIM-L or FAIM-S, as indicated, were transfected. When needed, empty vector pCDNA3 was co-transfected to reach 15  $\mu\text{g}$  of total DNA in the indicated conditions. After transfection, media was removed, and cells were maintained with supplemented culture media for 48 hrs. To achieve proteasome inhibition, six hrs before cell collection, cell culture media was replaced with supplemented medium containing 10  $\mu\text{M}$  of MG132 (Sigma Aldrich Cat# HY-13259) from a stock solution of 10 mg/ml of MG132 diluted in DMSO.

Before ubiquitin assay was performed, Anti-His affinity resin was washed in buffer A (**Table 8**) three times by shaking the tube in hand for 10 seconds. After centrifugation for one minute at 1,000g, the resin was pelleted and in the final wash resuspended in A buffer in a 1:1 ratio.

Then, ubiquitin assay was performed as follows. Cells were collected in PBS pH 7.0 and spun down at 1000g for five minutes. Cell pellets were resuspended in PBS and 20  $\mu\text{l}$  of input was stored. Cells were spun down again at 1000g for five minutes and pellets were resuspended in buffer A (6M guanidine pH8, 0.1M  $\text{Na}_2\text{PO}_4$  and 10mM Imidazol). Samples were sonicated and homogenised with 24 g insulin syringe and lysates were centrifugated at

16,000g for 15 minutes at 4°C. Supernatant was transferred to a new tube and 50 µl of resuspended Anti-His affinity resin was added.

**Table 8.** List of buffers for ubiquitin assay and its

<i>Buffer</i>	<i>Recipe</i>
<i>Buffer A</i>	6M guanidine-HCl 0.1M Na <sub>2</sub> PO <sub>4</sub> 10mM Imidazol pH=8 (adjust w. NaOH)
<i>Buffer T1</i>	25mM Tris-HCl 20mM Imidazol pH=6.8 (adjust w. HCl)
<i>Buffer A/T1</i>	1:3 ratio

Cell lysates were orbitally rotated for 4h at 4°C at 25 rpm. After a short spin, supernatant was discarded, and resin was washed twice with 800 µl of buffer A, four times in buffer A/T1 (1 volume of buffer A for 3 volumes of buffer T1), and twice in buffer T1 (25mM Tris-HCl, 20 mM Imidazol pH 6.8). After a short spin, a needle was used to aspirate the supernatant and 37.5 µl of T1 buffer supplemented with 25% Imidazol 1M was added to the resin. 12.5 µl of 4x Laemmli buffer (60 mM Tris-HCl pH 6.8, 4 mM EDTA, 10% glycerol, 2% SDS, 100 mM dithiothreitol (DTT) and traces of Bromophenol blue) was added to IP lysates and stored inputs and boiled at 95°C for 10 minutes for elution. Afterwards, lysates were loaded in SDS-PAGE for western blot analysis.

## **2.5.Statistical analyses**

We performed a pilot study to estimate sample size required for 0.8 power and two-sided 0.05 significance for retinal morphometric analysis. For the rest of analyses, we limited the number of animals to mice availability and

preliminary data. Data sets were plotted and analysed using GraphPad Prism v8.0.1, and no data was removed prior to analysis unless only repeated measures were used for analyses. Data was graphed before statistical test to check whether the data met the assumptions of the statistical approach. Statistical comparisons were made using a two-way ANOVA test followed by Sidak's post hoc test when analysing two or more ages between WT and Faim KO. Three-way ANOVA was used to assess three factors in electroretinogram analyses: light intensity, light damage, and genotype. Unpaired two-tailed Student's t test was used for parametric data when assessing only one factor. All p values lower than 0.05 were considered statistically significant. The ROUT method (with Q set to 1%) was used to detect outliers.



# Results

*“Understand well as I may, my  
comprehension can only be an infinitesimal  
fraction of all I want to understand”*

Ada Lovelace (1815-1852)



# Results

## Distribution of Results

The Results Section of this thesis is arranged in two different Chapters.

In *Chapter One* we studied histopathologically and structurally the retinas of mice in the absence of FAIM. Most of the data from this Chapter has already been published in “*Journal of Neuroscience Research*” (see *Annex One*).

➤ **TITLE: *Faim* knockout leads to gliosis and late-onset neurodegeneration of photoreceptors in the mouse retina.**

**AUTHORS: Anna Sirés, Mireia Turch-Anguera, Patricia Bogdanov, Joel Sampedro, Hugo Ramos, Agustín Ruíz Lasa, Jianxin Huo, Shengli Xu, Kong-Peng Lam, Joaquín López-Soriano, M. Jose Pérez- García, Cristina Hernández, Rafael Simó, Montse Solé, Joan X. Comella**

**DOI: 10.1002/jnr.24978**

In *Chapter Two* we studied possible functional alterations that stemmed from the results we obtained from *Chapter One*. Additionally, the contents of this chapter are ready to be published (see *Annex Two*).

➤ **TITLE: The absence of FAIM leads to a delay in dark adaptation and hampers Arrestin-1 translocation upon light reception in the retina**

**AUTHORS: Anna Sirés, Mateo Pazo, Alonso Sánchez, Joaquín López-Soriano, Enrique de la Rosa, Catalina Hernández, Pedro de la Villa, Joan X. Comella, Montse Solé**





# Chapter One

*“Above all, don’t fear difficult moments. The best comes from them.”*

Rita Levi-Montalcini (1909-2012)



# Chapter One

## 4.1.2. Rationale

FAIM is an important neuronal protein that has been reported to be implicated in neurodegenerative diseases, like AD (P Carriba et al. 2015) and Spinal Muscular Atrophy (SMA) (Sansa et al. 2021). Remarkably, FAIM-L levels are reduced in hippocampal samples from AD patients and in a transgenic mouse model of this disorder (APP/PS1) before neurodegeneration onset, thus indicating the potential clinical relevance of this isoform. While FAIM-S is ubiquitous, it holds multiple neuronal functions involved in neuritogenesis, but only CNS-specific isoform FAIM-L protects neurons against apoptosis (Segura et al. 2007; P Carriba et al. 2015).

Despite that both isoforms are constantly reported to be expressed in neurons, its expression has never been studied outside the brain, like in the neuroretina. The retina is a highly specialized tissue, and its degeneration has proved to precede pathological mechanisms of neurodegenerative diseases. Interestingly, data based on mRNA microarrays show that *Faim* transcripts are significantly downregulated in a mouse model of Norrie Disease (*Ndp* knockout mice), which is characterized by abnormal development of the retina that often results in blindness from birth (Q. Xu et al. 2004).

The lack of knowledge about the role of FAIM in the retina and the potential implication of this protein in retinal disorders prompted us to explore histologically and structurally this tissue in a *Faim* knockout (*Faim*<sup>-/-</sup>) mice in a short- and long-term manner.

#### **4.1.3. *Faim* is co-expressed with genes related to retinal function**

Data extracted from the Human Proteome Map portal and Protein Atlas showed that *Faim* transcripts are particularly enhanced in photoreceptor cells (**Figure 31A**) and that FAIM protein is highly expressed in the retina, in contrast to other adult and fetal tissues (**Figure 31B**). Here we analyzed and confirmed the protein expression of both FAIM-L and FAIM-S in WT retinas and their absence in *Faim*<sup>-/-</sup> mice (**Figure 31C**). We used online-available RNA-Seq data to construct a gene co-expression network, which allowed us to create gene associations with *Faim* that may indicate functional linkage among them. GO terms were applied to identify characteristic biological attributes of the *Faim* co-expression network in the organism. Unexpectedly, we found that the top 2 biological terms were related to retinal functions, such as sensory perception of light stimulus and photoreceptor differentiation (**Figure 31D**), which were distinctively and largely enriched. Of the 413 genes that are co-expressed with *Faim*, 58 of them are linked to the “Sensory perception of light stimulus” gene set, and 26 linked to “Photoreceptor cell differentiation” gene set. The top 10 biological terms, headed by retinal functions, are shown in **Figure 31E**.

#### **4.1.4. *Faim*<sup>-/-</sup> mice show photoreceptor death at 18 months**

FAIM performs important functions in neurons, but its role in the CNS has not been fully addressed *in vivo*. Given we observed that *Faim* is particularly enhanced in photoreceptors, here we examined the consequences of *Faim* loss in the retina. To this end, we analyzed the structure and morphometric parameters of the retina and quantified the cell number in different layers of this tissue. Cross-sections of the retina stained with Harris hematoxylin and eosin were examined in 2-, 12- and 18-month-old WT and in *Faim*<sup>-/-</sup> mice.

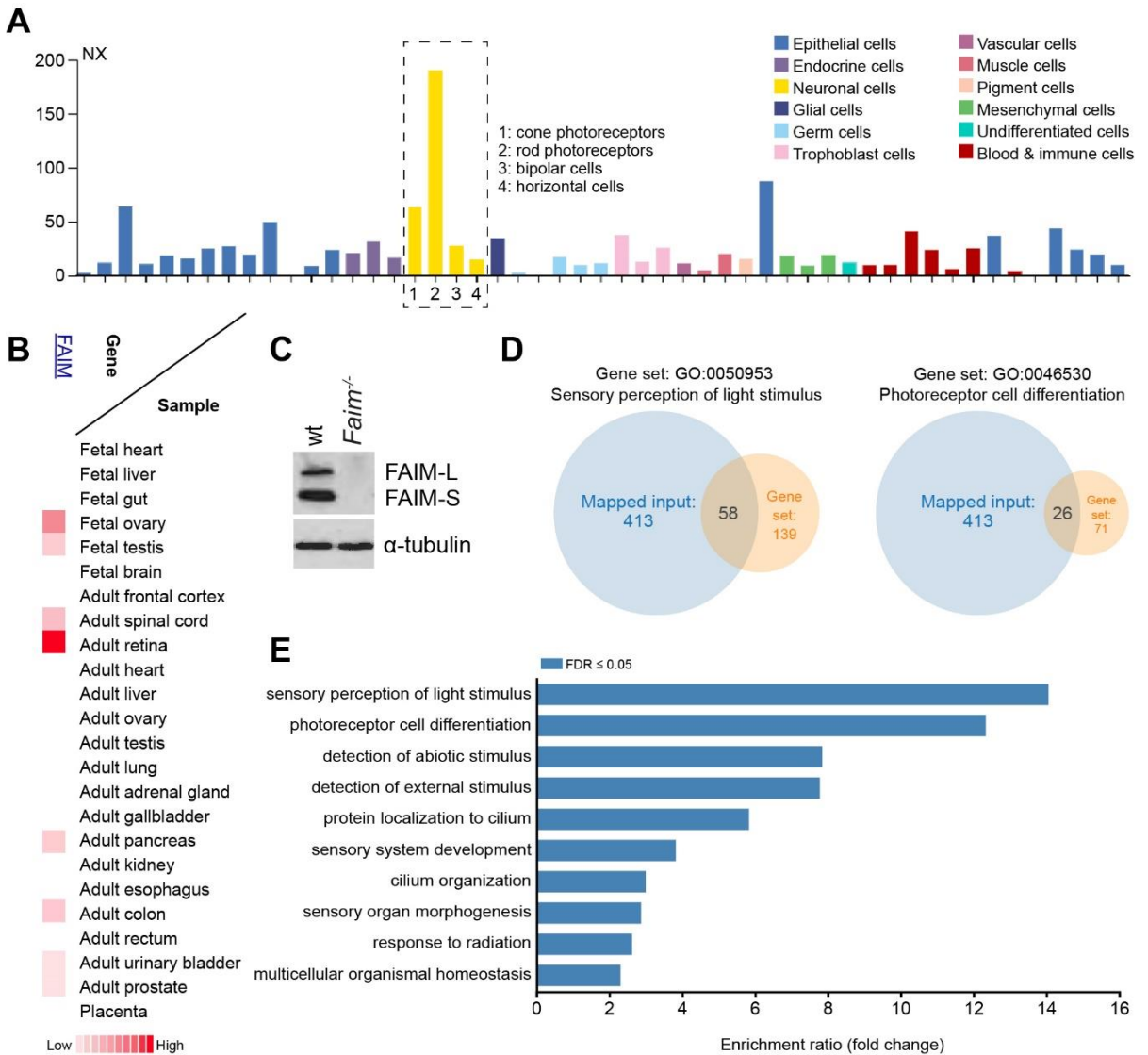


**Figure 31. FAIM expression in the retina. (A)** Graph deploying transcript expression values of FAIM in different cell types; data extracted from single-cell RNA from the Human Protein Atlas. Neuronal cells are highlighted by a discontinued line. **(B)** Diagram showing relative protein expression of FAIM in fetal and adult tissues; data extracted from the Human Proteome Map. **(C)** Retinal western blot of 2-month-old WT and *Faim*<sup>-/-</sup> mice showing both FAIM-L and FAIM-S protein expression.  $\alpha$ -tubulin was used as a loading control. **(D)** Venn diagram of the top 2 enriched GO terms, showing the number of coincidences between the mapped input containing *Faim* co-expressed genes and the pertinent GO term gene set. **(E)** Representation of the top 10 GO terms based on the biological function of genes co-expressed with *Faim* in mice.

We measured retinal thickness and the number of nuclei in the ONL and GCL. Our results revealed a decrease in the number of photoreceptor rows in the ONL by 18 months of age in *Faim*<sup>-/-</sup> mice (**Figure 32A-F**, M: two-way ANOVA, age,  $p = 0.0004$ ; genotype,  $p = 0.0884$ ; interaction,  $p = 0.4963$ ; Sidak's post-hoc test,  $p = 0.0476$ ).

Furthermore, at this age, the retinas of these mice manifested evident disorganization of layers, highly noticeable at the junction between the outer plexiform layer (OPL) and the ONL (**Figure 32F**, arrowheads). No changes were observed in the number of cells in the GCL (**Figure 32N**: two-way ANOVA: age,  $p = 0.0042$ ; genotype,  $p = 0.9847$ ; interaction,  $p = 0.8021$ ). Despite the decrease in photoreceptor rows in the ONL, no significant differences were found in the total retinal thickness of *Faim*<sup>-/-</sup> mice at any age when compared to WT mice (**Figure 32O**: two-way ANOVA: age,  $p = 0.0032$ ; genotype,  $p = 0.1886$ ; interaction,  $p = 0.7628$ ).

Upon seeing these results, we also analyzed retinal, INL and ONL thickness at 18 months through optical coherence tomography (OCT), which allows to assess layer thickness *in vivo*. In consonance, this methodology revealed a thinning of the ONL and of total thickness, but not the INL (**Figure 33**).

Although it has long been known that FAIM-S and FAIM-L are anti-apoptotic players, their roles have been studied only under stress conditions (P Carriba et al. 2015; Hiroaki Kaku and Rothstein 2020). Nonetheless, in view of their promising functions, we performed a TUNEL assay in retinal sections to ascertain whether the decrease in the number of photoreceptors was due to cell death. Indeed, TUNEL-stained positive cells in the ONL were significantly increased in *Faim*<sup>-/-</sup> retinas at 18 months of age (**Figure 32G-L**, P: unpaired two-tailed Student's *t* test,  $p = 0.0162$ ).

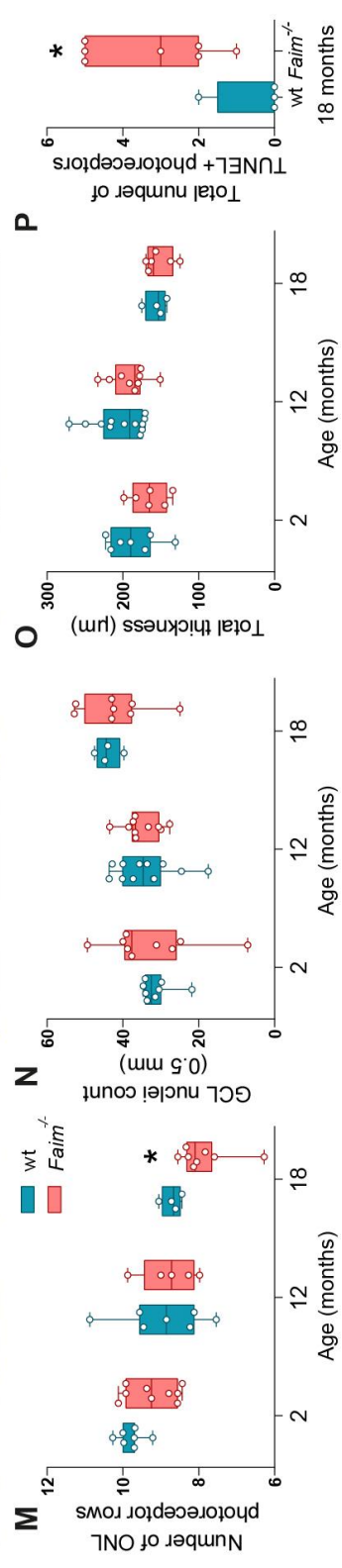
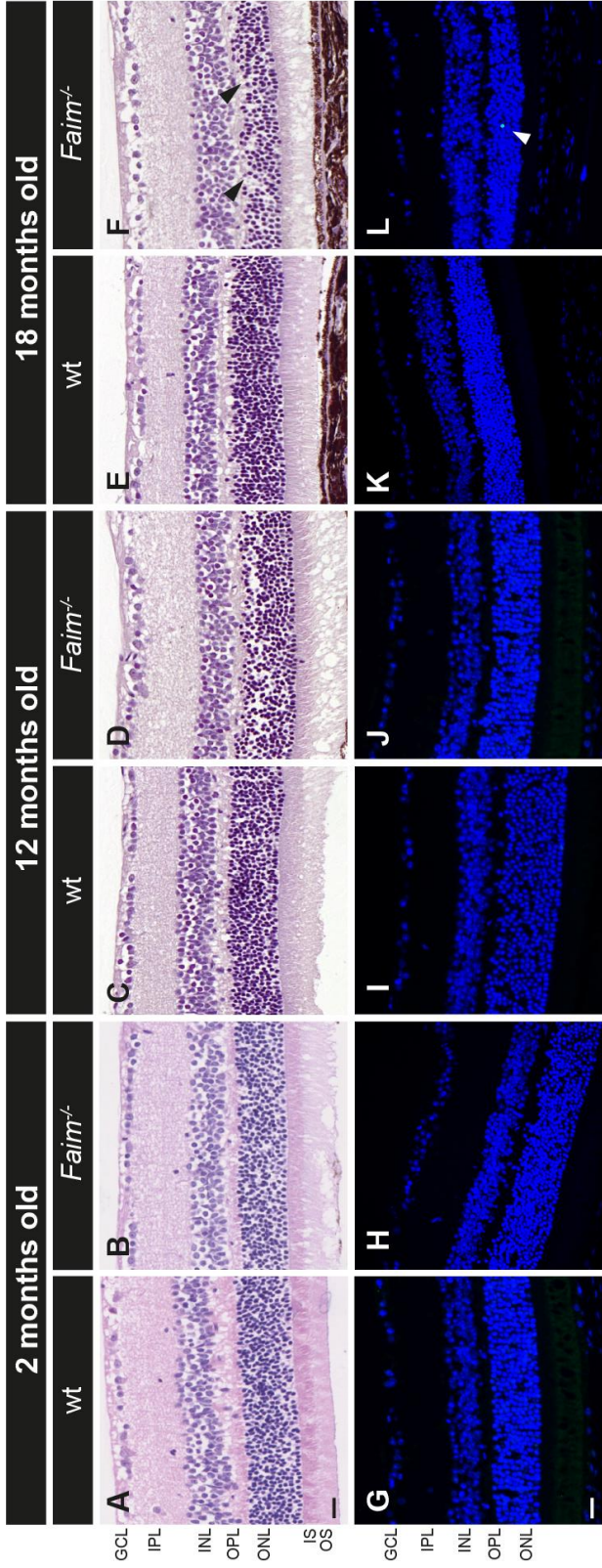




**Figure 32 Retinal degeneration in FAIM knockout mice (*Faim*<sup>-/-</sup>).** (A-F) Retinal sections of WT and *Faim*<sup>-/-</sup> mice stained with Harris hematoxylin and eosin and analyzed at different ages (2, 12 and 18 months). (F) At 18 months, significant loss of photoreceptor nuclei and disorganization of the ONL (black arrowheads) was observed. (G-L) Representative images of TUNEL (green) to quantify the number of apoptotic nuclei in the retina at the different ages. Sections were counterstained with Hoechst (blue). (M) At 18 months, the average number of ONL photoreceptor rows was decreased (n = 4–9 mice/group). (N, O) GCL nuclei count and retinal thickness were constant throughout the ages (n = 4–9 mice/group). (P) Quantification of the number of TUNEL+ photoreceptor cells in 18-month-old *Faim*<sup>-/-</sup> mice. Each symbol in the plots represents one retina. The white arrowhead points at a TUNEL+ photoreceptor. (n = 4–7 mice/group). Each box plot extends from the 25<sup>th</sup> to the 75<sup>th</sup> percentile and the median is plotted as a line in the box. Whiskers represent min to max values, and dot plots are overlaid. Statistical analysis was performed using a two-way ANOVA followed by Sidak's post hoc test for M, N and O, and an unpaired two-tailed Student's *t* test for P. \*p < 0.05. GCL: ganglion cellular layer, IPL: inner plexiform layer, INL: inner nuclear layer, OPL: outer plexiform layer, ONL: outer nuclear layer; and IS/OS: inner/outer segment. Scale bar: 20 μm.

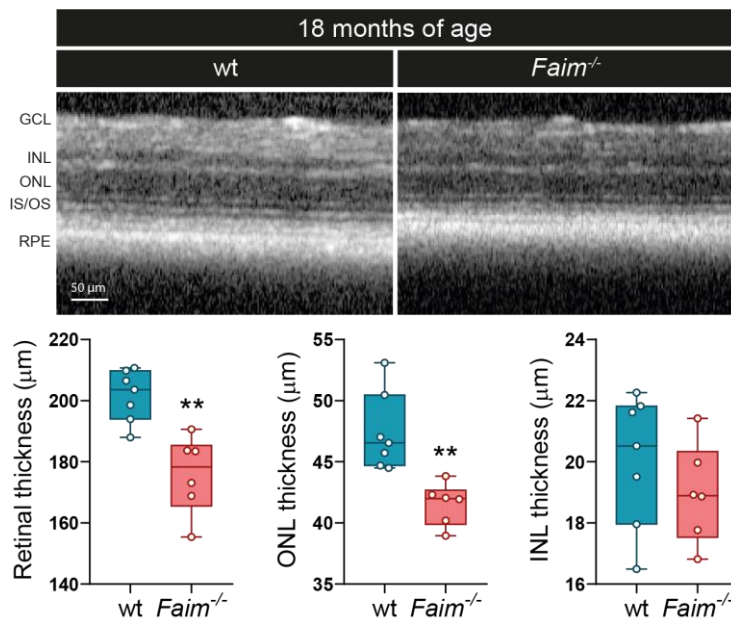


**Figure 33 Retinal and ONL thinning *Faim*<sup>-/-</sup> mice at 18 months of age.** Retinal images were obtained in vivo through OCT. A significant decrease of retinal and ONL thickness was found, but INL levels were similar to WT mice. Each box plot extends from the 25<sup>th</sup> to the 75<sup>th</sup> percentile and the median is plotted as a line in the box. Whiskers represent min to max values, and dot plots are overlaid. Statistical analysis was performed using unpaired two-tailed Student's *t* test. \*\*p < 0.01. GCL: ganglion cellular layer, IPL: inner plexiform layer, INL: inner nuclear layer, OPL: outer plexiform layer, ONL: outer nuclear layer; and IS/OS: inner/outer segment. Scale bar: 50 μm.

Thus, our results confirmed apoptosis in the ONL and suggest an active process of neurodegeneration under basal conditions.

#### 4.1.5. *Xiap* and *Tnf- $\alpha$* mRNA expression is increased in *Faim*<sup>-/-</sup> retinas

To expand on the previous results, we analyzed the mRNA expression of apoptotic mediators and FAIM-interacting partners by qRT-PCR (**Figure 34**).

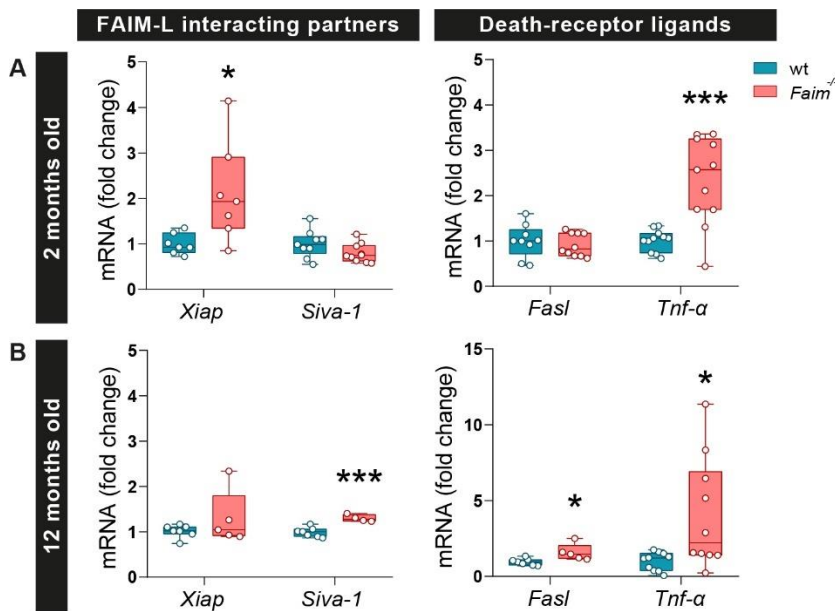


**Figure 34. Apoptosis-related gene markers are altered in *Faim*<sup>-/-</sup> mice.** mRNA levels of apoptotic-related markers of WT and *Faim*<sup>-/-</sup> retinas at (A) 2 and (B) 12 months of age, as determined by qRT-PCR. Each symbol in the plots represents one retina (n = 7–11 mice/group). Expression levels were normalized to *Actb* and data are plotted relative to WT values for each gene. Each box plot extends from the 25<sup>th</sup> to the 75<sup>th</sup> percentile and the median is plotted as a line in the box. Whiskers represent min to max values, and dot plots are overlaid. Statistical analyses were performed using an unpaired two-tailed Student's *t* test \* *p*<0.05, and \*\*\* *p*<0.001.

We recently described that SIVA-1, a pro-apoptotic protein, interacts with FAIM-L and XIAP. SIVA-1 interaction with XIAP displaces FAIM-L from

this complex, thus enabling XIAP auto-ubiquitination and subsequent caspase-3 activation (Moubarak et al. 2013). We detected an increase in *Xiap* mRNA expression in *Faim*<sup>-/-</sup> retinas at 2 months of age (unpaired two-tailed Student's *t* test,  $t = 2.657$ ,  $p = 0.0209$ ), and also an increase in *Siva-1* mRNA expression at 12 months (unpaired two-tailed Student's *t* test,  $p = 0.0006$ ). We also observed that mRNA levels of cytokine *Tnf- $\alpha$*  were upregulated at both ages (unpaired two-tailed Student's *t* test,  $p = 0.0003$  regarding 2 months of age;  $p = 0.0190$  regarding 12 months of age), and *Fasl* was upregulated at 12 months (unpaired two-tailed Student's *t* test,  $p = 0.0195$ ). These results suggest that apoptotic pathways are altered in *Faim*<sup>-/-</sup> retinas.

#### **4.1.6. Ubiquitin complexes accumulate in *Faim*<sup>-/-</sup> retinas**

To uncover likely events that may account for the late-photoreceptor death, we studied early pathogenic hallmarks of neurodegeneration, like protein aggregation. Ubiquitinated proteins usually become deactivated and tagged for degradation by the proteasome (Lecker, Goldberg, and Mitch 2006). However, disruption of this process causes the neurotoxic accumulation of ubiquitinated proteins, which can eventually lead to photoreceptor death (Schmidt et al. 2021).

To study whether this form of protein aggregation occurs in *Faim*<sup>-/-</sup> retinas, retinal sections of *Faim*<sup>-/-</sup> and WT mice were immunolabeled against multi-ubiquitin aggregates (**Figure 35**). We measured the number of ubiquitin-positive cells in the GCL and INL at 2 and 12 months of age and found a significant increase in both nuclear layers and ages in *Faim*<sup>-/-</sup> retinas (**Figure 35B**: two-way ANOVA: age,  $p = 0.0041$ ; genotype,  $p < 0.0001$ ; interaction  $p = 0.0639$ ) (Fig 3C: two-way ANOVA: age,  $p = 0.0515$ ; genotype,  $p = 0.0002$ ; interaction  $p = 0.0168$ ).

In addition, intense immunoreactivity against ubiquitin was revealed in the IPL, OPL, and inner segments (IS) of photoreceptors of *Faim*<sup>-/-</sup> retinas (**Figure 35A**), where the photoreceptor translation machinery is found (Kennedy and Malicki 2009). These results suggest that the ubiquitin-proteasome system is disrupted in *Faim*<sup>-/-</sup> retinas.

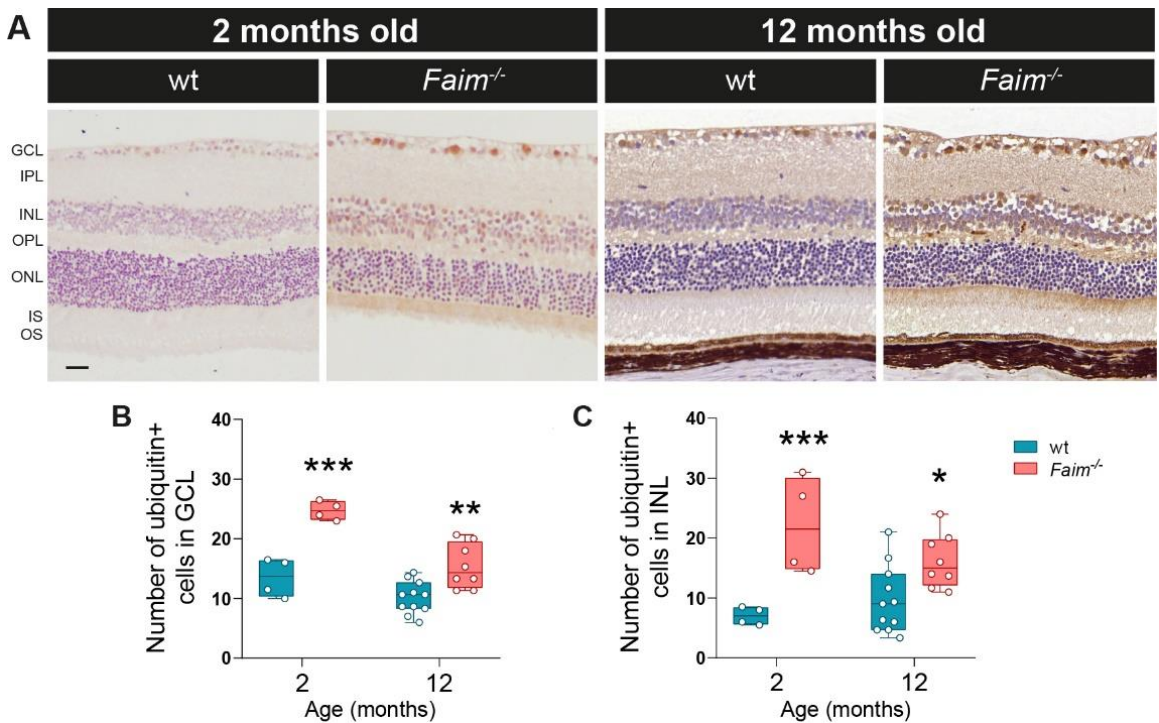


**Figure 35. Immunohistochemical analysis of ubiquitin aggregation in WT and *Faim*<sup>-/-</sup> retinas.** (A) Representative images of 4 μm paraffin sections of retinas taken from 2- and 12-month-old mice and immunolabeled with ubiquitin. (B) Ubiquitin-positive cells in the GCL at 2 and 12 months. (C) Ubiquitin-positive cells in the INL at 2 and 12 months. Each symbol in the plots represents one retina (n = 4–11 mice/group). Each box plot extends from the 25<sup>th</sup> to the 75<sup>th</sup> percentile and the median is plotted as a line in the box. Whiskers represent min to max values, and dot plots are overlaid. Statistical analysis was performed using a two-way ANOVA followed by Sidak's post hoc test. \*p < 0.05, \*\*\*p < 0.001. Scale bar: 20 μm.

#### 4.1.7. *Faim*<sup>-/-</sup> retinas present chronic reactive gliosis

The aggregation of ubiquitinated proteins can lead to inflammation of the retinal tissue (Leger et al. 2011). Müller cells activation is one of the hallmarks of retinal degeneration, and it can be characterized by an increased expression of Glial Fibrillary Acidic Protein (GFAP) (Luna et al. 2010). Consequently, we performed immunofluorescence against GFAP in the retinas of WT and *Faim*<sup>-/-</sup> mice and used an established procedure to assess the extent of Müller cell activation via a 5-point scoring system (**Figure 36**) (Anderson et al. 2008), which is explained in detail in Materials and Methods Section, *page 81*.

The retinas of *Faim*<sup>-/-</sup> mice showed an increased immunoreactivity of GFAP-positive glial processes extending from the endfeet of Müller cells in the GCL and deep into the tissue, towards the ONL (**Figure 36A-D**). This was reflected in higher GFAP scores at both 2 and 12 months of age (**Figure 36E**: two-way ANOVA: age,  $p = 0.6792$ ; genotype,  $F_{(1, 41)} = 19.18$ ,  $p < 0.0001$ ; interaction,  $p = 0.5341$ ).

Increased *Gfap* mRNA and GFAP protein expression was also confirmed by qRT-PCR and western blot at 2 (**Figure 36K**: unpaired two-tailed Student's *t* test: *Gfap* mRNA,  $p = 0.0001$ ; GFAP protein,  $p = 0.0091$ ) and 12 months of age (**Figure 36L**: unpaired two-tailed Student's *t* test: *Gfap* mRNA,  $p = 0.0229$ ; GFAP protein,  $p = 0.0256$ ), respectively.

Müller cells are known to activate an acute-phase response, which is associated with retinal upregulation of pro-inflammatory cytokines like Interleukin 1 Beta (IL-1 $\beta$ ). The IL-1 $\beta$  immunolabeling pattern in the retina traced Müller cell morphology (hence showing the same pattern as GFAP) (**Figure 36F-I**), and it depicted a higher score in 12-month-old *Faim*<sup>-/-</sup> retinas

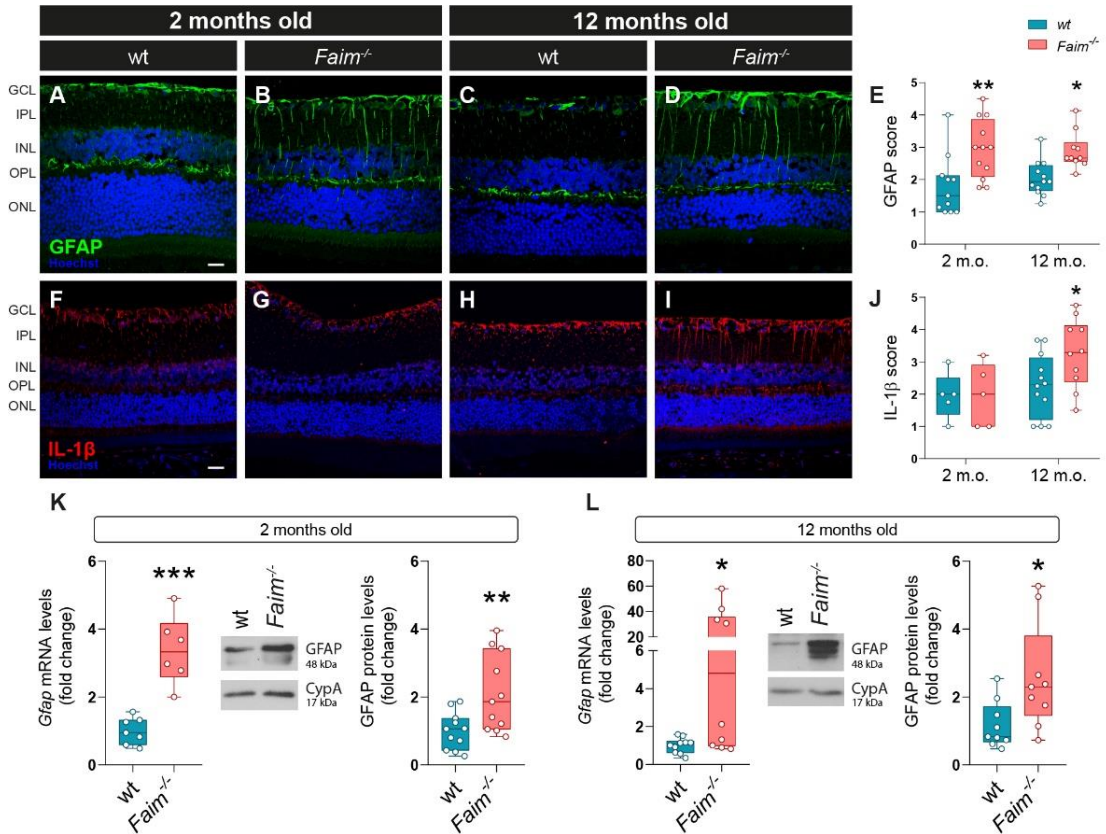


**Figure 36. Expression of GFAP and IL-1 $\beta$  in 2- and 12-month-old WT and *Faim*<sup>-/-</sup> mice. (A-D)** Representative images of GFAP (green) immunolabeling of paraffin-embedded sections of WT and *Faim*<sup>-/-</sup> retinas. GFAP expression is restricted to astrocytes in the GCL and to proximal prolongations of Müller cells. **(E)** GFAP immunolabeling score at 2 and 12 months, showing an increase in *Faim*<sup>-/-</sup> mice. **(F-I)** Representative images of IL-1 $\beta$  immunolabeling of paraffin-embedded sections from WT and *Faim*<sup>-/-</sup> retinas. **(J)** IL-1 $\beta$  immunolabeling score at both ages, showing an increase in *Faim*<sup>-/-</sup> mice at 12 months. **(K-L)** *Gfap* mRNA levels and protein levels are increased at 2 and 12 months of age (n = 6–11 mice/group). mRNA expression levels were normalized to *Actb*. Representative western blot images of GFAP levels of WT and *Faim*<sup>-/-</sup> retinas are shown. Protein levels were normalized to cyclophilin-A (CypA) and quantified in ImageJ. Data are plotted relative to WT values. Each box plot extends from the 25<sup>th</sup> to the 75<sup>th</sup> percentile and the median is plotted as a line in the box. Whiskers represent min to max values, and dot plots are overlaid. Statistical analysis was performed using a two-way ANOVA followed by Sidak's post

when compared to wt, but not at 2 months of age (**Figure 36J**: two-way ANOVA: age,  $p = 0.0429$ ; genotype  $p = 0.3482$ ; interaction  $p = 0.0492$ ; followed by Sidak's post-hoc test:  $p = 0.8077$  at 2;  $p = 0.0256$  at 12 months).

Microglia are the resident immune cell type of the CNS and play an important role in retinal homeostasis. To evaluate microglial activation status in the absence of *Faim*, we measured the mRNA levels of *Cd11b* and ionized calcium-binding adapter molecule 1 (*Iba-1*). Our results revealed an increase in both markers in the retinas of 2- (**Figure 37A**: unpaired two-tailed Student's *t* test: *Cd11b*,  $p = 0.0260$ ; *Iba-1*,  $p = 0.0022$ ) and 12-month-old (**Figure 37B**: unpaired two-tailed Student's *t* test: *Cd11b*,  $p = 0.0028$ ; *Iba-1*,  $p = 0.0343$ ) *Faim*<sup>-/-</sup> mice.

Taken together, these results show early glial activation in the absence of *Faim* in 2-month-old retinas that is sustained at 12 months of age.

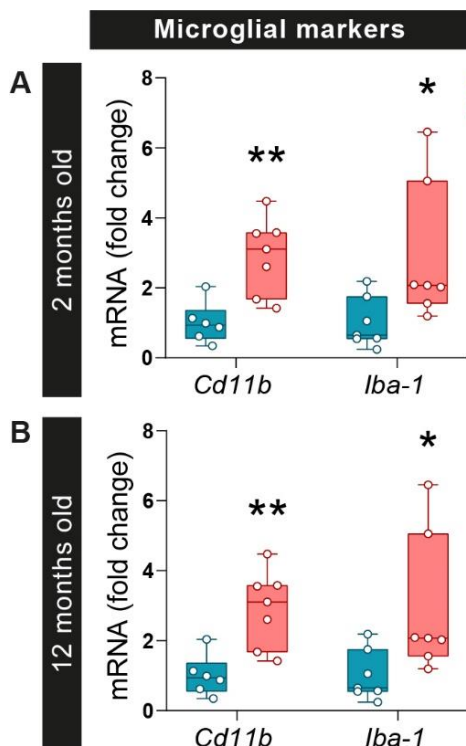


**Figure 37. Microglial markers are upregulated in 2- and 12-month-old *Faim*<sup>-/-</sup> mice.** Microglial mRNA markers of WT and *Faim*<sup>-/-</sup> retinas of mice aged **(A)** 2 and **(B)** 12 months, as determined by qRT-PCR. Each symbol in the plots represents one retina ( $n = 6-11$  mice/group). Expression levels were normalized to *Actb* and data are plotted relative to WT values for each gene. Each box plot extends from the 25<sup>th</sup> to the 75<sup>th</sup> percentile and the median is plotted as a line in the box. Whiskers represent min to max values, and dot plots are overlaid. Statistical analyses were performed using an unpaired two-tailed Student's *t* test \*  $p < 0.05$ , and \*\*  $p < 0.01$ .

#### 4.1.8. BRB homeostasis is disrupted in *Faim*<sup>-/-</sup> retinas

Retinal gliosis can promote leukocyte adhesion to the endothelium and the release of chemokines, cytokines, vascular permeability factors (TNF- $\alpha$  and vascular endothelial growth factor A (VEGF-A) (Giebel et al. 2005) and vascular endothelial adhesion molecules (intercellular adhesion molecule 1 (ICAM-1) and vascular cell adhesion protein 1 (VCAM-1), which act as pro-inflammatory mediators. Analysis of these molecular markers in the retina by qRT-PCR at 2 months of age revealed an upregulation of *Vcam-1* mRNA (Figure 38A: unpaired two-tailed Student's *t* test,  $p = 0.0228$ ). Additionally, *Vegfa* and *Vcam-1* were significantly upregulated at 12 months (Figure 38B: unpaired two-tailed Student's *t* test: *Vegfa*,  $p = 0.0332$ ; *Vcam-1*,  $p = 0.0310$ ). We also analyzed the mRNA levels of *Mmp9* and *Edn1*, which remained unchanged between WT and *Faim*<sup>-/-</sup> mice.

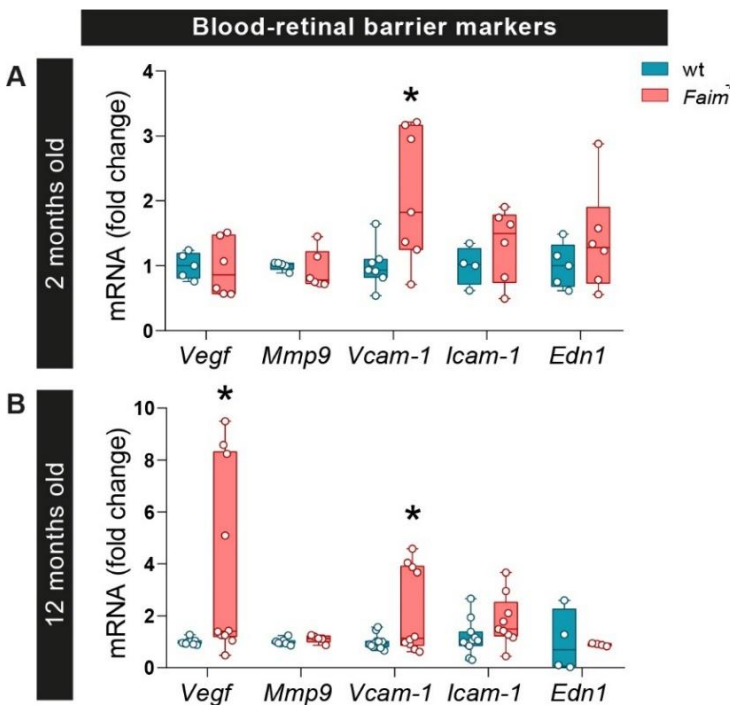


**Figure 38. Gene markers related to the maintenance of blood-retinal barrier homeostasis are altered in *Faim*<sup>-/-</sup> mice.** mRNA levels of different vascular genes related to the BRB function of WT and *Faim*<sup>-/-</sup> retinas of mice aged (A) 2 and (B) 12 months, as determined by qRT-PCR. Each symbol in the plots represents one retina ( $n = 4-11$  mice/group). Expression levels were normalized to *Actb* and data are plotted relative to WT values for each gene. Each box plot extends from the 25<sup>th</sup> to the 75<sup>th</sup> percentile and the median is plotted as a line in the box. Whiskers represent min to max values, and dot plots are overlaid. Statistical analyses were performed using an unpaired two-tailed Student's *t* test \*  $p < 0.05$ .



Vascular inflammation can evolve into impairment of the BRB function and the consequent breakdown of this barrier (E. S. Shin, Sorenson, and Sheibani 2014). Anatomically, the BRB is composed of an outer and inner component. The outer barrier is found in the retinal pigment epithelium, and the inner one is formed by tight junctions between retinal capillary endothelial cells. The inner BRB, in turn, is comprised of the retinal vascular endothelium. This structure can be explored by retinal whole-mounts, allowing the identification of the three vascular plexuses: the superficial vascular plexus (SVP), the intermediate capillary plexus (ICP), and the deep capillary plexus (DCP) (Campbell et al. 2017).

To study whether the BRB was impaired in *Faim*<sup>-/-</sup> mice, we analyzed vascular permeability by measuring albumin–Evans Blue complex leakage in retinal whole-mounts (**Figure 39**). Retinal vessels were sharply outlined in WT mice (**Figure 39A, I**), with no evidence of Evans Blue leakage from the vessels either in the SVP (**Figure 39B, J**), ICP (**Figure 39C, K**) or DCP (**Figure 39D, L**).

Interestingly, our results revealed sites of focal dye leakage into the retinal parenchyma of *Faim*<sup>-/-</sup> retinas at 2 and 12 months, with more obvious leakage at the latter age (**Figure 39E, M**).

Of note, these extravasations were specifically localized in the SVP (**Figure 39F, O**), which is the plexus that supplies the ICP and DCP by vertical anastomoses. In the SVP, the number of extravasations in *Faim*<sup>-/-</sup> mice retinas was not significant at 2 months of age (**Figure 39R**: Mann-Whitney test,  $p = 0.1032$ ), but the quantification of its intensity was significantly higher in *Faim*<sup>-/-</sup> mice compared to WT counterparts at this age (**Figure 39R'**: unpaired two-tailed Student's *t* test,  $p = 0.0478$ ).

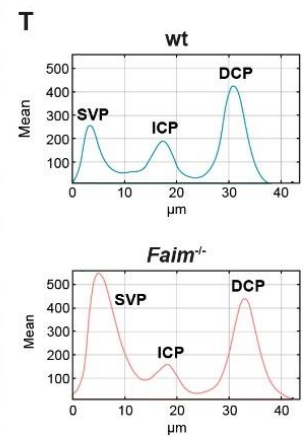
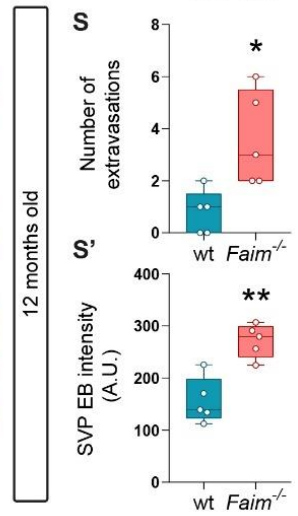
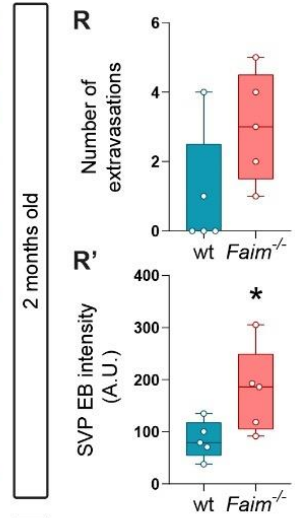
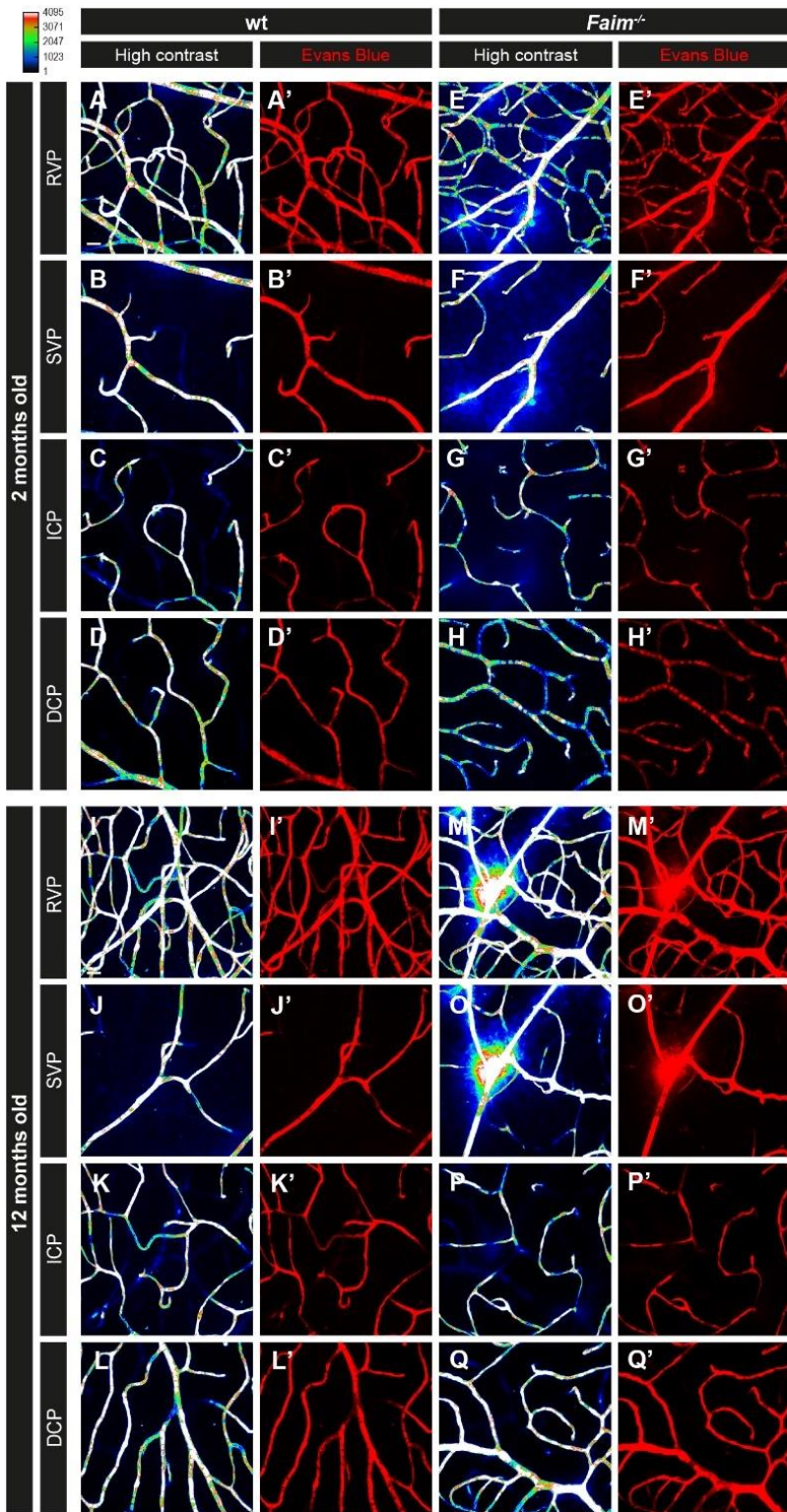


**Figure 39. Vascular BRB permeability in WT and *Faim*<sup>-/-</sup> mice observed in whole-mount retinas. (A-H, I-Q)** Representative confocal immunofluorescence images of Evans Blue maximum intensity projections observed under Spec3, a high contrast profile by FV100 Olympus confocal laser scanning microscope in 2- and 12-month-old WT and *Faim*<sup>-/-</sup> mice. **(R, S)** Total number of significant extravasations. **(R', S')** Intensity quantification of Evans Blue extravasations at 2 and 12 months **(T)** Representative plots of WT and *Faim*<sup>-/-</sup> Z-axis profiles of Evans Blue in retinal whole-mounts, showing the intensity of the different vascular plexuses and quantified in ImageJ. The number of extravasations was quantified in at least 8 images in a 60x field per mouse. All extravasations found were used to quantify extravasation intensity. Each symbol in the plots represents one retina (n = 4–5 mice/group). Each box plot extends from the 25<sup>th</sup> to the 75<sup>th</sup> percentile and the median is plotted as a line in the box. Whiskers represent min to max values, and dot plots are overlaid. Statistical analysis was performed using a Mann-Whitney test (number of extravasations) or Student's *t* test (intensity of extravasations). \*  $p < 0.05$ , and \*\*  $p < 0.01$ . RVP: retinal vascular plexus; SVP: superficial vascular plexus; ICP: intermediate capillary plexus; DCP: deep capillary plexus; EB: Evans blue; and A.U.: arbitrary units.

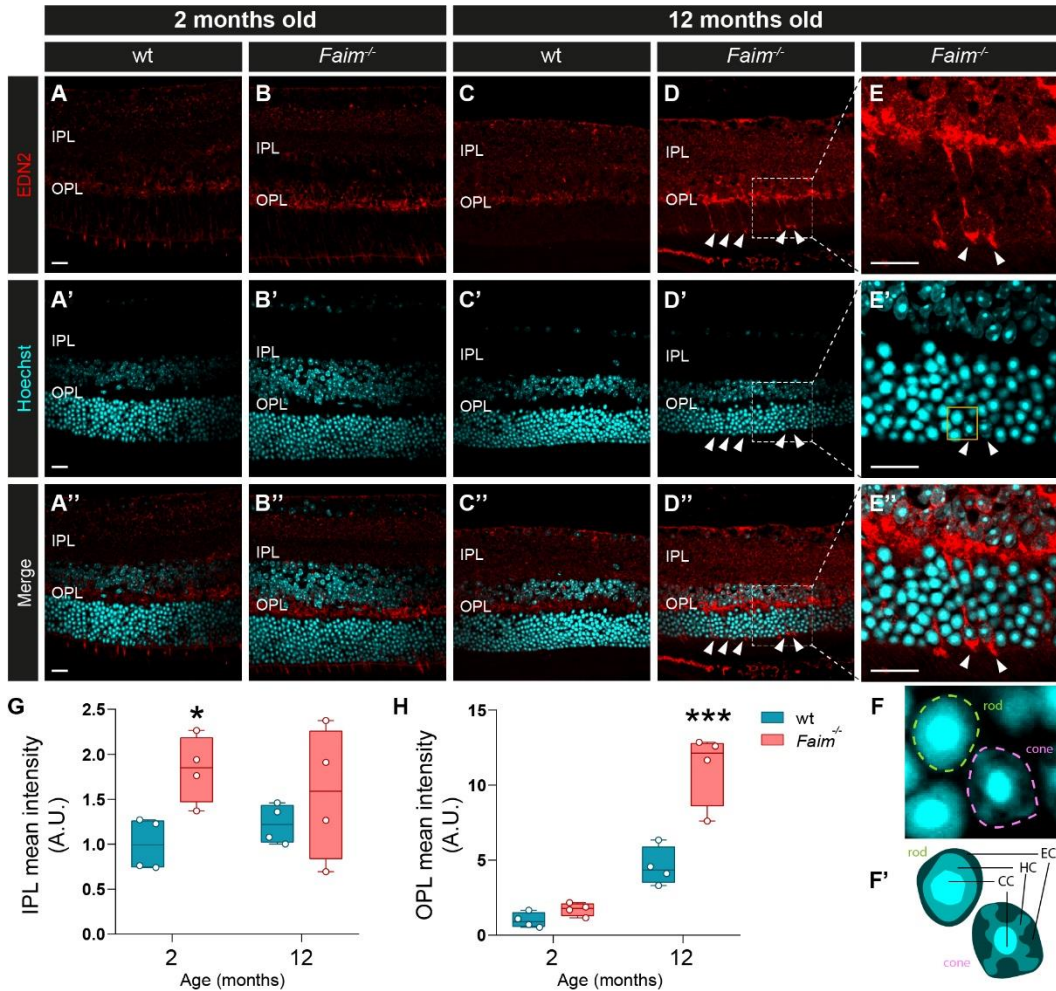
At 12 months of age, both the number (**Figure 39S**: Mann-Whitney test,  $p = 0.0238$ ) and the intensity (**Figure 39S'**: unpaired two-tailed Student's *t* test,  $p = 0.0015$ ) of the extravasations were significantly elevated in the SVP of *Faim*<sup>-/-</sup> retinas. No dye leakage was observed in the deeper retinal vascular plexuses (**Figure 39G-H, P-Q**). The Z-axis profile plots of Evans Blue retinal whole-mounts, representing the intensity of the different vascular plexuses, evidenced the presence of vascular extravasations in the SVP but not in the ICP or DCP (**Figure 39T**).

In summary, these results show evident vascular capillary leakage into the retinal parenchyma, caused by an impairment of the BRB at the SVP level.

#### 4.1.9. *Edn2/Fgf2* neuroprotective pathway could be activated in *Faim*<sup>-/-</sup> retinas

Photoreceptors may induce an endogenous protective response by triggering retinal gliosis through the production of endothelin-2 (EDN2) (Rattner, A.; Nathans 2005), a vasoconstrictive peptide. To test this notion, we performed EDN2 immunofluorescence staining in WT and *Faim*<sup>-/-</sup> retinal sections. EDN2 immunoreactivity was sparse in WT mice (**Figure 40A, C**). However, a strong increase in EDN2 signal intensity was observed in *Faim*<sup>-/-</sup> retinas (**Figure 40B, D-E**), being statistically significant in the IPL at 2 months (**Figure 40G**: two-way ANOVA: age,  $p = 0.8911$ ; genotype,  $p = 0.0724$ ; interaction  $p = 0.1938$ ; Sidak's post-hoc test:  $p = 0.0442$ ) and in the OPL at 12 months (**Figure 40H**: two-way ANOVA: age,  $p < 0.0001$ ; genotype  $p = 0.0002$ ; interaction,  $p = 0.0014$ , Sidak's post-hoc test:  $p < 0.0001$ ). At the latter age, we found a unique and distinctive EDN2 signal enclosing the nuclei of cone photoreceptors (but not rods) and following their axonal projections (**Figure 40D-F, F'**).

Also, we observed an upregulation of *Edn2* mRNA expression in retinas of 2-month-old *Faim*<sup>-/-</sup> mice (**Figure 41A**: unpaired two-tailed Student's *t* test,  $p = 0.0344$ ), and of *Edn2* receptors in Müller cells, endothelin receptor type B (*Ednrb*) (Jeon, Strettoi, and Masland 1998), at 12 months (**Figure 41B**: unpaired two-tailed Student's *t* test,  $p = 0.0251$ ). These events, in turn, can stimulate the expression of fibroblast growth factor 2 (*Fgf2*), which has also been shown to delay photoreceptor degeneration (H. Yamada et al. 2001; S. Joly et al. 2008; B. Spencer et al. 2001). Given these considerations, we analyzed *Fgf2* mRNA levels and found an upregulation at 12 months (**Figure 41B**: unpaired two-tailed Student's *t* test,  $p < 0.0001$ ).



These results suggest that the EDN2 survival signaling pathway is activated in *Faim*<sup>-/-</sup> retinas (**Figure 41C**).

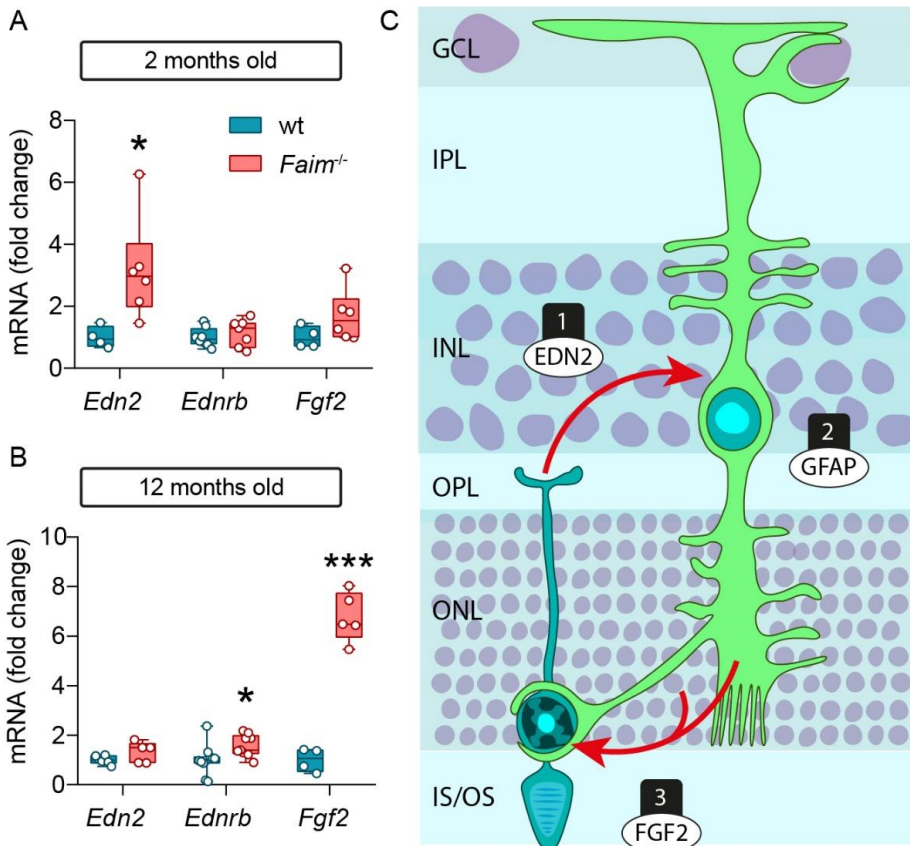


**Figure 41. Edn2 survival signaling loop is activated in *Faim*<sup>-/-</sup> mice. (A)** mRNA levels of *Edn2*, *Ednrb*, and *Fgf2* at 2 months, showing an increase in *Edn2*. **(B)** mRNA levels of *Edn2*, *Ednrb*, and *Fgf2* at 12 months, showing an increase in *Ednrb* and *Fgf2*. **(C)** Schematic representation of the EDN2-FGF2 hypothetical loop suggested by Rattner and Nathans (Rattner, A.; Nathans 2005). mRNA levels were assessed by qRT-PCR, and each symbol in the plots represents one retina (n = 4–7 mice/group). Expression levels were normalized to *Actb* and data are plotted relative to WT values for each gene. Each box plot extends from the 25<sup>th</sup> to the 75<sup>th</sup> percentile and the median is plotted as a line in the box. Whiskers represent min to max values, and dot plots are overlaid. Statistical analysis was performed using an unpaired two-tailed Student’s *t* test \* *p* < 0.05, and \*\*\* *p* < 0.005.

#### 4.1.10. Discussion

FAIM-S and FAIM-L play critical and distinct roles in neuronal outgrowth and survival. Nevertheless, FAIM function had never been studied *in vivo* in the CNS. Our analysis of the *Faim* co-expression network suggested that this gene is associated with the biological functions of photoreceptors and the retina. In the present study, we demonstrate the expression of both *Faim* isoforms in the retina for the first time, and we show that *Faim* depletion in mice leads to the accumulation of protein aggregates, retinal gliosis, leakage of the BRB, and photoreceptor death.

Photoreceptors, the light-sensitive neurons of the retina, are amongst the most specialized cells in the organism, rendering them highly vulnerable to any kind of stress. *Faim*<sup>-/-</sup> mice are viable and have a normal lifespan (J Huo et al. 2016), and loss of *Faim* is not enough to cause retinal degeneration at an early age. However, our data show that *Faim* depletion, without injury or stress-induction, can slowly but progressively damage the retina, culminating in photoreceptor death and retinal disorganization at 18 months. Consequently, after studying the earlier pathological events that may account for this late photoreceptor death, we found an aberrant accumulation of ubiquitinated protein aggregates, which was most notable in the GCL, INL and IS of photoreceptors. Accordingly, these experiments are consistent with previous results. In this respect, Kaku and Rothstein described how *Faim*-deficient cells accumulate ubiquitinated and aggregated proteins following oxidative stress *in vivo* (Hiroaki Kaku and Rothstein 2020), and that under the same oxidative conditions, FAIM is recruited to ubiquitinated complexes in WT cells. Those authors suggested that FAIM participates in the dynamics of protein aggregates by a mechanism that has yet to be elucidated. To expand these results, it would also be interesting to study the *Faim*<sup>-/-</sup> retina

under stress conditions that harm photoreceptors, such as light-induced damage (Bravo-Nuevo, Walsh, and Stone 2004).

Due to the unique anatomical distribution of the cytoplasm of photoreceptors, which is almost entirely found in the IS and outer segment (OS) compartments, quantification of ubiquitin-positive cells in the ONL was unattainable. However, our observation that the IS of photoreceptors in *Faim*<sup>-/-</sup> retinas showed an increase in ubiquitin expression has exciting implications. The IS is the major cytoplasmic compartment of the photoreceptor, where protein synthesis and the largest part of housekeeping functions take place. Therefore, it is reasonable to hypothesize that a disruption in the proteasome system of photoreceptors would result in the accumulation of misfolded proteins and ubiquitin aggregates in the IS.

The inability of neurons to undergo mitosis predisposes them to the cumulative pathogenic effects of protein misfolding and consequent aggregation (Mattson and Magnus 2006). Hence, it is imperative for neuronal cells such as photoreceptors to have good quality control mechanisms in place. Our data suggest that the sole absence of *Faim* causes a breakdown in protein quality control, which culminates in late photoreceptor death. The accumulation of protein aggregates in the retina is a major cause of cellular malfunction and it can trigger an inflammatory response, which can lead to retinal remodeling and photoreceptor death (Illing et al. 2002; Remé et al. 1998). Moreover, protein misfolding and aggregation are involved in several retinal dystrophies, including retinitis pigmentosa and age-related macular degeneration (Illing et al. 2002; Leger et al. 2011). These events resemble those in the brain, where numerous studies have demonstrated how ubiquitin-positive inclusions cause the loss of neuronal cells (Hara et al. 2006), and that protein aggregation is a common pathological hallmark of



neurodegeneration. For instance, abnormal amyloid beta and tau aggregation, disruption of the proteasome, and ubiquitin immunoreactivity in neurofibrillary tangles are characteristic features of Alzheimer's disease (Brion et al. 1985; Brion, Flament-Durand, and Dustin 1986; Sisodia et al. 1990; Harris, Jasem, and Licchesi 2020; Upadhyya and Hegde 2007). Given these considerations, research efforts into neurodegenerative diseases should focus on proteins that potentially play a role in protein aggregation, like FAIM.

Müller cells are the main resident glia of the retina and they exert many of the functions that in other CNS tissues are performed by astrocytes, oligodendrocytes or ependymal cells (Newman and Reichenbach 1996). Müller cells span the entire thickness of the retina and envelop every retinal cell type, thus providing structural and metabolic support. Under conditions of stress, such as protein aggregation, Müller cells are activated, triggering a reactive phenotype (A Bringmann, Reichenbach, and Wiedemann 2004), akin to astrocytes in the brain (Kato et al. 1998). Müller cell gliosis is characterized by morphological, phenotypical, and biochemical changes, such as GFAP upregulation and the release of pro-inflammatory cytokines like IL-1 $\beta$  and TNF- $\alpha$  (Sarthý and Fu 1989). These events are prompted in the form of acute gliosis to protect the nervous tissue. However, uncontrolled gliosis for prolonged periods in response to an unceasing event with multiple repercussions, like loss of FAIM, might harm the retina. Indeed, our data show how GFAP is already increased in *Faim*<sup>-/-</sup> retinas at 2 months of age, and that GFAP expression and immunoreactivity are even greater at 12 months. These alterations are emphasized by the increase in IL-1 $\beta$  immunoreactivity and *Tnf- $\alpha$*  mRNA expression detected in *Faim*<sup>-/-</sup> retinas, which can boost the retinal inflammatory response (Kany, Vollrath, and Relja 2019). The chronicity of reactive gliosis is likely to be one of the main

pathogenic events in *Faim*<sup>-/-</sup> retinas, as it is proven to occur in many neurodegenerative diseases (González et al. 2014).

Müller cells are also a major modulator of the neurovascular structure and an important player in the maintenance of BRB homeostasis (Tout et al. 1993). These cells envelop blood vessels, and thanks to this intimate anatomical association, they can rapidly perceive homeostatic changes and give an appropriate response. On the other hand, chronic gliosis can induce vascular permeability, leukocyte adhesion and leakage of blood into the retinal parenchyma, further exacerbating disease progression (Tout et al. 1993; Coughlin, Feenstra, and Mohr 2017). We examined retinal whole-mounts, which allowed us to visualize the three capillary plexuses and spatially analyze this information. Although we already found signs of vascular leakage in *Faim*<sup>-/-</sup> retinas at 2 months, it was not until 12 months that we discovered a substantial number of prominent extravasations. Surprisingly, every extravasation detected in the *Faim*<sup>-/-</sup> mice could be traced back to one area, namely the SVP. The SVP is found mainly in the GCL, where Müller cell endfeet and astrocytes converge (Coorey et al. 2012). We have shown how GFAP immunolabeling in Müller cell endfeet (and thus in the surroundings of the SVP) is heavily increased. This finding strengthens the hypothesis that reactive gliosis disrupts microvascular homeostasis in *Faim*<sup>-/-</sup> retinas. This vascular permeability is accompanied by an increase in the expression of cell adhesion molecules like *Vcam-1* and *Vegfa*, thus confirming the expansion of the inflammatory environment. BRB dysfunction and capillary permeability are potentially harmful and are typical attributes of microvascular diseases like macular oedema and diabetic retinopathy, in which photoreceptor viability is also affected (McDowell et al. 2018; Cunha-Vaz 2017).

To monitor retinal health conditions in such a short-term manner, Müller cells are thought to be able to specifically sense injuries on the basis of signaling molecules released from retinal cells (Senut, Gulati-Leekha, and Goldman 2004; Montgomery, Parsons, and Hyde 2010; Fimbel et al. 2007). Many studies have implicated Müller cells in neuroprotective pathways for photoreceptor survival (Andreas Bringmann et al. 2009; Goh et al. 2016). In particular, EDN2 is produced by photoreceptors in a wide variety of retinal injuries and early-stage diseases, and it has been proposed as an early biomarker for diabetic retinopathy (Binz et al. 2016). When we checked for the presence of this molecule in *Faim*<sup>-/-</sup> retinas, we found that both EDN2 immunoreactivity and mRNA expression were increased at 2 months, implying that photoreceptors may have already been impaired by harmful stimuli. We also distinguished a unique EDN2 pattern at 12 months. Surprisingly, at this age, EDN2 enveloped the soma of cone (but not rod) photoreceptors, which were identifiable through their distinctive euchromatin and heterochromatin conformations (Hughes et al. 2017; Solovei et al. 2009). Of note, in a microarray dataset of the *Nrl*<sup>-/-</sup> retinal model, which causes the conversion of rods into cones, both *Faim* and *Edn2* were upregulated as early as P21 (Hsiao et al. 2007). This finding suggests that FAIM has a specific function in cone photoreceptors. Cones mediate light perception in the daytime and are sensitive to color, whereas rods are more sensitive to light and they function for night vision. Accounting for roughly 3% of photoreceptors in humans and WT mice, cones are far sparser than rods in the retina (Jeon, Strettoi, and Masland 1998). If *Faim* was particularly important for cone survival, it would explain the reduced—but significant—number of apoptotic nuclei found in the *Faim*<sup>-/-</sup> retinas. Future studies assessing *Faim* levels in retinal pathologies that present cone degeneration might prove important.

Furthermore, EDN2 has been shown to trigger a neuroprotective response in Müller cells through EDNRB (S. Joly et al. 2008), and *Ednrb* mRNA levels were also upregulated in *Faim*<sup>-/-</sup> mice at 12 months. Rattner and Nathans (Rattner, A.; Nathans 2005) found a large increase in *Edn2* transcripts in a retinal degeneration slow (rds) mouse model. In that study, they proposed that photoreceptor-derived EDN2 functions as a general stress signal that activates Müller cells through EDNRB. This signal, in turn, can increase their sensitivity to EDN2 by upregulating EDNRB, inducing a gliotic response via GFAP upregulation. Those authors also suggested that, to support the survival of viable photoreceptors, activated Müller cells and/or other cells produce and release FGF2, which we also found upregulated in our model at 12 months. Moreover, FGF2 has been implicated in photoreceptor paracrine pathways linked to neuroprotective roles (Gao and Hollyfield 1996; Sandrine Joly et al. 2007; Wen et al. 1995). In animal models of inherited photoreceptor degeneration and light-induced retinal degeneration, FGF2 overexpression delays photoreceptor death (B. Spencer et al. 2001; H. Yamada et al. 2001). Also, in the *Ndp* knockout mouse (in which *Faim* is downregulated (Q. Xu et al. 2004)), *Edn2* and *Ednrb* expression were greatly increased. Nevertheless, to ascertain the causality between *Edn2* expression as a response to photoreceptor injury and reactive gliosis, further studies are required.

In addition to *Edn2* and *Fgf2*, we observed the upregulation of *Xiap*, which has also been linked to early neuroprotection in the retina. Its interaction with *Faim* has largely been characterized, but several studies propose that it also exerts important functions in the retina. In fact, *Xiap* mediates neuroprotection in various retinal pathologies and injuries such as retinal ischemia (Renwick et al. 2006), and its rapid delivery after retinal

detachment limits the acute damage that photoreceptors undergo in rats (Zadro-Lamoureux et al. 2009) and a feline model (Wassmer et al. 2017).

In summary, here we report that *Faim*<sup>-/-</sup> mice present photoreceptor neurodegeneration that is preceded by the aggregation of ubiquitinated proteins, GFAP upregulation and Müller cell activation, similarly to the aforementioned rds mouse models (Ekström et al. 1988). Over-compensatory expression of acute-phase proteins originally produced to support neuron survival, like EDN2, may give rise to chronic gliosis through the long-term activation of Müller cells. This activation, in turn, accounts for the absence of retinal homeostasis and leakage of the BRB, which contribute to this positive feedback loop. These pathogenic events converge into the perfect storm, culminating in photoreceptor death in *Faim*<sup>-/-</sup> retinas.

Since retinal alterations precede numerous pathological mechanisms in brain disorders (London, Benhar, and Schwartz 2013), finding biomarkers in the retina may facilitate the early diagnosis of neurodegenerative pathologies. Collectively, our results suggest that *Faim* plays a key role in the maintenance of retinal homeostasis, making it a plausible early marker for late photoreceptor and neuronal degeneration.

# Chapter Two

*“If you are not failing, you are not pushing  
boundaries”*

Elizabeth Blackburn  
Nobel Prize Winner, 2009



## Chapter Two

### 4.2.1. Rationale

In the previous chapter we described the histopathological alterations in Faim knockout (Faim KO) retinas, which present ubiquitin aggregates, chronic gliosis, vascular leakage, and photoreceptor cell death. In view of this, we wanted to study Faim KO retinas at the functional level and explore the possible mechanisms in which FAIM is involved.

It is important to highlight the role of the ubiquitin-proteasome system (UPS) as one of the primary mechanisms by which neuronal proteins are degraded to maintain cellular homeostasis (Flick and Kaiser 2012). Of interest, it has also been reported that ubiquitin participates in regulating the levels of mammalian phototransduction proteins in the retina (M. S. Obin et al. 1996a).

More recent studies have also shown ubiquitination as a regulator of light and dark-dependent translocation of proteins involved in phototransduction in rod photoreceptors. This process has been suggested to contribute to light and dark adaptation, given that signal amplification in the phototransduction cascade seems to be reduced after translocation (Majumder et al. 2013; Chaya et al. 2019). Nonetheless, the mechanism underlying this process has yet to be fully elucidated.

Phototransduction and light-dependending protein translocation are fine processes that need its partakers to act on time and to adjust perfectly on its role. Given that FAIM is involved in ubiquitination events and that FAIM knockout present a neurodegenerative phenotype in the retina, we assessed the potential role of FAIM in retinal function and phototransduction



modulation. We also studied whether these functional alterations could be linked to the role of FAIM in ubiquitinating events.

#### 4.2.2. Loss of FAIM leads to age-related rod photoreceptor and retinal ganglion cell defects

To assess whether the absence of FAIM in the retina leads to functional deficits, we performed dark-adapted (scotopic) and light-adapted (photopic) ERG assays. In previous studies we observed that neurodegeneration in Faim KO retinas occurred gradually and peaked at 18 months, when photoreceptor cell death was detected. In sight of this, we first analysed the responses of 18-month-old Faim KO mice.

Upon a light stimulus, the retinal cells produce electrical activity that can be captured through ERG (explained in detail in Methods Section, *page 72*). Responses from photoreceptors and bipolar cells elicit an electrical activity called a-wave and b-wave, respectively. Rod photoreceptors and rod-associated bipolar cells respond both in scotopic and mixed conditions, while cone photoreceptors and cone-associated bipolar cells only respond to photopic conditions. Scotopic and mixed ERG analyses revealed reduced amplitudes in both a-wave and b-wave (**Figure 42A**), suggesting that FAIM is important for maintenance of rod function during ageing. To detect a clean and unambiguous response of RGCs electrical activity after light stimulation, a low light intensity ( $-4.0 \log(\text{cd}\cdot\text{s}\cdot\text{m}^{-2})$ ) was used, which gives a positive scotopic threshold response (pSTR). At 18 months, the pSTR peak amplitude of Faim KO mice was reduced in comparison with its WT counterparts, suggesting that RGCs are compromised (**Figure 42A**).

Oscillatory potentials are ERG waveforms of high frequency and low amplitude that stem from the b-wave. They are obtained by bandpass filtering at 100 Hz the ERG responses at  $1.5 \log \text{cd}\cdot\text{s}\cdot\text{m}^{-2}$  of light intensity. At 18 months, neither OP1, OP2 or OP3 amplitudes were altered in Faim KO mice,

## Scotopic and photopic ERG at 18 months

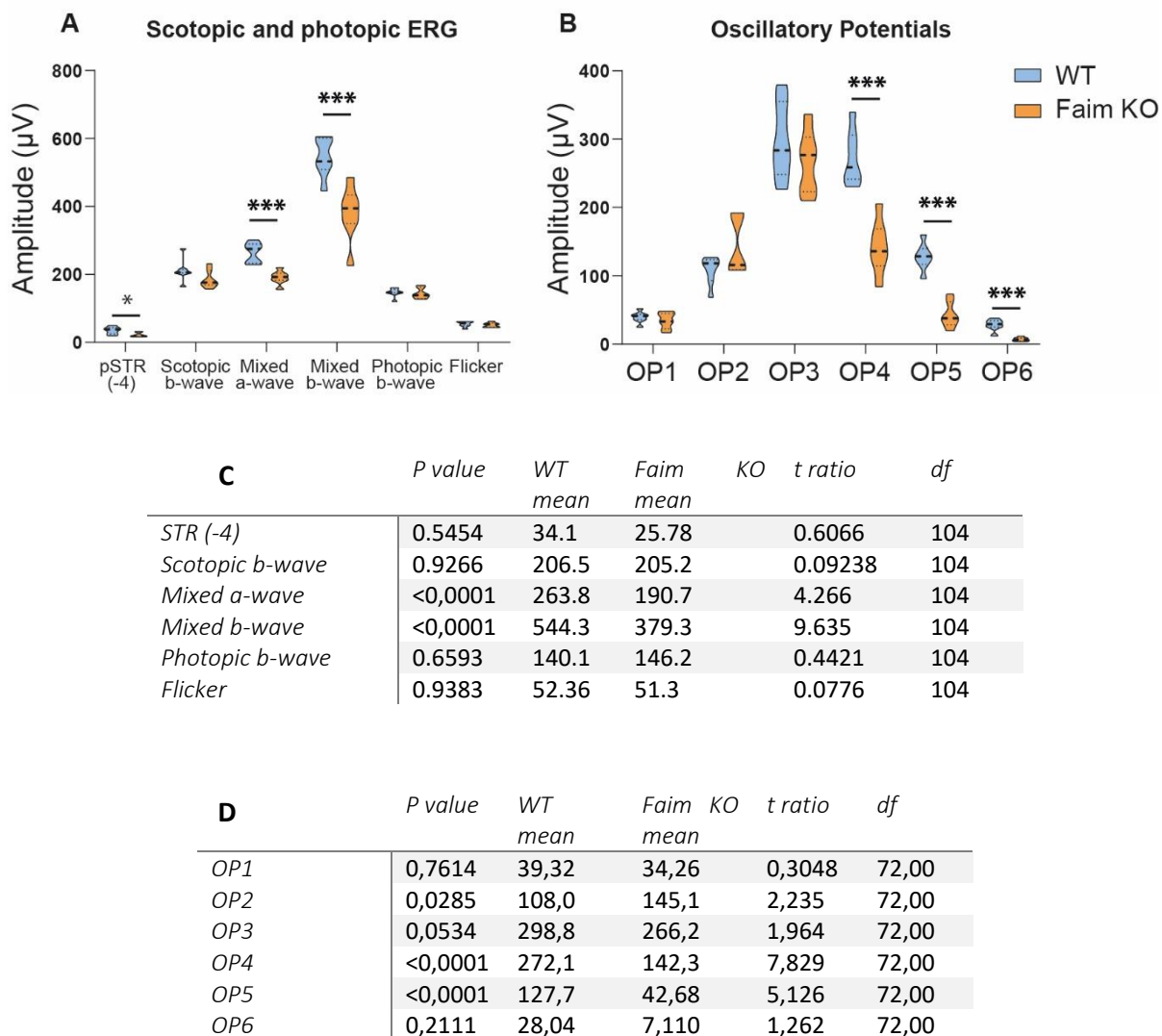


**Figure 42. Photoreceptors, bipolar cells and RGCs are altered in Faim KO mice at 18 months. (A)** Summary of ERG analysis of pSTR (-4) representing RGCs, scotopic b-wave, mixed a-wave, mixed b-wave, photopic b-wave and flicker (20 Hz). **(B)** Summary of the amplitudes recorded on ERG of the oscillatory potentials. OP1 corresponds to photoreceptors, OP2 and OP3 to bipolar and horizontal cells and OP4-6 to amacrine and RGCs (n = 7-14 mice/group). Each violin plot extends from the min to max values, the median is represented by a thick dashed line, and quartiles are represented by thin dotted lines. **(C)** Table with the results of statistical analysis using Student's t test of summary graphs. **(D)** Table with the results of statistical analysis using Student's t test of the oscillatory potentials. To summarize, data were plotted together \* p < 0.05, \*\* p < 0.01, \*\*\* p < 0.005.

but there was a significant decrease in OP4, OP5 and OP6 (see **Figure 42B**). OP4 to OP6 are thought to be linked to amacrine and RGCs, as they are the only neurons in the retina able to fire action potentials. These results suggest that the ganglion cell layer (GCL) may be also altered in Faim KO mice.

However, under photopic conditions, which are used to study cone photoreceptor pathways, b-wave amplitudes remained unchanged. Similarly, the rod-saturating flicker ERG recorded no alterations in Faim KO mice (see **Figure 42A**), indicating cone photoreceptors are not impaired.

We also checked the b:a ratio in scotopic conditions, which is used to assess electronegative ERGs and whether system dysfunction is found post-phototransduction, and found no alterations (**Figure 43**), indicating alterations stem from phototransduction.

Given that neurodegeneration in Faim KO retinas occurs progressively, we wondered whether retinal function could be already impaired at younger ages, when Faim KO mice already present a gliotic phenotype. As shown in **Figure 44**, retinal function was examined at 2 months but no alterations in amplitudes were found in either scotopic, photopic, pSTR, flicker or oscillatory potentials ERG analysis, suggesting that retinal functional alterations in Faim KO mice, just as photoreceptor cell death, is associated to aged retinas.

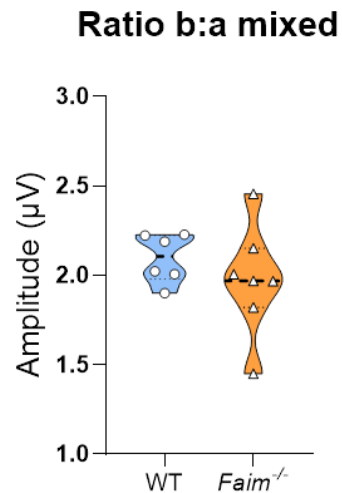


**Figure 43. b:a ratio is normal in Faim KO mice.** Ratio of mixed b-wave and mixed a-wave graphed as amplitude. Data are represented as violin plots. Each dot corresponds to a retina, the median is represented by a thick dashed line, and quartiles are represented by thin dotted lines. Below is shown a table with Student's t test statistical analysis, p value = 0.3949.

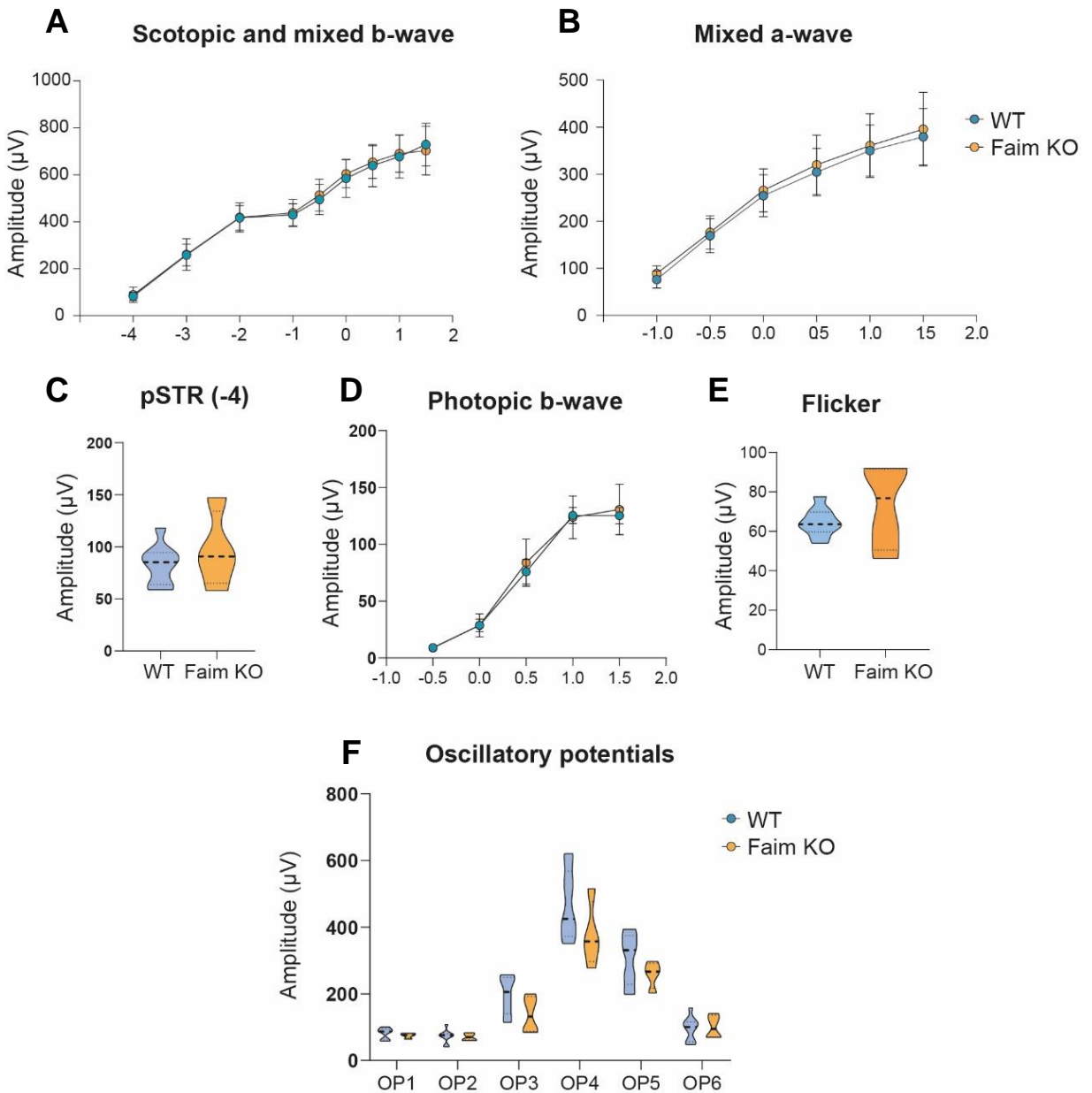


**Figure 44 Faim KO mice ERG analyses are not altered at 2 months of age.** ERG analyses of 2-month-old Faim KO mice. **(A)** Amplitudes of scotopic and mixed b-wave representing bipolar cells, ranging from -4 to 2 log cd-s-m<sup>-2</sup>. **(B)** Amplitudes of mixed a-wave representing photoreceptor cells, ranging from -1 to 1.5 log cd-s-m<sup>-2</sup>. **(C)** Amplitudes of pSTR at -4 log cds m2 representing RGCs. **(D)** Amplitudes from photopic b-wave responses ranging from -0.5 to 2 log cd-s-m<sup>-2</sup>, representing cone photoreceptors. **(E)** Flicker responses at Hz, representing cone photoreceptors. **(F)** Oscillatory potentials obtained from XXXX. Each violin plot extends from the min to max values, the median is represented by a thick dashed line, and quartiles are represented by thin dotted lines. Statistical analysis was used performing Two-way ANOVA.

Besides being associated with ageing processes, retinal degeneration can also be caused or influenced by extrinsic environmental conditions such as light damaging conditions (Hao et al. 2002; Christian Grimm and Remé 2013). Light stress induces the expression of endogenous molecular factors that confer protection to the retina and the eye (Pearson and Ali 2018; C. Liu et al. 1998). We previously showed that Endothelin-2 and FGF2 are upregulated in Faim KO mice without any additional stress. Interestingly, these proteins have been proposed to act as retinal neuroprotective factors after light damage exposure (Ueki et al. 2009; S. Joly et al. 2008; C. Liu et al. 1998). In sight of this, we decided to study whether Faim KO mice show increased sensitivity to light damage than its WT counterparts. To test whether we could emulate this impairment through an environmental stress, we exposed 2-month-old mice to light damage (LD). After applying 8h of continuous light exposure at 10,000 lux, we did not find any decrease in ERG amplitudes in scotopic ERG nor photopic ERG or OP (**Figure 45**).

Nonetheless, even though amplitudes under scotopic and photopic conditions were not significantly different, we observed unusual ERG shapes in Faim KO mice after light stimuli (**Figure 45A**).

For proper retinal function, photoresponse needs to terminate, and electrical activity must return to its resting state after light levels drop. ERG recordings showed that electrical activity decay differed between Faim KO and WT mice (**Figure 46A**). Hence, we analysed Faim KO and WT amplitudes at 200 ms after flash exposure of different intensities. Analysis revealed that Faim KO retinas are still firing electrical responses (**Figure 46B**) when WT have already returned to resting state. These results suggest that Faim KO mice could have a defective photoreceptor deactivation after stimulation, indicating alterations in adequate photoresponse termination.



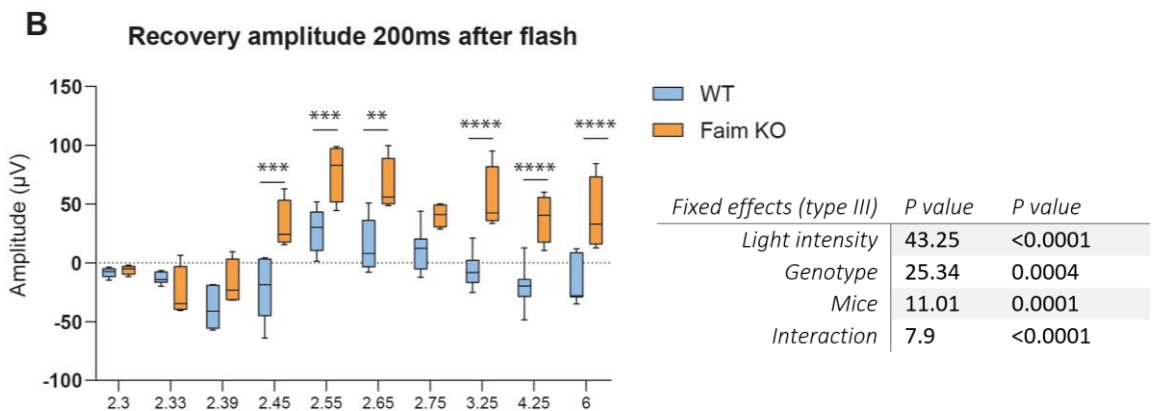
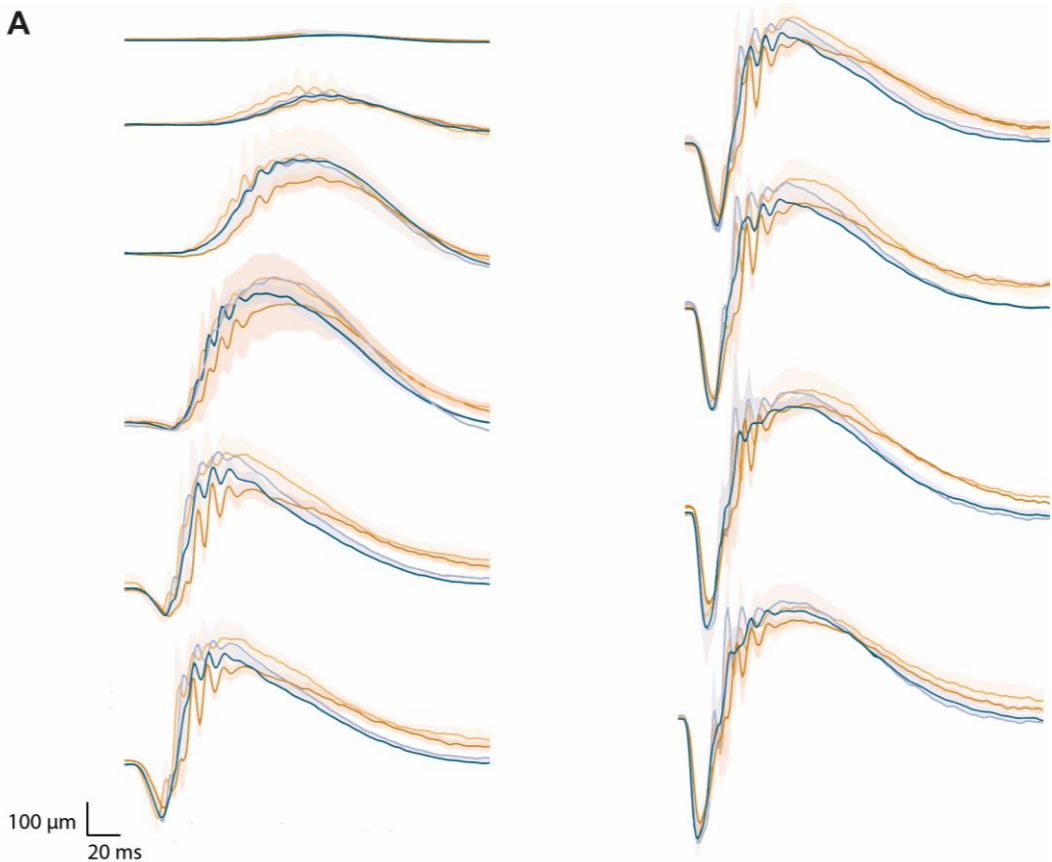


**Figure 46. Recovery amplitude in Faim KO mice is higher at 200 ms after light flash.** (A) From top to bottom and left to right, ERG responses from different light intensities are represented from WT and Faim KO mice before and after light damage. It can be observed how the shape in the recovery time of Faim KO differs from WT mice. (B) Recovery amplitude of WT and Faim KO mice pre-light damage 200 ms after the flash was evoked. The source of variation (light intensity, genotype, its interaction, and mice) and the total % of variation that accounts for the results and its p value are represented. Three-way ANOVA with repeated measures was performed. \*\*  $p < 0.01$ , \*\*\*  $p < 0.005$ , #  $p < 0.001$ .



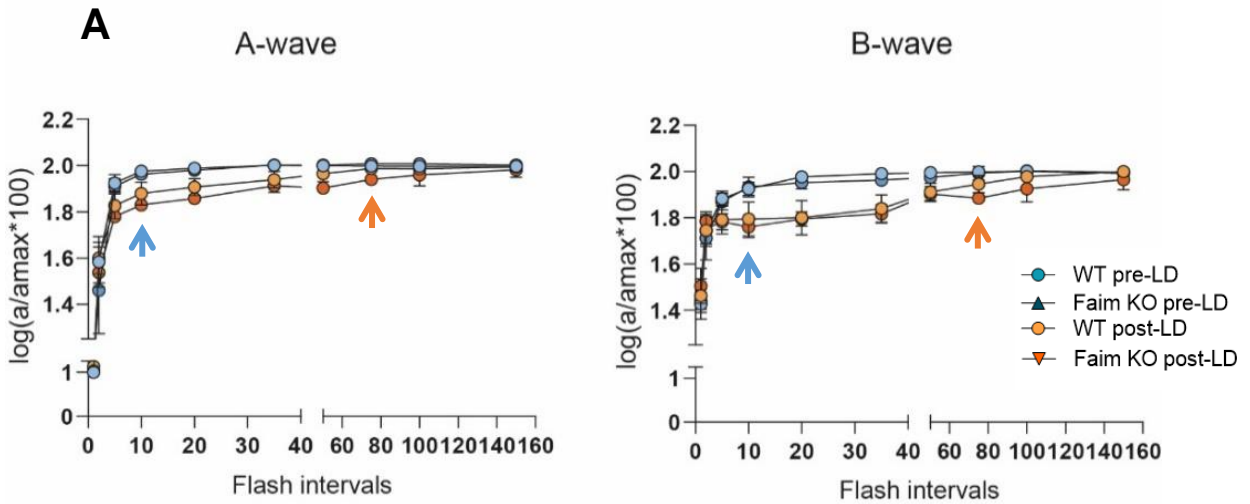
### 4.2.3. Faim depletion causes a delayed dark adaptation

The difference in amplitude shapes in scotopic ERG of Faim KO in comparison to WT mice (**Figure 46**) prompted us to study whether dark adaptation in Faim KO retinas was hindered, as this could be the consequence of a delayed photoresponse deactivation. To assess this, a double-flash protocol was performed to measure the photoresponse recovery at both 2 (**Figure 47**) and 18 months of age (**Figure 48**). We used ten different time intervals in between the two flashes to assess the rod recovery time.

The following full-field ERG resolved that Faim KO mice present a severe delay in dark-adaptation at both ages in comparison to WT mice (**Figure 47**, **Figure 48**). By 10 seconds, 2-month-old WT mice were able to recover and elicit the same amplitudes as the first flash (**Figure 47**, blue arrows), while it took approximately 75 seconds for Faim KO mice to achieve full photoreceptor and bipolar cell recovery (**Figure 47**, orange arrows).

We also studied whether light damage exacerbated this delay at 2 months of age given the reported effects of this stress specifically in photoreceptors and photoreceptor light and dark adaptation. Although the power size of the light damage effect may not be evident (**Figure 47A**), it is significant in photoreceptor response (**Figure 47B**, a-wave, light damage,  $p=0.0014^{**}$ ), but not at the bipolar response level (**Figure 47C**, b-wave, light damage,  $p=0.2409$ ). Moreover, the interaction between genotype and light damage in the a-wave is significant too (**Figure 47B**, a-wave, genotype \* light damage,  $p=0.013^{*}$ ), and thus observing our results **Figure 47A**, this indicates that light damage effect is more determinant in Faim KO dark adaptation than in WT mice.

## Dark adaptation at 2 months pre-LD and post-LD



### B

Three-way ANOVA, A-wave at 2 months old

Fixed effects (type III)	P value	P value	F (DFn, DFd)
Light intensity	<0,0001	****	F (9, 126) = 664,4
Genotype	<0,0001	****	F (1, 42) = 34,72
Light damage	0.0014	**	F (1, 14) = 15,73
Light intensity x Genotype	<0,0001	****	F (9, 42) = 7,364
Light intensity x Light damage	0.361	ns	F (9, 42) = 1,134
Genotype x Light damage	0.013	*	F (1, 42) = 6,736
Light intensity x Genotype x LD	0.4218	ns	F (9, 42) = 1,045

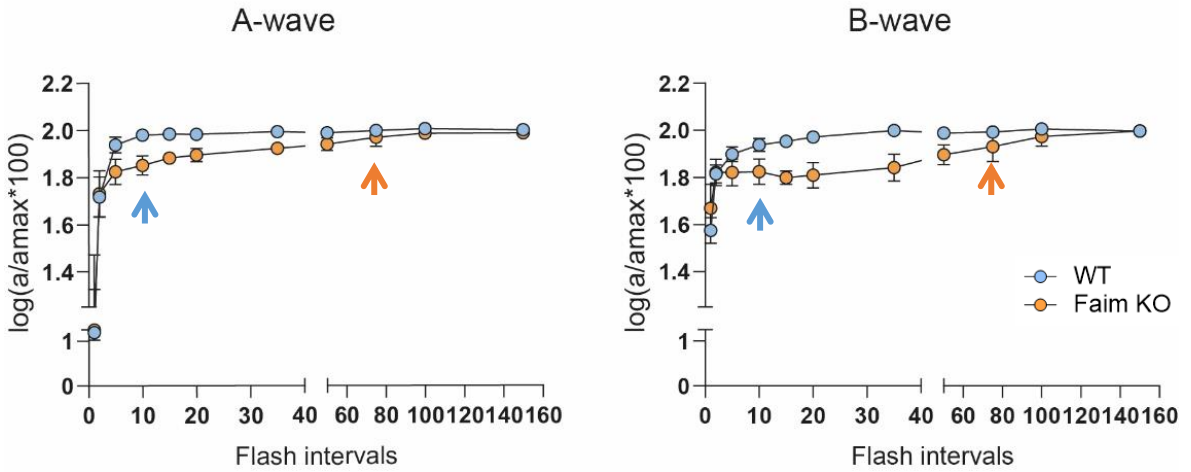
### C

Three-way ANOVA, B-wave at 2 months old

Fixed effects (type III)	P value	P value	F (DFn, DFd)
Light intensity	<0,0001	****	F (9, 126) = 357,7
Genotype	<0,0001	****	F (1, 42) = 45,60
Light damage	0.2409	ns	F (1, 14) = 1,500
Light intensity x Genotype	<0,0001	****	F (9, 42) = 20,90
Light intensity x Light damage	0.3724	ns	F (9, 42) = 1,117
Genotype x Light damage	0.8513	ns	F (1, 42) = 0,03559
Light intensity x Genotype x LD	0.1949	ns	F (9, 42) = 1,459

**Figure 47. Faim KO mice show a great delay in dark adaptation in comparison to WT mice at 2 months, but no differences are found after LD. (A)** Dark adaptation of WT and Faim KO mice at 2 months of age before and after light damage. Mice were dark-adapted overnight, and after anaesthesia double flash protocol was used to study a delay in dark adaptation using the following time intervals (s): 1, 2, 5, 10, 20, 35, 50, 75, 100, 150. Amax corresponds to the ERG responses after the first flash, and A corresponds to the second response after the second flash. Data are represented as  $\log(a/a_{max}) \cdot 100$  in XY table, and statistical analysis was performed using three-way ANOVA. Results are depicted in **(B)** for the a-wave and in **(C)** for the b-wave. 6-7 mice were for pre-LD analyses, and 4 mice were used for post-LD analyses.

## Dark adaptation at 18 months



### Two-way ANOVA, A-wave at 18 months

Fixed effects (type III)	P value	P value	F (DFn, DFd)
Interval time	<0,0001	****	F (1,516, 17,43) = 186,8
Genotype	0.0189	*	F (1, 12) = 7,353
Interval time x Genotype	0.0033	**	F (10, 115) = 2,849

### Two-way ANOVA, B-wave at 18 months

Fixed effects (type III)	P value	P value	F (DFn, DFd)
Interval time	<0,0001	****	F (3,714, 42,71) = 110,3
Genotype	0.0007	***	F (1, 12) = 20,62
Interval time x Genotype	<0,0001	****	F (10, 115) = 16,51

**Figure 48. Faim KO mice show a great delay in dark adaptation in comparison to WT mice at 18 months.** Dark adaptation of WT and Faim KO mice at 18 months of age. Mice were dark-adapted overnight, and after anaesthesia double flash protocol was used to study a delay in dark adaptation using the following time intervals (s): 1, 2, 5, 10, 20, 35, 50, 75, 100, 150. Amax corresponds to the ERG responses after the first flash, and A corresponds to the second response after the second flash. Arrowheads point towards the timepoint in which amax response was recovered (blue: WT, orange: Faim KO). Data are represented as  $\log(a/a_{max}) \cdot 100$  in XY table, and statistical analysis was performed using two-way ANOVA (depicted below) (n=6-7 mice/group).

#### **4.2.4. Light-dependent Arrestin-1 translocation is delayed in Faim KO mice**

To study the mechanism that could be lying beneath the delay in dark adaptation in Faim KO mice, we aimed to study the photoreceptor desensitizing process.

After dark-adaptation and upon light reception, Arrestin-1 and Transducin- $\alpha$  are translocated between the inner segment (IS) and the outer segment (OS) of photoreceptors in opposite directions (Mendez et al. 2003; Nair et al. 2005) (**Figure 49A**).

To assess whether this translocation is altered in Faim KO mice, Arrestin-1 (**Figure 49B**) and Transducin- $\alpha$  (**Figure 49C**) immunolocalization were examined in retinal sections. To this end, mice were dark-adapted overnight and exposed to 2,500 lux of white LED light for different periods of time.

Arrestin-1 in dark-adapted mice that were not exposed to light was completely localized in the IS both in WT and Faim KO mice. However, after 15 minutes of light exposure, 70% of Arrestin-1 was translocated to the OS in WT mice, while Faim KO mice roughly exhibited 20% of Arrestin-1 to the OS (**Figure 49D**). However, Transducin- $\alpha$  translocation levels from the OS to the IS upon light exposure were similar between Faim KO and WT mice (**Figure 49F**).

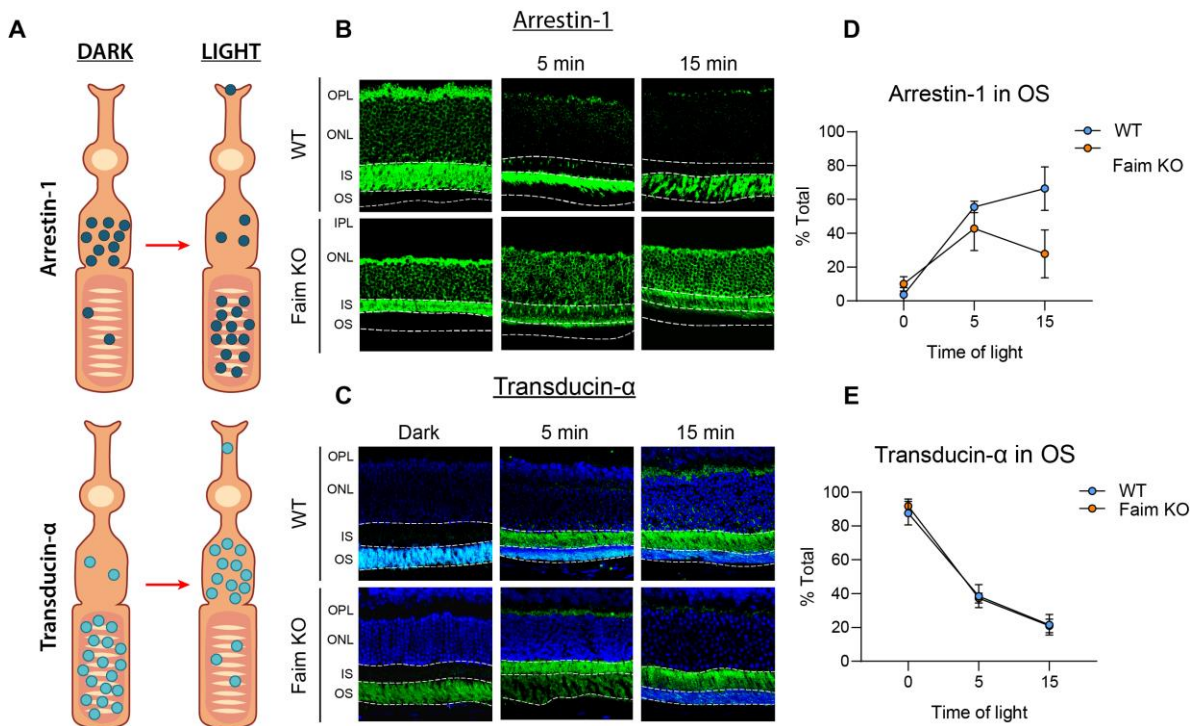


**Figure 49. Light dependent arrestin-1 and Transducin-1 localization at dark and translocation upon light reception for 5 and 15 minutes. (A)** Diagram representing the translocation of Arrestin-1 and Transducin- $\alpha$  in dark-adapted retinas that are exposed to light. **(B, C)** Retinal sections (4  $\mu$ m) were obtained from 2-month-old WT and Faim KO mice and immunofluorescence was performed with Arrestin-1 **(B)** or Transducin- $\alpha$  **(C)**. Mice were dark-adapted overnight, and pupils were dilated with tropicamide 1%. Mice were either euthanised in the dark or exposed to light for the indicated times. **(D)** Arrestin-1 translocation in Faim KO mice was delayed in comparison to WT mice, but Transducin- $\alpha$  translocation **(E)** remained normal. (n=4 mice/group). Data are represented as XY graphs, X= total % of protein translocated in the OS, Y= time of light exposure.

Moreover, we also checked Arrestin-1 and Transducin- $\alpha$  protein levels at 2 and 18 months of age and found a reduction of both Arrestin-1 and Transducin- $\alpha$  protein levels at 18 months (**Figure 50**).

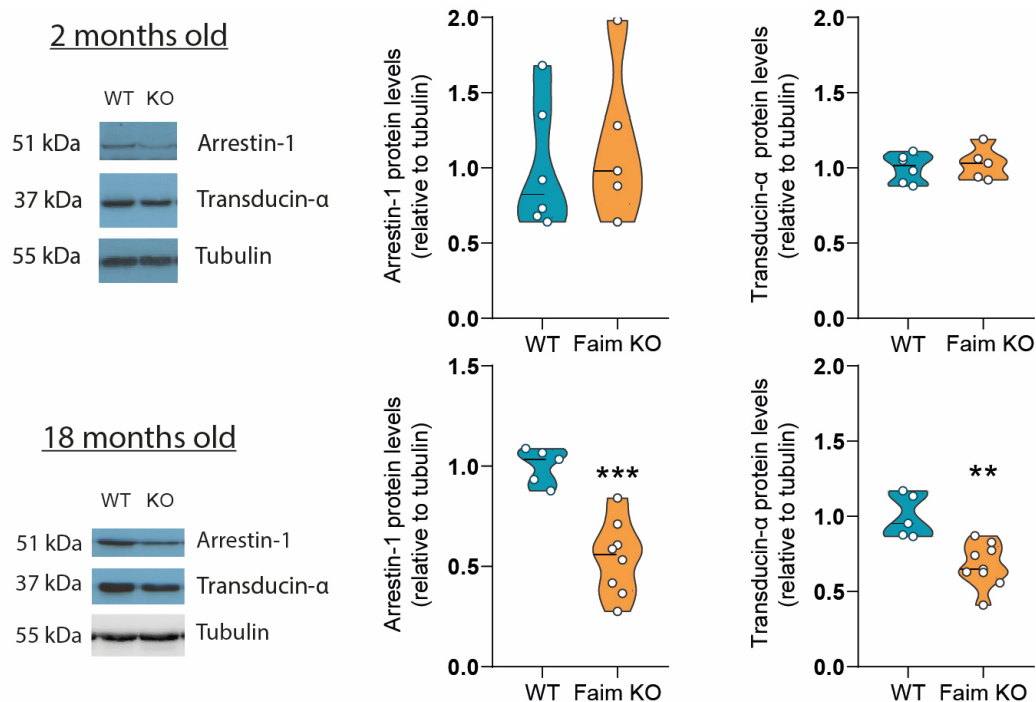


**Figure 50. Protein levels of Arrestin-1 and Transducin- $\alpha$  are reduced at 18 months in Faim KO mice, but not at 2 months.** Expression of Arrestin-1 and Transducin- $\alpha$  at 2 and 18 months of age in WT and Faim KO mice. Protein levels were normalized with tubulin- $\alpha$  and quantified in ImageJ. Data are plotted relative to WT values. Data are represented in violin plots. Each violin plot extends from the min to max values, the median is represented by a thick dashed line, and quartiles are represented by thin dotted lines. Statistical analysis was performed using Student's t test. \*\*  $p < 0.01$ , \*\*\*  $p < 0.005$ .

#### 4.2.5. Both FAIM isoforms prevent Arrestin-1 ubiquitination *in vitro*

To perform its anti-apoptotic function, FAIM regulates XIAP autoubiquitination by blocking its E3 ligase domain (Weissman, Shabek, and Ciechanover 2011; Martínez-Mármol et al. 2016; Moubarak et al. 2013). This affinity binding stabilizes the levels of XIAP and allows its ultimate function:

the inhibition of caspase-3 (Moubarak et al. 2013). Members of the Arrestin-1 family have also been found as a target of ubiquitination for signalling purposes, and E3 ubiquitin ligase proteins have been found to act as Transducin- $\alpha$  translocation modulators during light/dark adaptation (Taro Chaya, Ryotaro Tsutsumi, Leah Rie Varner, Yamato Maeda, 2019).

Since ubiquitination has been reported as a regulator of light and dark-dependent translocation of proteins involved in phototransduction in rod photoreceptors, and FAIM is a regulator of XIAP by ubiquitination, we tested whether FAIM could be associated to Arrestin-1 ubiquitination events. On that account, HEK293T cells were transfected with 6xHis-Ubiquitin encoding plasmid together with Arrestin-1-HA alone or Arrestin-1-HA with either FAIM-L-FLAG or FAIM-S-FLAG (**Figure 51**).

After ubiquitin immunoprecipitation and in the condition in which neither FAIM-L or FAIM-S were co-expressed, Arrestin-1-HA ubiquitination was abundant. However, FAIM-L and FAIM-S co-expression almost completely abrogated Arrestin-1-HA ubiquitination (**Figure 51**). Same ubiquitination assay was performed under the effects of inhibitor of proteasome MG132. As shown in the right panel, this condition increased the levels of ubiquitinated Arrestin-1 co-expressed with FAIM-L and FAIM-S, indicating that at least some of this ubiquitination is degradative via the proteasome.

Altogether, this result suggests that that both FAIM isoforms can negatively regulate Arrestin-1 ubiquitination and therefore play a role on the retinal phototransduction signalling.

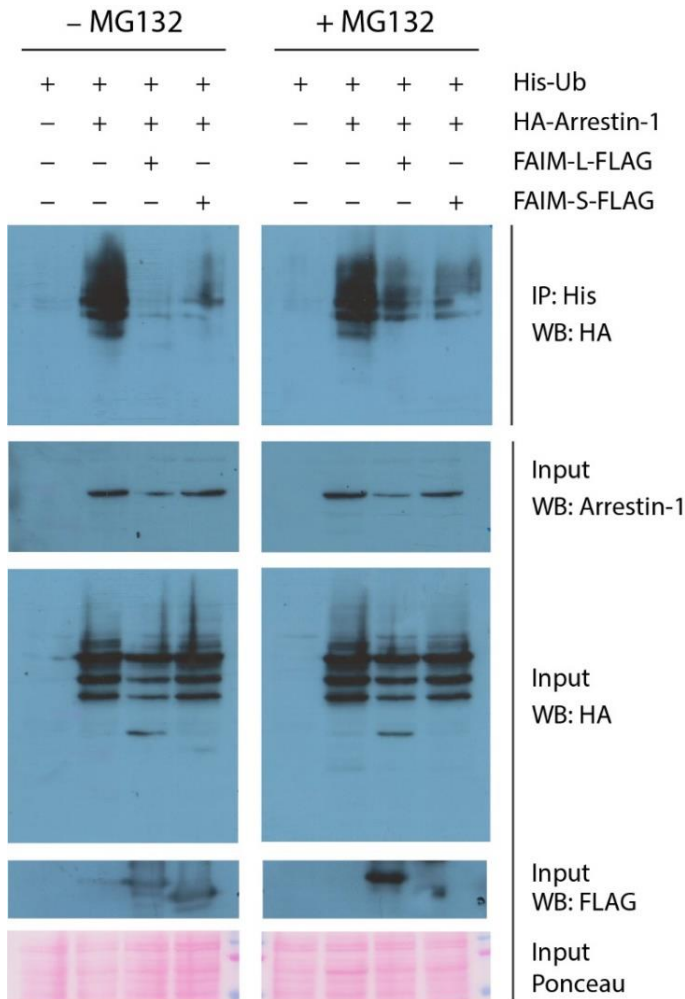


**Figure 51. FAIM-S and FAIM-L block Arrestin-1 ubiquitination *in vitro*.** HEK293T cells were transfected with the described plasmids, in the presence or absence of MG132 treatment as indicated. Successful transfection was confirmed by immunoblotting for HA and FLAG for Arrestin-1 and both FAIM-L and FAIM-S expression, respectively. Ponceau staining was used to check protein loading. Ubiquitin-His pull-down membrane was immunoblotted with HA. Evident ubiquitination is observed in the condition where Arrestin-1 is expressed alone with ubiquitin, and a significant decrease of ubiquitin is found both in FAIM-L and FAIM-S conditions.

#### 4.2.6. Photoreceptors in Faim KO mice are more sensitive after light damage

As mentioned above, functional alterations on standard scotopic and mixed ERG analyses were only observed in aged Faim KO mice, and 8h of light damage did not induce significant functional alterations in young mice. Retinal neurodegeneration and a decrease in its functionality are commonly associated to ageing processes. We previously described that aged retinas



with FAIM deficiency show increased retinal gliosis, accumulation of ubiquitinated aggregates, breakdown of the blood-retinal barrier and photoreceptor cell death (Sirés et al. 2021), so we hypothesized that Faim KO mice may be more susceptible to these alterations at early ages after stress induction.

There are several models that mimic degenerative retinal diseases, such as light-induced retinal damage (LIRD). These LIRD models have been used to study natural ageing processes, retinal pathologies like age-related macular disease (AMD) and retinitis pigmentosa (RP) (Christian Grimm and Remé 2019; 2013; Krigel et al. 2016; J. Yang et al. 2022), which are characterised by photoreceptor cell death.

To evaluate whether light stress renders Faim KO mice more sensible to neurodegenerative mechanisms, we exposed mice to cool LED light at 10,000 Lux for 8h and 24h and after two weeks we analysed the effects. As shown in **Figure 52A** after 8h of LIRD, Faim KO mice already exhibited accumulation of ubiquitinated proteins. We also studied retinal gliosis and found an increase in GFAP immunoreactivity (**Figure 52B**).

To determine the effect of LIRD in cell death we performed TUNEL assay, and a significant number of TUNEL-positive cells was found at both LIRD condition, with a significant increase in the more severe LIRD (8,000 lux for 24h) (**Figure 53**).

These results indicate that lack of FAIM renders the retina more sensible to light stress, suggesting that FAIM could confer protection to photoreceptors against light damage.



**Figure 52. Faim KO retinas are more prone to accumulate ubiquitin aggregates and express more GFAP than WT mice after light damage.** Representative images of 4  $\mu\text{m}$  paraffin sections of retinas taken from 2-month-old mice exposed normal light and to light damage for 8h (LD 8h) or light damage for 24h (LD 24h). **(A)** Ubiquitin-positive cells in the INL were counted, and at least 5 images per mice were used and averaged. **(B)** Total GFAP intensity was quantified with ImageJ, at least 5 images per mice were used and averaged. **(C)** Each violin plot extends from the min to max values, the median is represented by a thick dashed line, and quartiles are represented by thin dotted lines (n=4-6 mice/group). Statistical analysis was performed using Two-way ANOVA \*  $p < 0.05$ , \*\*  $p < 0.01$  \*\*\*\*  $p < 0.001$ .

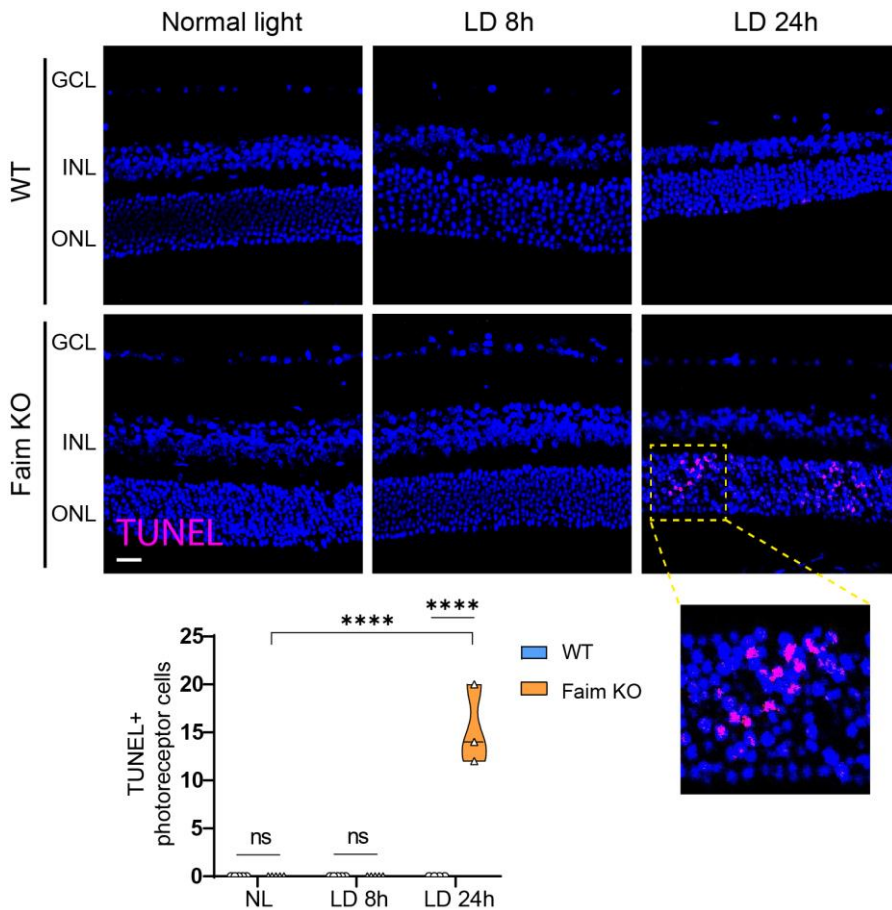


**Figure 53. Light-induced retinal degeneration (LIRD) in Faim KO mice after 24h of light exposure at 8,000 lux.** Representative images of 4  $\mu\text{m}$  paraffin sections of retinas taken from 2-month-old mice exposed normal light and to light damage for 8h (LD 8h) or light damage for 24h (LD 24h). Total number of TUNEL+ cells (*arrowheads*) per section were counted. Each violin plot extends from the min to max values, the median is represented by a thick dashed line, and quartiles are represented by thin dotted lines (n=4-6 mice/group). Statistical analysis was performed using Two-way ANOVA. \*\*\*\*  $p < 0.001$ .

Additionally, we recently performed bulk RNA-seq with mice exposed to LIRD for 24h at 8,000 lux to study whether Faim KO retinas countered light damage by overexpressing or downregulating a different set of genes in comparison to WT mice (**Figure 54**).

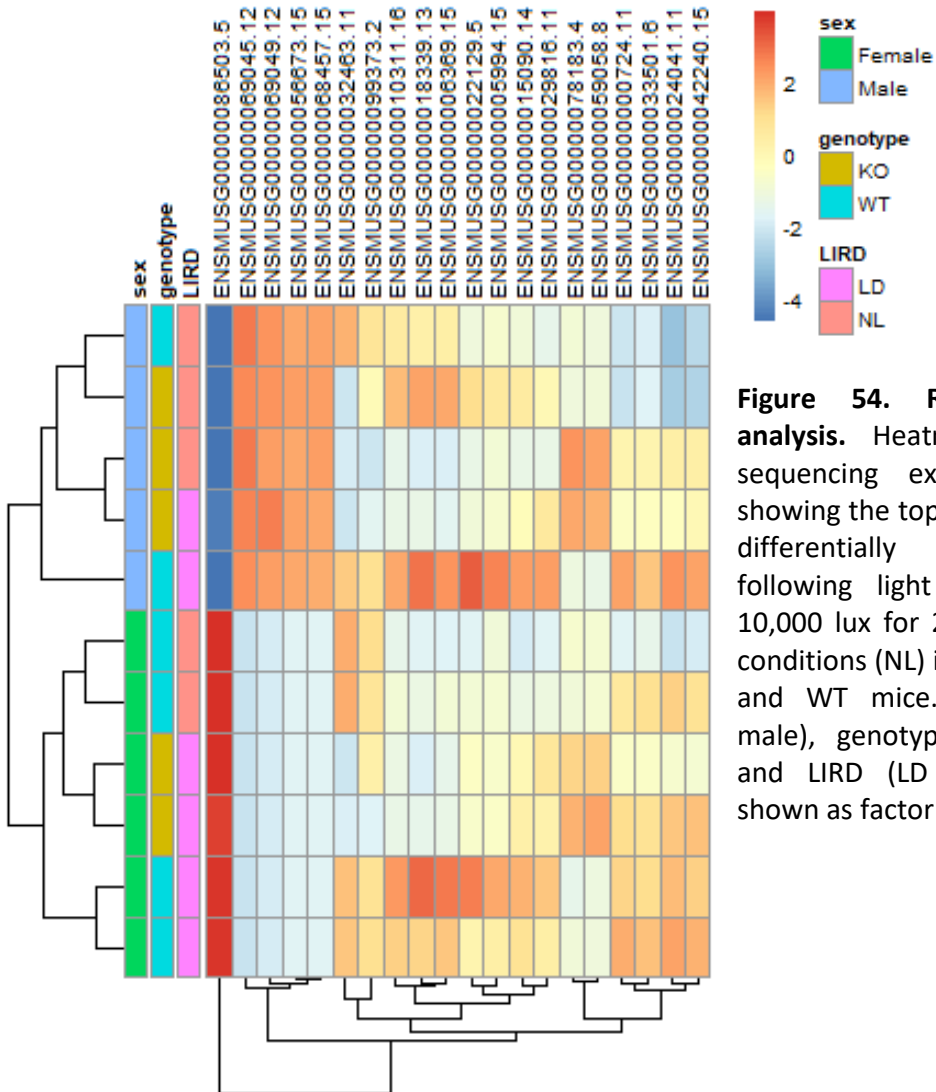


**Figure 54. RNA-seq data analysis.** Heatmap of RNA-sequencing expression data showing the top genes that are differentially regulated following light damage (LD, 10,000 lux for 24h) or normal conditions (NL) in Faim KO (KO) and WT mice. Sex (female, male), genotype (KO, WWT) and LIRD (LD and NL) are shown as factor conditions.

We used Gene Ontology (GO) terms for gene-enrichment analysis (Carbon et al. 2009; 2021) in order to identify potential associations. We found in preliminary results that Faim KO mice present a different response to WT against light damage and upregulate the expression of genes linked to inflammatory responses and cell death, and downregulate gene pathways linked to eye, retinal and neuronal development (**Table 9**).

**Table 9.** List of gene pathways upregulated or downregulated in Faim KO mice after light damage in comparison to WT mice.

<i>UPREGULATED GO pathway terms</i>	<i>DOWNREGULATED GO pathway terms</i>
GO:0006925 inflammatory cell apoptotic process	GO:0007423 sensory organ development
GO:0071346 cellular response to interferon-gamma	GO:0043010 camera-type eye development
GO:0006959 humoral immune response	GO:0002088 lens development in camera-type eye
GO:0002922 positive regulation of humoral immune response	GO:0045165 cell fate commitment
GO:0010939 regulation of necrotic cell death	GO:0048663 neuron fate commitment
GO:0070265 necrotic cell death	GO:0048568 embryonic organ

Therefore, this supports the notion that Faim KO mice behaves differently to WT mice in the presence of light damage, and that the consequences of the absence of FAIM are detrimental to the retina in response to light stress.

#### 4.2.7. Discussion

In the present work we report for the first time how the mouse retina is functionally impaired in the absence of FAIM, following our previous results in which we showed how *Faim* KO mice present a neurodegenerative phenotype. Remarkably, this is also the first time that the lack of FAIM has been reported to cause a functional deficit in the CNS *in vivo*, specifically in the retina.

After assessing the retinal function through ERG analyses, we found a rod-driven retinal malfunction in photoreceptor (a-wave) and bipolar cells (b-wave) at 18 months, while cone pathways remained unaltered. This is consistent with previous single-cell RNA-seq analyses, in which we found that *Faim* expression was heavily enriched in rod photoreceptor cells in comparison to other neuronal cell types, including cone photoreceptors. This photoreceptor malfunction could be a result of the cell death that we previously reported at this age, though the relatively low number of TUNEL-positive cells that we encountered may not be enough to explain such retinal malfunction.

RGCs responses were also reduced in aged *Faim* KO mice, although not severely. This decrease in RGC electrical activity could be explained by the chronic pro-inflammatory phenotype and blood-brain barrier (BRB) breakdown that was previously found in these mice, which progressively worsened with age. Similarly, the retinal neurodegeneration in a tauopathy mouse model (P301S) (Yoshiyama et al. 2007; Xia et al. 2021), presents a progression timeline that resembles the one in *Faim* KO retinas. In the P301S model, impairment of the BRB (which is caused by abnormal tau accumulation) is observed from early ages and increases progressively, but

RGC dysfunction only appears in aged mice (Xia et al. 2021), just like in Faim KO mice. Likewise, in glaucoma, a disease characterized by progressive damage of the optic nerve produced by RGCs death, it has been reported how glial activation and neurovascular alterations are associated to RGC degeneration, and that Müller cell gliosis may exacerbate RGC apoptosis (Munemasa and Kitaoka 2012; Fernández-Albarral et al. 2021; Q. Li et al. 2021).

Having observed at this point that a lack of Faim led to a neurodegenerative phenotype at late ages, we wanted to assess whether stress induction would trigger the same neurodegenerative phenotype at early ages. Hence, we used a protocol of mild light damage (10,000 lux for 8h) in 2 months-old mice. However, this light exposure was not enough to evoke the decrease in amplitude in the electrical responses of photoreceptors, bipolar cells or RGCs that we did observe at 18 months. Interestingly, although this protocol did not seem to alter retinal function, it was enough to elicit an increase in gliotic marker GFAP, ubiquitin aggregates and TUNEL-positive photoreceptor cells in Faim KO mice, both in respect to the WT mice exposed to the same conditions and to Faim KO mice without light damage. Although this phenotype could be predictive of a future retinal malfunction, our results were not conclusive on this end and additional light damage protocols with different light intensities and latency periods might be needed. This would allow us to ascertain whether Faim KO retinal function is sensible to light damage and whether FAIM confers protection against it, aside from a histopathological level.

Interestingly, it was described how after loss of half rod photoreceptors in murine retinas, rod bipolar cells were able to mitigate the deleterious effect by preserving their own voltage output and presenting normal b-wave

responses (Care et al. 2020). These compensating mechanisms could be another plausible explanation as to why mild (10,000 lux for 8h) LIRD did not alter electrical responses in Faim KO mice but did cause histopathological alterations in the form of ubiquitin aggregates and retinal gliosis.

In this regard, the effect of the substrain in which Faim KO mice were bred must be taken into account, as C57BL/6J mice are notoriously known in the ophthalmologic field for its light damage resistance (Bravo-Nuevo, Walsh, and Stone 2004). Hence, we cannot dismiss the possible limitations of this study, in which the specific conditions of light intensity and duration of light exposure may not have been enough to induce a significant LIRD.

Incidentally, a stronger LIRD protocol (10,000 lux for 24h) increased the accumulation of ubiquitin aggregates, the severity of retinal gliosis, and caused photoreceptor cell death, which was not present with milder conditions. To this end, it would be very useful to assess the retinal function of Faim KO and WT mice exposed to the more severe LIRD protocol, given these conditions may be enough to cause a deficit in retinal activity.

The use of LIRD protocols and mouse models allows to replicate the damage caused by environmental exposure to high levels of light in retinal diseases like AMD or inherited retinal dystrophies, which accelerate loss of vision (Remé et al. 1998; Wenzel et al. 2005). After light damage, a persistent bleaching of rhodopsin caused by excessive photon absorption follows, increasing the rate of rhodopsin deactivation and regeneration in photoreceptors in order to adapt to these conditions. This leads to the deleterious production of phototoxic products (Wenzel et al. 2005; C Grimm et al. 2000) that accumulate in photoreceptors, which are particularly sensible



to this kind of stress, ultimately causing photoreceptor death (Saari et al. 1998). In view of this, it could be interesting to explore whether Faim KO retinas exhibit accumulation of oxidative species in photoreceptors, which could be measured by normal phase HPLC (T. Maeda, Golczak, and Maeda 2012; A. Maeda et al. 2009; Rózanowska and Sarna 2005). This would provide us great insight of the possible mechanisms by which the absence of Faim leads to photoreceptor cell death.

To avoid the phototoxic effects of a persistent rhodopsin signalling it is essential to maintain an adequate photoresponse termination, which is also a key process for dark adaptation (Weiss 2020). To this end, transgenic mice that present functional alterations in proteins involved in rhodopsin deactivation, like Arrestin-1 and GRK1, have been studied (Coleman and Semple-Rowland 2005; Frederiksen et al. 2016; Aryan et al. 2020; Bayburt et al. 2011; Sokolov et al. 2004). For instance, in mouse models in which the SAG gene (which encodes Arrestin-1) is mutated or Arrestin-1 function is compromised, photoresponse is not properly inhibited and the retina is incapable of adequate dark adaptation, which can lead to night blindness (Gurevich and Gurevich 2019). Intriguingly, when we studied retinal function in Faim KO mice we found a severe delay in dark adaptation in young and aged mice, implying that FAIM could be involved in this mechanism.

Dark adaptation allows the retina to increase its sensitivity in the dark after bright light exposure, and it relies in adequate photoresponse termination (Kalloniatis and Luu 2007; J. Chen et al. 1995; J. Xu et al. 1997; C. K. Chen et al. 1999). Following disruption of dark adaptation, temporal resolution of vision is impaired, and it can lead to suboptimal eyesight and night blindness. This symptomatology is characteristic of congenital stationary night

blindness (CSNB) (Singhal et al. 2013), Oguchi disease (Fuchs et al. 1995; Yamamoto et al. 1997) or Retinitis Pigmentosa (RP), diseases that are directly linked to Arrestin-1 and GRK1 (J. Chen et al. 1999; Fuchs et al. 1995; Dai and Sun 2021; Aryan et al. 2020) and Rhodopsin and Transducin- $\alpha$  (Singhal et al. 2013; Zeitz, Robson, and Audo 2015; L. Kim 2019). This type of retinopathologies are rare, and there is no cure or treatment to date (Dai and Sun 2021; Singhal et al. 2013; R. G. Das et al. 2019). To explore a possible role of FAIM, it would be interesting to quantify the levels of FAIM-L and FAIM-S in retinas of mouse models or patients of these diseases.

To study the mechanism by which the absence of FAIM causes a dark adaptation delay, we focused on Arrestin-1 function, which is crucial for photoresponse termination. Hence, we assessed its process of translocation within photoreceptor segments, given this is a key event in phototransduction signalling (Sokolov et al. 2002; Majumder et al. 2013). We observed how Arrestin-1 translocation was delayed in Faim KO in comparison to WT mice, which suggests that FAIM could be important for adequate dark adaptation through the modulation of Arrestin-1 translocation.

The mechanism underlying the kinetics of this translocation is unknown, and different hypotheses have been enunciated (Sokolov et al. 2002; Nair et al. 2005). Protein-protein interactions in phototransduction are under a strict control for adaptational responses to light exposure and photoreceptor cell viability (Campello et al. 2013), and it has been described that ubiquitin holds a role in protein trafficking. For instance, a ubiquitin-dependent regulation of Transducin- $\alpha$  translocation has been proposed. In this model, Cul3-RetUbE3, an E3 ligase, modulates Transducin- $\alpha$  translocation through the ubiquitination and degradation of Unc119, an interacting partner of

Transducin- $\alpha$ . Thus, alterations in Cul3-RetUbE3 or Unc119 protein levels or function results in a delay in light and dark-dependent Transducin- $\alpha$  translocation (Chaya et al. 2019). Although we did not find alterations in Transducin- $\alpha$  translocation in Faim KO mice, its protein levels were reduced at 18 months of age. A significant reduction in Transducin- $\alpha$  could hinder phototransduction and even cause a decrease in a-wave amplitudes, which we observed in our Faim KO at the same age. Therefore, the study of possible alterations in the ubiquitination of Transducin-  $\alpha$  or its partner Unc119 would be interesting.

Curiously, there is not much available information regarding visual Arrestin-1 ubiquitination. Ubiquitination of the Arrestin family was first demonstrated for the mammalian and nonvisual  $\beta$ -Arrestin-2. After agonist stimulation,  $\beta$ -Arrestin-2 immunoprecipitates were accompanied by a smear of ubiquitination (Kommaddi and Shenoy 2013).

Previous results describe how FAIM has a role in modulating ubiquitination. For instance, we have shown FAIM-L blocks XIAP auto-ubiquitination (Moubarak et al. 2013), and Rothstein and colleagues established how in the absence of FAIM-S there was an accumulation of ubiquitin aggregates after oxidative stress (Hiroaki Kaku and Rothstein 2020). Upon seeing the roles of ubiquitin in protein translocation and after we found a specific delay in Arrestin-1 translocation in FAIM KO retinas, we studied Arrestin-1 ubiquitination and showed that 1) Arrestin-1 is susceptible to ubiquitination *in vitro*, and 2) its ubiquitination is greatly reduced after overexpressing FAIM-S or FAIM-L. Thus, in the presence of FAIM, Arrestin-1 ubiquitination is decreased and almost abrogated.

Interestingly, it has been reported how oxidative stress causes the aggregation of Rhodopsin and Transducin- $\alpha$ , and how this aggregation targets them for ubiquitin-mediated degradation (Illing et al. 2002; Schmidt et al. 2021; Shang and Taylor 2011). This field has not been extensively studied, and to the best of our knowledge, this is the first time that a visual Arrestin-1 has been shown to be susceptible of ubiquitination. To further explore this, it would be interesting to study whether oxidative stress generated by light damage causes Arrestin-1 ubiquitination and its consequent aggregation in WT mice, and whether the absence of Faim exacerbates this mechanism.

Moreover, it would be valuable to discern what type of Arrestin-1 ubiquitination is FAIM blocking. In this regard, performing ubiquitin assays in the presence of proteasome inhibitor MG132 provided valuable information, since we found that at least a fraction of the ubiquitination that FAIM is blocking is degradative. Agreeing with these results, we found a decrease in Arrestin-1 protein levels in Faim KO mice, meaning that Arrestin-1 is excessively being targeted for degradation via the UPS in the absence of FAIM. Given the mechanism of ubiquitin chain elongation, we could perform additional ubiquitin assays with mutated lysines to discern the type of ubiquitination that FAIM is blocking, namely polyubiquitination (which usually leads to proteasomal degradation), mono or multiubiquitination (linked to signalling properties or receptor endocytosis) (Haglund and Dikic 2005; Thrower et al. 2000).

In summary, we have observed that Faim KO mice present retinal malfunction at late ages and a delay in dark adaptation from two months, and we believe the latter could be linked to alterations in Arrestin-1 translocation upon light reception. Hence, it is possible that the ultimate goal of FAIM is to assist Arrestin-1 translocation through the modulation of its ubiquitination,

similarly to the process that regulates this movement in Transducin- $\alpha$  (Chaya et al. 2019). Therefore, in the absence of Faim, Arrestin-1 ubiquitination would be increased, hampering its translocation and causing a delay in dark adaptation. The obstruction of the role of Arrestin-1 in rhodopsin deactivation by a lack of FAIM could lead to impaired rhodopsin degradation, rendering photoreceptors more sensitive to age-related neurodegenerative events and to light damage, ultimately causing functional alterations in rod photoreceptor and bipolar cells.

Hereby, we propose that FAIM has a role in phototransduction termination through its ability to promote Arrestin-1 translocation, and as a result of this, Faim KO retinas present a symptomatology that is typically found in night blindness disorders. In view of this, we believe that research in proteins involved in the mechanisms underlying these diseases, such as FAIM, is of utmost importance.

# Global discussion

*What's the use of doing all this work if we  
don't get some fun out of this?"*

Rosalind Franklin (1920-1958)



# Global discussion

## 5.1. Faim throughout the years

Our group and others have thoroughly established how both FAIM-S (H. Kaku and Rothstein 2009; J Huo et al. 2016; Hiroaki Kaku and Rothstein 2020) and FAIM-L (Planells-Ferrer et al. 2016; Martínez-Mármol et al. 2016; Segura et al. 2007; Moubarak et al. 2013; P Carriba et al. 2015) act as powerful anti-apoptotic modulators and have a role in multiple mechanisms that avoid cell stress in the organism, specifically in neurons. Although FAIM-S is expressed ubiquitously, it holds specific and important functions in the CNS regarding neuritogenesis. However, FAIM-L, which only differs from FAIM-S by 22 additional amino acids, is only expressed in neurons (T. J. Schneider et al. 1999; Coccia et al. 2017). This neuronal specificity leads to many unresolved questions, like what is the unique and particular role of FAIM-L in neurons, or why is FAIM-S not able to exert these functions.

The importance of FAIM-L in the CNS has been a pivotal point of study for our group and others. Its ability to confer neuronal protection against apoptotic stimulus in neurons and its possible role in the pathophysiology of AD are of great interest (P Carriba et al. 2015; Segura et al. 2007; Hiroaki Kaku et al. 2021).

Evidently, this background brought us to think that a FAIM deficiency in an *in vivo* mouse model would result in a neurodegenerative phenotype. Given this, our group explored the phenotype of Faim KO brains to find possible neurodegenerative events that could be linked to a Faim deficiency, such as impairment of neuritogenesis, synaptic transmission and LTD (Martínez-Mármol et al. 2016; Sole et al. 2004; Coccia et al. 2020), and neuronal



apoptosis (Moubarak et al. 2013) already reported *in vitro*. Unexpectedly, no evident alterations were found in the brain of Faim KO mice (Calleja-Yagüe 2019). However, after using open-sourced bioinformatic to assess Faim expression and relative functions, we retrieved surprising information. Different analyses indicated that FAIM expression was greatly enriched in the retina among other neuronal tissues and the whole organism. This opened us a new unexplored research path for FAIM. We felt compelled to explore the possible implications of FAIM in the retina and, excitingly, found promising results that put this protein in the retinal scene. Additionally, this bioinformatic data could partly explain the lack of phenotype in the brain, where in physiological conditions the absence of FAIM does not impact neuronal homeostasis and an external toxic insult that promotes apoptosis might be needed.

According to the Human Proteome Map, which retrieves information from protein samples of human fetal and adult tissue, FAIM is particularly enriched in rod photoreceptors among every neuronal cell type in the brain and in the retina. Thus, although we could not obtain experimental data to be certain of this due to technical difficulties, we hypothesize that FAIM-L is indeed expressed in photoreceptor rods. We also used a bioinformatic tool that allows to explore networks of biological functions of genes that are coexpressed with the gene of interest. This tool significantly linked *Faim* functions to sensory perception of light stimulus and photoreceptor cell differentiation above others. Moreover, it also indicated that Faim expression is heavily linked to retinal function, given that Faim is actually one of the 83 genes that comprise the Phototransduction Cluster. Additionally, the Human Protein Atlas predicts the grouping of an individual gene using expression proximity. Thanks to this, we retrieved 15 genes that are close in function and expression with Faim, and within them we found photoreceptor-specific

proteins like Rhodopsin, SAG (the gene which encodes for Arrestin-1), Recoverin, PDE6G and Retbindin, among other retinal-specific genes.

To the best of our knowledge, this is the first time that both isoforms of FAIM have been reported to be expressed in the retina. Although FAIM-S is ubiquitously expressed, FAIM-L had only been reported to be expressed in brain samples and testes (Zhong et al. 2001). Unfortunately, since there is no available antibody suitable for immunohistochemistry for FAIM-L, we could not specifically determine which neurons express this isoform, and only could confirm its expression in the retina by western blot. However, if immunodetection of FAIM-L continues to be elusive, there are alternative methods that would be useful to detect its specific cellular expression. For instance, tissue microdissection to morphologically isolate the distinct population of retinal cells and layers could be useful, given it would allow us to perform a western blot afterwards.

In view of this, a great window of opportunity opened for us, since the retinal tissue was completely unexplored regarding FAIM. As a result of the studies that we performed in this thesis, we report novel roles for FAIM in the retina related to phototransduction and adequate dark adaptation, which will be discussed afterwards. Interestingly, these new mechanisms in which FAIM is involved are probably linked to functions that have already been described for FAIM, such as blocking of ubiquitination, protection against cell death and prevention of oxidative stress.

## **5.2. Photoreceptor stress and ubiquitin aggregates in Faim KO mice**

The first thing that we describe in the present thesis is how loss of FAIM leads to progressive neurodegeneration, which starts with accumulation of

ubiquitinated proteins and reactive gliosis and evolves to breakdown of the BRB and photoreceptor cell death.

It has been long established how FAIM holds anti-apoptotic properties throughout the organism in its short form (FAIM-S) and specifically in the nervous system in its long form (FAIM-L). Additionally, both FAIM-S and FAIM-L have housekeeping properties, such as protection against oxidative stress, modulation of proteostasis and inhibition of protein aggregation (Hiroaki Kaku and Rothstein 2020; Moubarak et al. 2013; Hiroaki Kaku et al. 2021), which reinforce our current results involving FAIM in the inhibition of deleterious ubiquitinating events.

Compared to other tissues and the rest of CNS, the retina is exceptionally prone to cell stress due to its high energetic demands and metabolic rate, rapid protein turnover, limited capacity of self-reparation and regeneration, and direct exposure to light (Wood et al. 2008; Roehlecke et al. 2009; Roehlecke et al. 2011). This greater sensitivity of photoreceptors and the retina could also explain why the neuronal phenotype in Faim KO mice is more severe in the retina than in the brain.

Incidentally, among all retinal structures, photoreceptor segments are particularly at risk. The OS oversees phototransduction and is comprised by highly specialized, disc-like structures enriched with lipids and proteins, molecules that are very susceptible to oxidative damage (Roehlecke et al. 2013; Sun et al. 2006). The IS is where protein synthesis and the largest part of housekeeping functions take place. Likewise, the IS is also susceptible to toxicity via misfolding mutations in retinal genes like Rhodopsin (Tam and Moritz 2006). Accumulation of misfolded proteins in the endoplasmic reticulum (ER) can lead to ER stress, form ubiquitinated aggregates and

cause UPS and proteasomal disruption, which are hallmarks of many neurodegenerative diseases (Qu, Zou, and Lin 2021; Hegde and Upadhya 2007)

Hence, accumulation of ubiquitin aggregates in photoreceptor segments like the ones we found in Faim KO mice are very detrimental to the retinal tissue, leading to serious photoreceptor stress and eventually triggering apoptotic cell death.

Arrestin-1 is the second most abundant protein in rod photoreceptors after Rhodopsin, and is localized in the photoreceptor segments (Strissel et al. 2006; Hanson et al. 2007; X Song et al. 2011). Since we observed a high accumulation of ubiquitinated proteins in the segments of photoreceptors in Faim KO mice, it would not be surprising that Ub-arrestin-1 accounts for most of this ubiquitin aggregation. As a result of this, alterations in Arrestin-1 ubiquitination could lead to a potent UPS dysfunction and photoreceptor stress.

Arrestin-1 is crucial for phototransduction given its role in photoresponse termination after rhodopsin deactivation. To deliver its functions, Arrestin-1 translocates from the IS to the OS (where Rhodopsin is localized) upon light reception, a process that is delayed in Faim KO mice. Like Arrestin-1, Transducin- $\alpha$  also initiates a relocation after light reception, but in opposite directions. In Faim KO mice, however, Transducin- $\alpha$  movement was unaltered. Although both Arrestin-1 and Transducin- $\alpha$  are implicated in light-dependent movement, their ultimate functions are contrary (Slepek and Hurley 2008), which could explain why FAIM is only linked to Arrestin-1 (but not Transducin- $\alpha$ ) translocation.

Interestingly, it has been described how Transducin- $\alpha$  migration within photoreceptor segments could be ubiquitin-dependent (Chaya et al. 2019), and although few, there are reports of this protein being ubiquitinated and degraded by the UPS and aggregated in neurodegenerative events (Campello et al. 2013; M. S. Obin et al. 1996a; M. Obin, Nowell, and Taylor 1994; M. S. Obin et al. 1996b). Nonetheless, to the best of our knowledge, Arrestin-1 has never been reported to be ubiquitinated and aggregated neither *in vivo* nor *in vitro*, nor we know for certainty the downstream consequences of this post-translational modification in Arrestin-1. In here, we report that Arrestin-1 is indeed susceptible of being ubiquitinated, and that FAIM modulates this ubiquitination and blocks it *in vitro*. In sight of this, we hypothesize that FAIM could be regulating Arrestin-1 translocation by blocking the latter's ubiquitination. In Faim KO mice, this would result in a delay in Arrestin-1 translocation upon light reception with subsequent functional alterations, and the severe delay in dark adaptation found in Faim KO retinas supports this point.

Furthermore, excessive ubiquitination of Arrestin-1 in the absence of FAIM could also be linked to a more detrimental and typical effect of this post-translational modification: degradation via the UPS. The involvement of the UPS in neurodegenerative disorders has been largely studied. Numerous studies have demonstrated how ubiquitin-positive inclusions cause the loss of neuronal cells (Hara et al. 2006), and that protein aggregation and proteasome disruption is a common pathological hallmark of neurodegeneration . For instance, abnormal A $\beta$  and tau aggregation, proteasome disruption, and ubiquitin immunoreactivity in neurofibrillary tangles are characteristic features of Alzheimer's disease (AD) (Brion et al. 1985; Brion, Flament-Durand, and Dustin 1986; Sisodia et al. 1990; Harris, Jasem, and Licchesi 2020; Upadhyya and Hegde 2007). Although we have not

checked for the presence of A $\beta$  or tau aggregation in the brain of Faim KO mice, we have observed how in AD mouse models, and in hippocampus and cortex samples of AD patients there is a significant reduction of FAIM-L levels (P Carriba et al. 2015). Moreover, Rothstein and Kaku described how in the presence of FAIM-S or FAIM-L, neuronal cells *in vitro* were able to eliminate A $\beta$  aggregates that were already formed (Hiroaki Kaku et al. 2021). In sight of this, it would be interesting to check the presence of A $\beta$  and tau aggregates in Faim KO mice, but also to induce toxicity to Faim KO retinas by injecting A $\beta$  and assessing aggregate levels, for instance.

Aside from the brain, proteasome overload is a common stress factor for multiple forms of inherited retinal degeneration and retinal dystrophies like RP and AMD (Illing et al. 2002; Leger et al. 2011; Lobanova et al. 2013). Several disease-causing mutations are specific to misfolding or mistrafficking events in photoreceptor-specific proteins, like the widely studied P23H mutation in rhodopsin, which has been used to develop a mouse model for RP. This alteration causes rhodopsin misfolding and ER stress, which ultimately contribute to rod photoreceptor cell death (J. Li et al. 2009). A similar pathophysiology is found in the retinal degeneration 10 (rd10) mouse model of RP, which is caused by a mutation in PDE6 $\gamma$  that results in its mislocalization, causing protein misfolding and aggregation and ultimately proteasome overload (Lobanova et al. 2013). Interestingly, when we checked *Faim-l* gene levels in rd10 mice we observed an upregulation at P17. This perfectly correlates with an upregulation of *Gfap* expression in response to retinal damage in rd10 mice, which happens just before evident neurodegeneration at P18 (Sánchez-Cruz et al. 2018). To continue with this, it would be interesting to explore protein levels of FAIM-S and FAIM-L in these mouse models to check whether its levels are reduced before

neurodegeneration, just like it happens in AD mouse models with FAIM-L (P Carriba et al. 2015).

Aside from morphological changes and photoreceptor cell death, misfolding and protein aggregation in the retina also cause retinal malfunction. For instance, a human frameshift mutation in the SAG gene (encoding Arrestin-1 protein) which in some cases leads to RP in the form of photoreceptor stress, has also been found to underlie Oguchi disease, a form of stationary night blindness (Nakazawa, Wada, and Tamai 1998; Gurevich and Gurevich 2019).

Night blindness is a feature of many retinal diseases that interfere with the complex molecular mechanism that is essential for dark adaptation. Excitingly, the retinal alterations that we found in Faim KO mice, namely the accumulation of ubiquitinated proteins, Arrestin-1 malfunction, delay in dark adaptation and photoreceptor cell death, are characteristic features of retinal diseases like RP and Oguchi disease. We believe research on Faim regarding the role of Arrestin-1 ubiquitination in dark adaptation would be groundbreaking and provide valuable information and insight on the mechanisms causing these diseases.

### **5.3. Neurodegeneration in Faim KO mice resembles the phenotype of several inherited and age-related retinal diseases**

As previously mentioned, it has been largely described how proteasome dysfunction causes photoreceptor stress, which triggers a survival response to the retinal glia to help reestablish proteostasis. To achieve this, damaged or degenerating photoreceptors release endogenous molecules that trigger the activation of Müller glia (Newton and Megaw 2020), a process that is found in many models of RP (Nomura-Komoike, Saitoh, and Fujieda 2020; Murakami et al. 2012). For instance, Rattner and Nathans described the

proliferation and activation of Müller glia in response to photoreceptor secretion of EDN2 in three mouse models of retinal neurodegeneration (rd7, rds<sup>-/-</sup> and prCAD<sup>-/-</sup>). Afterwards, Müller glia upregulate GFAP and respond by secreting FGF2 to allow photoreceptor survival (Rattner, A.; Nathans 2005; Rattner et al. 2013). In Faim KO retinas we found upregulation of GFAP from Müller cells, but also a specific EDN2 expression enveloping the soma of cones, but not rods. Intriguingly, we only found functional retinal alterations at the level of rod photoreceptors, but not cones. This could mean that cones are triggering a stress response to Müller cells, which are actually ensuring cone survival and function.

Nonetheless, if photoreceptor damage and Müller glia activation are sustained, detrimental retinal gliosis ensues and there is a upregulation of chemokines, cytokines and diverse inflammatory factors like IL-1 $\beta$  or TNF $\alpha$  (Andreas Bringmann et al. 2006; Andreas Bringmann and Wiedemann 2012), a feature that we observed in Faim KO mice.

In view of this, it is possible that in our model, ubiquitinated aggregates cause photoreceptor stress by proteasome overload and UPS dysfunction, thus leading to the release of survival molecules like EDN2. Upon reception through Müller glia receptors, these retinal cells would respond with GFAP upregulation, finally triggering a gliotic response. It has been described how retinal gliosis and a prolonged inflammatory context can result in BRB breakdown. In Faim KO mice, there are already mild vascular alterations at 2 months of age, but at 12 months of age there is a great extravasation of the retinal blood vessels. Remarkably, this happens almost exclusively at the GCL level, where RGCs are allocated. Ultimately, this loop of retinal gliosis and vascular alterations could cause the malfunction of RGCs, which we observed in our Faim KO mice at 18 months but not at 2, when



extravasations were still not evident at the GCL. To further support this, it would be useful to assess RGC function at 12 months, when the BRB is already severely compromised at the GCL.

Aside from retinitis pigmentosa, retinal gliosis is most present in DR. However, the most attributed cause and one of the most researched topics for retinal gliosis in DR is hyperglycemia. This metabolic alteration causes the accumulation of advanced glycation end-products and superoxide species in retinal blood vessels, which provokes vascular damage (E. S. Shin, Sorenson, and Sheibani 2014; Zong et al. 2010). Interestingly, Lam and colleagues (but not Rothstein) reported in their Faim KO systemic hyperglycemia, a feature that would be linked to FAIM-S given its implications in insulin signaling and energy homeostasis (Jianxin Huo, Xu, and Lam 2019; J Huo et al. 2016). Although we have not checked for glucose levels in our Faim KO mice bred in heterozygosity, this would be an interesting experiment that would allow us to explore alternative causes for the gliosis we observed.

Conversely, the research in DR pathophysiology has largely overlooked the potential (and detrimental) role of photoreceptors in early stages of the disease, despite many reports being available for decades (Greenstein et al. 1993; Amemiya 1977; Henson and North 1979). It has been described how in DR patients also diagnosed with RP, a disease characterized by photoreceptor cell death, the DR pathology was less severe than those without RP (Arden, Wolf, and Tsang 1998). Also, mice lacking photoreceptors due to a knockout of Rhodopsin showed less severity in microvascular alterations in a diabetic mouse model (De Gooyer et al. 2006). These results suggest that a lack of photoreceptors and phototransduction is beneficial for preventing the gliotic and microvascular alterations that are found in DR, meaning that they may have a role in its onset. Similarly, we have observed in Faim KO retinas

ubiquitin aggregates in photoreceptor segments and alterations in photoresponse termination at 2 months, which according to this hypothesis, would be broadening the regional gliosis and microvascular alterations that we already observe at 2 months, but that actually peak at 12.

A possible explanation for the deleterious effect of phototransduction in DR is linked to oxygen consumption of photoreceptors, which are the major oxygen consumers of the retina. Additionally, it has been reported how this metabolism is heavily increased in the dark (Ramsey and Arden 2015; Arden, Wolf, and Tsang 1998), when rod dark current is at its maximum (D. Y. Yu and Cringle 2001). Arden and colleagues suggested that photoreceptors induced hypoxia in DR retinas due to a higher photoreceptor metabolic activity during dark periods in an already compromised retinal vasculature (Arden, Wolf, and Tsang 1998). Agreeing with this, the elimination of phototransduction in diabetic mice through long-term deprivation of light caused a reduction of the levels of GFAP and pro-inflammatory markers in the retina, and led to an improvement of photoreceptor function as seen by ERG, preventing the development of DR (Thebeau et al. 2020).

Further corroborating these results, deleterious dark adaptation in DR was also observed in the form of dark adaptation delay and abnormal rod sensitivity in diabetic patients (Greenstein et al. 1993; Ramsey and Arden 2015; Amemiya 1977).

Curiously, this phenotype heavily resembles the one we found in Faim KO retinas, in which rod photoreceptor function is altered at late ages, but a severe dark adaptation delay already occurs at 2 months of age. To explore in depth these similarities we could expose mice to long-term dark or light-

adapted environments and compare the severity of retinal gliosis and malfunction.

In view of this, it is possible that lack of FAIM is not enough to cause retinal malfunction at early ages, but it may form a neurodegenerative and inflammatory context that eventually results in photoreceptor malfunction. Remarkably, our phenotype goes in line with the hypothesis in which photoreceptor stress contributes to the development and severity of DR (Kern and Berkowitz 2015; H. Liu et al. 2016).

Additionally, there have been several studies in which the expression of photoreceptor-specific proteins like Rhodopsin, Arrestin-1 and Recoverin among others are greatly downregulated in gliotic retinas, which may also justify photoreceptor stress and cell death during this process (Eastlake et al. 2018). Accordingly, expression of Arrestin-1 in Faim KO mice is also downregulated in the gliotic retina at 12 months of age.

It has also been largely studied how the gliotic phenotype is specifically sensitive in the retina among other tissues, given that the retina is consistently exposed to pro-inflammatory stimulus like continuous light exposure. In the retina, continuous light exposure in an already altered environment easily leads to oxidative stress, which positively feeds the gliotic loop (Wenzel et al. 2005; J. Chen et al. 1999). In this context, light stress triggers the expression of oxidative stress in the form of production of reactive oxygen species (ROS) in photoreceptors, which impairs the proteasome and causes aggregation of ubiquitinated proteins and gliosis in the retina (Campello et al. 2013). Precisely, we have described how a light damage protocol causes accumulation of ubiquitinated aggregates, retinal gliosis, and photoreceptor cell death in Faim KO, but not WT mice.

Incidentally, FAIM has been reported to avoid protein aggregates after oxidative stress (Hiroaki Kaku and Rothstein 2020). FAIM protein sequence is significantly low in cysteine residues (FAIM-S: 1.7%, FAIM-L: 1%) (Hiroaki Kaku and Rothstein 2020), a feature that helps avoid denaturation and protein aggregation caused by oxidative stress (Fuentes-Lemus et al. 2022).

If FAIM had a role in helping resist oxidative stress and Faim KO retinas were particularly susceptible to this stress, this could lead to the aggregation of ubiquitinated proteins, disruption of the UPS and finally photoreceptor cell death, which is exactly what we observed in Faim KO retinas. In consonance with this, there is a strong body of evidence that states that degradation of oxidized products is ubiquitin-dependent due to the loss of secondary and tertiary structures (Kelly, Wang, and Zhang 2018). According to this model, in the absence of FAIM there could be a disruption of the UPS, followed by accumulation of oxidized products that cannot be degraded due to proteasome overload, causing additional photoreceptor stress. In view of this, it would be meaningful to study whether oxidative stress and ROS products are also present in an exacerbated manner in Faim KO retinas after light damage.

Interestingly, light damage in the Faim KO retinas at 2 months phenocopied the histopathological alterations that we found in aged Faim KO mice without stress induction, suggesting that FAIM could be involved in photoreceptor survival processes that are also important for adequate ageing or senescence.

#### **5.4.FAIM in ageing and senescence**

Senescence is the process of gradual deterioration with age. At the cellular level, it is believed to be an irreversible arrest of cell division and an adaptive response to a variety of exogenous and endogenous stimulus. It has been long accepted how senescence is associated with detrimental events in cellular functions and increased oxidative damage, which can lead to protein misfolding, ubiquitin aggregations and even cell death (Hjelmeland et al. 1999; Decanini et al. 2007). An increasing body of literature has been linking senescence and oxidative stress to AMD, where age-associated changes such as telomere erosions, ROS production in photoreceptor segments and metabolic alterations occur (Ozawa et al. 2010; Balaiya et al. 2017; Ozawa 2020; Bellezza 2018). Interestingly, non-visual Arrestins have been also linked to senescence. For instance, non-visual Arrestin- $\beta$ -1 is important for telomerase activity by the prevention of the onset of cellular senescence in leukemia (Kallifatidis, Mamouni, and Lokeshwar 2020).

Although this topic has not been further explored, FAIM has also been reported to positively mediate the pro-survival actions of SRT1720, a molecule that regulates and ameliorates senescence in aged cells through the activation of sirtuin 1 (SIRT1) (X. Liu et al. 2017). SIRT1 is a NAD<sup>+</sup> dependent deacetylase, which among multiple other functions has important roles in neurodevelopment and brain senescence (Herskovits and Guarente 2014). It also controls the activity of numerous transcription factors that alleviate oxidative stress and associated damage. In the aforementioned study, this group reported how SRT1720 improved cell survival in aged human mesenchymal stem cells (hMSCs) in a Faim-dependent manner, and that Faim expression was positively regulated by SRT1720 (X. Liu et al. 2017).

Interestingly, SIRT1 has crucial roles in the retina through its protection against oxidative stress and retinal cell death (Ozawa et al. 2010; Mimura et al. 2013). It is expressed in the INL, ONL and GCL (Balaiya et al. 2017), and SIRT1 KO mouse present a thinning of the INL and ONL and a marked retinal disorganization. But, most importantly, SIRT1 has been linked to multiple retinal diseases, such as glaucoma, optic neuritis, AMD, RP and DR (reviewed in (Balaiya et al. 2017) (Mohammad et al. 2019)). There are multiple examples on how SIRT1 rescues retinal cell death. For instance, abnormal subcellular localization of SIRT1 accelerates retinal cell apoptosis in rd10, the RP mouse model (Ozawa et al. 2010; Jaliffa et al. 2009). Also, cell-selective AAV-mediated delivery of SIRT1 prevented RGC death in optic nerve injury (Ross et al. 2021). Moreover, in the db/db mice, a model of diabetes and diabetic retinopathy, pharmacological activation of SIRT-1 by SRT1720 prevented retinal cell death (Hammer et al. 2021).

Modulation of SIRT1 activity and levels has been a potent topic of research for many years. Remarkably, it was recently described how SIRT1 expression is modulated by E3 ubiquitin ligases, which mediate its ubiquitination and degradation (L. Yu et al. 2020; Ouyang et al. 2022; P. Y. Liu et al. 2021).

Piggybacking from these results, we could hypothesize that FAIM, in a mechanism that has yet to be elucidated but that essentially agrees with the work of Liu et al. (X. Liu et al. 2017), could be positively regulating SIRT1 levels through the blocking of the latter's ubiquitination, just as it happens with XIAP (Moubarak et al. 2013) and presumably with Arrestin-1. Interestingly, we have described in this thesis how Faim expression is decreased in rd10 mice, a model in which SIRT1 subcellular localization is abnormal (Ozawa et al. 2010; Jaliffa et al. 2009). Then, it can be

hypothesized that, just like with Arrestin-1, Faim might allow adequate subcellular colocalization of SIRT1 through the modulation of its ubiquitination. Hence, in the absence or downregulation of Faim in the retina, SIRT1 could not properly operate, leading to oxidative damage, accumulation of ubiquitinated proteins, retinal neurodegeneration and senescence.

In view of this, it would be extremely interesting to assess the levels, cellular and subcellular localization of SIRT1 in Faim KO mice, and also to study the presence of senescence markers like Beta Galactosidase.

Although reasonable connections can be made, SIRT1, XIAP and Arrestin-1 are fairly different molecules, with distinct expression patterns and diverse functions. The possibility that FAIM specifically abrogates the ubiquitination of these three unique proteins is certainly plausible, but other hypothesis in which Faim has a bigger role in the organism can be made. For instance, Faim could be directly regulating ubiquitination by its interaction with E2 ubiquitin-conjugating enzymes or E3 ubiquitin ligases. XIAP itself is an E3 ligase, and aside from blocking its ubiquitination, FAIM also immunoprecipitates with XIAP, indicating a direct binding of these two proteins, and thus agreeing with the possibility that FAIM directly interacts with ubiquitin-associated enzymes.

Interestingly, non-visual Arrestins have also been recently linked to ubiquitinating processes. It has been reported how  $\beta$ -Arrestins trigger the ubiquitination of receptors and are involved in multiple signaling pathways that are independent of G-proteins (like Transducin- $\alpha$  in the retina). They describe how  $\beta$ -Arrestins act like adaptors to allow the recruitment of E3 ubiquitin ligases, thereby promoting the downstream signaling of

ubiquitination (Lin et al. 2008; Sudha K. Shenoy et al. 2008; S. K. Shenoy et al. 2001; Jean-Charles, Rajiv, and Shenoy 2016).

This role, however, has not been researched for Arrestin-1. Nonetheless, the basic differences between visual and non-visual Arrestins lay almost exclusively in its targets. While visual Arrestins only bind to photopigments, non-visual Arrestins bind hundreds of GPCR subtypes. Given this, it is plausible that visual Arrestins are also able to recruit and act as E3 ligase adapters.

These results paint a colorful picture in which FAIM could be a distinctive subject and hold many (and much) more important roles than previously thought. Considering the multiple functions that we and others have reported that pivot around ubiquitin modulation, it could be hypothesized that FAIM interacts with E3 ligases in a competitive manner, thus blocking the ubiquitination of the enzyme targets.

### **5.5. Summarizing our results: FAIM in the retina**

This is the first time in which both FAIM-S and FAIM-L have been reported to be expressed in the neuroretina. FAIM-L had not been linked to more tissues other than brain (Coccia et al. 2017; Zhong et al. 2001); and although FAIM-S is thought to be ubiquitously expressed, it only had been reported to be expressed in brain, heart, kidney, spleen, thymus and liver (Zhong et al. 2001).

In here, we report completely novel FAIM functions that not only link FAIM to the retina but suggest that FAIM could have a role in phototransduction-associated protein translocation through the modulation of ubiquitination. In a retinal context, our results suggest that Faim would modulate arrestin-1



translocation, thus having a specific role in photoresponse termination and dark adaptation.

A new current of research has been focusing on the disruption of the UPS as one of the main mechanisms in the pathophysiology of retinal diseases, such as RP and Oguchi disease. Research on this topic is imperative, since these diseases have few available treatments that are only able to palliate its symptoms, but not cure the disease (Zeitze, Robson, and Audo 2015).

In view of this, exploring the roles of novel retinal players like FAIM that could influence the pathophysiology of these retinal diseases is of utmost importance.

Besides being implicated in dark adaptation, we have also linked Faim to retinal diseases that are characterised by retinal gliosis and microvasculature deficits.

Based on our results, we hypothesize the following model, in which FAIM has a role in adequate physiopathology and function of the retina and how its absence would be detrimental to this tissue:

- 1) Lack of Faim causes photoreceptor stress in the retina through the excessive ubiquitination of Arrestin-1, which causes proteasome overload, accumulation of ubiquitin aggregates in photoreceptor segments and UPS disruption.
- 2) Excessive ubiquitination of Arrestin-1 due to lack of Faim causes the disruption of the mechanism in which Arrestin-1 translocates from the IS to the OS upon light reception, causing additional aberrant accumulation of Arrestin-1 in photoreceptor segments.

- 3) Photoreceptor stress caused by ubiquitinated aggregates leads to activation of Müller glia through the secretion of survival signals. Persistent photoreceptor stress by a lack of Faim causes a chronic response of Müller glia, triggering retinal gliosis.
- 4) Retinal gliosis leads to breakdown of the blood-retinal barrier through the secretion of detrimental pro-inflammatory molecules that cause irreversible damage to retinal blood vessels, particularly at the GCL level.
- 5) These neurodegenerative events culminate in photoreceptor cell death, which could also enhance senescence development.

Furthermore, these molecular alterations have functional consequences on the retina:

- 1) As a result of abnormal Arrestin-1 translocation upon light reception, dark adaptation is severely delayed in Faim KO mice.
- 2) Rod photoreceptor, bipolar and retinal ganglion cells activity is hampered in Faim KO mice at late ages due to the detrimental effects of retinal gliosis and breakdown of the BRB, but also as a result of accelerated ageing and senescence.

In this thesis we have established new precedents and we suggest new possible roles for FAIM in the retina. Evidently, more work needs to be done to ascertain the specific molecular mechanism by which this role could be achieved, and whether the hypothesized functions are dependent of a specific FAIM isoform. Nonetheless, we believe this is a turning point for FAIM, and research on this topic will provide a great insight on the different mechanisms that allow adequate retinal homeostasis, adequate dark adaptation and overall retinal function. Therefore, beyond retinal physiology, further studying the

role of FAIM in the retina could lead to the discovery of new therapeutic targets that would alleviate the symptomatology of retinal diseases such as RP, DR, Oguchi disease and AMD.

# Conclusions

*“Lo importante es no tener arrugas en el cerebro”*

Margarita Salas (1938-2019)



## Conclusions

- i. **Absence of FAIM causes ubiquitinated proteins to aggregate in the retinal tissue**, specially to the inner nuclear layer (INL), ganglion cell layer (GCL) and photoreceptor segments.
- ii. **Absence of FAIM leads to a pro-inflammatory phenotype in the retina**, which is presented as retinal gliosis and breakdown of the blood-retinal barrier as early as 2 months of age.
- iii. **Faim KO retinas present a thinning of the ONL and photoreceptor cell death at 18 months of age.**
- iv. **Absence of Faim leads to an amplitude decrease of the electrical activity** of rod-mediated responses and RGCs to different light stimulus in scotopic conditions at 18 months of age.
- v. **Decreased amplitudes of electrical responses in scotopic conditions are age-dependent and not evident at 2 months in Faim KO mice**, despite the pro-inflammatory and neurodegenerative phenotype found at this age.
- vi. **The absence of FAIM leads to a severe delay in retinal dark adaptation at early and late ages**, as evidenced by a double-flash ERG protocol.
- vii. **Arrestin-1 translocation** upon light reception from the inner segment to the outer segment of photoreceptors **is obstructed in Faim KO mice, which could be causing the delay in dark adaptation.**
- viii. **Both FAIM-S and FAIM-L block Arrestin-1 ubiquitination in vitro**, and excessive ubiquitination in Faim KO mice could be hampering Arrestin-1 translocation.
- ix. **At 2 months of age, the absence of FAIM renders the retina more sensible to light damage** in the form of accumulation of ubiquitin

aggregates, retinal gliosis, and exacerbated photoreceptor cell death, which only occurs after 24h of light damage.

- x. **Light-induced damage for 8 h in the absence of FAIM at 2 months of age is not enough to elicit the retinal malfunction** that we observe at 18 months of age.
- xi. **Light-induced damage for 24h in Faim KO mice results in upregulation of cell death and inflammatory pathways and downregulation of retinal differentiation pathways**, as evidenced by RNA-seq analyses.
- xii. **The absence of FAIM leads to a neurodegenerative phenotype in the retina** that resembles the symptomatology of retinal pathologies like retinitis pigmentosa and diabetic retinopathy.
- xiii. **FAIM is involved in adequate retinal homeostasis and phototransduction, therefore research on the molecular mechanisms that allow Faim to exert its functions will provide a great value into the ophthalmologic field.**

# References

*“Never be limited by other people's limited  
imagination”*

Mae Jemison (1956)





## References

- Alexa, A, and J Rahnenfuhrer. 2022. "TopGO: Enrichment Analysis for Gene Ontology. R Package Version 2.48.0."
- Amemiya, Tsugio. 1977. "Dark Adaptation in Diabetics." *Ophthalmologica* 174: 322–26.
- Anderson, Peter Jb, Hr Watts, Cj Hille, Kl Philpott, P Clark, M Croucher S Gentleman, and Ling-Sun Jen. 2008. "Glial and Endothelial Blood-Retinal Barrier Responses to Amyloid-Beta in the Neural Retina of the Rat." *Clinical Ophthalmology (Auckland, N.Z.)* 2 (4): 801–16. <https://doi.org/10.2147/opth.s3967>.
- Araszkiewicz, Aleksandra, and Dorota Zozulinska-Ziolkiewicz. 2016. "Retinal Neurodegeneration in the Course of Diabetes-Pathogenesis and Clinical Perspective." *Current Neuropharmacology* 14 (8): 805. <https://doi.org/10.2174/1570159X14666160225154536>.
- Arden, G. B., J. E. Wolf, and Y. Tsang. 1998. "Does Dark Adaptation Exacerbate Diabetic Retinopathy? Evidence and a Linking Hypothesis." *Vision Research* 38 (11): 1723–29. [https://doi.org/10.1016/S0042-6989\(98\)00004-2](https://doi.org/10.1016/S0042-6989(98)00004-2).
- Arroba, Ana I., Alfonso M. Lechuga-Sancho, Laura M. Frago, Jesús Argente, and Julie A. Chowen. 2007. "Cell-Specific Expression of X-Linked Inhibitor of Apoptosis in the Anterior Pituitary of Streptozotocin-Induced Diabetic Rats." *Journal of Endocrinology* 192 (1): 215–27. <https://doi.org/10.1677/joe.1.06985>.

- Aryan, Hajar, Atekeh Bahadori, Dariush D. Farhud, Marjan Zarif Yeganeh, and Haniyeh Pourkalhor. 2020. "A Homozygote Mutation in S-Antigen Visual Arrestin SAG Gene in an Iranian Patient with Oguchi Type One: A Case Report." *Iranian Journal of Public Health* 49 (5).  
<https://doi.org/10.18502/ijph.v49i5.3219>.
- Ashkenazi, Avi, and Vishva M. Dixit. 1998. "Death Receptors: Signaling and Modulation." *Science (New York, N.Y.)* 281 (5381): 1305–8.  
<https://doi.org/10.1126/SCIENCE.281.5381.1305>.
- Athanasidou, Dimitra, Monica Aguila, James Bellingham, Wenwen Li, Caroline McCulley, Philip J Reeves, and Michael E Cheetham. 2018. "The Molecular and Cellular Basis of Rhodopsin Retinitis Pigmentosa Reveals Potential Strategies for Therapy." *Progress in Retinal and Eye Research*. <https://doi.org/10.1016/j.preteyeres.2017.10.002>.
- Balaiya, Sankarathi, Khaled K. Abu-Amero, Altaf A. Kondkar, and Kakarla V. Chalam. 2017. "Sirtuins Expression and Their Role in Retinal Diseases." *Oxidative Medicine and Cellular Longevity* 2017.  
<https://doi.org/10.1155/2017/3187594>.
- Bayburt, Timothy H., Sergey A. Vishnivetskiy, Mark A. McLean, Takefumi Morizumi, Chih Chin Huang, John J.G. Tesmer, Oliver P. Ernst, Stephen G. Sligar, and Vsevolod V. Gurevich. 2011. "Monomeric Rhodopsin Is Sufficient for Normal Rhodopsin Kinase (GRK1) Phosphorylation and Arrestin-1 Binding." *Journal of Biological Chemistry* 286 (2): 1420–28. <https://doi.org/10.1074/JBC.M110.151043>.
- Beard, Helen, Glyn Chidlow, Daniel Neumann, Nazzmer Nazri, Meghan Douglass, Paul J. Trim, Marten F. Snel, Robert J. Casson, and Kim M.

- Hemsley. 2020. "Is the Eye a Window to the Brain in Sanfilippo Syndrome?" *Acta Neuropathologica Communications* 8 (1): 1–16. <https://doi.org/10.1186/s40478-020-01070-w>.
- Behrens, Christian, Timm Schubert, Silke Haverkamp, Thomas Euler, and Philipp Berens. 2016. "Connectivity Map of Bipolar Cells and Photoreceptors in the Mouse Retina." *ELife* 5 (NOVEMBER2016). <https://doi.org/10.7554/ELIFE.20041>.
- Bellezza, Ilaria. 2018. "Oxidative Stress in Age-Related Macular Degeneration: NRF2 as Therapeutic Target." *Frontiers in Pharmacology* 9 (NOV): 1–7. <https://doi.org/10.3389/fphar.2018.01280>.
- Berger, Adeline, Sophie Cavallero, Elisa Dominguez, Peggy Barbe, Manuel Simonutti, José Alain Sahel, Florian Sennlaub, William Raoul, Michel Paques, and Alexis Pierre Bemelmans. 2014. "Spectral-Domain Optical Coherence Tomography of the Rodent Eye: Highlighting Layers of the Outer Retina Using Signal Averaging and Comparison with Histology." *PLoS ONE* 9 (5).
- Berkowitz, Bruce A., Robert H. Podolsky, Haohua Qian, Yichao Li, Ke Jiang, Jacob Nellissery, Anand Swaroop, and Robin Roberts. 2018. "Mitochondrial Respiration in Outer Retina Contributes to Light-Evoked Increase in Hydration In Vivo." *Investigative Ophthalmology & Visual Science* 59 (15): 5957. <https://doi.org/10.1167/IOVS.18-25682>.
- Berthelet, Jean, and Laurence Dubrez. 2013. "Regulation of Apoptosis by Inhibitors of Apoptosis (IAPs)." *Cells 2013, Vol. 2, Pages 163-187* 2 (1): 163–87. <https://doi.org/10.3390/CELLS2010163>.
- Binz, Nicolette, Elizabeth P. Rakoczy, Ireni S. Ali Rahman, Nermina N.

- Vagaja, and Chooi-May May Lai. 2016. "Biomarkers for Diabetic Retinopathy – Could Endothelin 2 Be Part of the Answer?" *PLOS ONE* 11 (8): e0160442. <https://doi.org/10.1371/JOURNAL.PONE.0160442>.
- Blanchard, Véronique, Saliha Moussaoui, Christian Czech, Nathalie Touchet, Bruno Bonici, Michel Planche, Thierry Canton, et al. 2003. "Time Sequence of Maturation of Dystrophic Neurites Associated with A $\beta$  Deposits in APP/PS1 Transgenic Mice." *Experimental Neurology* 184 (1): 247–63. [https://doi.org/10.1016/S0014-4886\(03\)00252-8](https://doi.org/10.1016/S0014-4886(03)00252-8).
- Boon, Camiel J.F., Anneke I. den Hollander, Carel B. Hoyng, Frans P.M. Cremers, B. Jeroen Klevering, and Jan E.E. Keunen. 2008. "The Spectrum of Retinal Dystrophies Caused by Mutations in the Peripherin/RDS Gene." *Progress in Retinal and Eye Research* 27 (2): 213–35. <https://doi.org/10.1016/J.PRETEYERES.2008.01.002>.
- Bramall, Alexa N., Michael J. Szego, Laura R. Pacione, Inik Chang, Eduardo Diez, Pedro D'Orleans-Juste, Duncan J. Stewart, William W. Hauswirth, Masashi Yanagisawa, and Roderick R. McInnes. 2013. "Endothelin-2-Mediated Protection of Mutant Photoreceptors in Inherited Photoreceptor Degeneration." *PLoS ONE* 8 (2). <https://doi.org/10.1371/journal.pone.0058023>.
- Bravo-Nuevo, Arturo, Natalie Walsh, and Jonathan Stone. 2004. "Photoreceptor Degeneration and Loss of Retinal Function in the C57BL/6-C2J Mouse." *Investigative Ophthalmology and Visual Science* 45 (6): 2005–12. <https://doi.org/10.1167/iovs.03-0842>.
- Bringmann, A, A Reichenbach, and P Wiedemann. 2004. "Pathomechanisms of Cystoid Macular Edema." *Ophthalmic Research* 36: 241–49.

Bringmann, Andreas, Ianors Iandiev, Thomas Pannicke, Antje Wurm, Margrit Hollborn, Peter Wiedemann, Neville N. Osborne, and Andreas Reichenbach. 2009. "Cellular Signaling and Factors Involved in Müller Cell Gliosis: Neuroprotective and Detrimental Effects." *Progress in Retinal and Eye Research*.  
<https://doi.org/10.1016/j.preteyeres.2009.07.001>.

Bringmann, Andreas, Thomas Pannicke, Jens Grosche, Mike Francke, Peter Wiedemann, Serguei N. Skatchkov, Neville N. Osborne, and Andreas Reichenbach. 2006. "Müller Cells in the Healthy and Diseased Retina." *Progress in Retinal and Eye Research* 25 (4): 397–424.  
<https://doi.org/10.1016/j.preteyeres.2006.05.003>.

Bringmann, Andreas, and Peter Wiedemann. 2012. "Müller Glial Cells in Retinal Disease." *Ophthalmologica* 227 (1): 1–19.  
<https://doi.org/10.1159/000328979>.

Brion, J P, A M Couck, E Passareiro, and J Flament-Durand. 1985. "Neurofibrillary Tangles of Alzheimer's Disease: An Immunohistochemical Study." *Journal of Submicroscopic Cytology* 17 (1): 89–96.

Brion, J P, J Flament-Durand, and P Dustin. 1986. "Alzheimer's Disease and Tau Proteins." *Lancet (London, England)*. England.  
[https://doi.org/10.1016/s0140-6736\(86\)90495-2](https://doi.org/10.1016/s0140-6736(86)90495-2).

Calleja-Yagüe, Isabel. 2019. "Neuronal Phenotype Characterization of FAIM KO Mice."

Campbell, J P, M Zhang, T S Hwang, S T Bailey, D J Wilson, Y Jia, and D Huang. 2017. "Detailed Vascular Anatomy of the Human Retina by

Projection-Resolved Optical Coherence Tomography Angiography.”  
*Scientific Reports* 7 (February): 42201.  
<https://doi.org/10.1038/srep42201>.

Campello, Laura, Julián Esteve-Rudd, Nicolás Cuenca, and José Martín-Nieto. 2013. “The Ubiquitin-Proteasome System in Retinal Health and Disease.” *Molecular Neurobiology* 47 (2): 790–810.  
<https://doi.org/10.1007/s12035-012-8391-5>.

Carbon, Seth, Eric Douglass, Benjamin M. Good, Deepak R. Unni, Nomi L. Harris, Christopher J. Mungall, Siddartha Basu, et al. 2021. “The Gene Ontology Resource: Enriching a GOld Mine.” *Nucleic Acids Research* 49 (D1): D325–34. <https://doi.org/10.1093/NAR/GKAA1113>.

Carbon, Seth, Amelia Ireland, Christopher J. Mungall, Shengqiang Shu, Brad Marshall, Suzanna Lewis, Jane Lomax, et al. 2009. “AmiGO: Online Access to Ontology and Annotation Data.” *Bioinformatics* 25 (2): 288–89. <https://doi.org/10.1093/BIOINFORMATICS/BTN615>.

Care, Rachel A., Ivan A. Anastassov, David B. Kastner, Yien Ming Kuo, Luca Della Santina, and Felice A. Dunn. 2020. “Mature Retina Compensates Functionally for Partial Loss of Rod Photoreceptors.” *Cell Reports* 31 (10): 107730. <https://doi.org/10.1016/j.celrep.2020.107730>.

Carpi-Santos, Raul, Ricardo A. de Melo Reis, Flávia Carvalho Alcantara Gomes, and Karin C. Calaza. 2022. “Contribution of Müller Cells in the Diabetic Retinopathy Development: Focus on Oxidative Stress and Inflammation.” *Antioxidants* 11 (4).  
<https://doi.org/10.3390/ANTIOX11040617>.

Carrasco, Esther, Cristina Hernández, Adela Miralles, Pere Huguet, Jaume

Farrés, and Rafael Simó. 2007. “Lower Somatostatin Expression Is an Early Event in Diabetic Retinopathy and Is Associated With Retinal Neurodegeneration.” *Diabetes Care* 30 (11): 2902–8.

<https://doi.org/10.2337/DC07-0332>.

Carriba, P, S Jimenez, V Navarro, and R S Moubarak. 2015. “Amyloid- $\beta$  Reduces the Expression of Neuronal FAIM-L , Thereby Shifting the Inflammatory Response Mediated by TNF  $\alpha$  from Neuronal Protection to Death.” *Cell Death and Disease* 6 (2): e1639-13.

<https://doi.org/10.1038/cddis.2015.6>.

Carriba, Paulina, and Joan X. Comella. 2014. “Amyloid Beta, TNF $\alpha$  and FAIM-L; Approaching New Therapeutic Strategies for AD.” *Frontiers in Neurology* 5 (DEC). <https://doi.org/10.3389/fneur.2014.00276>.

Chan, Priscilla, Julia Stolz, Susanne Kohl, Wei Chieh Chiang, and Jonathan H. Lin. 2016. “Endoplasmic Reticulum Stress in Human Photoreceptor Diseases.” *Brain Research* 1648 (October): 538–41.

<https://doi.org/10.1016/J.BRAINRES.2016.04.021>.

Chang, Min Lin, Ching Hsiang Wu, Ya Fen Jiang-shieh, Jeng Yung Shieh, and Chen Yuan Wen. 2007. “Reactive Changes of Retinal Astrocytes and Müller Glial Cells in Kainate-Induced Neuroexcitotoxicity.”

*Journal of Anatomy* 210 (1): 54. <https://doi.org/10.1111/J.1469-7580.2006.00671.X>.

Chaya, Taro, Ryotaro Tsutsumi, Leah Rie Varner, Yamato Maeda, Satoyo Yoshida, and Takahisa Furukawa. 2019. “Cul3-Klhl18 Ubiquitin Ligase Modulates Rod Transducin Translocation during Light-dark Adaptation.” *The EMBO Journal* 38 (23).



<https://doi.org/10.15252/emj.2018101409>.

Chen, Ching Kang, Marie E. Burns, Maribeth Spencer, Gregory A. Niemi, Jeannie Chen, James B. Hurley, Denis A. Baylor, and Melvin I. Simon. 1999. "Abnormal Photoresponses and Light-Induced Apoptosis in Rods Lacking Rhodopsin Kinase." *Proceedings of the National Academy of Sciences of the United States of America* 96 (7): 3718–22.

<https://doi.org/10.1073/pnas.96.7.3718>.

Chen, Jeannie, Clint L. Makino, Neal S. Peachey, Denis A. Baylor, and Melvin I. Simon. 1995. "Mechanisms of Rhodopsin Inactivation in Vivo as Revealed by a COOH-Terminal Truncation Mutant." *Science* 267 (5196): 374–77. <https://doi.org/10.1126/SCIENCE.7824934>.

Chen, Jeannie, Melvin I. Simon, Michael T. Matthes, Douglas Yasumura, and Matthew M. LaVail. 1999. "Increased Susceptibility to Light Damage in an Arrestin Knockout Mouse Model of Oguchi Disease (Stationary Night Blindness)." *Investigative Ophthalmology and Visual Science* 40 (12): 2978–82.

Chen, Tsung Yu, and King Wai Yau. 1994. "Direct Modulation by Ca(2+)-Calmodulin of Cyclic Nucleotide-Activated Channel of Rat Olfactory Receptor Neurons." *Nature* 368 (6471): 545–48.

<https://doi.org/10.1038/368545A0>.

Cheung, Ning, Paul Mitchell, and Tien Yin Wong. 2010. "Diabetic Retinopathy." In *The Lancet*, 376:124–36. Elsevier.

[https://doi.org/10.1016/S0140-6736\(09\)62124-3](https://doi.org/10.1016/S0140-6736(09)62124-3).

Chiquita, Samuel, Ana C. Rodrigues-Neves, Filipa I. Baptista, Rafael Carecho, Paula I. Moreira, Miguel Castelo-Branco, and António F.

- Ambrósio. 2019. “The Retina as a Window or Mirror of the Brain Changes Detected in Alzheimer’s Disease: Critical Aspects to Unravel.” *Molecular Neurobiology* 56 (8): 5416–35.  
<https://doi.org/10.1007/s12035-018-1461-6>.
- Ciechanover, Aaron, and Patrik Brundin. 2003. “The Ubiquitin Proteasome System in Neurodegenerative Diseases: Sometimes the Chicken, Sometimes the Egg.” *Neuron*. Cell Press. [https://doi.org/10.1016/S0896-6273\(03\)00606-8](https://doi.org/10.1016/S0896-6273(03)00606-8).
- Clifford, Luke J., Andrew M.J. Turnbull, and Anne M. Denning. 2013. “Reversible Night Blindness – A Reminder of the Increasing Importance of Vitamin A Deficiency in the Developed World.” *Journal of Optometry* 6 (3): 173. <https://doi.org/10.1016/J.OPTOM.2013.01.002>.
- Coccia, Elena, Isabel Calleja-Yagüe, Laura Planells-Ferrer, Blanca Sanuy, Joaquin Lo, Isabel Calleja-Yagüe, Laura Planells-Ferrer, et al. 2017. “Identification and Characterization of New Isoforms of Human Fas Apoptotic Inhibitory Molecule ( FAIM ).” *PLoS ONE* 12 (10): 1–21.  
<https://doi.org/10.1371/journal.pone.0185327>.
- Coccia, Elena, Laura Planells-Ferrer, Raquel Badillos-Rodríguez, Marta Pascual, Miguel F. Segura, Rita Fernández-Hernández, Joaquin López-Soriano, et al. 2020. “SIVA-1 Regulates Apoptosis and Synaptic Function by Modulating XIAP Interaction with the Death Receptor Antagonist FAIM-L.” *Cell Death and Disease* 11 (2).  
<https://doi.org/10.1038/s41419-020-2282-x>.
- Cohen, George B., Daniel D. Oprian, and Phyllis R. Robinson. 1992. “Mechanism of Activation and Inactivation of Opsin: Role of Glu113

and Lys296.” *Biochemistry* 31 (50): 12592–601.

<https://doi.org/10.1021/BI00165A008>.

Coleman, Jason E., and Susan L. Semple-Rowland. 2005. “GC1 Deletion Prevents Light-Dependent Arrestin Translocation in Mouse Cone Photoreceptor Cells.” *Investigative Ophthalmology and Visual Science* 46 (1): 12–16. <https://doi.org/10.1167/iovs.04-0691>.

Cooney, Theresa M., C. Starck Johnson, and Victor M. Elner. 2007. “Keratomalacia Caused by Psychiatric-Induced Dietary Restrictions.” *Cornea* 26 (8): 995–97.

<https://doi.org/10.1097/ICO.0B013E3180959A5D>.

Coorey, Nathan J, Weiyong Shen, Sook H Chung, Ling Zhu, and Mark C Gillies. 2012. “The Role of Glia in Retinal Vascular Disease.” *Clinical and Experimental Optometry* 95 (3): 266–81.

<https://doi.org/https://doi.org/10.1111/j.1444-0938.2012.00741.x>.

Corbett, James J., and Jian Chen. 2018. “The Visual System.” *Fundamental Neuroscience for Basic and Clinical Applications: Fifth Edition*, January, 286-305.e1. <https://doi.org/10.1016/B978-0-323-39632-5.00020-7>.

Cossu, Federica, Mario Milani, Eloise Mastrangelo, and Daniele Lecis. 2019. “Targeting the BIR Domains of Inhibitor of Apoptosis (IAP) Proteins in Cancer Treatment.” *Computational and Structural Biotechnology Journal* 17 (January): 142. <https://doi.org/10.1016/J.CSBJ.2019.01.009>.

Coughlin, Brandon A, Derrick J Feenstra, and Susanne Mohr. 2017. “Müller Cells and Diabetic Retinopathy.” *Vision Research* 139: 93–100.

<https://doi.org/https://doi.org/10.1016/j.visres.2017.03.013>.

- Criscuolo, Chiara, Elisa Cerri, Carlotta Fabiani, Simona Capsoni, Antonino Cattaneo, and Luciano Domenici. 2018. "The Retina as a Window to Early Dysfunctions of Alzheimer's Disease Following Studies with a 5xFAD Mouse Model." *Neurobiology of Aging* 67: 181–88.  
<https://doi.org/10.1016/j.neurobiolaging.2018.03.017>.
- Cunha-Vaz, José. 2017. "The Blood-Retinal Barrier in the Management of Retinal Disease: EURETINA Award Lecture." *Ophthalmologica. Journal International d'ophtalmologie. International Journal of Ophthalmology. Zeitschrift Fur Augenheilkunde*. Switzerland.  
<https://doi.org/10.1159/000455809>.
- Cunha-Vaz, José, Rui Bernardes, and Conceição Lobo. 2010. "Blood-Retinal Barrier:" *Https://Doi.Org/10.5301/EJO.2010.6049* 21 (SUPPL.6): 3–9.  
<https://doi.org/10.5301/EJO.2010.6049>.
- Dai, Ying, and Tao Sun. 2021. "Oguchi's Disease: Two Cases and Literature Review." *The Journal of International Medical Research* 49 (5).  
<https://doi.org/10.1177/03000605211019921>.
- Dantuma, Nico P., and Laura C. Bott. 2014. "The Ubiquitin-Proteasome System in Neurodegenerative Diseases: Precipitating Factor, yet Part of the Solution." *Frontiers in Molecular Neuroscience* 7 (JULY).  
<https://doi.org/10.3389/FNMOL.2014.00070>.
- Das, Kaberi P., Theresa M. Freudenrich, and William R. Mundy. 2004. "Assessment of PC12 Cell Differentiation and Neurite Growth: A Comparison of Morphological and Neurochemical Measures." *Neurotoxicology and Teratology* 26 (3): 397–406.  
<https://doi.org/10.1016/j.ntt.2004.02.006>.

- Das, Rueben G., Doreen Becker, Vidhya Jagannathan, Orly Goldstein, Evelyn Santana, Kendall Carlin, Raghavi Sudharsan, et al. 2019. “Genome-Wide Association Study and Whole-Genome Sequencing Identify a Deletion in LRIT3 Associated with Canine Congenital Stationary Night Blindness.” *Scientific Reports* 2019 9:1 9 (1): 1–12. <https://doi.org/10.1038/s41598-019-50573-7>.
- Decanini, Alejandra, Curtis L. Nordgaard, Xiao Feng, Deborah A. Ferrington, and Timothy W. Olsen. 2007. “Changes in Select Redox Proteins of the Retinal Pigment Epithelium in Age-Related Macular Degeneration.” *American Journal of Ophthalmology* 143 (4): 607. <https://doi.org/10.1016/J.AJO.2006.12.006>.
- Dehkordi, Mahshid H., Robert G.K. Munn, and Howard O. Fearnhead. 2022. “Non-Canonical Roles of Apoptotic Caspases in the Nervous System.” *Frontiers in Cell and Developmental Biology* 10 (February): 349. <https://doi.org/10.3389/FCELL.2022.840023/XML/NLM>.
- Descartes, René. 1664. “Traité de l’homme.” *Clerselier*.
- “Diabetic Retinopathy - NHS.” n.d. Accessed August 26, 2022. <https://www.nhs.uk/conditions/diabetic-retinopathy/>.
- Díaz-Coránguez, Mónica, Carla Ramos, and David A. Antonetti. 2017. “The Inner Blood-Retinal Barrier: Cellular Basis and Development.” *Vision Research* 139 (October): 123–37. <https://doi.org/10.1016/J.VISRES.2017.05.009>.
- Dikic, Ivan, Soichi Wakatsuki, and Kylie J. Walters. 2009. “Ubiquitin-Binding Domains from Structures to Functions.” *Nature Reviews Molecular Cell Biology* 10 (10): 659–71.

<https://doi.org/10.1038/nrm2767>.

Dobin, Alexander, Carrie A. Davis, Felix Schlesinger, Jorg Drenkow, Chris Zaleski, Sonali Jha, Philippe Batut, Mark Chaisson, and Thomas R. Gingeras. 2013. “STAR: Ultrafast Universal RNA-Seq Aligner.” *Bioinformatics (Oxford, England)* 29 (1): 15–21.  
<https://doi.org/10.1093/BIOINFORMATICS/BTS635>.

Donaldson, Kathryn M., Hongwei Yin, Nicholas Gekakis, Frantisek Supek, and Claudio A.P. Joazeiro. 2003. “Ubiquitin Signals Protein Trafficking via Interaction with a Novel Ubiquitin Binding Domain in the Membrane Fusion Regulator, Vps9p.” *Current Biology* 13 (3): 258–62.  
[https://doi.org/10.1016/S0960-9822\(03\)00043-5](https://doi.org/10.1016/S0960-9822(03)00043-5).

Dong, Cun Jian, Peter Agey, and William A. Hare. 2004. “Origins of the Electroretinogram Oscillatory Potentials in the Rabbit Retina.” *Visual Neuroscience* 21 (4): 533–43.  
<https://doi.org/10.1017/S0952523804214043>.

Du, Yunpeng, Alexander Veenstra, Krzysztof Palczewski, and Timothy S. Kern. 2013. “Photoreceptor Cells Are Major Contributors to Diabetes-Induced Oxidative Stress and Local Inflammation in the Retina.” *Proceedings of the National Academy of Sciences of the United States of America* 110 (41): 16586–91.  
<https://doi.org/10.1073/PNAS.1314575110/ASSET/8F0DD46B-00AD-463F-8BF0-3604B37C1848/ASSETS/GRAPHIC/PNAS.1314575110FIG07.JPEG>.

Duh, Elia J., Jennifer K. Sun, and Alan W. Stitt. 2017. “Diabetic Retinopathy: Current Understanding, Mechanisms, and Treatment

Strategies.” *JCI Insight* 2 (14).

<https://doi.org/10.1172/JCI.INSIGHT.93751>.

Duignan, Emma, Paul Kenna, Rosemarie Watson, Susan Fitzsimon, and Donal Brosnahan. 2015. “Ophthalmic Manifestations of Vitamin A and D Deficiency in Two Autistic Teenagers: Case Reports and a Review of the Literature.” *Case Reports in Ophthalmology* 6 (1): 24.

<https://doi.org/10.1159/000373921>.

Eastlake, Karen, Wendy E. Heywood, Phillip Banerjee, Emily Bliss, Kevin Mills, Peng T. Khaw, David Charteris, and G. Astrid Limb. 2018. “Comparative Proteomic Analysis of Normal and Gliotic PVR Retina and Contribution of Müller Glia to This Profile.” *Experimental Eye Research* 177 (December).

<https://doi.org/10.1016/J.EXER.2018.08.016>.

Ekshyyan, Oleksandr, and Tak Yee Aw. 2004. “Apoptosis in Acute and Chronic Neurological Disorders.” *Frontiers in Bioscience : A Journal and Virtual Library* 9: 1567–76. <https://doi.org/10.2741/1357>.

Ekström, P, S Sanyal, K Narfström, G J Chader, and T van Veen. 1988. “Accumulation of Glial Fibrillary Acidic Protein in Müller Radial Glia during Retinal Degeneration.” *Investigative Ophthalmology & Visual Science* 29 (9): 1363–71.

Elmore, Susan. 2007. “Apoptosis: A Review of Programmed Cell Death.” *Toxicologic Pathology* 35 (4): 495.

<https://doi.org/10.1080/01926230701320337>.

Esquerdo-Barragán, Mariona, Matthew J. Brooks, Vasileios Toulis, Anand Swaroop, and Gemma Marfany. 2019. “Expression of Deubiquitinating

Enzyme Genes in the Developing Mammal Retina.” *Molecular Vision* 25 (December): 800–813.

Esquerdo, Mariona, Xavier Grau-Bové, Alejandro Garanto, Vasileios Toulis, Sílvia Garcia-Monclús, Erica Millo, Ma José López-Iniesta, Víctor Abad-Morales, Iñaki Ruiz-Trillo, and Gemma Marfany. 2016. “Expression Atlas of the Deubiquitinating Enzymes in the Adult Mouse Retina, Their Evolutionary Diversification and Phenotypic Roles.” *PLoS ONE* 11 (3): 1–18. <https://doi.org/10.1371/journal.pone.0150364>.

Feher, Joseph. 2012. “Vision.” *Quantitative Human Physiology*, January, 386–400. <https://doi.org/10.1016/B978-0-12-382163-8.00041-4>.

Fernández-Albarral, José A., Juan J. Salazar, Rosa de Hoz, Eva M. Marco, Beatriz Martín-Sánchez, Elena Flores-Salguero, Elena Salobar-García, et al. 2021. “Retinal Molecular Changes Are Associated with Neuroinflammation and Loss of RGCs in an Experimental Model of Glaucoma.” *International Journal of Molecular Sciences* 22 (4): 1–29. <https://doi.org/10.3390/IJMS22042066>.

Fernández-Sánchez, Laura, Pedro Lax, Carolina Isiegas, Eduard Ayuso, José M. Ruiz, Pedro De La Villa, Fatima Bosch, Enrique J. De La Rosa, and Nicolás Cuenca. 2012. “Proinsulin Slows Retinal Degeneration and Vision Loss in the P23H Rat Model of Retinitis Pigmentosa.” *Human Gene Therapy* 23 (12): 1290–1300. <https://doi.org/10.1089/hum.2012.067>.

Fimbel, Shane M, Jacob E Montgomery, Christopher T Burket, and David R Hyde. 2007. “Regeneration of Inner Retinal Neurons after Intravitreal Injection of Ouabain in Zebrafish.” *The Journal of Neuroscience : The*



*Official Journal of the Society for Neuroscience* 27 (7): 1712–24.  
<https://doi.org/10.1523/JNEUROSCI.5317-06.2007>.

Flick, Karin, and Peter Kaiser. 2012. “Protein Degradation and the Stress Response.” *Semin Cell Dev Biol.* 23 (5): 515–22.  
<https://doi.org/10.1016/j.semcdb.2012.01.019>.

Frederiksen, Rikard, Soile Nymark, Alexander V. Kolesnikov, Justin D. Berry, Leopold Adler, Yiannis Koutalos, Vladimir J. Kefalov, and M. Carter Cornwall. 2016. “Rhodopsin Kinase and Arrestin Binding Control the Decay of Photoactivated Rhodopsin and Dark Adaptation of Mouse Rods.” *The Journal of General Physiology* 148 (1): 1–11.  
<https://doi.org/10.1085/JGP.201511538>.

Fu, Yingbin, and King-Wai Yau. 2007. “Phototransduction in Mouse Rods and Cones.” *Eur J Physiol*, no. 454: 805–819.  
<https://doi.org/10.1007/s00424-006-0194-y>.

Fu, Zhongjie, Shen Nian, Suk Yee Li, David Wong, Sookja K. Chung, and Amy C.Y. Lo. 2015. “Deficiency of Aldose Reductase Attenuates Inner Retinal Neuronal Changes in a Mouse Model of Retinopathy of Prematurity.” *Graefe’s Archive for Clinical and Experimental Ophthalmology* 253 (9): 1503–13. <https://doi.org/10.1007/S00417-015-3024-0>.

Fuchs, Sigrid, Mitsuru Nakazawa, Marion Maw, Makoto Tamai, Yoshihisa Oguchi, and Andreas Gal. 1995. “Oguchi Disease in Japanese” 10 (july): 360–62.

Fuente García, C., J.J. González-López, F.J. Muñoz-Negrete, and G. Rebolleda. 2018. “La Utilidad Diagnóstica Del Electrorretinograma

Negativo.” *Archivos de La Sociedad Española de Oftalmología* 93 (3): 126–35. <https://doi.org/10.1016/j.ofтал.2017.10.006>.

Fuentes-Lemus, Eduardo, Per Hägglund, Camilo López-Alarcón, and Michael J. Davies. 2022. “Oxidative Crosslinking of Peptides and Proteins: Mechanisms of Formation, Detection, Characterization and Quantification.” *Molecules* 27 (1): 1–31. <https://doi.org/10.3390/molecules27010015>.

Galbán, S, and C S Duckett. 2010. “XIAP as a Ubiquitin Ligase in Cellular Signaling.” *Cell Death and Differentiation* 17: 54–60. <https://doi.org/10.1038/cdd.2009.81>.

Gallego, Antonio. 1971. “Horizontal and Amacrine Cells in the Mammal’s Retina.” *Vision Research* 11 (SUPPL. 3): 33-IN24. [https://doi.org/10.1016/0042-6989\(71\)90029-0](https://doi.org/10.1016/0042-6989(71)90029-0).

Gao, H, and J G Hollyfield. 1996. “Basic Fibroblast Growth Factor: Increased Gene Expression in Inherited and Light-Induced Photoreceptor Degeneration.” *Experimental Eye Research* 62 (2): 181–89. <https://doi.org/10.1006/exer.1996.0022>.

Garcia-Ramírez, M., C. Hernández, M. Villarroel, F. Canals, M. A. Alonso, R. Fortuny, L. Masmiquel, A. Navarro, J. García-Arumí, and R. Simó. 2009. “Interphotoreceptor Retinoid-Binding Protein (IRBP) Is Downregulated at Early Stages of Diabetic Retinopathy.” *Diabetologia* 52 (12): 2633–41. <https://doi.org/10.1007/S00125-009-1548-8/FIGURES/5>.

Giebel, Stephen J, Gina Menicucci, Paul G McGuire, and Arup Das. 2005. “Matrix Metalloproteinases in Early Diabetic Retinopathy and Their

Role in Alteration of the Blood-Retinal Barrier.” *Laboratory Investigation; a Journal of Technical Methods and Pathology* 85 (5): 597–607. <https://doi.org/10.1038/labinvest.3700251>.

Goh, E.T., M.J. Way, S.R. Atkinson, A. McQuillin, and M.Y. Morgan. 2016. “Variations in the Promoter Region of the Glutaminase Gene and the Development of Hepatic Encephalopathy in Patients with Cirrhosis.” *Journal of Hepatology* 64 (2): S257. [https://doi.org/10.1016/s0168-8278\(16\)00283-x](https://doi.org/10.1016/s0168-8278(16)00283-x).

González, Hugo, Daniela Elgueta, Andro Montoya, and Rodrigo Pacheco. 2014. “Neuroimmune Regulation of Microglial Activity Involved in Neuroinflammation and Neurodegenerative Diseases.” *Journal of Neuroimmunology* 274 (1–2): 1–13. <https://doi.org/10.1016/j.jneuroim.2014.07.012>.

Gooyer, Tanyth E. De, Kathryn A. Stevenson, Pete Humphries, David A.C. Simpson, Tom A. Gardiner, and Alan W. Stitt. 2006. “Retinopathy Is Reduced during Experimental Diabetes in a Mouse Model of Outer Retinal Degeneration.” *Investigative Ophthalmology & Visual Science* 47 (12): 5561–68. <https://doi.org/10.1167/IOVS.06-0647>.

Gosbell, Andrew D., Nada Stefanovic, Lyndee L. Scurr, Josefa Pete, Ismail Kola, Ian Favilla, and Judy B. De Haan. 2006. “Retinal Light Damage: Structural and Functional Effects of the Antioxidant Glutathione Peroxidase-1.” *Investigative Ophthalmology and Visual Science* 47 (6): 2613–22. <https://doi.org/10.1167/iovs.05-0962>.

Greenstein, Vivienne C., Shari R. Thomas, Howard Blaustein, Karen Koenig, and Ronald E. Carr. 1993. “Effects of Early Diabetic Retinopathy on

Rod System Sensitivity.” *Optometry and Vision Science*.

<https://doi.org/10.1097/00006324-199301000-00005>.

Grimm, C, A Wenzel, F Hafezi, S Yu, T M Redmond, and C E Remé. 2000. “Protection of Rpe65-Deficient Mice Identifies Rhodopsin as a Mediator of Light-Induced Retinal Degeneration.” *Nature Genetics* 25 (1): 63–66. <https://doi.org/10.1038/75614>.

Grimm, Christian, and Charlotte E. Remé. 2013. “Light Damage as a Model of Retinal Degeneration.” *Methods in Molecular Biology* 935: 87–97. <https://doi.org/10.1007/978-1-62703-080-9-6>.

———. 2019. “Light Damage Models of Retinal Degeneration.” *Methods in Molecular Biology* 1834: 167–78. [https://doi.org/10.1007/978-1-4939-8669-9\\_12](https://doi.org/10.1007/978-1-4939-8669-9_12).

Groettrup, Marcus, Christiane Pelzer, Gunter Schmidtke, and Kay Hofmann. 2008. “Activating the Ubiquitin Family: UBA6 Challenges the Field.” *Trends in Biochemical Sciences* 33 (5): 230–37. <https://doi.org/10.1016/J.TIBS.2008.01.005>.

Gurevich, Vsevolod V, and Eugenia V Gurevich. 2019. “Arrestin Mutations: Some Cause Diseases, Others Promise Cure.” *Progress in Molecular Biology and Translational Science* 161: 29–45. <https://doi.org/10.1016/bs.pmbts.2018.09.004>.

Hack, Iris, Leo Peichl, and Johann Helmut Brandstätter. 1999. “An Alternative Pathway for Rod Signals in the Rodent Retina: Rod Photoreceptors, Cone Bipolar Cells, and the Localization of Glutamate Receptors.” *Proceedings of the National Academy of Sciences of the United States of America* 96 (24): 14130–35.

<https://doi.org/10.1073/PNAS.96.24.14130/ASSET/6F8AB1FE-0E9C-4406-8B97-41DFD8925C1B/ASSETS/GRAPHIC/PQ2493552006.JPEG>.

Haglund, Kaisa, and Ivan Dikic. 2005. "Ubiquitylation and Cell Signaling." *EMBO Journal* 24 (19): 3353–59.  
<https://doi.org/10.1038/SJ.EMBOJ.7600808>.

Hammer, Sandra S., Cristiano P. Vieira, Delaney McFarland, Maximilian Sandler, Yan Levitsky, Tim F. Dorweiler, Todd A. Lydic, et al. 2021. "Fasting and Fasting-Mimicking Treatment Activate SIRT1/LXR $\alpha$  and Alleviate Diabetes-Induced Systemic and Microvascular Dysfunction." *Diabetologia* 64 (7): 1674–89. <https://doi.org/10.1007/S00125-021-05431-5>.

Han, Ning, Li Yu, Zhidu Song, Lifu Luo, and Yazhen Wu. 2015. "Agmatine Protects Müller Cells from High-Concentration Glucose-Induced Cell Damage via N-Methyl-D-Aspartic Acid Receptor Inhibition." *Molecular Medicine Reports* 12 (1): 1098–1106.  
<https://doi.org/10.3892/MMR.2015.3540/HTML>.

Hanson, Susan M., Eugenia V. Gurevich, Sergey A. Vishnivetskiy, Mohamed R. Ahmed, Xiufeng Song, and Vsevolod V. Gurevich. 2007. "Each Rhodopsin Molecule Binds Its Own Arrestin." *Proceedings of the National Academy of Sciences of the United States of America* 104 (9): 3125–28. <https://doi.org/10.1073/PNAS.0610886104>.

Hao, Wenshan, Andreas Wenzel, Martin S. Obin, Ching Kang Chen, Elliott Brill, Nataliia V. Krasnoperova, Pamela Eversole-Cire, et al. 2002. "Evidence for Two Apoptotic Pathways in Light-Induced Retinal

Degeneration.” *Nature Genetics* 32 (2): 254–60.  
<https://doi.org/10.1038/ng984>.

Hara, Taichi, Kenji Nakamura, Makoto Matsui, Akitsugu Yamamoto, Yohko Nakahara, Rika Suzuki-Migishima, Minesuke Yokoyama, et al. 2006. “Suppression of Basal Autophagy in Neural Cells Causes Neurodegenerative Disease in Mice.” *Nature* 441 (7095): 885–89.  
<https://doi.org/10.1038/nature04724>.

Harris, Lee D, Sarah Jasem, and Julien D F Licchesi. 2020. “The Ubiquitin System in Alzheimer’s Disease.” *Advances in Experimental Medicine and Biology* 1233: 195–221. [https://doi.org/10.1007/978-3-030-38266-7\\_8](https://doi.org/10.1007/978-3-030-38266-7_8).

Hegde, Ashok N., and Sudarshan C. Upadhya. 2007. “The Ubiquitin-Proteasome Pathway in Health and Disease of the Nervous System.” *Trends in Neurosciences* 30 (11): 587–95.  
<https://doi.org/10.1016/j.tins.2007.08.005>.

Henriquez, Mauricio, Ricardo Armisen, Andres Stutzin, and Andrew Quest. 2008. “Cell Death by Necrosis, a Regulated Way to Go.” *Current Molecular Medicine* 8 (3): 187–206.  
<https://doi.org/10.2174/156652408784221289>.

Henson, D. B., and R. V. North. 1979. “Dark Adaptation in Diabetes Mellitus.” *British Journal of Ophthalmology* 63 (8): 539–41.  
<https://doi.org/10.1136/bjo.63.8.539>.

Herskovits, A Zara, and Leonard Guarente. 2014. “SIRT1 in Neurodevelopment and Brain Senescence.” *Neuron* 81 (3): 471–83.  
<https://doi.org/10.1016/j.neuron.2014.01.028>.

- Hicke, Linda, Heidi L. Schubert, and Christopher P. Hill. 2005. "Ubiquitin-Binding Domains." *Nature Reviews Molecular Cell Biology* 6 (8): 610–21. <https://doi.org/10.1038/nrm1701>.
- Hjelmeland, L M, V J Cristofolo, W Funk, E Rakoczy, and M L Katz. 1999. "Senescence of the Retinal Pigment Epithelium." *Molecular Vision* 5 (November): 33.
- Holcik, Martin. 2002. "The IAP Proteins." *Trends in Genetics* 18 (10): 537–38. [https://doi.org/10.1016/S0168-9525\(02\)02743-9](https://doi.org/10.1016/S0168-9525(02)02743-9).
- Hsiau, Timothy H.-C., Claudiu Diaconu, Connie A Myers, Jongwoo Lee, Constance L Cepko, and Joseph C Corbo. 2007. "The Cis-Regulatory Logic of the Mammalian Photoreceptor Transcriptional Network." *PLOS ONE* 2 (7): e643. <https://doi.org/10.1371/journal.pone.0000643>.
- Hu, Rendong, Qiaoyu Cao, Zhongqing Sun, Jinying Chen, Qing Zheng, and Fei Xiao. 2018. "A Novel Method of Neural Differentiation of PC12 Cells by Using Opti-MEM as a Basic Induction Medium." *International Journal of Molecular Medicine* 41 (1): 195. <https://doi.org/10.3892/IJMM.2017.3195>.
- Hu, Xi Min, Zhi Xin Li, Rui Han Lin, Jia Qi Shan, Qing Wei Yu, Rui Xuan Wang, Lv Shuang Liao, et al. 2021. "Guidelines for Regulated Cell Death Assays: A Systematic Summary, A Categorical Comparison, A Prospective." *Frontiers in Cell and Developmental Biology* 9 (March). <https://doi.org/10.3389/FCELL.2021.634690>.
- Hughes, Andrew E.O., Jennifer M. Enright, Connie A. Myers, Susan Q. Shen, and Joseph C. Corbo. 2017. "Cell Type-Specific Epigenomic Analysis Reveals a Uniquely Closed Chromatin Architecture in Mouse

- Rod Photoreceptors.” *Scientific Reports* 7 (October 2016): 1–16.  
<https://doi.org/10.1038/srep43184>.
- Hunter, Allison M., Eric C. LaCasse, and Robert G. Korneluk. 2007. “The Inhibitors of Apoptosis (IAPs) as Cancer Targets.” *Apoptosis* 12 (9): 1543–68. <https://doi.org/10.1007/s10495-007-0087-3>.
- Huo, J, Y Ma, J-J Liu, Y S Ho, S Liu, L Y Soh, S Chen, et al. 2016. “Loss of Fas Apoptosis Inhibitory Molecule Leads to Spontaneous Obesity and Hepatosteatosis.” *Cell Death and Disease* 7 (2): e2091.  
<https://doi.org/10.1038/cddis.2016.12>.
- Huo, J, S Xu, K Guo, Q Zeng, and K-p Lam. 2009. “Genetic Deletion of Faim Reveals Its Role in Modulating C-FLIP Expression during CD95-Mediated Apoptosis of Lymphocytes and Hepatocytes.” *Cell Death and Differentiation*, 1062–70. <https://doi.org/10.1038/cdd.2009.26>.
- Huo, Jianxin, Shengli Xu, and Kong-Peng Lam. 2019. “FAIM: An Antagonist of Fas-Killing and Beyond.” *Cells* 8 (6): 541.  
<https://doi.org/10.3390/cells8060541>.
- Iannaccone, Alessandro, David Man, Naushin Waseem, Barbara J. Jennings, Madhavi Ganapathiraju, Kevin Gallaher, Elisheva Reese, Shomi S. Bhattacharya, and Judith Klein-Seetharaman. 2006. “Retinitis Pigmentosa Associated with Rhodopsin Mutations: Correlation between Phenotypic Variability and Molecular Effects.” *Vision Research* 46 (27): 4556–67. <https://doi.org/10.1016/J.VISRES.2006.08.018>.
- Illing, Michelle E., Rahul S. Rajan, Neil F. Bence, and Ron R. Kopito. 2002. “A Rhodopsin Mutant Linked to Autosomal Dominant Retinitis Pigmentosa Is Prone to Aggregate and Interacts with the Ubiquitin



Proteasome System.” *The Journal of Biological Chemistry* 277 (37): 34150–60. <https://doi.org/10.1074/jbc.M204955200>.

Ishikawa, Hiroaki, and Wallace F. Marshall. 2011. “Ciliogenesis: Building the Cell’s Antenna.” *Nature Reviews. Molecular Cell Biology* 12 (4): 222–34. <https://doi.org/10.1038/NRM3085>.

Jaliffa, Carolina, Ilhame Ameqrane, Anouk Dansault, Julia Leemput, Véronique Vieira, Emmanuelle Lacassagne, Alexandra Provost, et al. 2009. “Sirt1 Involvement in Rd10 Mouse Retinal Degeneration.” *Investigative Ophthalmology & Visual Science* 50 (8): 3562–72. <https://doi.org/10.1167/IOVS.08-2817>.

Jean-Charles, Pierre Yves, Vishwaesh Rajiv, and Sudha K. Shenoy. 2016. “Ubiquitin-Related Roles of  $\beta$ -Arrestins in Endocytic Trafficking and Signal Transduction.” *Journal of Cellular Physiology* 231 (10): 2071–80. <https://doi.org/10.1002/JCP.25317>.

Jeon, Chang-Jin, Enrica Strettoi, and Richard Masland. 1998. “The Major Cell Populations of the Mouse Retina. J Neurosci.” *The Journal of Neuroscience : The Official Journal of the Society for Neuroscience* 18 (December): 8936–46. <https://doi.org/10.1523/JNEUROSCI.18-21-08936.1998>.

Jiang, Youde, Jayaprakash Pagadala, Duane Miller, and Jena J. Steinle. 2013. “Reduced Insulin Receptor Signaling in Retinal Müller Cells Cultured in High Glucose.” *Molecular Vision* 19 (April): 804. [/pmc/articles/PMC3626298/](https://pubmed.ncbi.nlm.nih.gov/pmc/articles/PMC3626298/).

JN, Pearing, Salinas RY, Baker SA, and Arshavsky VY. 2013. “Protein Sorting, Targeting and Trafficking in Photoreceptor Cells.” *Progress in*

*Retinal and Eye Research* 36.

<https://doi.org/10.1016/J.PRETEYERES.2013.03.002>.

Joly, S., C. Lange, M. Thiersch, M. Samardzija, and C. Grimm. 2008.

“Leukemia Inhibitory Factor Extends the Lifespan of Injured Photoreceptors In Vivo.” *Journal of Neuroscience* 28 (51): 13765–74.

<https://doi.org/10.1523/jneurosci.5114-08.2008>.

Joly, Sandrine, Vincent Pernet, Sylvain Chemtob, Adriana Di Polo, and

Pierre Lachapelle. 2007. “Neuroprotection in the Juvenile Rat Model of Light-Induced Retinopathy: Evidence Suggesting a Role for FGF-2 and CNTF.” *Investigative Ophthalmology & Visual Science* 48 (5): 2311–20.

<https://doi.org/10.1167/iovs.06-1205>.

Kaku, H., and T. L. Rothstein. 2009. “Fas Apoptosis Inhibitory Molecule

Expression in B Cells Is Regulated through IRF4 in a Feed-Forward Mechanism.” *The Journal of Immunology* 183 (9): 5575–81.

<https://doi.org/10.4049/jimmunol.0901988>.

Kaku, Hiroaki, Alexander V Ludlow, Michael F Gutknecht, and Thomas L

Rothstein. 2021. “Fas Apoptosis Inhibitory Molecule Blocks and Dissolves Pathological Amyloid- $\beta$  Species.” *Frontiers in Molecular Neuroscience* 14 (December): 1–11.

<https://doi.org/10.3389/fnmol.2021.750578>.

Kaku, Hiroaki, and Thomas L. Rothstein. 2020. “FAIM Is a Non-Redundant

Defender of Cellular Viability in the Face of Heat and Oxidative Stress and Interferes With Accumulation of Stress-Induced Protein

Aggregates.” *Frontiers in Molecular Biosciences* 7 (February): 1–10.

<https://doi.org/10.3389/fmolb.2020.00032>.

- Kallifatidis, Georgios, Kenza Mamouni, and Bal L. Lokeshwar. 2020. "The Role of  $\beta$ -Arrestins in Regulating Stem Cell Phenotypes in Normal and Tumorigenic Cells." *International Journal of Molecular Sciences* 21 (23): 1–16. <https://doi.org/10.3390/ijms21239310>.
- Kalloniatis, Michael, and Erica L. Fletcher. 2004. "Retinitis Pigmentosa: Understanding the Clinical Presentation, Mechanisms and Treatment Options." *Clinical and Experimental Optometry* 87 (2): 65–80. <https://doi.org/10.1111/J.1444-0938.2004.TB03152.X>.
- Kalloniatis, Michael, and Charles Luu. 2007. "Light and Dark Adaptation." *The Australasian Journal of Optometry* 18 (8): 384–85. <https://doi.org/10.1111/j.1444-0938.1935.tb05750.x>.
- Kany, Shinwan, Jan Tilmann Vollrath, and Borna Relja. 2019. "Cytokines in Inflammatory Disease." *International Journal of Molecular Sciences* 20 (23): 6008. <https://doi.org/10.3390/ijms20236008>.
- Kato, Senri, Toshikazu Gondo, Yoshinobu Hoshii, Mutsuo Takahashi, Michio Yamada, and Tokuhiro Ishihara. 1998. "Confocal Observation of Senile Plaques in Alzheimer's Disease: Senile Plaque Morphology and Relationship between Senile Plaques and Astrocytes." *Pathology International* 48 (5): 332–40. <https://doi.org/https://doi.org/10.1111/j.1440-1827.1998.tb03915.x>.
- Kaufmann, T., A. Strasser, and P. J. Jost. 2011. "Fas Death Receptor Signalling: Roles of Bid and XIAP." *Cell Death & Differentiation* 2012 19:1 19 (1): 42–50. <https://doi.org/10.1038/cdd.2011.121>.
- Kawamura, Satoru. 1993. "Rhodopsin Phosphorylation as a Mechanism of Cyclic GMP Phosphodiesterase Regulation by S-Modulin." *Nature* 1993

362:6423 362 (6423): 855–57. <https://doi.org/10.1038/362855a0>.

Kawamura, Satoru, and Shuji Tachibanaki. 2010. “Phototransduction in Rods and Cones.” *Vertebrate Photoreceptors: Functional Molecular Bases*, April, 23–45. [https://doi.org/10.1007/978-4-431-54880-5\\_2](https://doi.org/10.1007/978-4-431-54880-5_2).

Kelly, Kristen, Joshua Wang, and Sarah Zhang. 2018. “The Unfolded Protein Response Signaling and Retinal Müller Cell Metabolism.” *Neural Regeneration Research* 13 (11): 1861–70. <https://doi.org/10.4103/1673-5374.239431>.

Kennedy, Breandán, and Jarema Malicki. 2009. “What Drives Cell Morphogenesis: A Look inside the Vertebrate Photoreceptor.” *Developmental Dynamics* 238 (9): 2115–38. <https://doi.org/10.1002/dvdy.22010>.

Kermer, Pawel, Jan Liman, Jochen H Weishaupt, and Mathias Bähr. 2004. “Neuronal Apoptosis in Neurodegenerative Diseases: From Basic Research to Clinical Application.” *Review Neurodegenerative Dis* 1: 9–19. <https://doi.org/10.1159/000076665>.

Kern, Timothy S., and Bruce A. Berkowitz. 2015. “Photoreceptors in Diabetic Retinopathy.” *Journal of Diabetes Investigation* 6 (4): 371. <https://doi.org/10.1111/JDI.12312>.

Kim, Leo. 2019. “Congenital Stationary Night Blindness (CSNB),” 2019. [https://eyewiki.aao.org/Congenital\\_Stationary\\_Night\\_Blindness\\_\(CSNB\)](https://eyewiki.aao.org/Congenital_Stationary_Night_Blindness_(CSNB))).

Kim, Min-Sik, Sneha M Pinto, Derese Getnet, Raja Sekhar Nirujogi, Srikanth S Manda, Raghothama Chaerkady, Anil K Madugundu, et al. 2014. “A

- Draft Map of the Human Proteome.” *Nature* 509 (7502): 575–81.  
<https://doi.org/10.1038/nature13302>.
- Kinkl, Norbert, José Sahel, and David Hicks. 2001. “Alternate FGF2-ERK1/2 Signaling Pathways in Retinal Photoreceptor and Glial Cells in Vitro \*.” *Journal of Biological Chemistry* 276: 43871–78.  
<https://doi.org/10.1074/jbc.M105256200>.
- Koleva-Georgieva, Desislava N., Nelly P. Sivkova, and Dora Terzieva. 2011. “Serum Inflammatory Cytokines IL-1beta, IL-6, TNF-Alpha and VEGF Have Influence on the Development of Diabetic Retinopathy.” *Folia Medica* 53 (2): 44–50. <https://doi.org/10.2478/V10153-010-0036-8>.
- Kommaddi, Reddy Peera, and Sudha K. Shenoy. 2013. *Arrestins and Protein Ubiquitination. Progress in Molecular Biology and Translational Science*. 1st ed. Vol. 118. Elsevier Inc. <https://doi.org/10.1016/B978-0-12-394440-5.00007-3>.
- Kono, Masahiro, Patrice W. Goletz, and Rosalie K. Crouch. 2008. “11-Cis and All-Trans Retinols Can Activate Rod Opsin: Rational Design of the Visual Cycle.” *Biochemistry* 47 (28): 7567.  
<https://doi.org/10.1021/BI800357B>.
- Kowluru, Renu A., Qing Zhong, and Mamta Kanwar. 2010. “Metabolic Memory and Diabetic Retinopathy: Role of Inflammatory Mediators in Retinal Pericytes.” *Experimental Eye Research* 90 (5): 617–23.  
<https://doi.org/10.1016/j.exer.2010.02.006>.
- Kravtsova-Ivantsiv, Yelena, and Aaron Ciechanover. 2012. “Non-Canonical Ubiquitin-Based Signals for Proteasomal Degradation.” *Journal of Cell Science* 125 (3): 539–48. <https://doi.org/10.1242/JCS.093567>.

Krigel, A., M. Berdugo, E. Picard, R. Levy-Boukris, I. Jaadane, L. Jonet, M. Dernigoghossian, C. Andrieu-Soler, A. Torriglia, and F. Behar-Cohen. 2016. "Light-Induced Retinal Damage Using Different Light Sources, Protocols and Rat Strains Reveals LED Phototoxicity." *Neuroscience* 339 (October): 296–307.  
<https://doi.org/10.1016/j.neuroscience.2016.10.015>.

Krizaj, David, and David R Copenhagen. 2002. "Calcium Regulation in Photoreceptors." *Frontiers in Bioscience : A Journal and Virtual Library*. <https://doi.org/10.2741/a896>.

L, Zheng, and Kern TS. 2009. "Role of Nitric Oxide, Superoxide, Peroxynitrite and PARP in Diabetic Retinopathy." *Frontiers in Bioscience (Landmark Edition)* 14 (10): 3974.  
<https://doi.org/10.2741/3505>.

Lecker, Stewart H, Alfred L Goldberg, and William E Mitch. 2006. "Protein Degradation by the Ubiquitin-Proteasome Pathway in Normal and Disease States." *Journal of the American Society of Nephrology* 17 (7): 1807–19. <https://doi.org/10.1681/ASN.2006010083>.

Leger, François, Pierre-Olivier Fernagut, Marie-Hélène Canron, Sandy Léoni, Claude Vital, François Tison, Erwan Bezar, and Anne Vital. 2011. "Protein Aggregation in the Aging Retina." *Journal of Neuropathology & Experimental Neurology* 70 (1): 63–68.  
<https://doi.org/10.1097/NEN.0b013e31820376cc>.

Lenox, Austin R., Yogesh Bhootada, Oleg Gorbatyuk, Roderick Fullard, and Marina Gorbatyuk. 2015. "Unfolded Protein Response Is Activated in Aged Retinas." *Neuroscience Letters* 609: 30–35.

<https://doi.org/10.1016/j.neulet.2015.10.019>.

- Li, Fenge, Danye Jiang, and Melanie A. Samuel. 2019. "Microglia in the Developing Retina." *Neural Development* 2019 14:1 14 (1): 1–13. <https://doi.org/10.1186/S13064-019-0137-X>.
- Li, Jingming, Joshua J. Wang, Qiang Yu, Min Wang, and Sarah X. Zhang. 2009. "Endoplasmic Reticulum Stress Is Implicated in Retinal Inflammation and Diabetic Retinopathy." *FEBS Letters* 583 (9): 1521–27. <https://doi.org/10.1016/j.febslet.2009.04.007>.
- Li, Qian, Yun Cheng, Shenghai Zhang, Xinghuai Sun, and Jihong Wu. 2021. "TRPV4-Induced Müller Cell Gliosis and TNF- $\alpha$  Elevation-Mediated Retinal Ganglion Cell Apoptosis in Glaucomatous Rats via JAK2/STAT3/NF-KB Pathway." *Journal of Neuroinflammation* 2021 18:1 18 (1): 1–22. <https://doi.org/10.1186/S12974-021-02315-8>.
- Lin, Charles H., Jason A. MacGurn, Tony Chu, Christopher J. Stefan, and Scott D. Emr. 2008. "Arrestin-Related Ubiquitin-Ligase Adaptors Regulate Endocytosis and Protein Turnover at the Cell Surface." *Cell* 135 (4): 714–25. <https://doi.org/10.1016/J.CELL.2008.09.025>.
- Liu, Changdong, Min Peng, Alan M Laties, and Rong Wen. 1998. "Preconditioning with Bright Light Evokes a Protective Response against Light Damage in the Rat Retina." *The Journal of Neuroscience* 18 (4): 1337 LP – 1344. <https://doi.org/10.1523/JNEUROSCI.18-04-01337.1998>.
- Liu, Haitao, Jie Tang, Yunpeng Du, Aicha Saadane, Deoye Tonade, Ivy Samuels, Alex Veenstra, Krzysztof Palczewski, and Timothy S. Kern. 2016. "Photoreceptor Cells Influence Retinal Vascular Degeneration in

Mouse Models of Retinal Degeneration and Diabetes.” *Investigative Ophthalmology and Visual Science* 57 (10): 4272–81.  
<https://doi.org/10.1167/iovs.16-19415>.

Liu, Pei Yao, Cheng Cheung Chen, Chia Ying Chin, Te Jung Liu, Wen Chiu Tsai, Jian Liang Chou, Chuan Yu Huang, Yu Guang Chen, and Ying Chuan Chen. 2021. “E3 Ubiquitin Ligase Grail Promotes Hepatic Steatosis through Sirt1 Inhibition.” *Cell Death & Disease* 2021 12:4 12 (4): 1–15. <https://doi.org/10.1038/s41419-021-03608-9>.

Liu, Xianbao, Dexing Hu, Zhiru Zeng, Wei Zhu, Na Zhang, Hong Yu, Han Chen, et al. 2017. “SRT1720 Promotes Survival of Aged Human Mesenchymal Stem Cells via FAIM: A Pharmacological Strategy to Improve Stem Cell-Based Therapy for Rat Myocardial Infarction.” *Cell Death & Disease* 8 (4): e2731.  
<https://doi.org/10.1038/CDDIS.2017.107>.

Liu, Yang, Montserrat Costa, and Chiara Gerhardinger. 2012. “IL-1 $\beta$  Is Upregulated in the Diabetic Retina and Retinal Vessels: Cell-Specific Effect of High Glucose and IL-1 $\beta$  Autostimulation.” *PLoS ONE* 7 (5): 36949. <https://doi.org/10.1371/JOURNAL.PONE.0036949>.

Lobanova, Ekaterina S, Stella Finkelstein, Nikolai P Skiba, and Vadim Y Arshavsky. 2013. “Proteasome Overload Is a Common Stress Factor in Multiple Forms of Inherited Retinal Degeneration.” *Proceedings of the National Academy of Sciences* 110 (24): 9986 LP – 9991.  
<https://doi.org/10.1073/pnas.1305521110>.

London, Anat, Inbal Benhar, and Michal Schwartz. 2013. “The Retina as a Window to the Brain - From Eye Research to CNS Disorders.” *Nature*



*Reviews Neurology* 9 (1): 44–53.

<https://doi.org/10.1038/nrneurol.2012.227>.

Love, Michael I., Wolfgang Huber, and Simon Anders. 2014. “Moderated Estimation of Fold Change and Dispersion for RNA-Seq Data with DESeq2.” *Genome Biology* 15 (12): 1–21.

<https://doi.org/10.1186/S13059-014-0550-8/FIGURES/9>.

Luna, Gabriel, Geoffrey P Lewis, Christopher D Banna, Omar Skalli, and Steven K Fisher. 2010. “Expression Profiles of Nestin and Synemin in Reactive Astrocytes and Müller Cells Following Retinal Injury: A Comparison with Glial Fibrillar Acidic Protein and Vimentin.”

*Molecular Vision* 16 (November): 2511–23.

<https://pubmed.ncbi.nlm.nih.gov/21139996>.

Lyubarsky, A., S. Nikonov, and E. N. Pugh. 1996. “The Kinetics of Inactivation of the Rod Phototransduction Cascade with Constant  $Ca^{2+}$ .” *Journal of General Physiology* 107 (1): 19–34.

<https://doi.org/10.1085/jgp.107.1.19>.

MacDonald, Ian M, Stephanie Hoang, and Sari Tuupanen. 2019. “X-Linked Congenital Stationary Night Blindness.” *GeneReviews*®, July.

<https://www.ncbi.nlm.nih.gov/books/NBK1245/>.

Maeda, Akiko, Tadao Maeda, Marcin Golczak, Steven Chou, Amal Desai, Charles L. Hoppel, Shigemi Matsuyama, and Krzysztof Palczewski.

2009. “Involvement of All-Trans-Retinal in Acute Light-Induced Retinopathy of Mice.” *Journal of Biological Chemistry* 284 (22):

15173–83. <https://doi.org/10.1074/JBC.M900322200>.

Maeda, Tadao, Marcin Golczak, and Akiko Maeda. 2012. “Retinal

Photodamage Mediated by All-Trans-Retinal.” *Photochemistry and Photobiology* 88 (6): 1309–19. <https://doi.org/10.1111/j.1751-1097.2012.01143.x>.

Magnus, Hugo. 1901. *Die Augenheilkunde Der Alten*. Georg Olms Verlag.

Majumder, Anurima, Johan Pahlberg, Kimberly K. Boyd, Vasily Kerov, Saravanan Kolandaivelu, Visvanathan Ramamurthy, Alapakkam P. Sampath, and Nikolai O. Artemyev. 2013. “Transducin Translocation Contributes to Rod Survival and Enhances Synaptic Transmission from Rods to Rod Bipolar Cells.” *Proceedings of the National Academy of Sciences of the United States of America* 110 (30): 12468–73. <https://doi.org/10.1073/pnas.1222666110>.

Manohar, Sandhya, Samson Jacob, Jade Wang, Keira A. Wiechecki, Hiromi W.L. Koh, Vanessa Simões, Hyungwon Choi, Christine Vogel, and Gustavo M. Silva. 2019. “Polyubiquitin Chains Linked by Lysine Residue 48 (K48) Selectively Target Oxidized Proteins In Vivo.” *Antioxidants & Redox Signaling* 31 (15): 1133. <https://doi.org/10.1089/ARS.2019.7826>.

Martínez-Mármol, Ramón, Bruna Barneda-Zahonero, David Soto, Rosa Maria Andrés, Elena Coccia, Xavier Gasull, Laura Planells-Ferrer, Rana S. Moubarak, Eduardo Soriano, and Joan X. Comella. 2016. “FAIM-L Regulation of XIAP Degradation Modulates Synaptic Long-Term Depression and Axon Degeneration.” *Scientific Reports* 6 (November 2015): 1–16. <https://doi.org/10.1038/srep35775>.

Matamoros-Angles, A., A. Hervera, J. Soriano, E. Martí, P. Carulla, F. Llorens, M. Nuvolone, et al. 2022. “Analysis of Co-Isogenic Prion

Protein Deficient Mice Reveals Behavioral Deficits, Learning Impairment, and Enhanced Hippocampal Excitability.” *BMC Biology* 20 (1). <https://doi.org/10.1186/S12915-021-01203-0>.

Matamoros i Anglès, Andreu. 2019. “Noves Funcions de PrP(c) En Neurotransmissió, Neuroprotecció i Neurodegeneració.” *TDX (Tesis Doctorals En Xarxa)*. Universitat de Barcelona. <http://www.tdx.cat/handle/10803/667519>.

Matet, Alexandre, Francine Behar-Cohen, Nathalie Cassoux, Xavier Declèves, and Salvatore Cisternino. 2020. “Retinal and Choroidal Cancers: Blood-Retinal Barriers Considerations in Ocular Chemotherapy.” *Drug Efflux Pumps in Cancer Resistance Pathways: From Molecular Recognition and Characterization to Possible Inhibition Strategies in Chemotherapy*, 303–35. <https://doi.org/10.1016/B978-0-12-816434-1.00010-3>.

Mattson, Mark P, and Tim Magnus. 2006. “Ageing and Neuronal Vulnerability.” *Nature Reviews. Neuroscience* 7 (4): 278–94. <https://doi.org/10.1038/nrn1886>.

Maupin-Furlow, Julie. 2011. “Proteasomes and Protein Conjugation across Domains of Life.” *Nature Reviews Microbiology* 2012 10:2 10 (2): 100–111. <https://doi.org/10.1038/nrmicro2696>.

Mayo Clinic. 2021. “Diabetic Retinopathy - Diagnosis and Treatment -.” 2021. <https://www.mayoclinic.org/diseases-conditions/diabetic-retinopathy/diagnosis-treatment/drc-20371617>.

Mazzoni, Francesca, Hussein Safa, and Silvia C. Finnemann. 2014. “Understanding Photoreceptor Outer Segment Phagocytosis: Use and

Utility of RPE Cells in Culture.” *Experimental Eye Research* 126: 51–60. <https://doi.org/10.1016/J.EXER.2014.01.010>.

McDowell, Rosemary E, Peter Barabas, Josy Augustine, Olivier Chevallier, Philip McCarron, Mei Chen, J Graham McGeown, and Tim M Curtis. 2018. “Müller Glial Dysfunction during Diabetic Retinopathy in Rats Is Reduced by the Acrolein-Scavenging Drug, 2-Hydrazino-4,6-Dimethylpyrimidine.” *Diabetologia* 61 (12): 2654–67. <https://doi.org/10.1007/s00125-018-4707-y>.

McLaughlin, Todd, Andy Medina, Jacob Perkins, Maria Yera, Joshua J. Wang, and Sarah X. Zhang. 2022. “Cellular Stress Signaling and the Unfolded Protein Response in Retinal Degeneration: Mechanisms and Therapeutic Implications.” *Molecular Neurodegeneration* 17 (1): 1–19. <https://doi.org/10.1186/S13024-022-00528-W/FIGURES/3>.

Melia, Thomas J., Christopher W. Cowan, Joseph K. Angleson, and Theodore G. Wensel. 1997. “A Comparison of the Efficiency of G Protein Activation by Ligand-Free and Light-Activated Forms of Rhodopsin.” *Biophysical Journal* 73 (6): 3182–91. [https://doi.org/10.1016/S0006-3495\(97\)78344-9](https://doi.org/10.1016/S0006-3495(97)78344-9).

Mendez, Ana, Marie E. Burns, Angela Roca, Janis Lem, Lan Wing Wu, Melvin I. Simon, Denis A. Baylor, and Jeannie Chen. 2000. “Rapid and Reproducible Deactivation of Rhodopsin Requires Multiple Phosphorylation Sites.” *Neuron* 28 (1): 153–64. [https://doi.org/10.1016/S0896-6273\(00\)00093-3](https://doi.org/10.1016/S0896-6273(00)00093-3).

Mendez, Ana, Janis Lem, Melvin Simon, and Jeannie Chen. 2003. “Light-Dependent Translocation of Arrestin in the Absence of Rhodopsin

- Phosphorylation and Transducin Signaling.” *Journal of Neuroscience* 23 (8): 3124–29. <https://doi.org/10.1523/jneurosci.23-08-03124.2003>.
- Mendonca, Henrique, Raul Carpi-Santos, Karin Da Costa Calaza, and Ana Blanco Martinez. 2020. “Neuroinflammation and Oxidative Stress Act in Concert to Promote Neurodegeneration in the Diabetic Retina and Optic Nerve: Galectin-3 Participation.” *Neural Regeneration Research* 15 (4): 625–35. <https://doi.org/10.4103/1673-5374.266910>.
- Meyer, Hemmo H. 2002. “Direct Binding of Ubiquitin Conjugates by the Mammalian P97 Adaptor Complexes, P47 and Ufd1-Npl4.” *The EMBO Journal* 21 (21): 5645–52. <https://doi.org/10.1093/emboj/cdf579>.
- Micheau, Olivier, and Jürg Tschopp. 2003. “Induction of TNF Receptor I-Mediated Apoptosis via Two Sequential Signaling Complexes.” *Cell* 114 (2): 181–90. [https://doi.org/10.1016/S0092-8674\(03\)00521-X](https://doi.org/10.1016/S0092-8674(03)00521-X).
- Mimura, Tatsuya, Yuichi Kaji, Hidetaka Noma, Hideharu Funatsu, and Shinseiro Okamoto. 2013. “The Role of SIRT1 in Ocular Aging.” *Experimental Eye Research* 116 (November): 17–26. <https://doi.org/10.1016/J.EXER.2013.07.017>.
- Miyake, Yozo, and Kei Shinoda. 2012. “Clinical Electrophysiology.” *Retina Fifth Edition* 1: 202–26. <https://doi.org/10.1016/B978-1-4557-0737-9.00008-4>.
- Mohammad, Ghulam, Ghada Maher Abdelaziz, Mohammad Mairaj Siddiquei, Ajmal Ahmad, Gert De Hertogh, and Ahmed M. Abu El-Asrar. 2019. “Cross-Talk between Sirtuin 1 and the Proinflammatory Mediator High-Mobility Group Box-1 in the Regulation of Blood-Retinal Barrier Breakdown in Diabetic Retinopathy.”

<https://doi.org/10.1080/02713683.2019.1625406> 44 (10): 1133–43.  
<https://doi.org/10.1080/02713683.2019.1625406>.

Montgomery, Jacob E, Michael J Parsons, and David R Hyde. 2010. “A Novel Model of Retinal Ablation Demonstrates That the Extent of Rod Cell Death Regulates the Origin of the Regenerated Zebrafish Rod Photoreceptors.” *The Journal of Comparative Neurology* 518 (6): 800–814. <https://doi.org/10.1002/cne.22243>.

Morshedjian, Ala, and Gordon L. Fain. 2017. “The Evolution of Rod Photoreceptors.” *Philosophical Transactions of the Royal Society B: Biological Sciences* 372 (1717).  
<https://doi.org/10.1098/RSTB.2016.0074>.

Moubarak, R. S., L. Planells-Ferrer, J. Urresti, S. Reix, M. F. Segura, P. Carriba, F. Marques-Fernandez, et al. 2013. “FAIM-L Is an IAP-Binding Protein That Inhibits XIAP Ubiquitylation and Protects from Fas-Induced Apoptosis.” *Journal of Neuroscience* 33 (49): 19262–75.  
<https://doi.org/10.1523/JNEUROSCI.2479-13.2013>.

Mukhopadhyay, Debdyuti, and Howard Riezman. 2007. “Proteasome-Independent Functions of Ubiquitin in Endocytosis and Signaling.” *Science* 315 (5809): 201–5. <https://doi.org/10.1126/SCIENCE.1127085>.

Munemasa, Yasunari, and Yasushi Kitaoka. 2012. “Molecular Mechanisms of Retinal Ganglion Cell Degeneration in Glaucoma and Future Prospects for Cell Body and Axonal Protection.” *Frontiers in Cellular Neuroscience* 6 (DEC). <https://doi.org/10.3389/FNCEL.2012.00060>.

Murakami, Yusuke, Hidetaka Matsumoto, Miin Roh, Jun Suzuki, Toshio Hisatomi, Yasuhiro Ikeda, Joan W. Miller, and Demetrios G. Vavvas.

2012. “Receptor Interacting Protein Kinase Mediates Necrotic Cone but Not Rod Cell Death in a Mouse Model of Inherited Degeneration.” *Proceedings of the National Academy of Sciences of the United States of America* 109 (36): 14598–603.  
[https://doi.org/10.1073/PNAS.1206937109/SUPPL\\_FILE/PNAS.201206937SI.PDF](https://doi.org/10.1073/PNAS.1206937109/SUPPL_FILE/PNAS.201206937SI.PDF).

Murali, Aparna, Charmaine A. Ramlogan-Steel, Slawomir Andrzejewski, Jason C. Steel, and Christopher J. Layton. 2019. “Retinal Explant Culture: A Platform to Investigate Human Neuro-Retina.” *Clinical and Experimental Ophthalmology* 47 (2): 274–85.  
<https://doi.org/10.1111/ceo.13434>.

Nair, K. Saldas, Susan M. Hanson, Ana Mendez, Eugenia V. Gurevich, Matthew J. Kennedy, Valery I. Shestopalov, Sergey A. Vishnivetskiy, et al. 2005. “Light-Dependent Redistribution of Arrestin in Vertebrate Rods Is an Energy-Independent Process Governed by Protein-Protein Interactions.” *Neuron* 46 (4): 555–67.  
<https://doi.org/10.1016/j.neuron.2005.03.023>.

Nakajima, Yu Ichiro, and Erina Kuranaga. 2017. “Caspase-Dependent Non-Apoptotic Processes in Development.” *Cell Death & Differentiation* 2017 24:8 24 (8): 1422–30. <https://doi.org/10.1038/cdd.2017.36>.

Nakazawa, Mitsuru, Yuko Wada, and Makoto Tamai. 1998. “Arrestin Gene Mutations in Autosomal Recessive Retinitis Pigmentosa.” *Ophthalmic Molecular Genetics*, 116:498-501. <https://jamanetwork.com/>.

Nath, Deepa, and Sadaf Shadan. 2009. “The Ubiquitin System.” *Nature* 458 (7237): 421. <https://doi.org/10.1038/458421a>.

- Neel, Dylan V., Himanish Basu, Georgia Gunner, and Isaac M. Chiu. 2022. "Catching a Killer: Mechanisms of Programmed Cell Death and Immune Activation in Amyotrophic Lateral Sclerosis." *Immunological Reviews*. <https://doi.org/10.1111/IMR.13083>.
- Newman, Eric, and Andreas Reichenbach. 1996. "The Muller Cell: A Functional Element of the Retina." *Trends in Neurosciences* 19 (8): 307–12. [https://doi.org/10.1016/0166-2236\(96\)10040-0](https://doi.org/10.1016/0166-2236(96)10040-0).
- Newton, Fay, and Roly Megaw. 2020. "Mechanisms of Photoreceptor Death in Retinitis Pigmentosa." *Genes* 2020, Vol. 11, Page 1120 11 (10): 1120. <https://doi.org/10.3390/GENES11101120>.
- Nian, Shen, Amy C.Y. Lo, Yajing Mi, Kai Ren, and Di Yang. 2021. "Neurovascular Unit in Diabetic Retinopathy: Pathophysiological Roles and Potential Therapeutical Targets." *Eye and Vision (London, England)* 8 (1). <https://doi.org/10.1186/S40662-021-00239-1>.
- Nomura-Komoike, Kaori, Fuminori Saitoh, and Hiroki Fujieda. 2020. "Phosphatidylserine Recognition and Rac1 Activation Are Required for Müller Glia Proliferation, Gliosis and Phagocytosis after Retinal Injury." *Scientific Reports* 10 (1): 1–11. <https://doi.org/10.1038/s41598-020-58424-6>.
- O'Neal, Teri B., and Euil E. Luther. 2021. "Retinitis Pigmentosa." *StatPearls*, August. <https://www.ncbi.nlm.nih.gov/books/NBK519518/>.
- Obin, M., T. Nowell, and A. Taylor. 1994. "The Photoreceptor G-Protein Transducin (Gt) Is a Substrate for Ubiquitin-Dependent Proteolysis." *Biochemical and Biophysical Research Communications* 200 (3): 1169–76. <https://doi.org/10.1006/BBRC.1994.1574>.



- Obin, Martin S., Jessica Jahngen-Hodge, Thomas Nowell, and Allen Taylor. 1996a. "Ubiquitinylation and Ubiquitin-Dependent Proteolysis in Vertebrate Photoreceptors (Rod Outer Segments): EVIDENCE FOR UBIQUITINYLATION OF Gt AND RHODOPSIN." *Journal of Biological Chemistry* 271 (24): 14473–84. <https://doi.org/10.1074/JBC.271.24.14473>.
- . 1996b. "Ubiquitinylation and Ubiquitin-Dependent Proteolysis in Vertebrate Photoreceptors (Rod Outer Segments): EVIDENCE FOR UBIQUITINYLATION OF Gt AND RHODOPSIN \*." *Journal of Biological Chemistry* 271 (24): 14473–84. <https://doi.org/10.1074/JBC.271.24.14473>.
- Orlowski, Julius, Wolf Harmening, and Hermann Wagner. 2012. "Night Vision in Barn Owls: Visual Acuity and Contrast Sensitivity under Dark Adaptation." *Journal of Vision* 12 (13). <https://doi.org/10.1167/12.13.4>.
- Ouyang, Chenxi, Guang Lu, Weifeng He, Boon Huat Bay, and Han Ming Shen. 2022. "Post-Translational Modification in Control of SIRT1 Stability during DNA Damage Response." *International Journal of Biological Sciences* 18 (7): 2655–69. <https://doi.org/10.7150/IJBS.68587>.
- Ozawa, Yoko. 2020. "Oxidative Stress in the Light-Exposed Retina and Its Implication in Age-Related Macular Degeneration." *Redox Biology* 37: 101779. <https://doi.org/10.1016/j.redox.2020.101779>.
- Ozawa, Yoko, Shunsuke Kubota, Toshio Narimatsu, Kenya Yuki, Takashi Koto, Mariko Sasaki, and Kazuo Tsubota. 2010. "Retinal Aging and Sirtuins." *Ophthalmic Research* 44 (3): 199–203.

<https://doi.org/10.1159/000316484>.

Parmeggiani, Francesco, Francesco S. Sorrentino, Diego Ponzin, Vanessa Barbaro, Stefano Ferrari, and Enzo Di Iorio. 2011. "Retinitis Pigmentosa: Genes and Disease Mechanisms." *Current Genomics* 12 (4): 238. <https://doi.org/10.2174/138920211795860107>.

Pearson, Rachael A, and Robin R Ali. 2018. "Unlocking the Potential for Endogenous Repair to Restore Sight." *Neuron* 100 (3): 524–26. <https://doi.org/10.1016/j.neuron.2018.10.035>.

Planells-Ferrer, Laura, Jorge Urresti, Elena Coccia, Koen M.O. Galenkamp, Isabel Calleja-Yagüe, Joaquín López-Soriano, Paulina Carriba, Bruna Bareda-Zahonero, Miguel F. Segura, and Joan X. Comella. 2016. "Fas Apoptosis Inhibitory Molecules: More than Death-Receptor Antagonists in the Nervous System." *Journal of Neurochemistry* 139 (1): 11–21. <https://doi.org/10.1111/jnc.13729>.

Popova, Elka. 2014. "ON-OFF Interactions in the Retina: Role of Glycine and GABA." *Current Neuropharmacology* 12 (6): 509. <https://doi.org/10.2174/1570159X13999150122165018>.

Praefcke, Gerrit J.K., Marijn G.J. Ford, Eva M. Schmid, Lene E. Olesen, Jennifer L. Gallop, Sew Yeu Peak-Chew, Yvonne Vallis, M. Maclan Babu, Ian G. Mills, and Harvey T. McMahon. 2004. "Evolving Nature of the AP2  $\alpha$ -Appendage Hub during Clathrin-Coated Vesicle Endocytosis." *The EMBO Journal* 23 (22): 4371. <https://doi.org/10.1038/SJ.EMBOJ.7600445>.

Puller, Christian, Timm Schubert, and Silke Haverkamp. 2011. "The Glutamate Receptors of Mouse OFF Bipolar Cells." *Investigative*

*Ophthalmology & Visual Science* 52 (14): 4120–4120.

Purves, Dale, George J Augustine, David Fitzpatrick, Lawrence C Katz, Anthony-Samuel LaMantia, James O McNamara, and S Mark Williams. 2001. “Phototransduction.” <https://www.ncbi.nlm.nih.gov/books/NBK10806/>.

Qu, Junyan, Tingting Zou, and Zhenghong Lin. 2021. “The Roles of the Ubiquitin–Proteasome System in the Endoplasmic Reticulum Stress Pathway.” *International Journal of Molecular Sciences* 22 (4): 1–21. <https://doi.org/10.3390/ijms22041526>.

Raasi, Shahri, Irina Orlov, Karen G. Fleming, and Cecile M. Pickart. 2004. “Binding of Polyubiquitin Chains to Ubiquitin-Associated (UBA) Domains of HHR23A.” *Journal of Molecular Biology* 341 (5): 1367–79. <https://doi.org/10.1016/j.jmb.2004.06.057>.

Raina, Priyanka, Inês Lopes, Kasit Chatsirisupachai, Zoya Farooq, and João Pedro de Magalhães. 2021. “GeneFriends 2021: Updated Co-Expression Databases and Tools for Human and Mouse Genes and Transcripts.” *BioRxiv*, January, 2021.01.10.426125. <https://doi.org/10.1101/2021.01.10.426125>.

Ramaswamy, Madhu, Min Deng, and Richard M. Siegel. 2011. “Harnessing Programmed Cell Death as a Therapeutic Strategy in Rheumatic Diseases.” *Nature Reviews Rheumatology* 7 (3): 152–60. <https://doi.org/10.1038/NRRHEUM.2010.225>.

Ramón y Cajal, Santiago. 1891. “Notas Preventivas Sobre La Retina Y Gran Simpático De Los Mamíferos.” *Casa Provincial de Caridad*.

- Ramsey, David J., and G. B. Arden. 2015. "Hypoxia and Dark Adaptation in Diabetic Retinopathy: Interactions, Consequences, and Therapy." *Current Diabetes Reports* 15 (12). <https://doi.org/10.1007/s11892-015-0686-2>.
- Rattner, A.; Nathans, J. 2005. "The Genomic Response to Retinal Disease and Injury: Evidence for Endothelin Signaling from Photoreceptors to Glia." *Journal of Neuroscience* 25 (18): 4540–49. <https://doi.org/10.1523/jneurosci.0492-05.2005>.
- Rattner, Amir, Huimin Yu, John Williams, Philip M. Smallwood, and Jeremy Nathans. 2013. "Endothelin-2 Signaling in the Neural Retina Promotes the Endothelial Tip Cell State and Inhibits Angiogenesis." *Proceedings of the National Academy of Sciences of the United States of America* 110 (40). <https://doi.org/10.1073/pnas.1315509110>.
- Remé, C E, C Grimm, F Hafezi, A Marti, and A Wenzel. 1998. "Apoptotic Cell Death in Retinal Degenerations." *Progress in Retinal and Eye Research* 17 (4): 443–64. [https://doi.org/10.1016/s1350-9462\(98\)00009-3](https://doi.org/10.1016/s1350-9462(98)00009-3).
- Renwick, J., M. A. Narang, S. G. Coupland, J. Y. Xuan, A. N. Baker, J. Brousseau, D. Petrin, et al. 2006. "XIAP-Mediated Neuroprotection in Retinal Ischemia." *Gene Therapy* 13 (4): 339–47. <https://doi.org/10.1038/sj.gt.3302683>.
- Ristic, Gorica, Wei Ling Tsou, and Sokol V. Todi. 2014. "An Optimal Ubiquitin-Proteasome Pathway in the Nervous System: The Role of Deubiquitinating Enzymes." *Frontiers in Molecular Neuroscience* 7 (AUG): 72. <https://doi.org/10.3389/FNMOL.2014.00072/XML/NLM>.

- Rodrigues-Neves, Ana Catarina, Rafael Carecho, Sónia Catarina Correia, Cristina Carvalho, Elisa Julião Campos, Filipa Isabel Baptista, Paula Isabel Moreira, and António Francisco Ambrósio. 2021. "Retina and Brain Display Early and Differential Molecular and Cellular Changes in the 3xTg-AD Mouse Model of Alzheimer's Disease." *Molecular Neurobiology*. <https://doi.org/10.1007/s12035-021-02316-x>.
- Roehlecke, Cora, Annette Schaller, Lilla Knels, and Richard H.W. Funk. 2009. "The Influence of Sublethal Blue Light Exposure on Human RPE Cells." *Molecular Vision* 15 (September): 1929. [/pmc/articles/PMC2751800/](https://pubmed.ncbi.nlm.nih.gov/19292710/).
- Roehlecke, Cora, Ulrike Schumann, Marius Ader, Coy Brunssen, Silvia Bramke, Henning Morawietz, and Richard H.W. Funk. 2013. "Stress Reaction in Outer Segments of Photoreceptors after Blue Light Irradiation." *PLoS ONE* 8 (9). <https://doi.org/10.1371/JOURNAL.PONE.0071570>.
- Roehlecke, Cora, Ulrike Schumann, Marius Ader, Lilla Knels, and Richard H.W. W Funk. 2011. "Influence of Blue Light on Photoreceptors in a Live Retinal Explant System." *Molecular Vision* 17: 876. <http://www.molvis.org/molvis/v17/a98>.
- Romero-aroca, Pedro, L Maribel, Maria Asuncion Martinez-brocca, Alicia Pareja-r, Sara Artola, Josep Franch-nadal, Joan Fernandez-ballart, Jos Andonegui, and Marc Baget-bernaldez. 2022. "Changes in the Epidemiology of Diabetic Retinopathy in Spain : A Systematic Review and Meta-Analysis." *Healthcare MDPI*.
- Ross, Ahmara G., Devin S. McDougald, Reas S. Khan, Thu T. Duong,

- Kimberly E. Dine, Puya Aravand, Jean Bennett, Venkata Ramana Murthy Chavali, and Kenneth S. Shindler. 2021. "Rescue of Retinal Ganglion Cells in Optic Nerve Injury Using Cell-Selective AAV Mediated Delivery of SIRT1." *Gene Therapy* 2021 28:5 28 (5): 256–64. <https://doi.org/10.1038/s41434-021-00219-z>.
- Rózanowska, Małgorzata, and Tadeusz Sarna. 2005. "Light-Induced Damage to the Retina: Role of Rhodopsin Chromophore Revisited." *Photochemistry and Photobiology* 81 (6): 1305. <https://doi.org/10.1562/2004-11-13-ir-371>.
- RStudio Team. 2015. "RStudio: Integrated Development Environment for R." Boston, MA. <http://www.rstudio.com/>.
- Rungger-Brandle, Elisabeth, André A Dosso, and Peter M Leuenberger. 2000. "Glial Reactivity, an Early Feature of Diabetic Retinopathy." *Investigative Ophthalmology & Visual Science* 41 (7): 32–34.
- Russell, Bertrand. 1912. "The Problems of Philosophy." *The Philosophical Review* 22 (3): 329. <https://doi.org/10.2307/2178182>.
- Saari, John C. 2012. "Vitamin a Metabolism in Rod and Cone Visual Cycles." *Annual Review of Nutrition*. Annual Reviews. <https://doi.org/10.1146/annurev-nutr-071811-150748>.
- Saari, John C., Gregory G. Garwin, J. Preston Van Hooser, and Krzysztof Palczewski. 1998. "Reduction of All-Trans-Retinal Limits Regeneration of Visual Pigment in Mice." *Vision Research* 38 (10): 1325–33. [https://doi.org/10.1016/S0042-6989\(97\)00198-3](https://doi.org/10.1016/S0042-6989(97)00198-3).
- Samaranayake, Srimal, Sergey A. Vishnivetskiy, Camilla R. Shores,

- Kimberly C. Thibeault, Seunghyi Kook, Jeannie Chen, Marie E. Burns, Eugenia V. Gurevich, and Vsevolod V. Gurevich. 2020. “Biological Role of Arrestin-1 Oligomerization.” *Journal of Neuroscience* 40 (42): 8055–69. <https://doi.org/10.1523/JNEUROSCI.0749-20.2020>.
- Sánchez-Cruz, Alonso, Andrea C. Méndez, Ignacio Lizasoain, Pedro de la Villa, Enrique J. de la Rosa, and Catalina Hernández-Sánchez. 2021. “Tlr2 Gene Deletion Delays Retinal Degeneration in Two Genetically Distinct Mouse Models of Retinitis Pigmentosa.” *International Journal of Molecular Sciences* 22 (15). <https://doi.org/10.3390/ijms22157815>.
- Sánchez-Cruz, Alonso, Beatriz Villarejo-Zori, Miguel Marchena, Josefa Zaldivar-Díez, Valle Palomo, Carmen Gil, Ignacio Lizasoain, et al. 2018. “Modulation of GSK-3 Provides Cellular and Functional Neuroprotection in the Rd10 Mouse Model of Retinitis Pigmentosa.” *Molecular Neurodegeneration* 13 (1): 1–10. <https://doi.org/10.1186/s13024-018-0251-y>.
- Sansa, Alba, Sandra de la Fuente, Joan X. Comella, Ana Garcera, and Rosa M. Soler. 2021. “Intracellular Pathways Involved in Cell Survival Are Deregulated in Mouse and Human Spinal Muscular Atrophy Motoneurons.” *Neurobiology of Disease* 155: 105366. <https://doi.org/10.1016/j.nbd.2021.105366>.
- Sarthy, P V, and M Fu. 1989. “Transcriptional Activation of an Intermediate Filament Protein Gene in Mice with Retinal Dystrophy.” *DNA (Mary Ann Liebert, Inc.)* 8 (6): 437–46. <https://doi.org/10.1089/dna.1.1989.8.437>.
- Schauwecker, P. Elyse. 2011. “The Relevance of Individual Genetic

Background and Its Role in Animal Models of Epilepsy.” *Epilepsy Research* 97 (1–2): 1–11. <http://www.informatics.jax.org/>.

Schindelin, Johannes, Ignacio Arganda-Carreras, Erwin Frise, Verena Kaynig, Mark Longair, Tobias Pietzsch, Stephan Preibisch, et al. 2012. “Fiji: An Open-Source Platform for Biological-Image Analysis.” *Nature Methods* 9 (7): 676–82. <https://doi.org/10.1038/nmeth.2019>.

Schmidt, Marlene F., Zhong Yan Gan, David Komander, and Grant Dewson. 2021. “Ubiquitin Signalling in Neurodegeneration: Mechanisms and Therapeutic Opportunities.” *Cell Death and Differentiation* 28 (2): 570–90. <https://doi.org/10.1038/s41418-020-00706-7>.

Schneider, Caroline A, Wayne S Rasband, and Kevin W Eliceiri. 2012. “NIH Image to ImageJ: 25 Years of Image Analysis.” *Nature Methods* 9 (7): 671–75. <https://doi.org/10.1038/nmeth.2089>.

Schneider, T J, G M Fischer, T J Donohoe, T P Colarusso, and T L Rothstein. 1999. “A Novel Gene Coding for a Fas Apoptosis Inhibitory Molecule (FAIM) Isolated from Inducibly Fas-Resistant B Lymphocytes.” *The Journal of Experimental Medicine* 189 (6): 949–56. <https://doi.org/10.1084/jem.189.6.949>.

Schulze-Osthoff, Klaus, Davide Ferrari, Marek Los, Sebastian Wesselborg, and Marcus E. Peter. 1998. “Apoptosis Signaling by Death Receptors.” *European Journal of Biochemistry* 254 (3): 439–59. <https://doi.org/10.1046/J.1432-1327.1998.2540439.X>.

Sedmak, Tina, and Uwe Wolfrum. 2011. “Intraflagellar Transport Proteins in Ciliogenesis of Photoreceptor Cells.” *Biology of the Cell* 103 (10): 449–66. <https://doi.org/10.1042/BC20110034>.



- Segura, M. F., C. Sole, M. Pascual, R. S. Moubarak, M. Jose Perez-Garcia, R. Gozzelino, V. Iglesias, et al. 2007. "The Long Form of Fas Apoptotic Inhibitory Molecule Is Expressed Specifically in Neurons and Protects Them against Death Receptor-Triggered Apoptosis." *Journal of Neuroscience* 27 (42): 11228–41.  
<https://doi.org/10.1523/JNEUROSCI.3462-07.2007>.
- Semple, Colin A.M., Takahiro Arakawa, Piero Caminci, Jun Kawai, and Yoshihide Hayashizaki. 2003. "The Comparative Proteomics of Ubiquitination in Mouse." *Genome Research* 13 (6b): 1389.  
<https://doi.org/10.1101/GR.980303>.
- Senut, Marie-Claude, Abhilasha Gulati-Leekha, and Daniel Goldman. 2004. "An Element in the Alpha1-Tubulin Promoter Is Necessary for Retinal Expression during Optic Nerve Regeneration but Not after Eye Injury in the Adult Zebrafish." *The Journal of Neuroscience : The Official Journal of the Society for Neuroscience* 24 (35): 7663–73.  
<https://doi.org/10.1523/JNEUROSCI.2281-04.2004>.
- Shang, Fu, and Allen Taylor. 2011. "Ubiquitin-Proteasome Pathway and Cellular Responses to Oxidative Stress." *Free Radical Biology & Medicine* 51 (1): 5.  
<https://doi.org/10.1016/J.FREERADBIOMED.2011.03.031>.
- Shen, Weiyong, Shiyong Li, Sook Hyun Chung, and Mark C. Gillies. 2010. "Retinal Vascular Changes after Glial Disruption in Rats." *Journal of Neuroscience Research* 88 (7): 1485–99.  
<https://doi.org/10.1002/JNR.22317>.
- Shenoy, S. K., P. H. McDonald, T. A. Kohout, and R. J. Lefkowitz. 2001.

“Regulation of Receptor Fate by Ubiquitination of Activated B2-Adrenergic Receptor and  $\beta$ -Arrestin.” *Science* 294 (5545): 1307–13.  
[https://doi.org/10.1126/SCIENCE.1063866/SUPPL\\_FILE/1063866S2\\_THUMB.GIF](https://doi.org/10.1126/SCIENCE.1063866/SUPPL_FILE/1063866S2_THUMB.GIF).

Shenoy, Sudha K., Kunhong Xiao, Vidya Venkataramanan, Peter M. Snyder, Neil J. Freedman, and Allan M. Weissman. 2008. “Nedd4 Mediates Agonist-Dependent Ubiquitination, Lysosomal Targeting, and Degradation of the Beta2-Adrenergic Receptor.” *The Journal of Biological Chemistry* 283 (32): 22166–76.  
<https://doi.org/10.1074/JBC.M709668200>.

Shin, Eui Seok, Christine M Sorenson, and Nader Sheibani. 2014. “Diabetes and Retinal Vascular Dysfunction.” *Journal of Ophthalmic & Vision Research* 9 (3): 362–73. <https://doi.org/10.4103/2008-322X.143378>.

Shin, Hwain, Martin Ratus, Brendan P. Eckelman, Viviane A. Nunes, Claudio A.M. Sampaio, and Guy S. Salvesen. 2005. “The BIR Domain of IAP-like Protein 2 Is Conformationally Unstable: Implications for Caspase Inhibition.” *Biochemical Journal* 385 (Pt 1): 1.  
<https://doi.org/10.1042/BJ20041107>.

Shukla, Unnati V., and Koushik Tripathy. 2022. “Diabetic Retinopathy.” *StatPearls*, May. <https://www.ncbi.nlm.nih.gov/books/NBK560805/>.

Simó, Rafael, and Cristina Hernández. 2014. “Neurodegeneration in the Diabetic Eye: New Insights and Therapeutic Perspectives.” *Trends in Endocrinology and Metabolism* 25 (1): 23–33.  
<https://doi.org/10.1016/j.tem.2013.09.005>.

Singhal, Ankita, Martin K. Ostermaier, Sergey A. Vishnivetskiy, Valérie

- Panneels, Kristoff T. Homan, John J.G. Tesmer, Dmitry Veprintsev, et al. 2013. “Insights into Congenital Stationary Night Blindness Based on the Structure of G90D Rhodopsin.” *EMBO Reports* 14 (6): 520–26. <https://doi.org/10.1038/embor.2013.44>.
- Sirés, Anna, Mireia Turch-Anguera, Patricia Bogdanov, Joel Sampedro, Hugo Ramos, Agustín Ruíz Lasa, J. Huo, et al. 2021. “Faim Knockout Leads to Gliosis and Late-onset Neurodegeneration of Photoreceptors.” *Journal of Neuroscience Research* 99: 3103–20. <https://doi.org/https://doi.org/10.1002/jnr.24978>.
- Sisodia, S S, E H Koo, K Beyreuther, A Unterbeck, and D L Price. 1990. “Evidence That Beta-Amyloid Protein in Alzheimer’s Disease Is Not Derived by Normal Processing.” *Science (New York, N.Y.)* 248 (4954): 492–95. <https://doi.org/10.1126/science.1691865>.
- Slepek, Vladlen Z., and James B. Hurley. 2008. “Mechanism of Light-Induced Translocation of Arrestin and Transducin in Photoreceptors: Interaction-Restricted Diffusion.” *IUBMB Life* 60 (1): 2. <https://doi.org/10.1002/IUB.7>.
- Smith, Heather L, and Giovanna R Mallucci. 2016. “The Unfolded Protein Response : Mechanisms and Therapy of Neurodegeneration,” 2113–21. <https://doi.org/10.1093/brain/aww101>.
- Sokolov, Maxim, Arkady L Lyubarsky, Katherine J Strissel, Andrey B Savchenko, Viktor I Govardovskii, Edward N Pugh, and Vadim Y Arshavsky. 2002. “Massive Light-Driven Translocation of Transducin between the Two Major Compartments of Rod Cells: A Novel Mechanism of Light Adaptation.” *Neuron* 33: 1–12.

Sokolov, Maxim, Katherine J. Strissel, Ilya B. Leskov, Norman A. Michaud, Viktor I. Govardovskii, and Vadim Y. Arshavsky. 2004. "Phosducin Facilitates Light-Driven Transducin Translocation in Rod Photoreceptors: Evidence from the Phosducin Knockout Mouse." *Journal of Biological Chemistry* 279 (18): 19149–56. <https://doi.org/10.1074/jbc.M311058200>.

Sole, Carme, Xavier Dolcet, Miguel F. Segura, Humberto Gutierrez, Maria Teresa Diaz-Meco, Raffaella Gozzelino, Daniel Sanchis, et al. 2004. "The Death Receptor Antagonist FAIM Promotes Neurite Outgrowth by a Mechanism That Depends on ERK and NF-KB Signaling." *Journal of Cell Biology* 167 (3): 479–92. <https://doi.org/10.1083/jcb.200403093>.

Solovei, Irina, Moritz Kreysing, Christian Lanctôt, Süleyman Kösem, Leo Peichl, Thomas Cremer, Jochen Guck, and Boris Joffe. 2009. "Nuclear Architecture of Rod Photoreceptor Cells Adapts to Vision in Mammalian Evolution." *Cell* 137 (2): 356–68. <https://doi.org/10.1016/j.cell.2009.01.052>.

Song, X, S A Vishnivetskiy, J Seo, J Chen, E. V Gurevich, and V V Gurevich. 2011. "Arrestin-1 Expression Level in Rods: Balancing Functional Performance and Photoreceptor Health." *Neuroscience* 174: 37–49. <https://doi.org/10.1016/j.neuroscience.2010.11.009>.

Song, Xiufeng, Dayanidhi Raman, Eugenia V. Gurevich, Sergey A. Vishnivetskiy, and Vsevolod V. Gurevich. 2006. "Visual and Both Non-Visual Arrestins in Their 'Inactive' Conformation Bind JNK3 and Mdm2 and Relocalize Them from the Nucleus to the Cytoplasm." *Journal of Biological Chemistry* 281 (30): 21491–99. <https://doi.org/10.1074/jbc.M603659200>.

- Sorrentino, Francesco Saverio, Silvia Matteini, Claudio Bonifazzi, Adolfo Sebastiani, and Francesco Parmeggiani. 2018. "Diabetic Retinopathy and Endothelin System: Microangiopathy versus Endothelial Dysfunction." *Eye* 32 (7): 1157. <https://doi.org/10.1038/S41433-018-0032-4>.
- Spencer, Brian, Seema Agarwala, Laura Gentry, and Curtis R. Brandt. 2001. "HSV-1 Vector-Delivered FGF2 to the Retina Is Neuroprotective but Does Not Preserve Functional Responses." *Molecular Therapy* 3 (5): 746–56. <https://doi.org/10.1006/mthe.2001.0307>.
- Spencer, William J., Tylor R. Lewis, Jillian N. Pearring, and Vadim Y. Arshavsky. 2020. "Photoreceptor Discs: Built Like Ectosomes." *Trends in Cell Biology* 30 (11): 904–15. <https://doi.org/10.1016/j.tcb.2020.08.005>.
- Stewart, Mikaela D., Tobias Ritterhoff, Rachel E. Klevit, and Peter S. Brzovic. 2016. "E2 Enzymes: More than Just Middle Men." *Cell Research* 26:4 26 (4): 423–40. <https://doi.org/10.1038/cr.2016.35>.
- Strissel, Katherine J, Maxim Sokolov, Lynn H Trieu, and Vadim Y Arshavsky. 2006. "Arrestin Translocation Is Induced at a Critical Threshold of Visual Signaling and Is Superstoichiometric to Bleached Rhodopsin." *Journal of Neuroscience* 26 (4): 1146–53. <https://doi.org/10.1523/JNEUROSCI.4289-05.2006>.
- Sun, Mingjiang, Silvia C. Finnemann, Maria Febbraio, Lian Shan, Suresh P. Annangudi, Eugene A. Podrez, George Hoppe, et al. 2006. "Light-Induced Oxidation of Photoreceptor Outer Segment Phospholipids Generates Ligands for CD36-Mediated Phagocytosis by Retinal Pigment

Epithelium: A Potential Mechanism for Modulating Outer Segment Phagocytosis Under Oxidant Stress Conditions\*.” *The Journal of Biological Chemistry* 281 (7): 4222.

<https://doi.org/10.1074/JBC.M509769200>.

Szikra, Tamas, and David Križaj. 2007. “Intracellular Organelles and Calcium Homeostasis in Rods and Cones.” *Visual Neuroscience* 24 (5): 733–43. <https://doi.org/10.1017/S0952523807070587>.

Tam, Beatrice M., and Orson L. Moritz. 2006. “Characterization of Rhodopsin P23H-Induced Retinal Degeneration in a *Xenopus Laevis* Model of Retinitis Pigmentosa.” *Investigative Ophthalmology & Visual Science* 47 (8): 3234–41. <https://doi.org/10.1167/IOVS.06-0213>.

Taylor, Rebecca C., Sean P. Cullen, and Seamus J. Martin. 2008. “Apoptosis: Controlled Demolition at the Cellular Level.” *Nature Reviews Molecular Cell Biology* 9 (3): 231–41. <https://doi.org/10.1038/nrm2312>.

Teo, Zhen Ling, Yih Chung Tham, Marco Yu, Miao Li Chee, Tyler Hyungtaek Rim, Ning Cheung, Mukharram M. Bikbov, et al. 2021. “Global Prevalence of Diabetic Retinopathy and Projection of Burden through 2045: Systematic Review and Meta-Analysis.” *Ophthalmology* 128 (11): 1580–91. <https://doi.org/10.1016/J.OPHTHA.2021.04.027>.

Terakita, Akihisa. 2005. “The Opsins.” *Genome Biology* 6 (3): 213. <https://doi.org/10.1186/GB-2005-6-3-213>.

Tessier-Lavigne, Marc. 2020. “Visual Processing by the Retina The Retina Contains the Eye’s Receptor Sheet.” *Neuroscience Online*.

Thebeau, Christina, Sheng Zhang, Alexander V. Kolesnikov, Vladimir J.

- Kefalov, Clay F. Semenkovich, and Rithwick Rajagopal. 2020. "Light Deprivation Reduces the Severity of Experimental Diabetic Retinopathy." *Neurobiology of Disease* 137 (April): 104754.  
<https://doi.org/10.1016/J.NBD.2020.104754>.
- Thrower, Julia S., Laura Hoffman, Martin Rechsteiner, and Cecile M. Pickart. 2000. "Recognition of the Polyubiquitin Proteolytic Signal." *The EMBO Journal* 19 (1): 94–102.  
<https://doi.org/10.1093/EMBOJ/19.1.94>.
- Tout, S., T. Chan-Ling, H. Holländer, and J. Stone. 1993. "The Role of Müller Cells in the Formation of the Blood-Retinal Barrier." *Neuroscience* 55 (1): 291–301.  
[https://doi.org/https://doi.org/10.1016/0306-4522\(93\)90473-S](https://doi.org/https://doi.org/10.1016/0306-4522(93)90473-S).
- Trachsel-Moncho, Laura, Soledad Benlloch-Navarro, Ángel Fernández-Carbonell, Dolores Tania Ramírez-Lamelas, Teresa Olivar, Dolores Silvestre, Enric Poch, and María Miranda. 2018. "Oxidative Stress and Autophagy-Related Changes during Retinal Degeneration and Development." *Cell Death & Disease* 2018 9:8 9 (8): 1–12.  
<https://doi.org/10.1038/s41419-018-0855-8>.
- Tse, Man Kit, Kam Hui, Yinhua Yang, Si-Tao Yin, Hong-Yu Hu, Bing Zou, Benjamin Chun, Yu Wong, and Kong Hung Sze. 2011. "Structural Analysis of the UBA Domain of X-Linked Inhibitor of Apoptosis Protein Reveals Different Surfaces for Ubiquitin-Binding and Self-Association." *PLoS ONE* 6 (12).  
<https://doi.org/10.1371/journal.pone.0028511>.
- Ueki, Yumi, Yun Zheng Le, Srinivas Chollangi, Werner Muller, and John D.

- Ash. 2009. "Preconditioning-Induced Protection of Photoreceptors Requires Activation of the Signal-Transducing Receptor Gp130 in Photoreceptors." *Proceedings of the National Academy of Sciences of the United States of America* 106 (50): 21389–94.  
<https://doi.org/10.1073/pnas.0906156106>.
- Uhlén, Mathias, Linn Fagerberg, Björn M Hallström, Cecilia Lindskog, Per Oksvold, Adil Mardinoglu, Åsa Sivertsson, et al. 2015. "Tissue-Based Map of the Human Proteome." *Science* 347 (6220): 1260419.  
<https://doi.org/10.1126/science.1260419>.
- Upadhyaya, Sudarshan C, and Ashok N Hegde. 2007. "Role of the Ubiquitin Proteasome System in Alzheimer's Disease." *BMC Biochemistry* 8 Suppl 1 (Suppl 1): S12–S12. <https://doi.org/10.1186/1471-2091-8-S1-S12>.
- Vainchtein, Ilia D., and Anna V. Molofsky. 2020. "Astrocytes and Microglia: In Sickness and in Health." *Trends in Neurosciences* 43 (3): 144.  
<https://doi.org/10.1016/J.TINS.2020.01.003>.
- Vecino, Elena, F. David Rodriguez, Noelia Ruzafa, Xandra Pereiro, and Sansar C. Sharma. 2016. "Glial-Neuron Interactions in the Mammalian Retina." *Progress in Retinal and Eye Research* 51 (March): 1–40.  
<https://doi.org/10.1016/J.PRETEYERES.2015.06.003>.
- Velasco Cruz, Antonio Augusto, Flávia A. Attié-Castro, Sandra L. Fernandes, Jussara Fialho F. Cortes, Paulo De Tarso P. Pierre-Filho, Eduardo Melani Rocha, and Júlio Sérgio Marchini. 2005. "Adult Blindness Secondary to Vitamin A Deficiency Associated with an Eating Disorder." *Nutrition (Burbank, Los Angeles County, Calif.)* 21



(5): 630–33. <https://doi.org/10.1016/J.NUT.2004.12.003>.

Veleri, Shobi, Csilla H. Lazar, Bo Chang, Paul A. Sieving, Eyal Banin, and Anand Swaroop. 2015. “Biology and Therapy of Inherited Retinal Degenerative Disease: Insights from Mouse Models.” *Disease Models & Mechanisms* 8 (2): 109–29. <https://doi.org/10.1242/DMM.017913>.

Volland, Stefanie, Julian Esteve-Rudd, Juyea Hoo, Claudine Yee, and David S. Williams. 2015. “A Comparison of Some Organizational Characteristics of the Mouse Central Retina and the Human Macula.” *PLOS ONE* 10 (4): e0125631. <https://doi.org/10.1371/JOURNAL.PONE.0125631>.

Wang, Jing, Dexter Duncan, Zhiao Shi, and Bing Zhang. 2013. “WEB-Based GENE SeT AnaLysis Toolkit (WebGestalt): Update 2013.” *Nucleic Acids Research* 41 (W1): W77–83. <https://doi.org/10.1093/nar/gkt439>.

Wang, Xu, Lian Zhao, Jun Zhang, Robert N. Fariss, Wenxin Ma, Friedrich Kretschmer, Minhua Wang, et al. 2016. “Requirement for Microglia for the Maintenance of Synaptic Function and Integrity in the Mature Retina.” *The Journal of Neuroscience* 36 (9). <https://doi.org/10.1523/JNEUROSCI.3575-15.2016>.

Wassmer, Sarah J, Brian C Leonard, Stuart G Coupland, Adam N Baker, John Hamilton, William W Hauswirth, and Catherine Tsilfidis. 2017. “Overexpression of the X-Linked Inhibitor of Apoptosis Protects Against Retinal Degeneration in a Feline Model of Retinal Detachment.” *Human Gene Therapy* 28 (6): 482–92. <https://doi.org/10.1089/hum.2016.161>.

Weiss, Ellen. 2020. “Shedding Light on Dark Adaptation.” *Biochemist* 42

(5): 44–50. <https://doi.org/10.1042/BIO20200067>.

- Weissman, Allan M, Nitzan Shabek, and Aaron Ciechanover. 2011. “The Predator Becomes the Prey: Regulating the Ubiquitin System by Ubiquitylation and Degradation.” *Nature Reviews Molecular Cell Biology* 12 (9): 605–20. <https://doi.org/10.1038/nrm3173>.
- Wen, R, Y Song, T Cheng, M T Matthes, D Yasumura, M M LaVail, and R H Steinberg. 1995. “Injury-Induced Upregulation of BFGF and CNTF MRNAS in the Rat Retina.” *Journal of Neuroscience* 15 (11): 7377–85. <https://doi.org/10.1523/JNEUROSCI.15-11-07377.1995>.
- Wenzel, Andreas, Christian Grimm, Marijana Samardzija, and Charlotte E. Remé. 2005. “Molecular Mechanisms of Light-Induced Photoreceptor Apoptosis and Neuroprotection for Retinal Degeneration.” *Progress in Retinal and Eye Research* 24 (2): 275–306. <https://doi.org/10.1016/j.preteyeres.2004.08.002>.
- Werblin, F. S., and J. E. Dowling. 1969. “Organization of the Retina of the Mudpuppy, *Necturus Maculosus*. II. Intracellular Recording.” <https://doi.org/10.1152/Jn.1969.32.3.339> 32 (3): 339–55. <https://doi.org/10.1152/JN.1969.32.3.339>.
- Wijk, Anne Eva van der, Ilse M.C. Vogels, Henk A. van Veen, Cornelis J.F. van Noorden, Reinier O. Schlingemann, and Ingeborg Klaassen. 2018. “Spatial and Temporal Recruitment of the Neurovascular Unit during Development of the Mouse Blood-Retinal Barrier.” *Tissue and Cell* 52 (April): 42–50. <https://doi.org/10.1016/j.tice.2018.03.010>.
- Wood, John P. M., Gerassimos Lascaratos, Anthony J. Bron, and Neville N. Osborne. 2008. “The Influence of Visible Light Exposure on Cultured

RGC-5 Cells.” *Molecular Vision* 14 (February): 334.  
[/pmc/articles/PMC2254956/](https://pubmed.ncbi.nlm.nih.gov/1612254956/).

Wright, Alan F., Christina F. Chakarova, Mai M. Abd El-Aziz, and Shomi S. Bhattacharya. 2010. “Photoreceptor Degeneration: Genetic and Mechanistic Dissection of a Complex Trait.” *Nature Reviews. Genetics* 11 (4): 273–84. <https://doi.org/10.1038/NRG2717>.

Xi, Xia, Ling Gao, Denise A. Hatala, Dawn G. Smith, Maria C. Codispoti, Bendi Gong, Timothy S. Kern, and Jin Zhong Zhang. 2005. “Chronically Elevated Glucose-Induced Apoptosis Is Mediated by Inactivation of Akt in Cultured Müller Cells.” *Biochemical and Biophysical Research Communications* 326 (3): 548–53.  
<https://doi.org/10.1016/J.BBRC.2004.11.064>.

Xia, Fan, Yonju Ha, Shuizhen Shi, Yi Li, Shengguo Li, Jonathan Luisi, Rakez Kayed, Massoud Motamedi, Hua Liu, and Wenbo Zhang. 2021. “Early Alterations of Neurovascular Unit in the Retina in Mouse Models of Tauopathy.” *Acta Neuropathologica Communications* 9 (1): 1–16.  
<https://doi.org/10.1186/s40478-021-01149-y>.

Xu, Jun, Robert L. Dodd, Clint L. Makino, Melvin I. Simon, Denis A. Baylor, and Jeannle Chen. 1997. “Prolonged Photoresponses in Transgenic Mouse Rods Lacking Arrestin.” *Nature* 389 (6650): 505–9.  
<https://doi.org/10.1038/39068>.

Xu, Qiang, Yanshu Wang, Alain Dabdoub, Philip M Smallwood, John Williams, Chad Woods, Matthew W Kelley, et al. 2004. “Vascular Development in the Retina and Inner Ear: Control by Norrin and Frizzled-4, a High-Affinity Ligand-Receptor Pair.” *Cell* 116 (6): 883–

95. [https://doi.org/10.1016/s0092-8674\(04\)00216-8](https://doi.org/10.1016/s0092-8674(04)00216-8).

Yamada, Akiko, Rieko Arakaki, Masako Saito, Yasusei Kudo, and Naozumi Ishimaru. 2017. "Dual Role of Fas/FasL-Mediated Signal in Peripheral Immune Tolerance." *Frontiers in Immunology* 8 (APR): 403. <https://doi.org/10.3389/FIMMU.2017.00403/XML/NLM>.

Yamada, Haruhiko, Eri Yamada, Akira Ando, Noriko Esumi, Naba Bora, Jina Saikia, Ching Hwa Sung, Donald J. Zack, and Peter A. Campochiaro. 2001. "Fibroblast Growth Factor-2 Decreases Hyperoxia-Induced Photoreceptor Cell Death in Mice." *American Journal of Pathology* 159 (3): 1113–20. [https://doi.org/10.1016/S0002-9440\(10\)61787-7](https://doi.org/10.1016/S0002-9440(10)61787-7).

Yamamoto, Shuichi, Masanori Hayashi, Shinobu Takeuchi, Yutaka Shirao, Katsutoshi Kita, and Kazuo Kawasaki. 1997. "Normal S Cone Electroretinogram B-Wave in Oguchi's Disease." *The British Journal of Ophthalmology* 81 (12): 1043–45. <https://doi.org/10.1136/BJO.81.12.1043>.

Yang, Jun, Yujuan Song, Alexander D. Law, Conner J. Rogan, Kelsey Shimoda, Danijel Djukovic, Jeffrey C. Anderson, Doris Kretzschmar, David A. Hendrix, and Jadwiga M. Giebultowicz. 2022. "Chronic Blue Light Leads to Accelerated Aging in Drosophila by Impairing Energy Metabolism and Neurotransmitter Levels." *Frontiers in Aging* 0 (August): 94. <https://doi.org/10.3389/FRAGI.2022.983373>.

Yang, Quan, Jinyao Zhao, Dan Chen, and Yang Wang. 2021. "E3 Ubiquitin Ligases: Styles, Structures and Functions." *Molecular Biomedicine* 2021 2:1 2 (1): 1–17. <https://doi.org/10.1186/S43556-021-00043-2>.

Yau, Joanne W.Y., Sophie L. Rogers, Rho Kawasaki, Ecosse L. Lamoureux, Jonathan W. Kowalski, Toke Bek, Shih Jen Chen, et al. 2012. “Global Prevalence and Major Risk Factors of Diabetic Retinopathy.” *Diabetes Care* 35 (3): 556–64. <https://doi.org/10.2337/DC11-1909>.

Yildiz, Ozge, and Hemant Khanna. 2012. “Ciliary Signaling Cascades in Photoreceptors.” *Vision Research* 75 (December): 112–16. <https://doi.org/10.1016/J.VISRES.2012.08.007>.

Yoshiyama, Yasumasa, Makoto Higuchi, Bin Zhang, Shu Ming Huang, Nobuhisa Iwata, Takaomi C C. Saido, Jun Maeda, Tetsuya Suhara, John Q. Trojanowski, and Virginia M.Y. Lee. 2007. “Synapse Loss and Microglial Activation Precede Tangles in a P301S Tauopathy Mouse Model.” *Neuron* 53 (3): 337–51. <https://doi.org/10.1016/j.neuron.2007.01.010>.

Yu, Dao Yi, and Stephen J. Cringle. 2001. “Oxygen Distribution and Consumption within the Retina in Vascularised and Avascular Retinas and in Animal Models of Retinal Disease.” *Progress in Retinal and Eye Research* 20 (2): 175–208. [https://doi.org/10.1016/S1350-9462\(00\)00027-6](https://doi.org/10.1016/S1350-9462(00)00027-6).

Yu, Le, Ling Dong, Hui Li, Zhaojian Liu, Zhong Luo, Guangjie Duan, Xiaotian Dai, and Zhenghong Lin. 2020. “Ubiquitination-Mediated Degradation of SIRT1 by SMURF2 Suppresses CRC Cell Proliferation and Tumorigenesis.” *Oncogene* 39 (22): 4450–64. <https://doi.org/10.1038/S41388-020-1298-0>.

Yuan, Junying, and Bruce A. Yankner. 2000. “Apoptosis in the Nervous System.” *Nature* 407 (6805): 802–9. <https://doi.org/10.1038/35037739>.

- Zadro-Lamoureux, Laura A., David N. Zacks, Adam N. Baker, Qiong Duan Zheng, William W. Hauswirth, and Catherine Tsilfidis. 2009. "Effects on XIAP Retinal Detachment-Induced Photoreceptor Apoptosis." *Investigative Ophthalmology and Visual Science* 50 (3): 1448–53. <https://doi.org/10.1167/iovs.08-2855>.
- Zeit, Christina. 2007. "Molecular Genetics and Protein Function Involved in Nocturnal Vision." *Expert Review of Ophthalmology* 2 (3): 467–85. <https://doi.org/10.1586/17469899.2.3.467>.
- Zeit, Christina, Anthony G. Robson, and Isabelle Audo. 2015. "Congenital Stationary Night Blindness: An Analysis and Update of Genotype-Phenotype Correlations and Pathogenic Mechanisms." *Progress in Retinal and Eye Research* 45: 58–110. <https://doi.org/10.1016/j.preteyeres.2014.09.001>.
- Zhang, Sarah X., Emily Sanders, Steven J. Fliesler, and Joshua J. Wang. 2014. "Endoplasmic Reticulum Stress and the Unfolded Protein Responses in Retinal Degeneration." *Experimental Eye Research* 125: 30–40. <https://doi.org/10.1016/J.EXER.2014.04.015>.
- Zhang, Ying, Yanjiang Wang, Ce Shi, Meixiao Shen, and Fan Lu. 2021. "Advances in Retina Imaging as Potential Biomarkers for Early Diagnosis of Alzheimer's Disease." *Translational Neurodegeneration* 10 (1): 1–9. <https://doi.org/10.1186/s40035-021-00230-9>.
- Zheng, Ning, and Nitzan Shabek. 2017. "Ubiquitin Ligases: Structure, Function, and Regulation." *Annual Review of Biochemistry* 86: 129–57. <https://doi.org/10.1146/annurev-biochem-060815-014922>.
- Zhong, Xuemei, Thomas J. Schneider, Deborah S. Cabral, Terrence J.

Donohoe, and Thomas L. Rothstein. 2001. “An Alternatively Spliced Long Form of Fas Apoptosis Inhibitory Molecule (FAIM) with Tissue-Specific Expression in the Brain.” *Molecular Immunology* 38 (1): 65–72. [https://doi.org/10.1016/S0161-5890\(01\)00035-9](https://doi.org/10.1016/S0161-5890(01)00035-9).

Zong, H., M. Ward, A. Madden, P. H. Yong, G. A. Limb, T. M. Curtis, and A. W. Stitt. 2010. “Hyperglycaemia-Induced pro-Inflammatory Responses by Retinal Müller Glia Are Regulated by the Receptor for Advanced Glycation End-Products (RAGE).” *Diabetologia* 53 (12): 2656–66. <https://doi.org/10.1007/S00125-010-1900-Z>.

# Annex

*“Reserve your right to think, for even to think  
wrongly is better than not to think at all”*





Hypatia (355-415)





# **Annex One**

# *Faim* knockout leads to gliosis and late-onset neurodegeneration of photoreceptors in the mouse retina

Anna Sirés<sup>1,2,3</sup>  | Mireia Turch-Anguera<sup>1,3,4,5</sup> | Patricia Bogdanov<sup>4,5</sup> | Joel Sampedro<sup>4,5</sup> | Hugo Ramos<sup>4,5</sup> | Agustín Ruíz Lasa<sup>2,6</sup>  | Jianxin Huo<sup>7</sup> | Shengli Xu<sup>7</sup> | Kong-Peng Lam<sup>7</sup> | Joaquín López-Soriano<sup>1,2,3</sup> | M. Jose Pérez-García<sup>1,2</sup> | Cristina Hernández<sup>4,5</sup> | Rafael Simó<sup>4,5</sup> | Montse Solé<sup>1,2,3</sup>  | Joan X. Comella<sup>1,2,3</sup> 

<sup>1</sup>Cell Signaling and Apoptosis Group, Vall d'Hebron Institute of Research (VHIR), Barcelona, Spain

<sup>2</sup>Centro de Investigación Biomédica en Red sobre Enfermedades Neurodegenerativas (CIBERNED), ISCIII, Madrid, Spain

<sup>3</sup>Departament de Bioquímica i Biologia Molecular, Facultat de Medicina, Universitat Autònoma de Barcelona (UAB), Bellaterra, Spain

<sup>4</sup>Diabetes and Metabolism Research Unit, Vall d'Hebron Institute of Research (VHIR), Barcelona, Spain

<sup>5</sup>Centro de Investigación Biomédica en Red de Diabetes y Enfermedades Metabólicas Asociadas (CIBERDEM), ISCIII, Madrid, Spain

<sup>6</sup>Research Center and Memory Clinic. Fundació ACE, Institut Català de Neurociències Aplicades, Universitat Internacional de Catalunya (UIC), Barcelona, Spain

<sup>7</sup>Singapore Immunology Network (SiGN), A\*STAR (Agency for Science, Technology and Research), Singapore, Singapore

## Correspondence

Montse Solé and Joan X. Comella, Cell Signaling and Apoptosis Group, Vall d'Hebron Institute of Research (VHIR), Pg. Vall d'Hebron, 119-129, Barcelona 08135, Spain.

Email: montserrat.sole@vhir.org (M. S.) and joan.comella@vhir.org (J. X. C.)

## Funding information

This work was funded by grants awarded to J.X.C by the Spanish "Ministerio de Economía y Competitividad" (SAF2016-80236-R and PID2019-107286RB-I00), CIBERNED (CBO6/05/1104), and the Generalitat de Catalunya (2017SGR996)

## Abstract

Fas Apoptotic Inhibitory Molecule protein (FAIM) is a death receptor antagonist and an apoptosis regulator. It encodes two isoforms, namely FAIM-S (short) and FAIM-L (long), both with significant neuronal functions. FAIM-S, which is ubiquitously expressed, is involved in neurite outgrowth. In contrast, FAIM-L is expressed only in neurons and it protects them from cell death. Interestingly, FAIM-L is downregulated in patients and mouse models of Alzheimer's disease before the onset of neurodegeneration, and *Faim* transcript levels are decreased in mouse models of retinal degeneration. However, few studies have addressed the role of FAIM in the central nervous system, yet alone the retina. The retina is a highly specialized tissue, and its degeneration has proved to precede pathological mechanisms of neurodegenerative diseases. Here we describe that *Faim* depletion in mice damages the retina persistently and leads to late-onset photoreceptor death in older mice. Immunohistochemical analyses showed that *Faim* knockout (*Faim*<sup>-/-</sup>) mice present ubiquitinated aggregates throughout the retina from early ages. Moreover, retinal cells released stress signals that can signal to Müller cells, as shown by immunofluorescence and qRT-PCR. Müller cells monitor retinal homeostasis and trigger a gliotic response in *Faim*<sup>-/-</sup> mice that becomes pathogenic when sustained. In this regard, we observed pronounced vascular leakage at later ages, which may be caused by persistent inflammation. These results suggest that FAIM is an important player in the maintenance of retinal homeostasis, and they support the premise that FAIM is a plausible early marker for late photoreceptor and neuronal degeneration.

## KEYWORDS

inflammation, neurodegeneration, photoreceptor, protein aggregation, retina, RRID:AB\_141359, RRID:AB\_143165, RRID:AB\_2169115, RRID:AB\_257896, RRID:AB\_258431, RRID:AB\_2714189, RRID:AB\_2888627, RRID:AB\_2892773, RRID:AB\_2892776, RRID:AB\_305808, RRID:AB\_308765, RRID:AB\_477579, RRID:AB\_628423, RRID:IMSR\_JAX:000664, RRID:SCR\_002285, RRID:SCR\_002798,

RRID:SCR\_003070, RRID:SCR\_006710, RRID:SCR\_006786, RRID:SCR\_015560,  
RRID:SCR\_021625, vascular leakage

## 1 | INTRODUCTION

Fas Apoptotic Inhibitory Molecule protein (FAIM) is a death receptor antagonist that was first described as an inhibitor of Fas-mediated apoptosis in B lymphocytes (Schneider et al., 1999). *Faim* is an evolutionarily conserved and unique gene that is unrelated to any homologous protein, suggesting that it plays a distinctive role in the organism. The *Faim* knockout mouse (*Faim*<sup>-/-</sup>) has been reported to present an increased sensitivity to Fas-triggered apoptosis in B lymphocytes, thymocytes, and hepatocytes, along with several metabolic alterations (Huo et al., 2016, 2019). Also, in a different *Faim*<sup>-/-</sup> mouse that was recently generated, *Faim*-deficient cells accumulate ubiquitinated and aggregated proteins after an oxidative stress insult, both *in vivo* and *in vitro* (Kaku & Rothstein, 2020).

*Faim* gives rise to two distinct products generated by alternative splicing, named FAIM-short (FAIM-S) and FAIM-long (FAIM-L). While FAIM-S is ubiquitously expressed throughout the organism, FAIM-L, which contains 22 extra N-terminal amino acid residues coded in exons 2b and 3a, is expressed only in neurons (Zhong et al., 2001). These two isoforms play diverse and important roles in the central nervous system (CNS). FAIM-S is required for neurite outgrowth through the activation of the MAPK/ERK and NFκB pathways (Sole et al., 2004), and although it protects B lymphocytes from Fas activation, it does not confer the same protection in neurons. In contrast, FAIM-L protects neurons at two different levels: first, by activating death receptors through both Fas and tumor necrosis factor receptor 1 (TNFR1), and second, by interacting with an endogenous inhibitor of caspases, X-linked inhibitor of apoptosis protein (XIAP). At the first level, our group showed that FAIM-L binds to Fas receptor and prevents caspase activation (Segura et al., 2007). Also, we demonstrated that FAIM-L is essential to confer tumor necrosis factor alpha (TNF-α) the ability to protect against amyloid beta toxicity, although the exact mechanism is still unknown (Carriba et al., 2015). At the second level, the interaction of FAIM-L with XIAP blocks the XIAP auto-ubiquitination site, thus hampering XIAP degradation and enabling it to inhibit the apoptotic executioner caspase-3 (Moubarak et al., 2013; Scott et al., 2005).

We have also reported that FAIM-L levels are reduced in hippocampal samples from patients with Alzheimer's disease and in a transgenic mouse model of this disorder (APP/PS1) before neurodegeneration onset, thus indicating the potential clinical relevance of this isoform. Furthermore, we also determined that amyloid-β downregulates FAIM-L protein expression in cultures of primary cortical neurons. This downregulation, in turn, causes the loss of the aforementioned TNF-α-mediated protection against amyloid beta, thus contributing to a neurodegenerative phenotype (Carriba et al., 2015). Moreover, FAIM-L might also be involved in the pathogenesis of spinal muscular atrophy (SMA), a severe neuromuscular

### Significance

Fas apoptotic inhibitory molecule (FAIM) is a protein involved in key functions in the central nervous system, like neuronal survival and neurite outgrowth. FAIM expression is decreased in patients with Alzheimer's disease and mouse models of retinal pathologies, thereby suggesting that this protein plays a significant role in neurodegenerative events. In this study, we found that the absence of FAIM causes the accumulation of aggregated proteins, inflammation, vascular leakage, and activation of survival pathways in the mouse retina, culminating in photoreceptor death. Our results suggest that FAIM is crucial for neuronal survival, thus pointing to its potential as a plausible early marker for late neuronal degeneration.

disorder, since motoneurons from SMA mutant mice show altered FAIM-L mRNA and protein levels (Sansa et al., 2021). However, few studies have focused on the functions of FAIM in other neuronal tissues. Data based on mRNA microarrays show that *Faim* transcripts are significantly downregulated in a mouse model of Norrie disease (*Ndp* knockout mice), which is characterized by abnormal development of the retina that often results in blindness from birth (Xu et al., 2004). Also, miRNA-1 and 133b, which target *Faim* at the 3'-UTR site and downregulate its expression (Coccia, Masanas, et al., 2020), are massively overexpressed in mouse models of retinitis pigmentosa (rd1 and rd10 (Lauterbur, 1973; Loscher et al., 2007)), a disease characterized by photoreceptor death and retinal neurodegeneration. While miRNAs are key regulators of gene expression and functionality, the 3'-UTR sites of a gene are frequently overlooked. Interestingly, a study exploring de novo noncoding single-nucleotide variations in patients with intellectual disability identified the *Faim* 3'-UTR site as a putative regulatory region (Devanna et al., 2018).

The retina has long been considered a window to the brain. Anatomically and developmentally, the retina shares multiple similarities with the brain and spinal cord. Neurodegenerative diseases manifest earlier in the retina, and its accessibility makes it exceptionally useful for studying processes in the CNS and for developing non-invasive diagnostic methods. The lack of knowledge about the role of FAIM in the retina and the potential implication of this protein in retinal disorders prompted us to explore this tissue in *Faim* knockout (*Faim*<sup>-/-</sup>) mice in a short- and long-term manner. Here we report that *Faim*<sup>-/-</sup> mice present neurodegenerative traits in the retina, including photoreceptor loss, accumulation of protein aggregates, chronic gliosis, and disruption of the blood-retinal barrier (BRB).

## 2 | MATERIALS AND METHODS

### 2.1 | Weighted-gene co-expression network analysis

Data from the Human Proteome Map (Research Resource Identifier, RRID:SCR\_015560) (Kim et al., 2014) and Human Protein Atlas v20.0 (HPA, RRID:SCR\_006710) (Uhlén et al., 2015) were used. The former consists of LC-MS/MS data that show relative expression of the proteins of interest in fetal and adult tissues, while the latter deploys RNA single-cell type specificity in the form of transcript expression values.

The GeneFriends tool (GeneFriends, RRID:SCR\_021625) (van Dam et al., 2015) was used to generate an unsupervised mouse co-expression gene map based on 34,322 RNA-seq samples containing 31,236 genes. To this end, we calculated the distance for each possible gene paired with *Faim*. The mutual rank, which was obtained by taking a geometric average of Pearson's correlation coefficients from each pair of genes bidirectionally, was used as the threshold parameter at 1,306. WebGestalt (WEB-based GENE SeT AnaLysis Toolkit, RRID:SCR\_006786) (Wang et al., 2013) was then used to conduct a Gene Ontology (GO) term enrichment analysis of biological processes among the resulting *Faim* co-expressed genes. The Overrepresentation Analyses (ORA) approach was used to determine the enrichment for gene sets based on some shared theme, in this case, GO terms. The false discovery rate (FDR), which estimates the probability that a gene set with a given enrichment score is a false-positive finding, was used to filter the results.

### 2.2 | Animals

All mouse experiments were conducted in compliance with European Union Council directives (2010/63/EU) and with the Spanish legislation for the use of laboratory animals (BOE 34/11370-421, 2013). Experimental protocols were approved by the Ethics Committee for Animal Experimentation of the Vall d'Hebron Research Institute (VHIR) (CEEA 20/15) and the Generalitat de Catalunya (DARP 8594).

Homozygous *Faim*<sup>-/-</sup> mice were kindly provided by Dr. Lam (Huo et al., 2016) and crossbred with C57BL/6J wild-type (wt) mice (Envigo, France) (IMSR Cat# JAX:000664, RRID:IMSR\_JAX:000664). Heterozygous mice were used to breed *Faim*<sup>-/-</sup> and wt littermates for experimental procedures. Animals were bred and maintained in the animal facility at VHIR. They were housed in groups of a maximum of five animals per Tecniplast GM-500 cage (36 × 19 × 13.5 cm) under standard laboratory conditions at 22 ± 2°C, under a 12-hr light/dark cycle (8 a.m. to 8 p.m.) and relative humidity of 50%–60%. Animals had access to water and food ad libitum (Teklad Global 18% Protein Rodent diet, Envigo, France). An equal number of females and males per study group was selected, and at least four animals per genotype were used for each experiment.

Genotypes were confirmed by PCR analysis. A tail snip was used for DNA extraction. The tail sample was digested in alkaline solution with Proteinase K (0.24 Units/sample) (Qiagen, Hilden, Germany) for 120 min at 55°C. The following primers were used to perform a semiquantitative PCR: *Faim*-P1-Fw 5'-GAGACTGAGACAGGAGAAGCC-3'; *Faim*-P2-Fw 5'-GCTCTCA GCAATATC-ACGGG-3' and *Faim*-P3-Rev 5'-GCTCAGGTAAAGTG AAGTGCG-3'.

### 2.3 | Tissue collection and processing

Mice were euthanized by cervical dislocation and eyes were enucleated. The retina was extracted from the left eye and snap-frozen in liquid nitrogen for protein or mRNA extraction. The right eye was fixed in 4% paraformaldehyde for 5 hr and embedded in paraffin blocks. Next, 4-μm-thick sections were cut on a microtome (Microm HM 355 S, ThermoFisher Scientific, Waltham, USA), and three or four sections were placed on one slide. Slides were stored at room temperature until analysis. Experiments were performed using samples from 2-, 12-, and 18-month-old mice, and at least four animals per group were used in each experiment.

### 2.4 | Western blotting

Retinal proteins were extracted in RIPA lysis buffer (150 mM NaCl, 1% IGEPAL® CA-630, 0.5% sodium deoxycholate, 0.1% SDS, and 50 mM Tris pH 8.0) containing 1× cOmplete™ EDTA-free protease inhibitor cocktail (11873580001, Roche, Darmstadt, Germany). Extracts were kept ice-cold and supernatants were collected after centrifugation at 9,300× g for 15 min at 4°C. Protein concentration was quantified using the Modified Lowry kit (DC protein assay; Bio-Rad, Hercules, CA, USA). Next, 20 to 40 μg of total protein was resolved by SDS-PAGE and transferred onto PVDF Immobilon-P transfer membranes (Millipore Iberica, Madrid, Spain). Membranes were blocked with Tris-buffered saline with 0.1% TWEEN®-20 and 5% nonfat dry milk for 1 hr at room temperature and then probed overnight with the appropriate primary antibody (*Faim*: in-house antibody, Cat# SCIA\_001, RRID:AB\_2892776, 1:2,000; GFAP: DAKO, Jena, Germany, Cat# Z0334, RRID:AB\_2714189, 1:4,000; α-tubulin: Sigma-Aldrich, Saint Louis, MO, USA, Cat# T5168, RRID:AB\_477579, 1:60,000; cyclophilin A (CypA): Enzo Lifesciences, Farmingdale, NY, USA, Cat# BML-SA296, RRID:AB\_2169115, 1:10,000) (for details of antibody, see Table S1). Blots were then incubated with the corresponding peroxidase-conjugated secondary antibodies (Goat anti-Rabbit IgG, Sigma-Aldrich, Cat# A0545, RRID:AB\_257896, 1:20,000; Rabbit anti-mouse IgG, Sigma-Aldrich, Cat# A9044, RRID:AB\_258431, 1:20,000) for 1 hr at room temperature, developed using the EZ-ECL Enhanced Chemiluminescence Detection Kit for HRP (Biological Industries, Kibbutz Beit Haemek, Israel), and captured with Fuji X-ray films Super RX-N (Fujifilm, Tokyo, Japan). Band intensities were quantified with ImageJ software, version 1.53e

(RRID:SCR\_003070) (Schneider et al., 2012). To control equal loading, housekeeping  $\alpha$ -tubulin or CypA were used to normalize protein expression.

## 2.5 | Histology and retinal morphometry analysis

Slides were heated at 60°C for 1 hr, deparaffinized in xylene, rehydrated in a graded ethanol series, and stained with Harris hematoxylin and eosin. Whole digital scans were taken using a NanoZoomer 2.0HT high-resolution whole-slide scanner (Hamamatsu). At least four mice per group were measured for each morphometric analysis, and three sections were averaged per mouse.

The thickness of the whole retina was measured manually using the ruler tool of NanoZoomer software at a distance of 0.6 mm from both sides of the optic nerve and then averaged.

To manually measure the number of rows of photoreceptor nuclei in the outer nuclear layer (ONL), we also took two segments of the retina at 0.6 mm from the optic nerve. At least 11 columns per segment were manually counted using ImageJ software and then averaged.

The number of nuclei in the ganglion cell layer (GCL) and the inner nuclear layer (INL) was manually counted in ImageJ using 0.5-mm wide segments (at 0.6 mm from both sides of the optic nerve), and at least four comparable segments per section were averaged. All measurements were taken in three distinct slices per mouse in a double-blinded manner.

## 2.6 | TUNEL assay

Slides were deparaffinized and rehydrated as above. They were then permeabilized for 8 min in 0.1% sodium citrate containing 0.1% Triton X-100. Slides were placed in a plastic jar containing 200 ml of 0.1 M citrate buffer pH 6.0 and irradiated at 750W in a microwave for 1 min for antigen retrieval. Next, they were immediately cooled by adding room temperature ddH<sub>2</sub>O, and washed with PBS pH 7.4. Slides were immersed in Tris-HCl 0.1 M pH 7.5 containing 3% BSA and 20% fetal bovine serum for 30 min at room temperature and then washed with PBS. The slides were incubated for 1 hr at 37°C with TUNEL (Terminal deoxynucleotidyl transferase dUTP nick end labeling) reaction mixture (11767291910 and 11767305001, TUNEL Label Mix and TUNEL Enzyme, Roche), following the manufacturer's instructions. The mixture was added individually to each retinal section. Negative controls were incubated with TUNEL reaction mixture without TUNEL enzyme. Slides were rinsed with PBS and counterstained with Hoechst 33342 (0.05  $\mu$ g/ml, ab228551, Abcam) for 10 min and rinsed again with PBS. Finally, slides were mounted in Prolong™ Gold Antifade Mountant (P36930, Thermofisher) and 40 $\times$  images were taken with Olympus FV1000 spectral confocal microscope in the High Technology Unit (UAT) at VHIR. TUNEL-positive cells in retinal sections were manually counted using ImageJ software. Three distinct retinal sections per mouse were analyzed and averaged, and at least four animals per group were used.

## 2.7 | Immunohistochemistry and quantification

Slides were deparaffinized and rehydrated as stated above. Antigen retrieval was achieved by immersing the slides in antigen retrieval solution (0.1 M citrate buffer pH 6.0) and placing them in a pressure cooker at 150°C for 4 min. Nonspecific binding sites were blocked for 1 hr at room temperature with PBS containing 10% NGS. After blocking, sections were incubated with multiubiquitin primary antibody (Santa Cruz Biotechnology, Cat# sc-8017, RRID:AB\_628423, 1:2,000) overnight at 4°C (for details of antibody, see Table S3). The following day, they were incubated for 1 hr at room temperature with HRP-conjugated antibodies (listed in Table S3). Antibody labeling was visualized with EnVision Detection System (Dako, Agilent mouse Cat# K5007, RRID:AB\_2888627, 1:2,000) and slides were counterstained with Harris hematoxylin and mounted in DPX (255254, PanReac AppliChem, Chicago, USA). Samples without primary antibodies were used as negative controls. Images were taken under a Nikon ECLIPSE 80i microscope at 20 $\times$  and 40 $\times$  in the Histology Service Unit at the Neurosciences Institute, UAB. Pictures were analyzed in a double-blinded manner by two researchers.

To quantify ubiquitin immunostaining, ubiquitin-positive cells in the GCL and INL were manually counted. Measurements of ubiquitin-positive cells were averaged for the INL and GCL to obtain the number of ubiquitin-positive GCL cells in 0.6-mm segments, and the number of ubiquitin-positive INL cells in 0.4-mm segments. Four equally sized random segments across the retinal section were selected, and three retinal sections per mouse were used.

## 2.8 | Immunofluorescence and quantification

Slides were deparaffinized and rehydrated as stated above. They were then fixed in ice-cold methanol-acetic acid solution (95% methanol, 5% glacial acetic acid) for 1 min and washed with PBS. Antigen retrieval was achieved by immersing the slides in antigen retrieval solution (0.1 M citrate buffer pH 6.0) and placing them in a pressure cooker at 150°C for 4 min. Nonspecific binding sites were blocked for 1 hr at room temperature with PBS containing 5% NGS, 0.2% Triton X-100, and 1% BSA. After blocking, sections were incubated with the corresponding primary antibody overnight at 4°C (GFAP: Abcam, Cat #ab7260, RRID:AB\_305808, 1:100; IL-1 $\beta$ : Abcam, Cat# ab9722, RRID:AB\_308765, 1:100; EDN2: Cat# orb445105, RRID:AB\_2892773, 1:500).

The following day, sections were incubated for 1 hr at room temperature in the dark with the fluorescent secondary antibodies (Goat Anti-Rabbit IgG Alexa Fluor 488 Conjugated, Cat# A-11008, RRID:AB\_143165, 1:600; Goat Anti-Rabbit IgG Alexa Fluor 594 Conjugated, Cat# A-11012, RRID:AB\_141359, 1:600) (for details of antibody, see Table S3). Nuclei were stained with Hoechst 33342 and sections were mounted with Prolong™ Gold Antifade Mountant. Samples without primary antibodies were used as negative controls. Images were taken at 20 $\times$ , 40 $\times$ , and 60 $\times$  in an Olympus FV1000

spectral confocal microscope in the UAT at VHIR. Pictures were analyzed in a double-blinded manner by two researchers.

For EDN2 fluorescence intensity, regions of interest (ROI) corresponding to the inner plexiform layer (IPL) and outer plexiform layer (OPL) were manually drawn, and average intensity was measured for each ROI in ImageJ. Four photomicrographs of the retina, each separated by at least 0.6 mm, were used for each retinal section, and three retinal sections were used per mouse.

The score of GFAP and IL-1 $\beta$  expression and immunolocalization was estimated using a previously established 5-point scoring system following (Anderson et al., 2008), as follows: staining only in Müller cell end feet region or GCL (score 1); GCL plus a few proximal processes (score 2); GCL plus many processes, but not extending to ONL (score 3); GCL plus processes throughout, with some in the ONL (score 4); and GCL plus many processes to the outer margin of the ONL (score 5).

## 2.9 | Measurement of retinal vessel leakage

BRB permeability and vascular leakage were quantified using Evans blue dye (E2129 Sigma-Aldrich), which binds irreversibly to serum albumin. Under anesthesia, five animals per group were injected intraperitoneally with a solution of Evans blue (17 mg/kg dissolved in PBS) via the tail vein. After 2 hr, the eyes were enucleated and immediately immersed in 2% paraformaldehyde for 2 hr. The retinas were then dissected and flat-mounted for whole-mounts with the vitreous side up. Images from multiple random fields of the retina were acquired under an Olympus FV1000 spectral confocal microscope and the number of extravasations per field of 60x was counted in a double-blinded manner. Extravasation intensity was measured in Fiji (Fiji, RRID:SCR\_002285) (Schindelin et al., 2012). A ROI was manually drawn following the outlines of the retinal vessels in each photomicrograph. Z-stack images corresponding to the SVP were selected and used to calculate maximum intensity.

## 2.10 | RNA isolation and qRT-PCR

Total RNA was isolated from mouse retinas using the RNeasy kit (Qiagen) and following the manufacturer's instructions. RNA concentration and integrity were determined using a NanoDrop spectrophotometer (ThermoFisher Scientific). At least 250 ng of RNA was reverse-transcribed using the High-Capacity cDNA Reverse Transcription Kit (ThermoFisher Scientific). qRT-PCR was performed in 384-well plates (ThermoFisher Scientific) using PowerUp™ SYBR™ Green Master Mix (ThermoFisher Scientific) under standard conditions: 2 min at 50°C, 10 min at 95°C, 40 cycles of 15 s at 95°C, 1 min at 60°C, and 15 s at 95°C and followed by 15 s at 60°C and 15 s at 95°C in the 7900HT Fast Real-Time PCR System (ThermoFisher Scientific).

Each sample was measured in triplicate, relative fold change gene expression levels were calculated with the presented formula  $2^{-(\Delta\Delta Ct)}$ , and  $\beta$ -actin (*ActB*) was used as an internal control. Each pair of primers used to perform qRT-PCR is listed in Table S2.

## 2.11 | Statistical analysis

We performed a pilot study to estimate the sample size required for 0.8 power and two-sided 0.05 significance for retinal morphometric analysis. For the rest of analyses, we limited the number of animals to mice availability.

Data sets were plotted and analyzed using GraphPad Prism, v8.0.1 (RRID:SCR\_002798), and no data were removed prior to analysis. Data were graphed before statistical test to check whether the data met the assumptions of the statistical approach. Statistical comparisons were made using a two-way ANOVA test followed by Sidak's post hoc test when analyzing two or more ages between wt and *Faim*<sup>-/-</sup>, an unpaired two-tailed Student's *t* test for parametric data, and the Mann-Whitney test for nonparametric data. All *p*-values lower than 0.05 were considered statistically significant. The ROUT method (with *Q* set to 1%) was used to detect outliers.

## 3 | RESULTS

### 3.1 | *Faim* is co-expressed with genes related to retinal function

Data extracted from the Human Proteome Map portal and Protein Atlas showed that *Faim* transcripts are particularly enhanced in photoreceptor cells (Figure 1a) and that FAIM protein is highly expressed in the retina, in contrast to other adult and fetal tissues (Figure 1b). Here we analyzed and confirmed the protein expression of both FAIM-L and FAIM-S in wt retinas and their absence in *Faim*<sup>-/-</sup> mice (Figure 1c). We used RNA-Seq data to construct a gene co-expression network, which allowed us to create gene associations with *Faim* that may indicate functional linkage among them. GO terms were applied to identify characteristic biological attributes of the *Faim* co-expression network. Of note, we found that the top two biological terms were related to retinal functions such as sensory perception of light stimulus and photoreceptor differentiation (Figure 1d), and they were distinctively and largely enriched. The top 10 biological terms, headed by retinal functions, are shown in Figure 1e.

### 3.2 | *Faim*<sup>-/-</sup> mice show photoreceptor death at 18 months

FAIM performs important functions in neurons, but its role in the CNS has not been addressed. Given our previous results, which revealed that *Faim* is particularly enhanced in photoreceptors, here we examined the consequences of *Faim* loss in the retina. To this end, we analyzed the structure and morphometric parameters of the retina and quantified the cell number in different layers of this tissue. Cross-sections of the retina stained with Harris hematoxylin and eosin were examined in 2-, 12-, and 18-month-old wt and *Faim*<sup>-/-</sup> mice. We measured retinal thickness and the number of nuclei in the ONL and GCL. Our results strikingly revealed a decrease

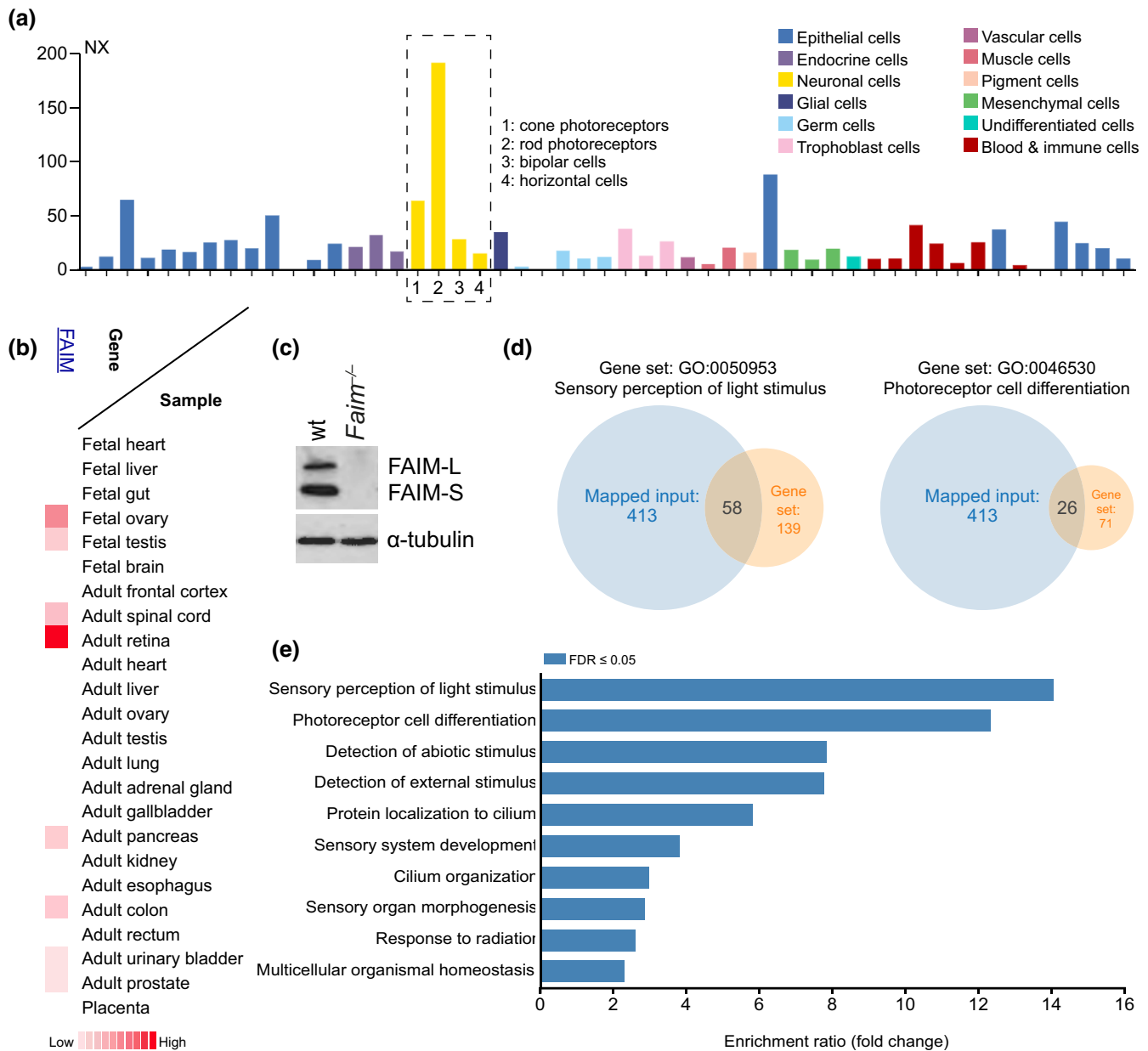


**FIGURE 1** FAIM expression in the retina. (a) Graph deploying transcript expression values of FAIM in different cell types; data extracted from single-cell RNA from the Human Protein Atlas. Neuronal cells are highlighted by a discontinued line. (b) Diagram showing relative protein expression of FAIM in fetal and adult tissues; data extracted from the Human Proteome Map. (c) Retinal western blot of 2-month-old wild-type (wt) and *Faim*<sup>-/-</sup> mice showing both FAIM-L and FAIM-S protein expression.  $\alpha$ -Tubulin was used as a loading control. (d) Venn diagram of the top two enriched GO terms, showing the number of coincidences between the mapped input containing *Faim* co-expressed genes and the pertinent GO term gene set. (e) Representation of the top 10 GO terms based on the biological function of genes co-expressed with *Faim* in mice

in the number of photoreceptor rows in the ONL by 18 months of age in *Faim*<sup>-/-</sup> mice (Figure 2a–f, M: two-way ANOVA, age,  $F_{(1,616, 16,16)} = 14.84$ ,  $p = 0.0004$ ; genotype,  $F_{(1,14)} = 3.354$ ,  $p = 0.0884$ ; interaction,  $F_{(2,20)} = 0.7258$ ,  $p = 0.4963$ ; Sidak's post hoc test,  $p = 0.0476$ ). Furthermore, at this age, the retinas of these mice manifested evident disorganization of layers, highly noticeable at the junction between the OPL and the ONL (Figure 2f). No changes were observed in the number of cells in the GCL (Figure 2n: two-way ANOVA: age,  $F_{(1,954, 24,43)} = 6.966$ ,  $p = 0.0042$ ; genotype,  $F_{(1,20)} = 0.0003761$ ,

$p = 0.9847$ ; interaction,  $F_{(2,25)} = 0.2225$ ,  $p = 0.8021$ ) or INL (data not shown). Despite the decrease in photoreceptor rows in the ONL, no significant differences were found in the total retinal thickness of *Faim*<sup>-/-</sup> mice at any age when compared to wt mice (Figure 2o: two-way ANOVA: age,  $F_{(1,529, 29,06)} = 8.119$ ,  $p = 0.0032$ ; genotype,  $F_{(1,38)} = 1.792$ ,  $p = 0.1886$ ; interaction,  $F_{(2,38)} = 0.2727$ ,  $p = 0.7628$ ).

Although it has long been known that FAIM-S and FAIM-L are anti-apoptotic players, their roles have been studied only under stress conditions (Uhlén et al., 2015). Nonetheless, in view of their promising



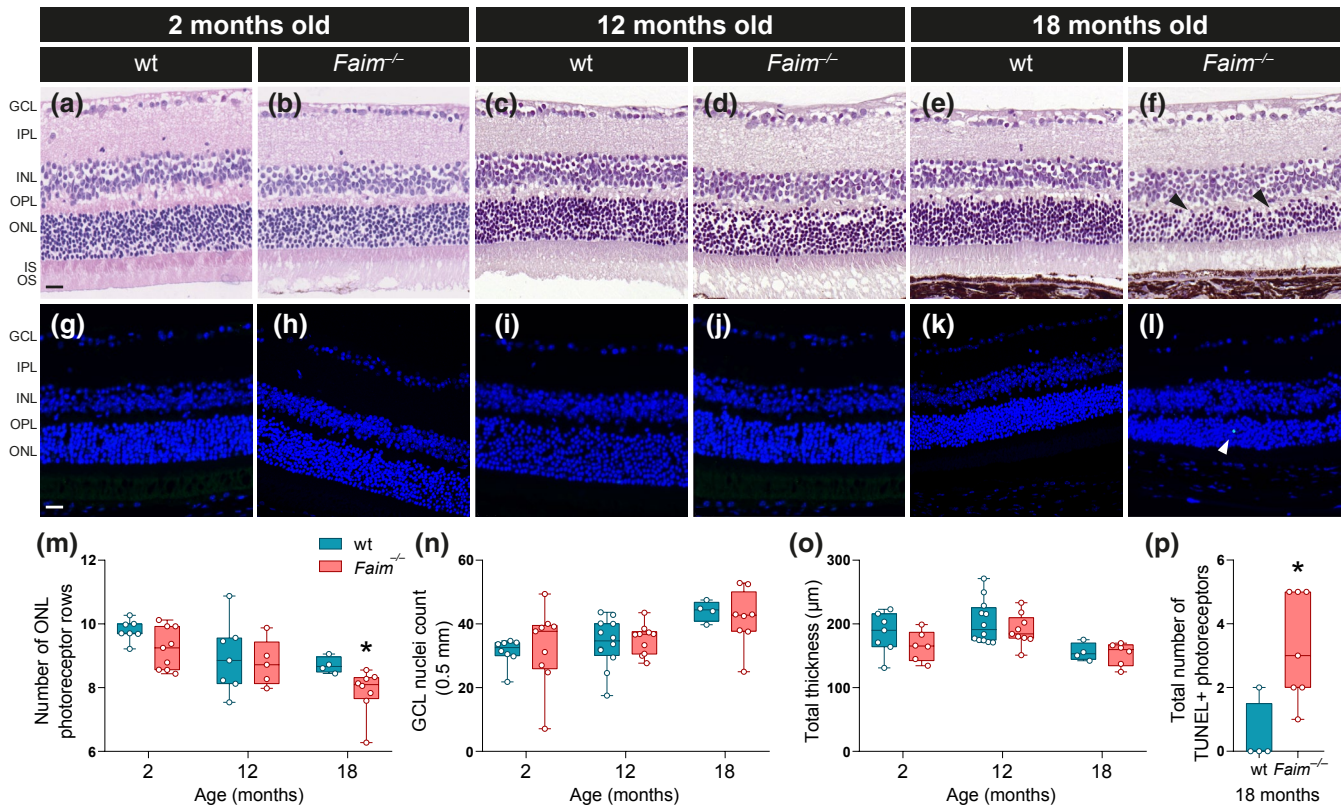


**FIGURE 2** Retinal degeneration in *Faim*<sup>-/-</sup> mice. (a–f) Retinal sections of wt and *Faim*<sup>-/-</sup> mice stained with Harris hematoxylin and eosin and analyzed at different ages (2, 12, and 18 months). (f) At 18 months, significant loss of photoreceptor nuclei and disorganization of the ONL (black arrowheads) was observed. (g–l) Representative images of TUNEL (green) to quantify the number of apoptotic nuclei in the retina at the different ages. Sections were counterstained with Hoechst (blue). (m) At 18 months, the average number of ONL photoreceptor rows was decreased ( $n = 4–9$  mice/group). (n, o) GCL nuclei count and retinal thickness were constant throughout the ages ( $n = 4–9$  mice/group). (p) Quantification of the number of TUNEL + photoreceptor cells in 18-month-old *Faim*<sup>-/-</sup> mice. Each symbol in the plots represents one retina. The white arrowhead points at a TUNEL + photoreceptor. ( $n = 4–7$  mice/group). Each box plot extends from the 25th to the 75th percentile and the median is plotted as a line in the box. Whiskers represent min to max values, and dot plots are overlaid. Statistical analysis was performed using a two-way ANOVA followed by Sidak's post hoc test for m, n, and o, and an unpaired two-tailed Student's *t* test for p. \* $p < 0.05$ . GCL: ganglion cellular layer, IPL: inner plexiform layer, INL: inner nuclear layer, OPL: outer plexiform layer, ONL: outer nuclear layer; and IS/OS: inner/outer segment. Scale bar: 20  $\mu\text{m}$

functions, we performed a TUNEL assay in retinal sections to ascertain whether the decrease in the number of photoreceptors was due to cell death. Indeed, TUNEL-stained positive cells in the ONL were significantly increased in *Faim*<sup>-/-</sup> retinas at 18 months of age (Figure 2g–l, P: unpaired two-tailed Student's *t* test,  $t = 2.950$ ,  $p = 0.0162$ ). Thus, our results confirmed apoptosis in the ONL and suggest an active process of neurodegeneration under basal conditions.

### 3.3 | *Xiap* and *Tnf- $\alpha$* mRNA expression is increased in *Faim*<sup>-/-</sup> retinas

To expand on the previous results, we analyzed the mRNA expression of apoptotic mediators and FAIM-interacting partners by qRT-PCR. We recently described that SIVA-1, a pro-apoptotic protein, interacts with FAIM-L and XIAP. SIVA-1 interaction with XIAP displaces FAIM-L from this complex, thus enabling XIAP auto-ubiquitination and subsequent caspase-3 activation (Coccia et al., 2020). We detected an

increase in *Xiap* mRNA expression in *Faim*<sup>-/-</sup> retinas at 2 months of age (unpaired two-tailed Student's *t* test,  $t = 2.657$ ,  $p = 0.0209$ ), and also an increase in *Siva-1* mRNA expression at 12 months (unpaired two-tailed Student's *t* test,  $t = 5.111$ ,  $p = 0.0006$ ). We also observed that mRNA levels of cytokine *Tnf- $\alpha$*  were upregulated at both ages (unpaired two-tailed Student's *t* test,  $t = 4.409$ ,  $p = 0.0003$  regarding 2 months of age;  $t = 2.578$ ,  $p = 0.0190$  regarding 12 months of age), and *FasI* was upregulated at 12 months (unpaired two-tailed Student's *t* test,  $t = 2.779$ ,  $p = 0.0195$ ) (Figure S1). These results suggest that apoptotic pathways are altered in *Faim*<sup>-/-</sup> retinas.

### 3.4 | Ubiquitin complexes accumulate in *Faim*<sup>-/-</sup> retinas

To uncover likely events that may account for the late photoreceptor death, we studied early pathogenic hallmarks of neurodegeneration, like protein aggregation. Ubiquitinated proteins usually become

deactivated and tagged for degradation by the proteasome (Lecker et al., 2006; Lobanova et al., 2013). However, disruption of this process causes the neurotoxic accumulation of ubiquitinated proteins, which can eventually lead to photoreceptor death (Schneider et al., 2012). To study whether this form of protein aggregation occurs in *Faim*<sup>-/-</sup> retinas, retinal sections of *Faim*<sup>-/-</sup> and wt mice were immunolabeled against multiubiquitin aggregates. We measured the number of ubiquitin-positive cells in the GCL and INL at 2 and 12 months of age and found a significant increase in both nuclear layers and ages in *Faim*<sup>-/-</sup> retinas (Figure 3b: two-way ANOVA: age,  $F_{(1,5)} = 24.99$ ,  $p = 0.0041$ ; genotype,  $F_{(1,18)} = 41.53$ ,  $p < 0.0001$ ; interaction  $F_{(1,5)} = 5.618$ ,  $p = 0.0639$ ) (Figure 3c: two-way ANOVA: age,  $F_{(1,5)} = 6.485$ ,  $p = 0.0515$ ; genotype  $F_{(1,18)} = 21.10$ ,  $p = 0.0002$ ; interaction  $F_{(1,5)} = 12.42$ ,  $p = 0.0168$ ). In addition, intense immunoreactivity against ubiquitin was revealed in the IPL, OPL, and inner segments (IS) of photoreceptors of *Faim*<sup>-/-</sup> retinas (Figure 3a), where the photoreceptor translation machinery is found (Kennedy & Malicki, 2009). These results suggest that the ubiquitin-proteasome system is disrupted in *Faim*<sup>-/-</sup> retinas.

### 3.5 | *Faim*<sup>-/-</sup> retinas present chronic reactive gliosis

The aggregation of ubiquitinated proteins can lead to inflammation of the retinal tissue (Leger et al., 2011). Müller cell activation is one of the hallmarks of retinal degeneration, and it can be characterized by an increased expression of glial fibrillary acidic protein (GFAP) (Luna et al., 2010). Consequently, we performed immunofluorescence

against GFAP in the retinas of wt and *Faim*<sup>-/-</sup> mice and used an established procedure to assess the extent of Müller cell activation via a 5-point scoring system (Anderson et al., 2008). The retinas of *Faim*<sup>-/-</sup> mice showed an increased immunoreactivity of GFAP-positive glial processes extending from the end feet of Müller cells in the GCL and deep into the tissue, toward the ONL (Figure 4a-d). This was reflected in higher GFAP scores at both 2 and 12 months of age (Figure 4e: two-way ANOVA: age,  $F_{(1,41)} = 0.1735$ ,  $p = 0.6792$ ; genotype,  $F_{(1,41)} = 19.18$ ,  $p < 0.0001$ ; interaction,  $F_{(1,41)} = 0.3933$ ,  $p = 0.5341$ ). Increased *Gfap* mRNA and GFAP protein expression was also confirmed by qRT-PCR and western blot at 2 (Figure 4k: unpaired two-tailed Student's *t* test: *Gfap* mRNA,  $p = 0.0001$ ; GFAP protein,  $p = 0.0091$ ) and 12 months of age (Figure 4l; unpaired two-tailed Student's *t* test: *Gfap* mRNA,  $p = 0.0229$ ; GFAP protein,  $p = 0.0256$ ), respectively. Müller cells are known to activate an acute phase response, which is associated with retinal upregulation of pro-inflammatory cytokines like interleukin-1 beta (IL-1 $\beta$ ). The IL-1 $\beta$  immunolabeling pattern in the retina traced Müller cell morphology (hence showing the same pattern as GFAP) (Figure 4f-i), and it depicted a higher score in 12-month-old *Faim*<sup>-/-</sup> retinas when compared to wt, but not at 2 months of age (Figure 4j: two-way ANOVA: age,  $F_{(1,8)} = 5.783$ ,  $p = 0.0429$ ; genotype  $F_{(1,19)} = 0.9253$ ,  $p = 0.3482$ ; interaction  $F_{(1,8)} = 5.365$ ,  $p = 0.0492$ ; followed by Sidak's post hoc test:  $p = 0.8077$  at 2 months;  $p = 0.0256$  at 12 months). Microglia are the resident immune cell type of the CNS and play an important role in retinal homeostasis. To evaluate microglial activation status in the absence of *Faim*, we measured the mRNA levels of *Cd11b* and ionized calcium-binding adapter molecule 1 (*Iba-1*). Our results revealed an

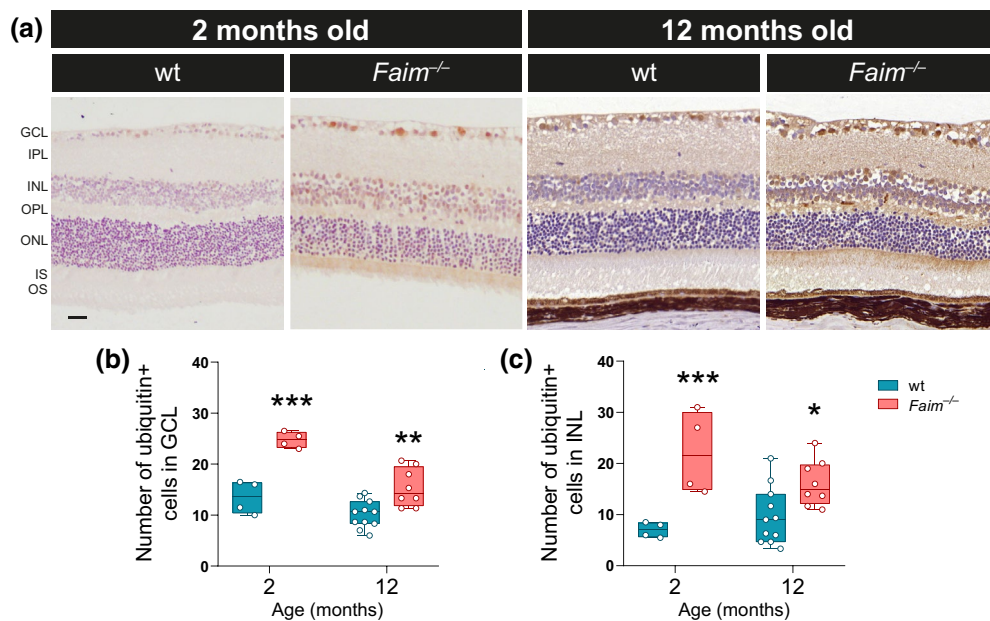


**FIGURE 3** Immunohistochemical analysis of ubiquitin aggregation in wt and *Faim*<sup>-/-</sup> retinas. (a) Representative images of 4- $\mu$ m paraffin sections of retinas taken from 2- and 12-month-old mice and immunolabeled with ubiquitin. (b) Ubiquitin-positive cells in the GCL at 2 and 12 months. (c) Ubiquitin-positive cells in the INL at 2 and 12 months. Each symbol in the plots represents one retina ( $n = 4$ –11 mice/group). Each box plot extends from the 25th to the 75th percentile and the median is plotted as a line in the box. Whiskers represent min to max values, and dot plots are overlaid. Statistical analysis was performed using a two-way ANOVA followed by Sidak's post hoc test. \* $p < 0.05$  and \*\*\* $p < 0.001$ . Scale bar: 20  $\mu$ m

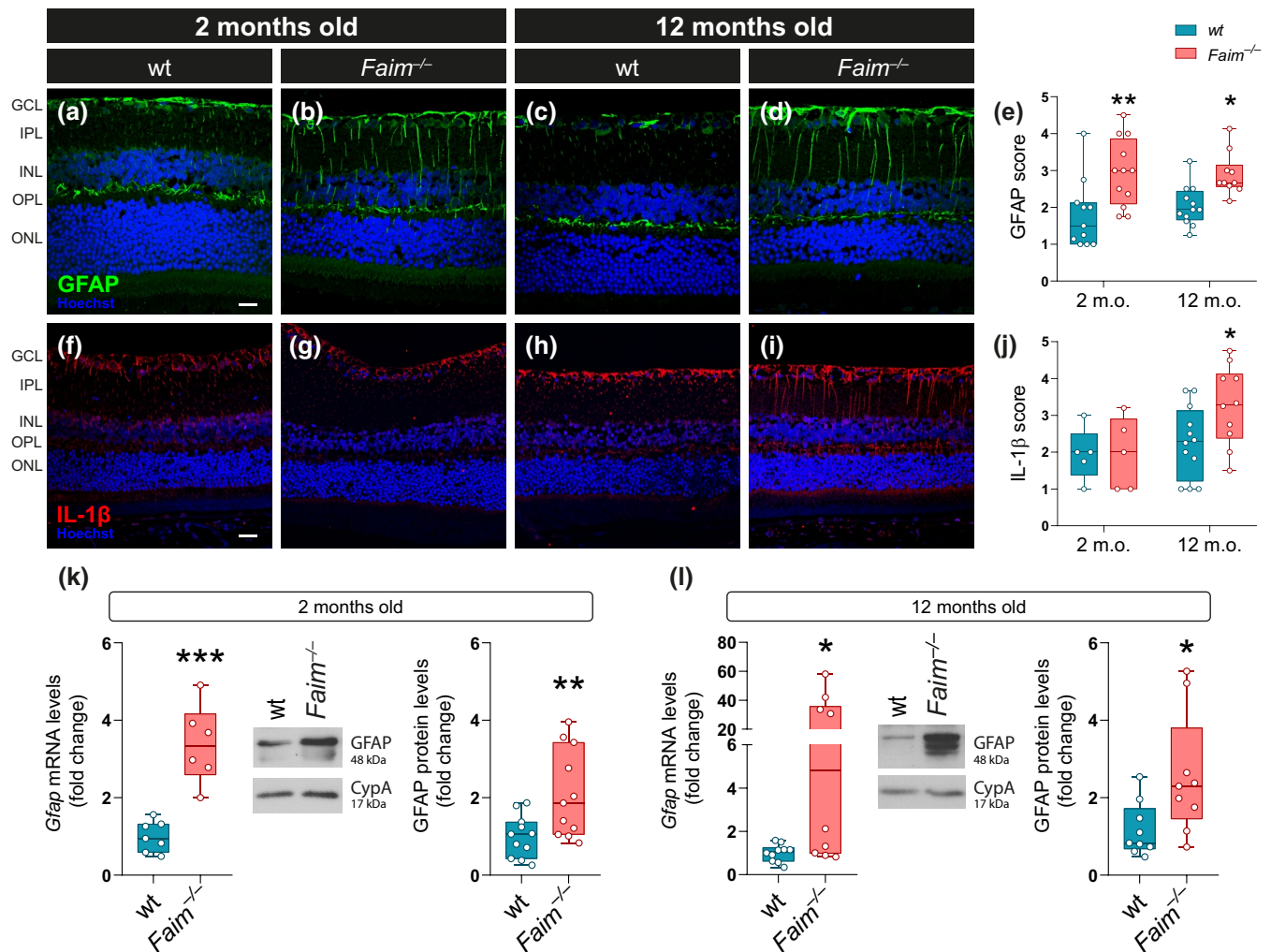


**FIGURE 4** Expression of GFAP and IL-1 $\beta$  in 2- and 12-month-old wt and *Faim*<sup>-/-</sup> mice. (a–d) Representative images of GFAP (green) immunolabeling of paraffin-embedded sections of wt and *Faim*<sup>-/-</sup> retinas. GFAP expression is restricted to astrocytes in the GCL and to proximal prolongations of Müller cells. (e) GFAP immunolabeling score at 2 and 12 months, showing an increase in *Faim*<sup>-/-</sup> mice. (f–i) Representative images of IL-1 $\beta$  immunolabeling of paraffin-embedded sections from wt and *Faim*<sup>-/-</sup> retinas. (j) IL-1 $\beta$  immunolabeling score at both ages, showing an increase in *Faim*<sup>-/-</sup> mice at 12 months. (k–l) *Gfap* mRNA levels and protein levels are increased at 2 and 12 months of age ( $n = 6$ – $11$  mice/group). mRNA expression levels were normalized to *Actb*. Representative western blot images of GFAP levels of wt and *Faim*<sup>-/-</sup> retinas are shown. Protein levels were normalized to cyclophilin A (CypA) and quantified in ImageJ. Data are plotted relative to wt values. Each box plot extends from the 25th to the 75th percentile and the median is plotted as a line in the box. Whiskers represent min to max values, and dot plots are overlaid. Statistical analysis was performed using a two-way ANOVA followed by Sidak's post hoc test. \* $p < 0.05$ , \*\* $p < 0.01$ , and \*\*\* $p < 0.001$ . Scale bar: 20  $\mu$ m

increase in both markers in the retinas of 2- (Figure S2a: unpaired two-tailed Student's  $t$  test: *Cd11b*,  $p = 0.0260$ ; *Iba-1*,  $p = 0.0022$ ) and 12-month-old (Figure S2b: unpaired two-tailed Student's  $t$  test: *Cd11b*,  $p = 0.0028$ ; *Iba-1*,  $p = 0.0343$ ) *Faim*<sup>-/-</sup> mice.

Taken together, these results show early glial activation in the absence of *Faim* in 2-month-old retinas that is sustained at 12 months of age.

### 3.6 | BRB homeostasis is disrupted in *Faim*<sup>-/-</sup> retinas

Retinal gliosis can promote leukocyte adhesion to the endothelium and the release of chemokines, cytokines, vascular permeability factors (TNF- $\alpha$  and vascular endothelial growth factor A (VEGF-A)

(Giebel et al., 2005) and vascular endothelial adhesion molecules (intercellular adhesion molecule 1 (ICAM-1) and vascular cell adhesion protein 1 (VCAM-1), which act as pro-inflammatory mediators. The analysis of these molecular markers in the retina by qRT-PCR at 2 months of age revealed an upregulation of *Vcam-1* mRNA (Figure S3a: unpaired two-tailed Student's  $t$  test,  $p = 0.0228$ ). Although the great variability may reflect biological or technical issues, *Vegfa* and *Vcam-1* were significantly upregulated at 12 months (Figure S3b: unpaired two-tailed Student's  $t$  test: *Vegfa*,  $p = 0.0332$ ; *Vcam-1*,  $p = 0.0310$ ). We also analyzed the mRNA levels of *Mmp9* and *Edn1*, which remained unchanged between wt and *Faim*<sup>-/-</sup> mice.

Vascular inflammation can evolve into impairment of the BRB function and the consequent breakdown of this barrier (Shin et al., 2014).

**FIGURE 5** Vascular BRB permeability in wt and *Faim*<sup>-/-</sup> mice observed in whole-mount retinas. (a–q) Representative confocal immunofluorescence images of Evans blue maximum intensity projections observed under Spec3, a high-contrast profile by FV100 Olympus confocal laser scanning microscope in 2- and 12-month-old wt and *Faim*<sup>-/-</sup> mice. (r, s) Total number of significant extravasations. (r', s') Intensity quantification of Evans blue extravasations at 2 and 12 months. (t) Representative plots of wt and *Faim*<sup>-/-</sup> z axis profiles of Evans blue in retinal whole-mounts, showing the intensity of the different vascular plexuses and quantified in ImageJ. The number of extravasations was quantified in at least eight images in a 60x field per mouse. All extravasations found were used to quantify extravasation intensity. Each symbol in the plots represents one retina ( $n = 4\text{--}5$  mice/group). Each box plot extends from the 25th to the 75th percentile and the median is plotted as a line in the box. Whiskers represent min to max values, and dot plots are overlaid. Statistical analysis was performed using a Mann–Whitney test (number of extravasations) or Student's *t* test (intensity of extravasations). \* $p < 0.05$  and \*\* $p < 0.01$ . A.U., arbitrary units; DCP, deep capillary plexus; EB, Evans blue; ICP: intermediate capillary plexus; RVP, retinal vascular plexus; and SVP, superficial vascular plexus. Spec3 intensity scale is shown in the upper left area. Scale bar: 20  $\mu\text{m}$

Anatomically, the BRB is composed of an outer and inner component. The outer barrier is found in the retinal pigment epithelium, and the inner one is formed by tight junctions between retinal capillary endothelial cells. The inner BRB, in turn, is comprised of the retinal vascular endothelium. This structure can be explored by retinal whole-mounts, allowing the identification of the three vascular plexuses: the superficial vascular plexus (SVP), the intermediate capillary plexus (ICP), and the deep capillary plexus (DCP) (Campbell et al., 2017).

To study whether the BRB was impaired in *Faim*<sup>-/-</sup> mice, we analyzed vascular permeability by measuring albumin–Evans blue complex leakage in retinal whole-mounts (Figure 5). Retinal vessels were sharply outlined in wt mice (Figure 5a,i), with no evidence of Evans blue leakage from the vessels either in the SVP (Figure 5b,j), ICP (Figure 5c,k), or in the DCP (Figure 5d,l). Interestingly, our results revealed sites of focal dye leakage into the retinal parenchyma of *Faim*<sup>-/-</sup> retinas at 2 and 12 months, with more obvious leakage at the latter age (Figure 5e,m). Of note, these extravasations were specifically localized in the SVP (Figure 5f,o), which is the plexus that supplies the ICP and DCP by vertical anastomoses. In the SVP, the number of extravasations in *Faim*<sup>-/-</sup> mice retinas was not significant at 2 months of age (Figure 5r: Mann–Whitney test,  $p = 0.1032$ ), but the quantification of its intensity was significantly higher in *Faim*<sup>-/-</sup> mice compared to wt counterparts at this age (Figure 5r': unpaired two-tailed Student's *t* test,  $p = 0.0478$ ). At 12 months of age, both the number (Figure 5s: Mann–Whitney test,  $p = 0.0238$ ) and the intensity (Figure 5s': unpaired two-tailed Student's *t* test,  $p = 0.0015$ ) of the extravasations were significantly elevated in the SVP of *Faim*<sup>-/-</sup> retinas. No dye leakage was observed in the deeper retinal vascular plexuses (Figure 5g,h,p,q). The z axis profile plots of Evans blue retinal whole-mounts, representing the intensity of the different vascular plexuses, evidenced the presence of vascular extravasations in the SVP but not in the ICP or DCP (Figure 5t).

In summary, these results show evident vascular capillary leakage into the retinal parenchyma, caused by an impairment of the BRB at the SVP level.

### 3.7 | Edn2/Fgf2 neuroprotective pathway could be activated in *Faim*<sup>-/-</sup> retinas

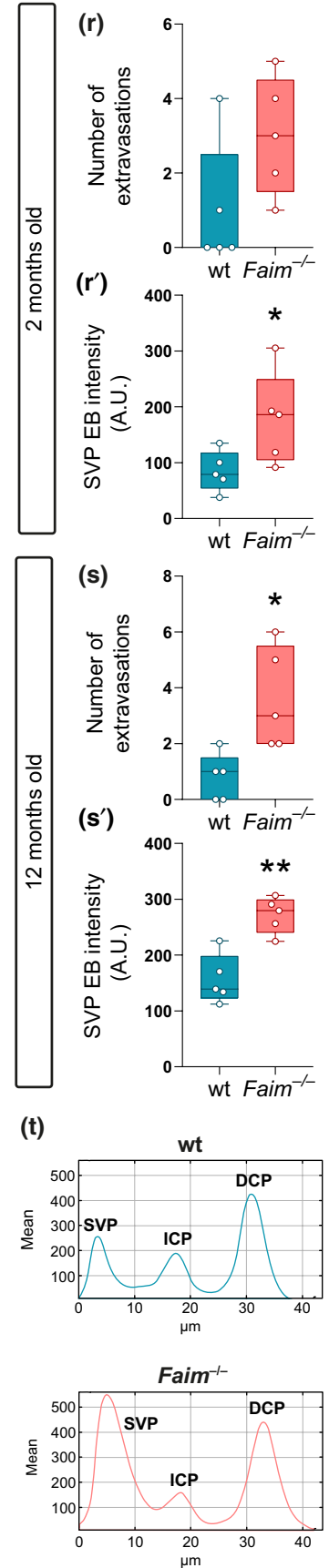
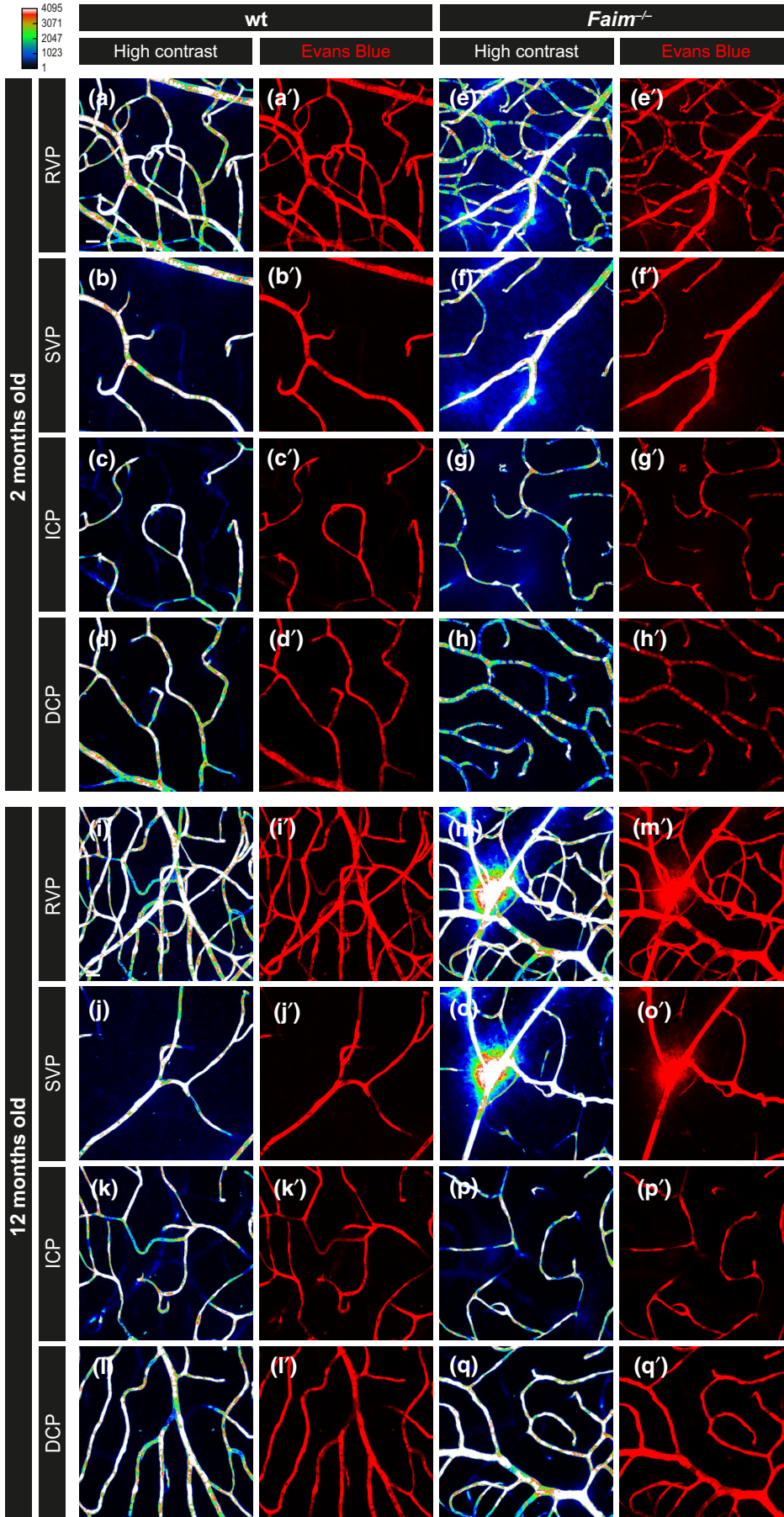
Photoreceptors may induce an endogenous protective response by triggering retinal gliosis through the production of endothelin-2

(EDN2) (Rattner & Nathans, 2005), a vasoconstrictive peptide. To test this notion, we performed EDN2 immunofluorescence staining in wt and *Faim*<sup>-/-</sup> retinal sections. EDN2 immunoreactivity was sparse in wt mice (Figure 6a,c). However, a strong increase in EDN2 signal intensity was observed in *Faim*<sup>-/-</sup> retinas (Figure 6b,d,e), being statistically significant in the IPL at 2 months (Figure 6g: two-way ANOVA: age,  $F_{(1,6)} = 0.02038$ ,  $p = 0.8911$ ; genotype,  $F_{(1,6)} = 4.737$ ,  $p = 0.0724$ ; interaction  $F_{(1,6)} = 2.140$ ,  $p = 0.1938$ ; Sidak's post hoc test:  $p = 0.0442$ ) and in the OPL at 12 months (Figure 6h: two-way ANOVA: age,  $F_{(1,12)} = 84.89$ ,  $p < 0.0001$ ; genotype,  $F_{(1,12)} = 26.78$ ,  $p = 0.0002$ ; interaction,  $F_{(1,12)} = 17.21$ ,  $p = 0.0014$ , Sidak's post hoc test:  $p < 0.0001$ ). At the latter age, we found a unique and distinctive EDN2 signal enclosing the nuclei of cone photoreceptors (but not rods) and following their axonal projections (Figure 6d–f). Also, we observed an upregulation of *Edn2* mRNA expression in retinas of 2-month-old *Faim*<sup>-/-</sup> mice (Figure 7a: unpaired two-tailed Student's *t* test,  $p = 0.0344$ ), and of *Edn2* receptors in Müller cells, endothelin receptor type B (*Ednrb*) (Jeon et al., 1998), at 12 months (Figure 7b: unpaired two-tailed Student's *t* test,  $p = 0.0251$ ). These events, in turn, can stimulate the expression of fibroblast growth factor 2 (*Fgf2*), which has also been shown to delay photoreceptor degeneration (Leger et al., 2011; Luna et al., 2010). Given these considerations, we analyzed *Fgf2* mRNA levels and found an upregulation at 12 months (Figure 7b: unpaired two-tailed Student's *t* test,  $p < 0.0001$ ). These results suggest that the EDN2 survival signaling pathway is activated in *Faim*<sup>-/-</sup> retinas (Figure 7c).

## 4 | DISCUSSION

FAIM-S and FAIM-L play critical and distinct roles in neuronal outgrowth and survival. Nevertheless, FAIM function had never been studied *in vivo* in the CNS. Our analysis of the *Faim* co-expression network suggested that this gene is associated with the biological functions of photoreceptors and the retina. In the present study, we demonstrate the expression of both *Faim* isoforms in the retina for the first time, and we show that *Faim* depletion in mice leads to the accumulation of protein aggregates, retinal gliosis, leakage of the BRB, and photoreceptor death.

Photoreceptors, the light-sensitive neurons of the retina, are among the most specialized cells in the organism, rendering them highly vulnerable to any kind of stress. *Faim*<sup>-/-</sup> mice are viable and



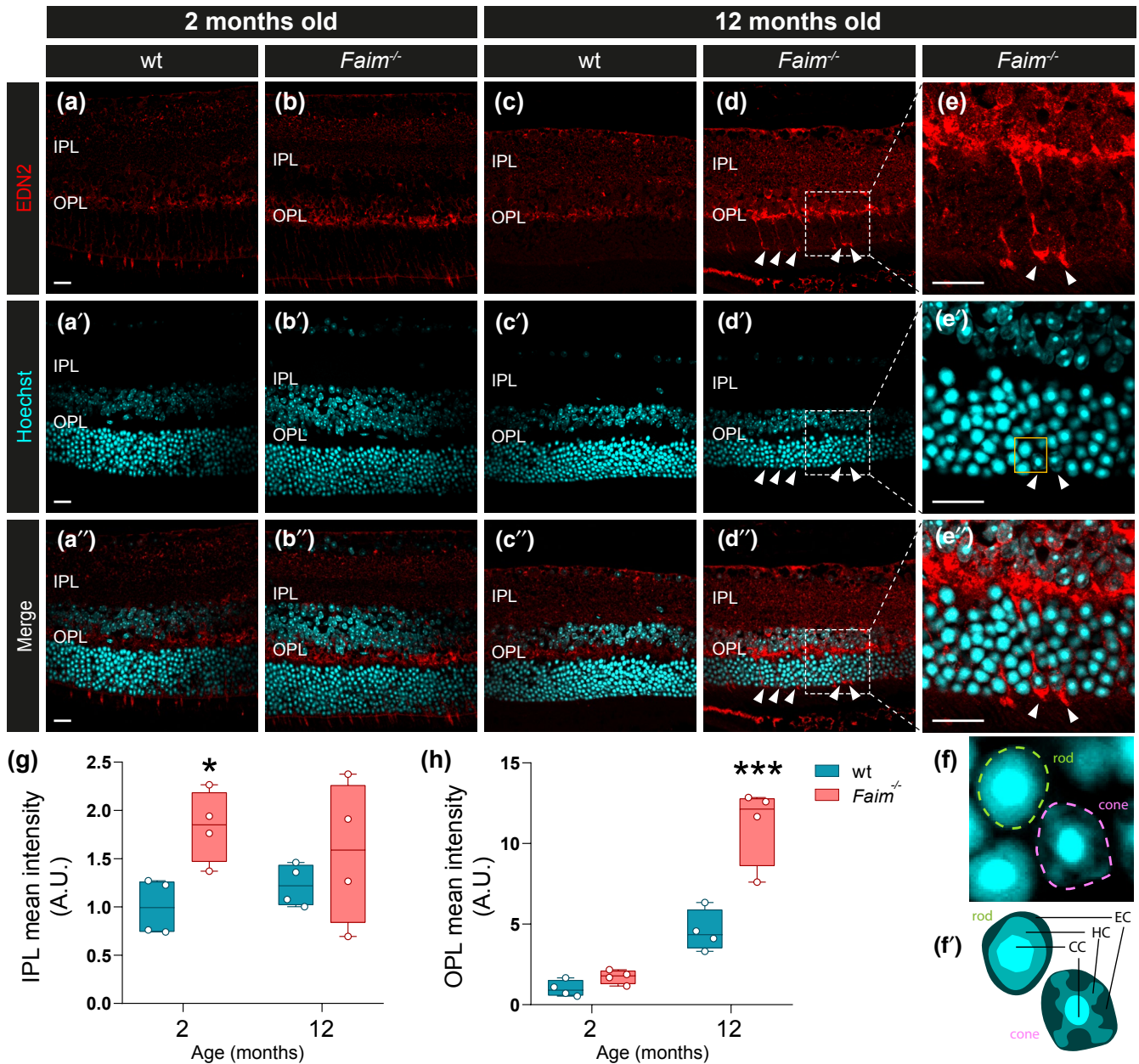


**FIGURE 6** EDN2 immunolabeling is increased at 2 and 12 months in *Faim*<sup>-/-</sup> retinas. (a–d) Representative images of 4- $\mu$ m paraffin sections of retinas immunolabeled with endothelin-2 (EDN2). (a'–d') Hoechst counterstaining. (a'–d'') Merged immunofluorescence of EDN2 and Hoechst. (e, e', e'') Panels showing magnified boxed areas highlighted in d, d', and d''. (f) Magnification of yellow boxed area in e' showing the distinctive nuclei of cones and rods. (f') Diagram showing the nuclei of representative cones and rods. (g) Quantification of EDN2 immunolabeling performed in the IPL and showing an increase at 2 months. (h) Quantification of EDN2 immunolabeling performed in the OPL and showing an increase at 12 months. Each symbol in the plots represents one retina ( $n = 4$  mice/group). Data are plotted relative to wt values for each measure. Each box plot extends from the 25th to the 75th percentile and the median is plotted as a line in the box. Whiskers represent min to max values, and dot plots are overlaid. Statistical analysis was performed using a two-way ANOVA followed by Sidak's post hoc test. \* $p < 0.05$  and \*\*\* $p < 0.001$ . CC, chromocenter; EC, euchromatin; HC, heterochromatin. Scale bar: 20  $\mu$ m

have a normal life span (Huo et al., 2016), and loss of *Faim* is not enough to cause retinal degeneration at an early age. However, our data show that *Faim* depletion, without injury or stress-induction, can slowly but progressively damage the retina, culminating in photoreceptor death and retinal disorganization at 18 months. Consequently, after studying the earlier pathological events that

may account for this late photoreceptor death, we found an aberrant accumulation of ubiquitinated protein aggregates, which was most notable in the GCL, INL, and IS of photoreceptors. Accordingly, these experiments are consistent with previous results. In this respect, Kaku and Rothstein described how *Faim*-deficient cells accumulate ubiquitinated and aggregated proteins following oxidative

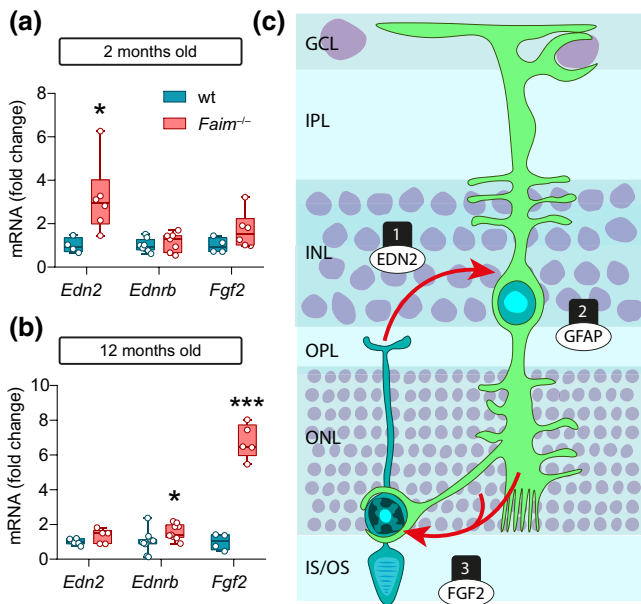


**FIGURE 7** EDN2 survival signaling loop is activated in *Faim*<sup>-/-</sup> mice. (a) mRNA levels of *Edn2*, *Ednrb*, and *Fgf2* at 2 months, showing an increase in *Edn2*. (b) mRNA levels of *Edn2*, *Ednrb*, and *Fgf2* at 12 months, showing an increase in *Ednrb* and *Fgf2*. (c) Schematic representation of the EDN2-FGF2 hypothetical loop suggested by Rattner and Nathans (Rattner & Nathans, 2005). mRNA levels were assessed by qRT-PCR, and each symbol in the plots represents one retina ( $n = 4-7$  mice/group). Expression levels were normalized to *Actb* and data are plotted relative to wt values for each gene. Each box plot extends from the 25th to the 75th percentile and the median is plotted as a line in the box. Whiskers represent min to max values, and dot plots are overlaid. Statistical analyses was performed using an unpaired two-tailed Student's *t* test \* $p < 0.05$  and \*\*\* $p < 0.005$

stress *in vivo* (Kaku & Rothstein, 2020), and that under the same oxidative conditions, FAIM is recruited to ubiquitinated complexes in wt cells. Those authors suggested that FAIM participates in the dynamics of protein aggregates by a mechanism that has yet to be elucidated. To expand these results, it would also be interesting to study the *Faim*<sup>-/-</sup> retina under stress conditions that harm photoreceptors, such as light-induced damage (Bravo-Nuevo et al., 2004).

Due to the unique anatomical distribution of the cytoplasm of photoreceptors, which is almost entirely found in the IS and outer segment (OS) compartments, quantification of ubiquitin-positive cells in the ONL was unattainable. However, our observation that the IS of photoreceptors in *Faim*<sup>-/-</sup> retinas showed an increase in ubiquitin expression has exciting implications. The IS is the major cytoplasmic compartment of the photoreceptor, where protein synthesis and the largest part of housekeeping functions take place. Therefore, it is reasonable to hypothesize that a disruption in the proteasome system of photoreceptors would result in the accumulation of misfolded proteins and ubiquitin aggregates in the IS.

The inability of neurons to undergo mitosis predisposes them to the cumulative pathogenic effects of protein misfolding and

consequent aggregation (Mattson & Magnus, 2006). Hence, it is imperative for neuronal cells such as photoreceptors to have good quality control mechanisms in place. Our data suggest that the sole absence of *Faim* causes a breakdown in protein quality control, which culminates in late photoreceptor death. The accumulation of protein aggregates in the retina is a major cause of cellular malfunction and it can trigger an inflammatory response, which can lead to retinal remodeling and photoreceptor death (Illing et al., 2002; Remé et al., 1998). Moreover, protein misfolding and aggregation are involved in several retinal dystrophies, including retinitis pigmentosa and age-related macular degeneration (Illing et al., 2002; Leger et al., 2011). These events resemble those in the brain, where numerous studies have demonstrated how ubiquitin-positive inclusions cause the loss of neuronal cells (Hara et al., 2006), and that protein aggregation is a common pathological hallmark of neurodegeneration. For instance, abnormal amyloid beta and tau aggregation, disruption of the proteasome, and ubiquitin immunoreactivity in neurofibrillary tangles are characteristic features of Alzheimer's disease (Brion et al., 1985, 1986; Harris et al., 2020; Sisodia et al., 1990; Upadhyay & Hegde et al., 2007). Given these considerations, research efforts into neurodegenerative diseases should focus on proteins that potentially play a role in protein aggregation, like FAIM.

Müller cells are the main resident glia of the retina and they exert many of the functions that in other CNS tissues are performed by astrocytes, oligodendrocytes, or ependymal cells (Newman & Reichenbach et al., 1996). Müller cells span the entire thickness of the retina and envelop every retinal cell type, thus providing structural and metabolic support. Under conditions of stress, such as protein aggregation, Müller cells are activated, triggering a reactive phenotype (Bringmann et al., 2004), akin to astrocytes in the brain (Kato et al., 1998). Müller cell gliosis is characterized by morphological, phenotypical, and biochemical changes, such as GFAP upregulation and the release of pro-inflammatory cytokines like IL-1 $\beta$  and TNF- $\alpha$  (Sarthy & Fu, 1989). These events are prompted in the form of acute gliosis to protect the nervous tissue. However, uncontrolled gliosis for prolonged periods in response to an unceasing event with multiple repercussions, like loss of FAIM, might harm the retina. Indeed, our data show how GFAP is already increased in *Faim*<sup>-/-</sup> retinas at 2 months of age, and that GFAP expression and immunoreactivity are even greater at 12 months. These alterations are emphasized by the increase in IL-1 $\beta$  immunoreactivity and *Tnf- $\alpha$*  mRNA expression detected in *Faim*<sup>-/-</sup> retinas, which can boost the retinal inflammatory response (Kany et al., 2019). The chronicity of reactive gliosis is likely to be one of the main pathogenic events in *Faim*<sup>-/-</sup> retinas, as it is proven to occur in many neurodegenerative diseases (González et al., 2014).

Müller cells are also a major modulator of the neurovascular structure and an important player in the maintenance of BRB homeostasis (Tout et al., 1993). These cells envelop blood vessels, and thanks to this intimate anatomical association, they can rapidly perceive homeostatic changes and give an appropriate response. On the other hand, chronic gliosis can induce vascular permeability, leukocyte adhesion, and leakage of blood into the retinal parenchyma,

further exacerbating disease progression (Coughlin et al., 2017; Tout et al., 1993). We examined retinal whole-mounts, which allowed us to visualize the three capillary plexuses and spatially analyze this information. Although we found signs of vascular leakage in *Faim*<sup>-/-</sup> retinas at 2 months, it was not until 12 months that we discovered a substantial number of prominent extravasations. Surprisingly, every extravasation detected in the *Faim*<sup>-/-</sup> mice could be traced back to one area, namely the SVP. The SVP is found mainly in the GCL, where Müller cell end feet and astrocytes converge (Coorey et al., 2012). We have shown how GFAP immunolabeling in Müller cell end feet (and thus in the surroundings of the SVP) is heavily increased. This finding strengthens the hypothesis that reactive gliosis disrupts microvascular homeostasis in *Faim*<sup>-/-</sup> retinas. This vascular permeability is accompanied by an increase in the expression of cell adhesion molecules like *Vcam-1* and *Vegfa*, thus confirming the expansion of the inflammatory environment. BRB dysfunction and capillary permeability are potentially harmful and are typical attributes of microvascular diseases like macular edema and diabetic retinopathy, in which photoreceptor viability is also affected (Cunha-Vaz, 2017; McDowell et al., 2018).

To monitor retinal health conditions in such a short-term manner, Müller cells are thought to be able to specifically sense injuries on the basis of signaling molecules released from retinal cells (Fimbel et al., 2007; Montgomery et al., 2010; Senut et al., 2004). Many studies have implicated Müller cells in neuroprotective pathways for photoreceptor survival (Bringmann et al., 2009; Goh et al., 2016). In particular, EDN2 is produced by photoreceptors in a wide variety of retinal injuries and early stage diseases, and it has been proposed as an early biomarker for diabetic retinopathy (Binz et al., 2016; Bramall et al., 2013; Braunger et al., 2013). When we checked for the presence of this molecule in *Faim*<sup>-/-</sup> retinas, we found that both EDN2 immunoreactivity and mRNA expression were increased at 2 months, implying that photoreceptors may have already been impaired by harmful stimuli. We also distinguished a unique EDN2 pattern at 12 months. Surprisingly, at this age, EDN2 enveloped the soma of cone (but not rod) photoreceptors, which were identifiable through their distinctive euchromatin and heterochromatin conformations (Hughes et al., 2017; Solovei et al., 2009). Of note, in a microarray data set of the *Nrl*<sup>-/-</sup> retinal model, which causes the conversion of rods into cones, both *Faim* and *Edn2* were upregulated as early as P21 (Hsiau et al., 2007). This finding suggests that FAIM has a specific function in cone photoreceptors. Cones mediate light perception in the daytime and are sensitive to color, whereas rods are more sensitive to light and they function for night vision. Accounting for roughly 3% of photoreceptors in humans and wt mice, cones are far sparser than rods in the retina (Jeon et al., 1998). If *Faim* was particularly important for cone survival, it would explain the reduced—but significant—number of apoptotic nuclei found in the *Faim*<sup>-/-</sup> retinas. Future studies assessing *Faim* levels in retinal pathologies that present cone degeneration might prove important.

Furthermore, EDN2 has been shown to trigger a neuroprotective response in Müller cells through EDNRB (Joly et al., 2008), and *Ednrb*

mRNA levels were also upregulated in *Faim*<sup>-/-</sup> mice at 12 months. Rattner and Nathans (Rattner & Nathans, 2005) found a large increase in *Edn2* transcripts in a retinal degeneration slow (rds) mouse model. In that study, they proposed that photoreceptor-derived EDN2 functions as a general stress signal that activates Müller cells through EDNRB. This signal, in turn, can increase their sensitivity to EDN2 by upregulating EDNRB, inducing a gliotic response via GFAP upregulation. Those authors also suggested that, to support the survival of viable photoreceptors, activated Müller cells and/or other cells produce and release FGF2, which we also found upregulated in our model at 12 months. Moreover, FGF2 has been implicated in photoreceptor paracrine pathways linked to neuroprotective roles (Gao & Hollyfield, 1996; Joly et al., 2007; Wen et al., 1995). In animal models of inherited photoreceptor degeneration and light-induced retinal degeneration, FGF2 overexpression delays photoreceptor death (Spencer et al., 2001; Yamada et al., 2001). Also, in the *Ndp* knockout mouse (in which *Faim* is downregulated (Xu et al., 2004)), *Edn2* and *Ednrb* expression were greatly increased. Nevertheless, to ascertain the causality between *Edn2* expression as a response to photoreceptor injury and reactive gliosis, further studies are required.

In addition to *Edn2* and *Fgf2*, we observed the upregulation of *Xiap*, which has also been linked to early neuroprotection in the retina. Its interaction with *Faim* has largely been characterized, but several studies propose that it also exerts important functions in the retina. In fact, *Xiap* mediates neuroprotection in various retinal pathologies and injuries such as retinal ischemia (Renwick et al., 2006), and its rapid delivery after retinal detachment limits the acute damage that photoreceptors undergo in rats (Zadro-Lamoureux et al., 2009) and a feline model (Wassmer et al., 2017).

## 5 | CONCLUSIONS

In summary, here we report that *Faim*<sup>-/-</sup> mice present photoreceptor neurodegeneration that is preceded by the aggregation of ubiquitinated proteins, GFAP upregulation, and Müller cell activation, similar to the aforementioned rds mouse models (Ekström et al., 1988). Overcompensatory expression of acute phase proteins originally produced to support neuron survival, like EDN2, may give rise to chronic gliosis through the long-term activation of Müller cells. This activation, in turn, accounts for the absence of retinal homeostasis and leakage of the BRB, which contribute to this positive feedback loop. These pathogenic events converge into the perfect storm, culminating in photoreceptor death in *Faim*<sup>-/-</sup> retinas.

Since retinal alterations precede numerous pathological mechanisms in brain disorders (London et al., 2013), finding biomarkers in the retina may facilitate the early diagnosis of neurodegenerative pathologies. Collectively, our results suggest that *Faim* plays a key role in the maintenance of retinal homeostasis, making it a plausible early marker for late photoreceptor and neuronal degeneration.



## DECLARATION OF TRANSPARENCY

The authors, reviewers and editors affirm that in accordance to the policies set by the *Journal of Neuroscience Research*, this manuscript presents an accurate and transparent account of the study being reported and that all critical details describing the methods and results are present.

## ACKNOWLEDGMENTS

The authors thank Dr. Isabel Calleja-Yagüe for her relentless and generous work in the establishment and maintenance of the *Faim*<sup>-/-</sup> mouse colony. They are grateful to Raquel Badillos for her invaluable skills with animal handling. They especially thank Marta Valeri for helping with confocal image acquisition and Sandra Mancilla for technical support. Histological processing and staining were performed by the ICTS "NANBIOSIS," specifically by Unit 20 of CIBER in Bioengineering, Biomaterials and Nanomedicine (CIBER-BBN) at the Vall d'Hebron Institute of Research (VHIR).

## CONFLICT OF INTEREST

The authors declare that they have no competing interests.

## AUTHOR CONTRIBUTIONS

*Conceptualization*, A.S., J.X.C., R.S., M.S.; *Methodology*, A.S., M.T.A., P.B., M.S., J.S., H.R., A.R., J.H., S.X., K.P.L., J.L.S.; *Validation*, A.S., M.T.A.; *Formal analysis*, A.S., M.T.A.; *Investigation*, A.S., M.T.A., P.B.; *Resources*, P.B., C.H., R.S., J.X.C.; *Writing – Original draft*, A.S.; *Writing – Review & editing*, M.S., A.S.; *Visualization*, A.S.; *Supervision*, J.X.C., M.S., P.B., M.J.P.G.; *Project administration*, J.X.C.; *Funding acquisition*, J.X.C., R.S., C.H. All authors read and approved the final manuscript.

## PEER REVIEW

The peer review history for this article is available at <https://publons.com/publon/10.1002/jnr.24978>.

## DATA AVAILABILITY STATEMENT

The data sets analyzed in this study are available in the GeneFriends, Human Proteome Map, and Protein Atlas repositories: <https://genefriends.org/>, <https://www.proteinatlas.org/ENSG00000158234-FAIM/celltype>, <http://www.humanproteomemap.org/query.php>. The rest of the data that support the findings of this study are available from the corresponding author upon reasonable request.

## ORCID

Anna Sirés  <https://orcid.org/0000-0002-0588-0153>

Agustín Ruíz Lasa  <https://orcid.org/0000-0003-2633-2495>

Montse Solé  <https://orcid.org/0000-0003-4240-6562>

Joan X. Comella  <https://orcid.org/0000-0002-6218-0786>

## REFERENCES

- Anderson, P. J., Watts, H., Hille, C., Philpott, K., Clark, P., Gentleman, M. C. S., & Jen, L. S. (2008). Glial and endothelial blood-retinal barrier responses to amyloid-beta in the neural retina of the rat. *Clinical Ophthalmology*, 2, 801–816. <https://doi.org/10.2147/oph.s3967>.

- Binz, N., Rakoczy, E. P., Ali Rahman, I. S., Vagaja, N. N., & Lai, C.-M. (2016). Biomarkers for diabetic retinopathy—Could endothelin 2 be part of the answer? *PLoS ONE*, 1, e0160442. <https://doi.org/10.1371/journal.pone.0160442>
- Bramall, A. N., Szego, M. J., Pacione, L. R., Chang, I., Diez, E., D'Orleans-Juste, P., Stewart, D. J., Hauswirth, W. W., Yanagisawa, M., & McInnes, R. R. (2013). Endothelin-2-mediated protection of mutant photoreceptors in inherited photoreceptor degeneration. *PLoS ONE*, 8. <https://doi.org/10.1371/journal.pone.0058023>
- Braunger, B. M., Ohlmann, A., Koch, M., Tanimoto, N., Volz, C., Yang, Y., Bösl, M. R., Cvekl, A., Jägle, H., Seeliger, M. W., & Tamm, E. R. (2013). Constitutive overexpression of *Norrin* activates *Wnt/β-catenin* and endothelin-2 signaling to protect photoreceptors from light damage. *Neurobiology of Diseases*, 50, 1–12. <https://doi.org/10.1016/j.nbd.2012.09.008>
- Bravo-Nuevo, A., Walsh, N., & Stone, J. (2004). Photoreceptor degeneration and loss of retinal function in the C57BL/6-C2J mouse. *Investigative Ophthalmology & Visual Science*, 45, 2005–2012. <https://doi.org/10.1167/iov.03-0842>
- Bringmann, A., Landiev, I., Pannicke, T., Wurm, A., Hollborn, M., Wiedemann, P., Osborne, N. N., & Reichenbach, A. (2009). Cellular signaling and factors involved in Müller cell gliosis: Neuroprotective and detrimental effects. *Progress in Retinal and Eye Research*, 28, 423–451. <https://doi.org/10.1016/j.preteyeres.2009.07.001>
- Bringmann, A., Reichenbach, A., & Wiedemann, P. (2004). Pathomechanisms of cystoid macular edema. *Ophthalmic Research*, 36, 241–249. <https://doi.org/10.1159/000081203>
- Brion, J. P., Couck, A. M., Passareiro, E., & Flament-Durand, J. (1985). Neurofibrillary tangles of Alzheimer's disease: An immunohistochemical study. *Journal of Submicroscopic Cytology*, 17, 89–96.
- Brion, J. P., Flament-Durand, J., & Dustin, P. (1986). Alzheimer's disease and tau proteins. *The Lancet*, 328, 1098. [https://doi.org/10.1016/s0140-6736\(86\)90495-2](https://doi.org/10.1016/s0140-6736(86)90495-2)
- Campbell, J. P., Zhang, M., Hwang, T. S., Bailey, S. T., Wilson, D. J., Jia, Y., & Huang, D. (2017). Detailed vascular anatomy of the human retina by projection-resolved optical coherence tomography angiography. *Scientific Reports*, 7, 42201. <https://doi.org/10.1038/srep42201>
- Carriba, P., Jimenez, S., Navarro, V., & Moubarak, R. S. (2015). Amyloid-β reduces the expression of neuronal FAIM-L, thereby shifting the inflammatory response mediated by TNF α from neuronal protection to death. *Cell Death & Disease*, 6, e1639-13. <https://doi.org/10.1038/cddis.2015.6>
- Coccia, E., Masanas, M., López-Soriano, J., Segura, M. F., Comella, J. X., & Pérez-García, M. J. (2020). FAIM Is Regulated by MiR-206, MiR-1-3p and MiR-133b. *Frontiers in Cell and Developmental Biology*, 8, 1–3. <https://doi.org/10.3389/fcell.2020.584606>
- Coccia, E., Planells-Ferrer, L., Badillos-Rodríguez, R., Pascual, M., Segura, M. F., Fernández-Hernández, R., López-Soriano, J., Garí, E., Soriano, E., Barneda-Zahonero, B., Moubarak, R. S., Pérez-García, M. J., & Comella, J. X. (2020). SIVA-1 regulates apoptosis and synaptic function by modulating XIAP interaction with the death receptor antagonist FAIM-L. *Cell Death & Disease*, 11, 584606. <https://doi.org/10.1038/s41419-020-2282-x>
- Coorey, N. J., Shen, W., Chung, S. H., Zhu, L., & Gillies, M. C. (2012). The role of glia in retinal vascular disease. *Clinical and Experimental Optometry*, 95, 266–281. <https://doi.org/10.1111/j.1444-0938.2012.00741.x>
- Coughlin, B. A., Feenstra, D. J., & Mohr, S. (2017). Müller cells and diabetic retinopathy. *Vision Research*, 139, 93–100. <https://doi.org/10.1016/j.visres.2017.03.013>
- Cunha-Vaz, J. (2017). The blood-retinal barrier in the management of retinal disease: EURETINA award lecture. *Ophthalmologica*, 237, 1–10. <https://doi.org/10.1159/000455809>

- Devanna, P., van de Vorst, M., Pfundt, R., Gilissen, C., & Vernes, S. C. (2018). Genome-wide investigation of an ID cohort reveals de novo 3'UTR variants affecting gene expression. *Human Genetics*, *137*, 717–721. <https://doi.org/10.1007/s00439-018-1925-9>
- Ekström, P., Sanyal, S., Narfström, K., Chader, G. J., & van Veen, T. (1988). Accumulation of glial fibrillary acidic protein in Müller radial glia during retinal degeneration. *Investigative Ophthalmology & Visual Science*, *29*, 1363–1371.
- Fimbel, S. M., Montgomery, J. E., Burket, C. T., & Hyde, D. R. (2007). Regeneration of inner retinal neurons after intravitreal injection of Ouabain in zebrafish. *Journal of Neuroscience*, *27*, 1712–1724. <https://doi.org/10.1523/JNEUROSCI.5317-06.2007>
- Gao, H., & Hollyfield, J. G. (1996). Basic fibroblast growth factor: Increased gene expression in inherited and light-induced photoreceptor degeneration. *Experimental Eye Research*, *62*, 181–189. <https://doi.org/10.1006/exer.1996.0022>
- Giebel, S. J., Menicucci, G., McGuire, P. G., & Das, A. (2005). Matrix metalloproteinases in early diabetic retinopathy and their role in alteration of the blood-retinal barrier. *Laboratory Investigation*, *85*, 597–607. <https://doi.org/10.1038/labinvest.3700251>
- Goh, E. T., Way, M. J., Atkinson, S. R., McQuillin, A., & Morgan, M. Y. (2016). Variations in the promoter region of the glutaminase gene and the development of hepatic encephalopathy in patients with cirrhosis. *Journal of Hepatology*, *64*(2), S257. <https://doi.org/10.7326/0003-4819-153-5-201009070-00002>
- González, H., Elgueta, D., Montoya, A., & Pacheco, R. (2014). Neuroimmune regulation of microglial activity involved in neuroinflammation and neurodegenerative diseases. *Journal of Neuroimmunology*, *274*, 1–13. <https://doi.org/10.1016/j.jneuroim.2014.07.012>
- Hara, T., Nakamura, K., Matsui, M., Yamamoto, A., Nakahara, Y., Suzuki-Migishima, R., Yokoyama, M., Mishima, K., Saito, I., Okano, H., & Mizushima, N. (2006). Suppression of basal autophagy in neural cells causes neurodegenerative disease in mice. *Nature*, *441*, 885–889. <https://doi.org/10.1038/nature04724>
- Harris, L. D., Jasem, S., & Licchesi, J. D. F. (2020). The ubiquitin system in Alzheimer's disease. *Advances in Experimental Medicine and Biology*, *1233*, 195–221. [https://doi.org/10.1007/978-3-030-38266-7\\_8](https://doi.org/10.1007/978-3-030-38266-7_8)
- Hsiau, T.-H.-C., Diaconu, C., Myers, C. A., Lee, J., Cepko, C. L., & Corbo, J. C. (2007). The Cis-regulatory logic of the mammalian photoreceptor transcriptional network. *PLoS One*, *2*, e643. <https://doi.org/10.1371/journal.pone.0000643>
- Hughes, A. E. O., Enright, J. M., Myers, C. A., Shen, S. Q., & Corbo, J. C. (2017). Cell type-specific epigenomic analysis reveals a uniquely closed chromatin architecture in mouse rod photoreceptors. *Scientific Reports*, *7*, 1–16. <https://doi.org/10.1038/srep43184>
- Huo, J., Ma, Y., Liu, J.-J., Ho, Y. S., Liu, S., Soh, L. Y., Chen, S., Xu, S., Han, W., Hong, A., Lim, S. C., & Lam, K.-P. (2016). Loss of Fas apoptosis inhibitory molecule leads to spontaneous obesity and hepatosteatosis. *Cell Death & Disease*, *7*, e2091. <https://doi.org/10.1038/cddis.2016.12>
- Huo, J., Xu, S., & Lam, K.-P. (2019). FAIM: An antagonist of Fas-killing and beyond. *Cells*, *8*(6), 541. <http://doi.org/10.3390/cells8060541>
- Illing, M. E., Rajan, R. S., Bence, N. F., & Kopito, R. R. (2002). A rhodopsin mutant linked to autosomal dominant retinitis pigmentosa is prone to aggregate and interacts with the ubiquitin proteasome system. *Journal of Biological Chemistry*, *277*, 34150–34160. <https://doi.org/10.1074/jbc.M204955200>
- Jeon, C.-J., Strettoi, E., & Masland, R. (1998). The major cell populations of the mouse retina. *Journal of Neuroscience*, *18*, 8936–8946. <https://doi.org/10.1523/JNEUROSCI.18-21-08936.1998>
- Joly, S., Lange, C., Thiersch, M., Samardzija, M., & Grimm, C. (2008). Leukemia inhibitory factor extends the lifespan of injured photoreceptors in vivo. *Journal of Neuroscience*, *28*, 13765–13774. <https://doi.org/10.1523/JNEUROSCI.5114-08.2008>
- Joly, S., Pernet, V., Chemtob, S., Di Polo, A., & Lachapelle, P. (2007). Neuroprotection in the juvenile rat model of light-induced retinopathy: Evidence suggesting a role for FGF-2 and CNTF. *Investigative Ophthalmology & Visual Science*, *48*, 2311–2320.
- Kaku, H., & Rothstein, T. L. (2020). FAIM is a non-redundant defender of cellular viability in the face of heat and oxidative stress and interferes with accumulation of stress-induced protein aggregates. *Frontiers in Molecular Biosciences*, *7*, 1–10. <https://doi.org/10.3389/fmolb.2020.00032>
- Kany, S., Vollrath, J., & Relja, B. (2019). Cytokines in Inflammatory Disease. *International Journal of Molecular Sciences*, *20*(23), 6008. <http://doi.org/10.3390/ijms20236008>
- Kato, S., Gondo, T., Hoshii, Y., Takahashi, M., Yamada, M., & Ishihara, T. (1998). Confocal observation of senile plaques in Alzheimer's disease: Senile plaque morphology and relationship between senile plaques and astrocytes. *Pathology International*, *48*(5), 332–340. <http://doi.org/10.1111/j.1440-1827.1998.tb03915.x>
- Kennedy, B., & Malicki, J. (2009). What drives cell morphogenesis: A look inside the vertebrate photoreceptor. *Developmental Dynamics*, *238*, 2115–2138. <https://doi.org/10.1002/dvdy.22010>
- Kim, M.-S., Pinto, S. M., Getnet, D., Nirujogi, R. S., Manda, S. S., Chaerkady, R., Madugundu, A. K., Kelkar, D. S., Isserlin, R., Jain, S., Thomas, J. K., Muthusamy, B., Leal-Rojas, P., Kumar, P., Sahasrabudhe, N. A., Balakrishnan, L., Advani, J., George, B., Renuse, S., ... Pandey, A. (2014). A draft map of the human proteome. *Nature*, *509*, 575–581. <https://doi.org/10.1038/nature13302>
- Lauterbur, P. C. (1973). Image formation by induced local interactions: Examples employing nuclear magnetic resonance. *Nature*, *242*, 119–190. <https://doi.org/10.1038/242190a0>
- Lecker, S. H., Goldberg, A. L., & Mitch, W. E. (2006). Protein degradation by the ubiquitin-proteasome pathway in normal and disease states. *Journal of the American Society of Nephrology*, *17*, 1807–1819. <https://doi.org/10.1681/ASN.2006010083>
- Leger, F., Fernagut, P.-O., Canon, M.-H., Léoni, S., Vital, C., Tison, F., Bezard, E., & Vital, A. (2011). Protein aggregation in the aging retina. *Journal of Neuropathology & Experimental Neurology*, *70*, 63–68. <https://doi.org/10.1097/NEN.0b013e31820376cc>
- Lobanova, E. S., Finkelstein, S., Skiba, N. P., & Arshavsky, V. Y. (2013). Proteasome overload is a common stress factor in multiple forms of inherited retinal degeneration. *Proceedings of the National Academy of Sciences*, *110*, 9986–9991. <https://doi.org/10.1073/pnas.1305521110>
- London, A., Benhar, I., & Schwartz, M. (2013). The retina as a window to the brain—From eye research to CNS disorders. *Nature Reviews Neurology*, *9*, 44–53. <https://doi.org/10.1038/nrnneurol.2012.227>
- Loscher, C. J., Hokamp, K., Kenna, P. F., Ivens, A. C., Humphries, P., Palfi, A., & Farrar, G. J. (2007). Altered retinal microRNA expression profile in a mouse model of retinitis pigmentosa. *Genome Biology*, *8*, R248. <https://doi.org/10.1186/gb-2007-8-11-r248>
- Luna, G., Lewis, G. P., Banna, C. D., Skalli, O., & Fisher, S. K. (2010). Expression profiles of nestin and synemin in reactive astrocytes and Müller cells following retinal injury: A comparison with glial fibrillary acidic protein and vimentin. *Molecular Vision*, *16*, 2511–2523. <https://pubmed.ncbi.nlm.nih.gov/21139996>
- Mattson, M. P., & Magnus, T. (2006). Ageing and neuronal vulnerability. *Nature Reviews Neuroscience*, *7*, 278–294. <https://doi.org/10.1038/nnr1886>
- McDowell, R. E., Barabas, P., Augustine, J., Chevallier, O., McCarron, P., Chen, M., McGeown, J. G., & Curtis, T. M. (2018). Müller glial dysfunction during diabetic retinopathy in rats is reduced by the acrolein-scavenging drug, 2-hydrazino-4,6-dimethylpyrimidin e. *Diabetologia*, *61*, 2654–2667. <https://doi.org/10.1007/s00125-018-4707-y>
- Montgomery, J. E., Parsons, M. J., & Hyde, D. R. (2010). A novel model of retinal ablation demonstrates that the extent of rod cell death

- regulates the origin of the regenerated zebrafish rod photoreceptors. *Journal of Comparative Neurology*, 518, 800–814. <https://doi.org/10.1002/cne.22243>
- Moubarak, R. S., Planells-Ferrer, L., Urresti, J., Reix, S., Segura, M. F., Carriba, P., Marques-Fernandez, F., Sole, C., Llecha-Cano, N., Lopez-Soriano, J., Sanchis, D., Yuste, V. J., & Comella, J. X. (2013). FAIM-L is an IAP-binding protein that inhibits XIAP ubiquitylation and protects from Fas-induced apoptosis. *Journal of Neuroscience*, 33, 19262–19275. <https://doi.org/10.1523/JNEUROSCI.2479-13.2013>
- Newman, E., & Reichenbach, A. (1996). The Müller cell: A functional element of the retina. *Trends in Neurosciences*, 19(8), 307–312. [http://doi.org/10.1016/0166-2236\(96\)10040-0](http://doi.org/10.1016/0166-2236(96)10040-0)
- Rattner, A., & Nathans, J. (2005). The genomic response to retinal disease and injury: Evidence for endothelin signaling from photoreceptors to glia. *Journal of Neuroscience*, 25, 4540–4549. <https://doi.org/10.1523/JNEUROSCI.0492-05.2005>
- Remé, C. E., Grimm, C., Hafezi, F., Marti, A., & Wenzel, A. (1998). Apoptotic cell death in retinal degenerations. *Progress in Retinal and Eye Research*, 17, 443–464. [https://doi.org/10.1016/s1350-9462\(98\)00009-3](https://doi.org/10.1016/s1350-9462(98)00009-3)
- Renwick, J., Narang, M. A., Coupland, S. G., Xuan, J. Y., Baker, A. N., Brousseau, J., Petrin, D., Munger, R., Leonard, B. C., Hauswirth, W. W., Korneluk, R. G., & Tsilfidis, C. (2006). XIAP-mediated neuroprotection in retinal ischemia. *Gene Therapy*, 13, 339–347. <https://doi.org/10.1038/sj.gt.3302683>
- Sansa, A., de la Fuente, S., Comella, J. X., Garcera, A., & Soler, R. M. (2021). Intracellular pathways involved in cell survival are deregulated in mouse and human spinal muscular atrophy motoneurons. *Neurobiology of Disease*, 155, 105366. <https://doi.org/10.1016/j.nbd.2021.105366>
- Sarthy, P. V., & Fu, M. (1989). Transcriptional activation of an intermediate filament protein gene in mice with retinal dystrophy. *DNA*, 8, 437–446. <https://doi.org/10.1089/dna.1.1989.8.437>
- Schindelin, J., Arganda-Carreras, I., Frise, E., Kaynig, V., Longair, M., Pietzsch, T., Preibisch, S., Rueden, C., Saalfeld, S., Schmid, B., Tinevez, J.-Y., White, D. J., Hartenstein, V., Eliceiri, K., Tomancak, P., & Cardona, A. (2012). Fiji: An open-source platform for biological-image analysis. *Nature Methods*, 9, 676–682. <https://doi.org/10.1038/nmeth.2019>
- Schneider, C. A., Rasband, W. S., & Eliceiri, K. W. (2012). NIH Image to ImageJ: 25 years of image analysis. *Nature Methods*, 9, 671–675. <https://doi.org/10.1038/nmeth.2089>
- Schneider, T. J., Fischer, G. M., Donohoe, T. J., Colarusso, T. P., & Rothstein, T. L. (1999). A novel gene coding for a Fas apoptosis inhibitory molecule (FAIM) isolated from inducibly Fas-resistant B lymphocytes. *Journal of Experimental Medicine*, 189, 949–956. <https://doi.org/10.1084/jem.189.6.949>
- Scott, F. L., Denault, J.-B., Riedl, S. J., Shin, H., Renatus, M., & Salvesen, G. S. (2005). XIAP inhibits caspase-3 and -7 using two binding sites: Evolutionarily conserved mechanism of IAPs. *The EMBO Journal*, 24(3), 645–655. <http://doi.org/10.1038/sj.emboj.7600544>
- Segura, M. F., Sole, C., Pascual, M., Moubarak, R. S., Jose Perez-Garcia, M., Gozzelino, R., Iglesias, V., Badiola, N., Bayascas, J. R., Llecha, N., Rodriguez-Alvarez, J., Soriano, E., Yuste, V. J., & Comella, J. X. (2007). The long form of Fas apoptotic inhibitory molecule is expressed specifically in neurons and protects them against death receptor-triggered apoptosis. *Journal of Neuroscience*, 27, 11228–11241. <http://www.jneurosci.org/cgi/doi/https://doi.org/10.1523/JNEUROSCI.3462-07.2007>
- Senut, M.-C. (2004). An element in the 1-Tubulin promoter is necessary for retinal expression during optic nerve regeneration but not after eye injury in the adult Zebrafish. *Journal of Neuroscience*, 24(35), 7663–7673. <http://doi.org/10.1523/jneurosci.2281-04.2004>
- Shin, E. S., Sorenson, C. M., & Sheibani, N. (2014). Diabetes and retinal vascular dysfunction. *Journal of Ophthalmic & Vision Research*, 9, 362–373. <https://pubmed.ncbi.nlm.nih.gov/25667739>
- Sisodia, S. S., Koo, E. H., Beyreuther, K., Unterbeck, A., & Price, D. L. (1990). Evidence that beta-amyloid protein in Alzheimer's disease is not derived by normal processing. *Science*, 248, 492–495. <https://doi.org/10.1126/science.1691865>
- Sole, C., Dolcet, X., Segura, M. F., Gutierrez, H., Diaz-Meco, M. T., Gozzelino, R., Sanchis, D., Bayascas, J. R., Gallego, C., Moscat, J., Davies, A. M., & Comella, J. X. (2004). The death receptor antagonist FAIM promotes neurite outgrowth by a mechanism that depends on ERK and NF- $\kappa$ B signaling. *Journal of Cell Biology*, 167, 479–492. <https://doi.org/10.1083/jcb.200403093>
- Solovei, I., Kreysing, M., Lanctôt, C., Kösem, S., Peichl, L., Cremer, T., Guck, J., & Joffe, B. (2009). Nuclear architecture of rod photoreceptor cells adapts to vision in mammalian evolution. *Cell*, 137, 356–368. <https://doi.org/10.1016/j.cell.2009.01.052>
- Spencer, B., Agarwala, S., Gentry, L., & Brandt, C. R. (2001). HSV-1 vector-delivered FGF2 to the retina is neuroprotective but does not preserve functional responses. *Molecular Therapy*, 3, 746–756. <https://doi.org/10.1006/mthe.2001.0307>
- Tout, S., Chan-Ling, T., Holländer, H., & Stone, J. (1993). The role of Müller cells in the formation of the blood-retinal barrier. *Neuroscience*, 55, 291–301. [https://doi.org/10.1016/0306-4522\(93\)90473-S](https://doi.org/10.1016/0306-4522(93)90473-S)
- Uhlen, M., Fagerberg, L., Hallstrom, B. M., Lindskog, C., Oksvold, P., Mardinoglu, A., ... Ponten, F. (2015). Tissue-based map of the human proteome. *Science*, 347(6220), 1260419–1260419. <http://doi.org/10.1126/science.1260419>
- Upadhyay, S. C., & Hegde, A. N. (2007). Role of the ubiquitin proteasome system in Alzheimer's disease. *BMC Biochemistry*, 8(Suppl 1), S12. <http://doi.org/10.1186/1471-2091-8-s1-s12>
- van Dam, S., Craig, T., & de Magalhães, J. (2015). GeneFriends: A human RNA-seq-based gene and transcript co-expression database. *Nucleic Acids Research*, 43(D1), D1124–D1132. <http://doi.org/10.1093/nar/gku1042>
- Wang, J., Duncan, D., Shi, Z., & Zhang, B. (2013). WEB-based GENE Set Analysis Toolkit (WebGestalt): update 2013. *Nucleic Acids Research*, 41, W77–W83. <https://doi.org/10.1093/nar/gkt439>
- Wassmer, S. J., Leonard, B. C., Coupland, S. G., Baker, A. N., Hamilton, J., Hauswirth, W. W., & Tsilfidis, C. (2017). Overexpression of the X-linked inhibitor of apoptosis protects against retinal degeneration in a feline model of retinal detachment. *Human Gene Therapy*, 28, 482–492. <https://doi.org/10.1089/hum.2016.161>
- Wen, R., Song, Y., Cheng, T., Matthes, M. T., Yasumura, D., LaVail, M. M., & Steinberg, R. H. (1995). Injury-induced upregulation of bFGF and CNTF mRNAs in the rat retina. *The Journal of Neuroscience*, 15(11), 7377–7385. <http://doi.org/10.1523/jneurosci.15-11-07377.1995>
- Xu, Q., Wang, Y., Dabdoub, A., Smallwood, P. M., Williams, J., Woods, C., Kelley, M. W., Jiang, L., Tasman, W., Zhang, K., & Nathans, J. (2004). Vascular development in the retina and inner ear: Control by Norrin and Frizzled-4, a high-affinity ligand-receptor pair. *Cell*, 116, 883–895. [https://doi.org/10.1016/s0092-8674\(04\)00216-8](https://doi.org/10.1016/s0092-8674(04)00216-8)
- Yamada, H., Yamada, E., Ando, A., Esumi, N., Bora, N., Saikia, J., Sung, C.-H., Zack, D. J., & Campochiaro, P. A. (2001). Fibroblast growth factor-2 decreases hyperoxia-induced photoreceptor cell death in mice. *American Journal of Pathology*, 159, 1113–1120. [https://doi.org/10.1016/S0002-9440\(10\)61787-7](https://doi.org/10.1016/S0002-9440(10)61787-7)
- Zadro-Lamoureux, L. A., Zacks, D. N., Baker, A. N., Zheng, Q. D., Hauswirth, W. W., & Tsilfidis, C. (2009). Effects on XIAP retinal detachment-induced photoreceptor apoptosis. *Investigative Ophthalmology & Visual Science*, 50, 1448–1453. <https://doi.org/10.1167/iovs.08-2855>
- Zhong, X., Schneider, T. J., Cabral, D. S., Donohoe, T. J., & Rothstein, T. L. (2001). An alternatively spliced long form of Fas apoptosis inhibitory molecule (FAIM) with tissue-specific expression in the brain. *Molecular Immunology*, 38, 65–72. [https://doi.org/10.1016/S0161-5890\(01\)00035-9](https://doi.org/10.1016/S0161-5890(01)00035-9)

**SUPPORTING INFORMATION**

Additional supporting information may be found in the online version of the article at the publisher's website.

**TABLE S1** List of antibodies used for western blot

**TABLE S2** Sequence of primers used for qRT-PCR

**TABLE S3** List of antibodies used for immunohistochemistry and immunofluorescence

**FIGURE S1** Apoptosis-related gene markers are altered in *Faim*<sup>-/-</sup> mice. mRNA levels of apoptotic-related markers of wt and *Faim*<sup>-/-</sup> retinas at (a) 2 and (b) 12 months of age, as determined by qRT-PCR. Each symbol in the plots represents one retina ( $n = 7$ –11 mice/group). Expression levels were normalized to *Actb* and data are plotted relative to wt values for each gene. Each box plot extends from the 25th to the 75th percentile and the median is plotted as a line in the box. Whiskers represent min to max values, and dot plots are overlaid. Statistical analyses was performed using an unpaired two-tailed Student's *t* test \* $p < 0.05$ , and \*\*\* $p < 0.001$

**FIGURES2** Microglial markers are upregulated in 2- and 12-month-old *Faim*<sup>-/-</sup> mice. Microglial mRNA markers of wt and *Faim*<sup>-/-</sup> retinas of mice aged (a) 2 and (b) 12 months, as determined by qRT-PCR. Each symbol in the plots represents one retina ( $n = 6$ –11 mice/group). Expression levels were normalized to *Actb* and data are plotted relative to wt values for each gene. Each box plot extends from the 25th to the 75th percentile and the median is plotted as a line in the

box. Whiskers represent min to max values, and dot plots are overlaid. Statistical analyses was performed using an unpaired two-tailed Student's *t* test \* $p < 0.05$ , and \*\* $p < 0.01$

**FIGURE S3** Gene markers related to the maintenance of blood-retinal barrier homeostasis are altered in *Faim*<sup>-/-</sup> mice. mRNA levels of different vascular genes related to the BRB function of wt and *Faim*<sup>-/-</sup> retinas of mice aged (a) 2 and (b) 12 months, as determined by qRT-PCR. Each symbol in the plots represents one retina ( $n = 4$ –11 mice/group). Expression levels were normalized to *Actb* and data are plotted relative to wt values for each gene. Each box plot extends from the 25th to the 75th percentile and the median is plotted as a line in the box. Whiskers represent min to max values, and dot plots are overlaid. Statistical analyses was performed using an unpaired two-tailed Student's *t* test \* $p < 0.05$

Transparent Peer Review Report

Transparent Science Questionnaire for Authors

**How to cite this article:** Sirés, A., Turch-Anguera, M., Bogdanov, P., Sampedro, J., Ramos, H., Ruíz Lasa, A., Huo, J., Xu, S., Lam, K.-P., López-Soriano, J., Pérez-García, M. J., Hernández, C., Simó, R., Solé, M., & Comella, J. X. (2021). *Faim* knockout leads to gliosis and late-onset neurodegeneration of photoreceptors in the mouse retina. *Journal of Neuroscience Research*, 99, 3103–3120. <https://doi.org/10.1002/jnr.24978>

# **Annex Two**

# **The absence of FAIM leads to a delay in dark adaptation and hampers Arrestin-1 translocation upon light reception in the retina**

**Anna Sirés<sup>1,2,3</sup>, Mateo Pazo<sup>4,5</sup>, Alonso Sánchez<sup>4</sup>, Joaquín López<sup>1,2,3</sup>, Enrique de la Rosa<sup>4</sup>, Catalina Hernández<sup>4</sup>, Pedro de la Villa<sup>5</sup>, Joan X. Comella<sup>1,2,3</sup>, Montse Solé<sup>1,2,3</sup>**

<sup>1</sup>Cell Signaling and Apoptosis Group, Vall d'Hebron Institute of Research (VHIR), Barcelona, Spain.

<sup>2</sup>Centro de Investigación Biomédica en Red sobre Enfermedades Neurodegenerativas (CIBERNED), ISCIII, Madrid, Spain.

<sup>3</sup>Departament de Bioquímica i Biologia Molecular, Facultat de Medicina, Universitat Autònoma de Barcelona (UAB), Bellaterra, Spain.

<sup>4</sup>Departments of Molecular Biomedicine (3D Lab) and Structural and Chemical Biology (IPSBB Unit), Centro de Investigaciones Biológicas-CSIC, C/ Ramiro de Maeztu 9, E-28040 Madrid, Spain

<sup>5</sup>Department of Systems Biology, Facultat de Medicina, Universidad de Alcalá, Alcalá de Henares, Spain.

## **1. Introduction**

The retina has now long been considered as a window to the brain. Several neurodegenerative disorders have also been reported to manifest in the retina, and remarkably, ocular manifestations often precede symptoms in the brain (London, Benhar, and Schwartz 2013). Age is a major risk factor to most of blindness and vision loss cases (Wang et al. 2013), and in view of our current demographic trends, it is not surprising that retinal pathologies and neurodegeneration are an emerging cause of visual impairment in the developing world (Bourne et al. 2021). Therefore, finding strategies to prevent or delay the onset of retinal pathology and photoreceptor degeneration is a major challenge. Although retinal degeneration has been widely studied, most mechanisms underlying such alterations are relatively unexplored. One plausible approach to strengthen our knowledge is to study pro-survival as well as anti-apoptotic modulators that are already in place and can be potentially modulated to achieve therapeutic effects.

We have previously established Fas Apoptotic Inhibitory Molecule (FAIM) as a powerful anti-apoptotic protein (Segura et al. 2007; Sole et al. 2004; Carriba et al. 2015). We have also described the potential neuroprotective role of FAIM in photoreceptors, since Faim knockout (Faim KO) mice present ubiquitin aggregates, chronic gliosis and vascular leakage in the retina. Those alterations eventually culminate with a late-onset photoreceptor cell death (Sirés et al. 2021).. Likewise, FAIM has also been reported to be recruited to ubiquitinated protein aggregates and FAIM-deficient cells accumulate ubiquitinated proteins after stress induction (Kaku and Rothstein 2020).

In view of this, it is important to highlight the role of the ubiquitin-proteasome system (UPS) as one of the primary mechanisms by which neuronal proteins are degraded to maintain cellular homeostasis (Flick and Kaiser 2012).

Although protein degradation is the most well-studied feature of UPS, ubiquitination also serves as an additional posttranslational modification to many neuronal functions. For instance, UPS is crucial for synaptic plasticity and self-renewal of neurons

(Schwartz and Ciechanover, 2009 REF). It is also involved in cell signaling regulation by controlling the endocytosis of receptors in plasma membrane, and ubiquitin modifications can result in alterations on protein-protein interactions or protein localization (Mukhopadhyay and Riezman 2007).

Protein-protein interactions in phototransduction, the process in which light is converted into electrical signals in the retina, are under a strict control for adaptational response to light and photoreceptor cell viability (Campello et al. 2013). In addition, it has been reported that ubiquitin participates in regulating the levels of mammalian phototransduction proteins in the retina (Obin et al. 1996). For instance, the beta gamma subunit complex of the G-protein Transducin- $\alpha$ , as well as the G protein-coupled receptor rhodopsin, were shown to be a substrate of ubiquitin-mediated degradation (Obin et al., 2002; Shang and Taylor, 2004). More recent studies have also shown ubiquitination as a regulator of light and dark-dependent translocation of proteins involved in phototransduction in rod photoreceptors. This process has been suggested to contribute to light and dark adaptation, given that signal amplification in the phototransduction cascade seems to be reduced after translocation (Majumder et al. 2013; Chaya et al. 2019). Nonetheless, the mechanism underlying this process has yet to be fully elucidated.



Phototransduction and light-dependent protein translocation are fine processes that need its partakers to act on time and to adjust perfectly on its role. Given that FAIM is involved in ubiquitination events and that FAIM knockout present a neurodegenerative phenotype in the retina, we assessed the potential role of FAIM in retinal function and phototransduction modulation. We also studied whether these functional alterations could be linked to the role of FAIM in ubiquitinating events.

We report that Faim KO mice present a delay in dark adaptation from early ages and retinal malfunction at the rod photoreceptor, bipolar and RGCs level

## 2. Methods

### 2.1. Animal care

All experimental procedures were conducted in compliance with European Union Council directives (2010/63/EU) and with the Spanish legislation for the use of laboratory animals (BOE 34/11370-421, 2013). Protocols were approved by the Ethics Committee for Animal Experimentation of the Vall d'Hebron Research Institute (VHIR) (CEEA 07/23 and 20/15) and Generalitat de Catalunya (DARP 11769 and 8594).

Homozygous Faim knockout (*Faim*<sup>-/-</sup> or Faim KO) mice were kindly provided by Dr. Lam (Huo et al. 2009) and crossbred with C57BL/6J OlaHsd wild-type mice (WT) (Envigo, France) (IMSR Cat# JAX:000664) for at least 10 generations before using them, and no epileptic phenotype was observed.

Heterozygous mice were used to breed Faim KO mice and WT littermates for experimental procedures. Animals were bred and maintained in the animal facility at VHIR. They were housed in groups of a maximum of five animals per Tecniplast GM-500 cage (36 x 19 x 13.5 cm) under standard laboratory conditions at 22 ± 2°C, under a 12 h light/dark cycle (8 am to 8 pm) and relative humidity of 50-60%. Animals had access to water and food *ad libitum* (Teklad Global 18% Protein Rodent diet, Envigo, France). An equal number of females and males per study group was selected, and at least four animals per genotype were used for each experiment.

Genotypes were confirmed by PCR analysis. A tail snip was used for DNA extraction. The tail sample was digested in alkaline solution with Proteinase K (0.24 Units/sample) (Qiagen, Hilden, Germany) for 120 min at 55°C. The following primers were used to perform a semiquantitative PCR: FAIM-P1-Fw 5'-GAGACTGAGACAGGAGAAGCC-3'; FAIM-P2-Fw 5'-

GCTCTTCAGCAATATC-ACGGG-3' and FAIM-P3-Rev 5'-GCTCAGGTAAAGTGAAGTGCG-3'.

## **2.2.Optical tomography coherence**

For optical tomography coherence (OCT) analyses, a Spectralis OCT machine was used (Heidelberg Engineering GmbH ©, Germany). Mice were anesthetized intraperitoneally with a mixture of ketamine (37 mg/kg) (Ketolar® 50mg/mL, Pfizer, Madrid, Spain) and xylazine (10 mg/kg), and the eye pupils were dilated with atropine 1% (Colircusí®, Novartis Farmacéutica, S.A., Madrid, Spain). After anesthesia, the analysed eye (right eye) was covered with a contact lens, while the non-used eye was humidified with saline teardrops to avoid drying. After the mice were immobilized, the eye bottom was focused (0.5–1.5 optic dioptres) and images were captured with a high-resolution mode in two scanning modalities: radial (six radius per image) and longitudinal. For total retina, INL and ONL thickness, nine longitudinal sections separated by 50 µm were averaged per each mouse.

## **2.3.Electroretinography**

Retinal function was assessed by electroretinography (ERG), which measures the electrical activity of the retina in response to a light stimulus. Protocols used were previously described elsewhere (Sánchez-Cruz et al. 2021; Fernández-Sánchez et al. 2012).

Briefly, mice were dark-adapted overnight in their own cages in a separate dark room only illuminated with red light and covered with reflective black covers. Just before ERG analyses, mice were anesthetized intraperitoneally with a mixture of ketamine (70 mg/kg) and xylazine (10 mg/kg). Mice were placed on a heating pad maintained at 37°C. Corneal surface was protected with a drop

of non-irritating ionic conductive solution (contact lens solutions containing sodium chloride and 0.5% methylcellulose). Then, a golden loop electrode was placed over the cornea of the right eye. A needle reference and ground electrodes were inserted into the cheek and subcutaneously on the side of the mouse, respectively. Electrical activity of the retinal cells was measured as amplitude ( $\mu\text{V}$ ) in response to a light stimulus in a scotopic or photopic manner (see below for protocol specification) (**Figure 1**).

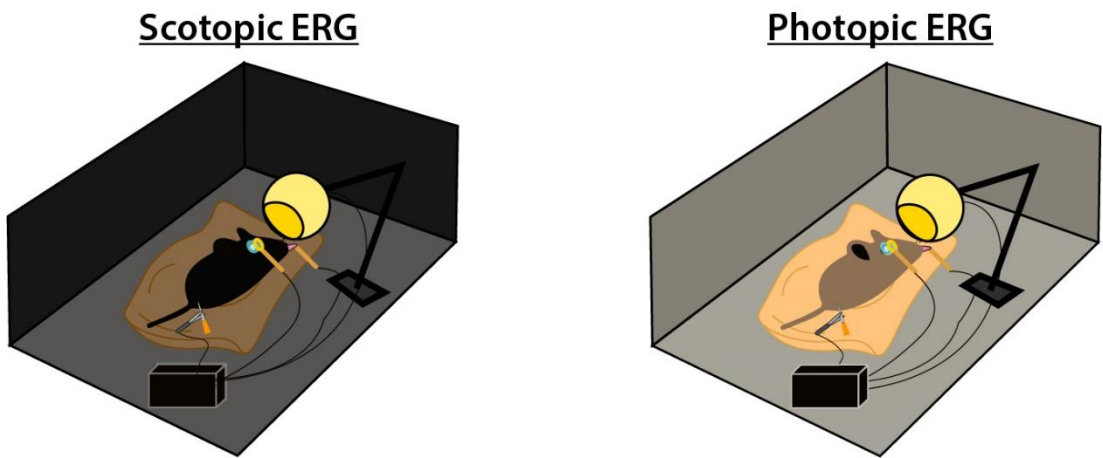


**Figure 1.** Representation of a mouse in its cage and lighting depending on ERG conditions. Left, scotopic conditions in dark-adapted mice. Right, photopic conditions in light-adapted mice.

### ➤ **Scotopic and photopic ERG**

After dark-adaptation overnight, mice were stimulated by flashing lights of different intensities, ranging from  $-5.0$  to  $2$  log scotopic candlepower ( $\text{cd}\cdot\text{s}/\text{m}^2$ ) in a Ganzfeld dome (Sánchez-Cruz et al. 2021). There was a pause of 15 to 120 seconds between flashes depending on light intensity to allow photoresponse recovery. For each intensity, electrical responses after 4-60 consecutive light flashes were averaged.

Each range of light intensities allows recording currents arising from specific cell types (**Figure 26**). In dark-adapted (scotopic) ERG recordings, RGC activity is detected from  $-5$  to  $-4$   $\text{cd}\cdot\text{s}/\text{m}^2$ ; rod-mediated responses from  $-4$  to  $-1.52$   $\text{cd}\cdot\text{s}/\text{m}^2$ ; mixed rod and cone responses from  $-1.42$  to  $0.48$   $\text{cd}\cdot\text{s}/\text{m}^2$ ; and oscillatory potentials are detected at  $0.48$   $\text{cd}\cdot\text{s}/\text{m}^2$  and at recording frequency range of  $100$ - $1000$  Hz.

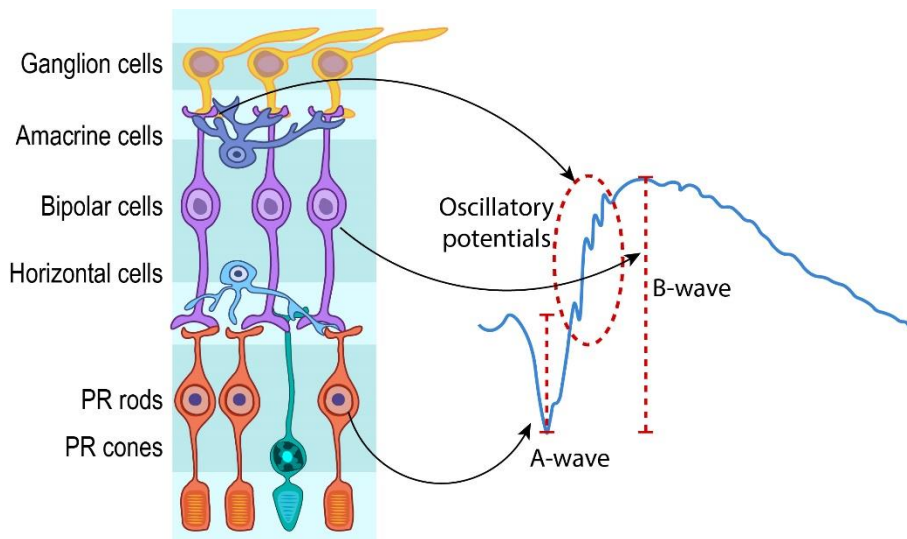


**Figure 2** Diagram representing retinal cell-specific responses on scotopic ERG.

For light-adapted (photopic) ERG recordings, a background of  $30$   $\text{cd}\cdot\text{s}/\text{m}^2$  was applied for five minutes to suppress rod stimulation, and from  $-0.52$  to  $1.48$   $\log$   $\text{cd}\cdot\text{s}/\text{m}^2$  cone-mediated electrical responses were recorded. Also, at  $1.48$   $\text{cd}\cdot\text{s}/\text{m}^2$  flicker responses were recorded ( $20$  Hz) (**Figure 27**).



**Figure 3.** Representation of light flashes (yellow stars) in Flicker ERG.

### ➤ **Double-flash ERG for dark adaptation assessment**

For the assessment of dark adaptation, a double-flash protocol was performed (Samaranayake et al. 2020; Lyubarsky, Nikonov, and Pugh 1996). Mice were dark-adapted overnight, handled, and anesthetized as stated before ERG analyses. A first (test) flash was delivered to suppress rod circulating current. Then, a second (probe) flash was delivered to monitor the recovery of rod current. The time interval between the two flashes increased with each set, ranging from 1 to 150 seconds. The intensity of the flashes was  $2 \text{ cd}\cdot\text{s}/\text{m}^2$ , and there was a delay with each subsequent set of double-flash ranging from two to five minutes. The amplitude of response recorded in the second flash is plotted as a function of time interval between flashes (**Figure 28**).

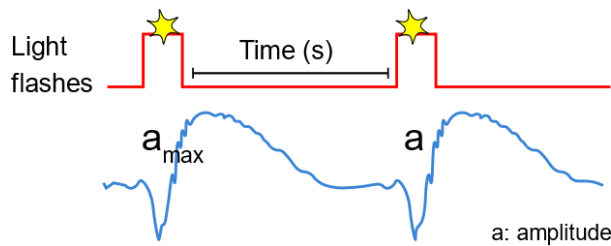


**Figure 4** Representation of double-flash protocol. Light flashes are represented by yellow stars. The first flash elicits the maximum electrical response: “ $a_{\text{max}}$ ”, while the second flash elicits “ $a$ ”.

### **2.4. Light exposure protocol**

Two-month-old Faim KO and WT mice were dark-adapted overnight and exposed to bright light in a cage with LED panels (2,500 lux) for different time periods (30 seconds, 5 minutes, and 15 minutes) after their pupils were dilated with a topical drop of 1% tropicamide, a mydriatic drug. For the dark-adapted condition, mice were euthanized after overnight dark adaptation. Eyes were collected in the dark, under a dim infrared light for immunofluorescence analysis.

## 2.5. Light damage protocol

For light-induced retinal damage (LIRD), two-month-old Faim KO and WT mice were dark-adapted overnight and then exposed to LED light at 10,000 lux in non-reflective cages for 8 or 24h (**Figure 29**) after pupils were dilated with drops of 0.5% tropicamide and 2.5% phenylephrine hydrochloride. During light-stress, mice were allowed free access to food and water.

For ERG measurements and consequent sample collection for biochemical or immunohistological analyses, mice were kept in their cages after 8h LIRD for two weeks and dark-adapted overnight before the ERG procedure.

For RNAseq analyses, mice were immediately euthanized after 24h LIRD. Left-eye retinas were rapidly collected and submerged in 1ml of RNAlater (ThermoFisher) and maintained at 4°C overnight before freezing at -20° for a maximum of 5 days. Right-eye retinas were snap-frozen in liquid nitrogen and stored at -80°C until further use.

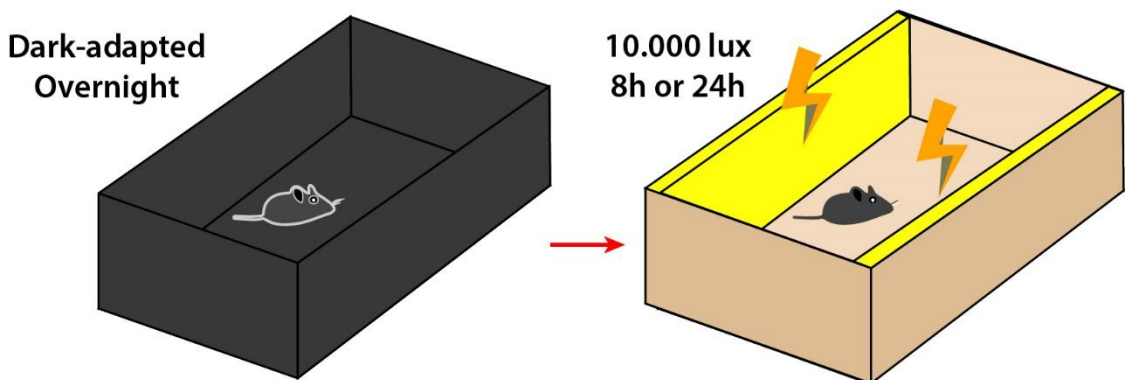


**Figure 5.** Representation of the protocol of light damage Animals are dark-adapted overnight (left), and exposed to 10,000 luxes for 8 or 24h depending on the protocol (right). After two weeks, animals were euthanized.

## 2.6. Tissue collection and processing

Mice were euthanized by cervical dislocation and eyes were enucleated. The retina was extracted from the left eye and snap-frozen in liquid nitrogen for protein or mRNA extraction, unless stated otherwise. The right eye was fixed in 4% paraformaldehyde for 5 h, washed five times for 10 minutes in PBS and embedded in paraffin blocks. Next, 4- $\mu$ m-thick sections were cut on a microtome (Microm HM 355 S, ThermoFisher Scientific, Waltham, USA), and three or four sections were placed on one slide. Slides were stored at room temperature until analysis. Experiments were performed using samples from 2-, 12- or 18-month-old mice, and at least four animals per group were used in each experiment.

## 2.7. Histology and retinal morphometry analysis

Slides were heated at 60°C for 1 h, deparaffinized in xylene, rehydrated in a graded ethanol (EtOH) series as described in **Table 1**.

**Table 1** Series of graded rehydration.

<i>Product</i>	<i>Time</i>
<i>Xylene,</i>	6 minutes
<i>Xylene/EtOH 1:1,</i>	6 minutes
<i>100% EtOH,</i>	6 minutes
<i>95% EtOH,</i>	6 minutes
<i>70% EtOH,</i>	3 min
<i>50% EtOH,</i>	3 min
<i>ddH<sub>2</sub>O</i>	3 min



Then, slides were stained with Harris hematoxylin for 8 minutes (VWR chemicals, Cat# 351945s) and rinsed with water to remove excess. They were submerged in eosin (Alfa Aesar, Karlsruhe, Alemania, Cat# B24535) immediately afterwards for one minute. Finally, slides were rehydrated oppositely as stated above (50%, 70%, 95%, 100% EtOH) for one minute each condition. After, slides were submerged in xylene for 6 minutes. Slides were fixed with DPX mounting media (VWR Chemicals, Cat# 1.005.790.500) and a coverslip was attached. Whole digital scans were taken using a NanoZoomer 2.0HT high-resolution whole-slide scanner (Hamamatsu).

The thickness of the whole retina was measured manually using the ruler tool of NanoZoomer software at 0.6 mm from both sides of the optic nerve and then averaged, as based on (Berger et al. 2014; Fu et al. 2015).

To manually measure the number of rows of photoreceptor nuclei in the outer nuclear layer (ONL), we also took two segments of the retina at 0.6 mm from the optic nerve. At least 11 columns per segment were manually counted using ImageJ software and then averaged, as based on (Gosbell et al. 2006; Trachsel-Moncho et al. 2018).

The number of nuclei in the ganglion cell layer (GCL) and the inner nuclear layer (INL) was manually counted in ImageJ using 0.5 mm-wide segments (at 0.6 mm from both sides of the optic nerve).

At least four mice per group were measured for each morphometric analyses, at least three sections per animal were used, and at least four comparable segments per section were averaged. All measurements were taken in a double-blinded manner.

## 2.8. Immunohistochemistry and quantification

Slides were deparaffinized and rehydrated as stated above. Antigen retrieval was achieved by immersing the slides in antigen retrieval solution (0.1M citrate buffer pH 6.0) and placing them in a pressure cooker at 150°C for 4 min. Slides were washed in PBS for 10 minutes each wash without agitation until room temperature was achieved.

Slides were individually shaken, and the surroundings of the tissue were dried with a paper towel to remove PBS excess and placed in a humidity chamber. Then, non-specific binding sites were blocked for 1 h at room temperature with PBS containing 10% NGS. After blocking, sections were delimited with a hydrophobic pen (Dako Pen, Agilent, Cat# S2002) and incubated with 20 µl of multiubiquitin primary antibody in blocking solution (Santa Cruz Biotechnology, Cat# sc-8017, 1:2,000) overnight at 4°C (for details of antibody, see **Table 2**) in a humidity chamber.

**Table 2.** List of primary antibodies for immunohistochemistry and immunofluorescence

<i>Antibody</i>	<i>Supplier information</i>	<i>Immunogen</i>	<i>Dilution</i>
<i>Multi-ubiquitin</i>	Santa Cruz Biotechnology mouse monoclonal antibody Cat# sc-8017	UBB human, mouse, rat	1:2,000
<i>GFAP</i>	Abcam rabbit polyclonal Cat# ab7260	Full-length human recombinant GFAP expressed in bacteria and highly purified	1:2,000
<i>IL-1β</i>	Abcam rabbit polyclonal Cat# ab9722	IL1 beta mouse	1:100
<i>EDN2</i>	Biorbyt rabbit polyclonal Cat# orb445105	KLH conjugated synthetic peptide derived from human Endothelin 2	1:500
<i>Arrestin-1</i>	Rabbit polyclonal antibody provided by Dr. Ana Méndez	C10C10 epitope (residues 290-297 of bovine arrestin)	1:1,000

<i>Transducin-α</i>	Rabbit polyclonal antibody, Residues 85–103 provided by Dr. Ana Méndez	1:2,000
---------------------	--	---------

The following day, slides were washed three times with PBS for 10 minutes each wash, and they were incubated for 1 h at room temperature with 40 µl of HRP-conjugated antibody (listed in **Table 3**) in blocking buffer. Slides were washed three times with PBS for 10 minutes. Antibody labeling was visualized with EnVision Detection System (Dako, Agilent mouse Cat# K5007, 1:2,000) and slides were counterstained with Harris hematoxylin as stated above and mounted in DPX (255254, PanReac AppliChem, Chicago, USA). Samples without primary antibodies were used as negative controls. Images were taken under a Nikon ECLIPSE 80i microscope at 20x and 40x in the Histology Service Unit at the Neurosciences Institute, UAB. Pictures were taken and analyzed in a double-blinded manner by two researchers.

**Table 3.** List of secondary antibodies for immunohistochemistry and immunofluorescence

<i>Antibody</i>	<i>Supplier information</i>	<i>Immunogen</i>	<i>Dilution</i>
<i>Dako REAL EnVision Detection System, Peroxidase/DAB, Rabbit/Mouse, HRP Kit</i>	Agilent mouse Cat# K5007	IgG rabbit, mouse	1:2,000
<i>Goat Anti-Rabbit IgG (H+L) Antibody, Alexa Fluor 488 Conjugated</i>	Molecular Probes polyclonal Cat# A-11008	rabbit Rabbit (H+L)	IgG 1:600
<i>Goat Anti-Rabbit IgG (H+L) Antibody, Alexa Fluor 594 Conjugated</i>	Molecular Probes Cat# A-11012	rabbit Rabbit (H+L)	IgG 1:600

To quantify ubiquitin immunostaining, ubiquitin-positive cells in the GCL and INL were manually counted. Measurements of ubiquitin-positive cells were averaged for the INL and GCL to obtain the number of ubiquitin-positive GCL

cells in 0.6 mm segments, and the number of ubiquitin-positive INL cells in 0.4 mm segments. Four equally sized random segments across the retinal section were selected, and three retinal sections per mouse were used. All measurements were taken in a double-blinded manner.

## **2.9. Immunofluorescence and quantification**

Slides were deparaffinized and rehydrated as stated above. They were then post-fixed in ice-cold methanol-acetic acid solution (95% methanol, 5% glacial acetic acid) for 1 min and washed three times with PBS for 10 minutes. Antigen retrieval was achieved by immersing the slides in antigen retrieval solution (0.1M citrate buffer pH 6.0) and placing them in a pressure cooker at 150°C for 4 min.

After washing with PBS three times for 10 minutes, PBS excess was removed shaking slides and drying the surroundings of the tissue with a paper towel. Slides were placed in a humidity chamber and non-specific binding sites were blocked for 1 h at room temperature with PBS containing 0.2% Triton X-100 and 1% BSA. After blocking, sections were washed three times for 10 minutes in PBS and incubated with the corresponding primary antibody overnight at 4°C (see **Table 2**).

The following day, sections were washed three times for 10 minutes 3x10 in PBS and incubated for 1 h at room temperature in the dark with the fluorescent secondary antibodies (see **Table 3**).

Nuclei were stained with Hoechst 33342 at 1:10.000 in PBS for 10 minutes and washed three times for 10 minutes in PBS afterwards. Sections were mounted with Prolong™ Gold Antifade Mountant. Samples without primary antibodies were used as negative controls. Images were taken at 20x, 40x and

60x in an Olympus FV1000 spectral confocal microscope in the UAT at VHIR. Pictures were analyzed in a double-blinded manner by two researchers.

For Edn2 fluorescence intensity, regions of interest (ROI) corresponding to the inner plexiform layer (IPL) and outer plexiform layer (OPL) were manually drawn, and average intensity was measured for each ROI in ImageJ. Four photomicrographs of the retina, each separated by at least 0.6 mm, were used for each retinal section, and three retinal sections were used per mouse.

The degree of GFAP and IL-1 $\beta$  expression and immunolocalization in Results – Chapter 1, was estimated using a previously established 5-point scoring system (Anderson et al. 2008), as follows: staining only in Müller cell endfeet region or GCL (score 1); GCL plus a few proximal processes (score 2); GCL plus many processes, but not extending to ONL (score 3); GCL plus processes throughout, with some in the ONL (score 4); and GCL plus many processes to the outer margin of the ONL (score 5) (**Error! No s'ha trobat l'origen de la referència.**).

### **2.9.1. Arrestin-1 and Transducin- $\alpha$ immunofluorescence**

Slides were heated at 60°C for 1 h, deparaffinized in xylene and rehydrated in a graded ethanol series as stated before. Tissue sections were subjected to antigen retrieval by placing slides in a glass-staining container with antigen retrieval solution (PBS with 0.1 mg/ml proteinase K (Roche)) at room temperature for two minutes and heating slides at 70°C for 6-8 seconds individually.

Non-specific binding sites were blocked and permeabilized for 1 h at room temperature with and PBS 0.2% Triton X-100 and 5% BSA in a humidity chamber. Afterwards, blocking solution was removed by shaking the slides and

the surroundings of the tissue were dried with a paper towel. Sections were individually isolated with Dako pen and incubated with the corresponding primary antibody overnight at 4°C (see **Table 2**) in a humidity chamber. The following day, slides were washed three times for 10 minutes in PBS and Dako pen was reapplied. Slides were incubated in the dark in a humidity box for 1 h at room temperature with 20 µl of the corresponding fluorescent secondary antibodies (see **Table 3**). Hoechst 33342 was used to stain the nuclei and sections were mounted with Prolong™ Gold Antifade Mountant, and slides were washed five times for 10 minutes with PBS.

Immunofluorescence signal intensities were measured and quantified using ImageJ software (National Institutes of Health NIH). Signal was quantified using Region of Interest (ROI) tool of ImageJ, which was used to outline the whole photoreceptor inner (IS) and outer segments (OS) of the retinal image in order to calculate the percentage of Arrestin-1 and Transducin- $\alpha$  signal that was located in the OS.

### **2.10. TUNEL assay**

Slides were deparaffinized and rehydrated as above. They were then permeabilized for 8 min in 0.1% sodium citrate containing 0.1% Triton X-100 and rinsed twice with PBS for 10 minutes. Slides were afterwards placed in a plastic jar containing 200 ml of 0.1M citrate buffer pH 6.0 and irradiated at 750W in a microwave for 1 min for antigen retrieval. Next, they were immediately cooled by adding room temperature ddH<sub>2</sub>O, and washed three times with PBS for five minutes before blocking.

Slides were immersed in Tris-HCl 0.1M pH 7.5 containing 3% BSA and 20% fetal bovine serum for 30 min at room temperature for blocking and then washed with PBS three times for 10 minutes. Excess of PBS was removed by

shaking and drying with a paper towel and sections were transferred to a humidity chamber. The slides were incubated for 1 h at 37°C with 20 µl TUNEL (Terminal deoxynucleotidyl transferase dUTP Nick End Labeling) reaction mixture (11767291910 and 11767305001, TUNEL Label Mix and TUNEL Enzyme, Roche), following the manufacturer's instructions. The mixture was added individually to each retinal section. Negative controls were incubated with TUNEL reaction mixture without TUNEL enzyme. Slides were rinsed three times for five minutes with PBS and counterstained with Hoechst 33342 (0.05 µg/ml, ab228551, Abcam) for 10 min and rinsed again with PBS three times for five minutes. Finally, slides were mounted in Prolong™ Gold Antifade Mountant (P36930, Thermofisher) and 40x images were taken with Olympus FV1000 spectral confocal microscope in the High Technology Unit (UAT) at VHIR. TUNEL-positive cells in retinal sections were manually counted in a blind manner using ImageJ software. Three distinct whole retinal sections per mouse were analyzed and averaged, and at least four animals per group were used.

## **2.11. Western blotting**

Retinal proteins were homogenized mechanically by pipetting the tissue up and down with different-sized pipette tips and insulin syringes with RIPA lysis buffer (150 mM NaCl, 1% IGEPAL® CA-630, 0.5% sodium deoxycholate, 0.1% SDS, and 50 mM Tris pH 8.0) containing 1x cOmplete™ EDTA-free protease inhibitor cocktail (11873580001, Roche, Darmstadt, Germany). Extracts were kept ice-cold and supernatants from the homogenates were collected after centrifugation at 9300 x g for 15 min at 4°C. Protein concentration was quantified using the Modified Lowry kit (DC protein assay; Bio-Rad, Hercules, CA, USA).

Next, 20 to 40 µg of total protein was resolved by SDS-PAGE and transferred onto PVDF Immobilon-P transfer membranes (Millipore Iberica, Madrid, Spain). Membranes were blocked with Tris-buffered saline with 0.1% TWEEN®-20 and 10% non-fat dry milk for 1 h at room temperature and then probed overnight with the appropriate primary antibody (**Table 4**).

**Table 4** List of primary antibodies used for western

<i>Antibody</i>	<i>Supplier information</i>	<i>Immunogen</i>	<i>MW (kDa)</i>	<i>Dilution</i>
<i>Anti-FAIM</i>	In-house rabbit polyclonal antibody [5]	Recombinant protein corresponding to full-length rat FAIM	21, 23	1:2,000
<i>Anti-GFAP</i>	DAKO rabbit polyclonal Cat# Z0334	GFAP isolated from cow spinal cord	48, 50	1:4,000
<i>Arrestin-1</i>	Rabbit polyclonal antibody provided by Dr. Ana Méndez	C10C10 epitope (residues 290-297 of bovine arrestin)	48	1:10,000
<i>Transducin-α</i>	Rabbit polyclonal antibody, provided by Dr. Ana Méndez	Residues 85–103 of transducin-α	40	1:5,000
<i>Multiubiquitin</i>	Santa Cruz Biotechnology mouse monoclonal antibody Cat# sc 8017	UBB human, mouse, rat		1:6,000
<i>Anti-α-tubulin</i>	Rabbit monoclonal antibody Cat# T5168	by the fusion of mouse myeloma cells and splenocytes from an immunized mouse		1:60,000
<i>Anti-cyclophilin A</i>	Enzo Life Sciences Cat# BML-SA296	Recombinant human cyclophilin A conjugated to KLH	17	1:10,000
<i>Anti-GAPDH</i>	Enzo Life Sciences, Cat# ADI-CSA-335	Pig GAPDH, clone ID4	36	1:8,000

Blots were then incubated with the corresponding peroxidase-conjugated secondary antibodies (listed in **Table 5**) for 1 h at room temperature, developed using the EZ-ECL Enhanced Chemiluminescence Detection Kit for HRP (Biological Industries, Kibbutz Beit Haemek, Israel), and captured with Fuji X-ray films Super RX-N (Fujifilm, Tokyo, Japan). Band intensities were quantified with ImageJ software, version 1.53e (Schneider, Rasband, and



Eliceiri 2012). To control equal loading, housekeeping  $\alpha$ -tubulin, actin, GAPDH or cyclophilin A (cypA) were used to normalize protein expression.

<i>Antibody</i>	<i>Supplier information</i>	<i>Immunogen</i>	<i>Dilution</i>
<i>Goat anti-Rabbit IgG</i>	Sigma-Aldrich goat Cat# A0545	Purified rabbit IgG	1:20,000
<i>Rabbit anti-mouse IgG</i>	Sigma-Aldrich rabbit polyclonal antibody Cat# A9044	Purified mouse IgG	1:20,000

## 2.12. RNA-sequencing and analysis

Immediately after LIRD protocol (24h at 10,000 lux) or normal light exposure, mice were euthanised, eyes were enucleated, and retinas were rapidly obtained and preserved in RNAlater at 4°C overnight and frozen the following day. Total RNA was obtained using RNeasy kit following the manufacturer's instructions. RNA concentration was determined with NanoDrop spectrophotometer (ThermoFisher Scientific). RIN integrity, RNA quality assessment, library preparation and Illumina sequencing was performed in the Genomic Unit of the Centre de Regulació Genòmica (CRG) facility (Agilent Technologies).

A cDNA library for every RNA sample was made using 5-10  $\mu$ g of RNA to prepare the RNA-seq library using TruSeq RNA Sample Prep Kits (Illumina). First, the RNA was isolated from the sample and traces of contaminating DNA was removed with DNase. The polyA containing mRNA molecules were purified using poly-T oligo-attached magnetic beads. Then, the mRNA is reverse transcribed into double-stranded cDNA, and sequence adapters are added to the ends of the fragments. cDNA library was made by synthesizing

the first-strand cDNA using reverse transcriptase and random primers and followed by synthesis of the second-strand cDNA using DNA polymerase I and RNase H. After construction of the libraries, paired-end sequencing on Illumina HiSeq 2000 platform was performed using the nucleotide sequences of the ends of the fragments, from now on called “reads”, and 2x100 bp reads were obtained.

The raw reads (in fastq format) were aligned with an indexed mouse reference genome (GRcm39) with Spliced Transcripts Alignment to a Reference (STAR) (Dobin et al. 2013). Transcript quantification and differential analysis of count data was performed with count-based statistical method DESeq2 (Love, Huber, and Anders 2014) in RStudio (RStudio Team 2015). Exploratory data analysis for quality assessment and to explore the relationship between the samples was made. Variance stabilizing transformation was performed with rlog and VST, and sample distances to assess similarity was calculated with VST data and plotted with principal components analysis (PCA).

### **2.13. Cell culture conditions**

HEK293T cells were cultured in DMEM (ATCC Cat# CRL-3216) supplemented with 10% of heat-inactivated foetal bovine serum (FBS) (Invitrogen), 20 U/ml penicillin and 20 ug/ml streptomycin. Cells were maintained at 37°C in a 5% CO<sub>2</sub> atmosphere in a humidified incubator.

To subculture cells, medium was removed, and dissociation was performed with a 1:5 dilution of 0.25% trypsin-EDTA in PBS. Cells were incubated at 37°C until they were detached and the enzymatic effect of trypsin-EDTA was blocked with FBS-containing fresh culture media. Cells were harvested, centrifugated, counted using a hemocytometer chamber and seeded in culture

dishes with fresh media. Subcultures were performed when an 80% of cell confluence was achieved.

To cryopreserve HEK293T cells, they were harvested and pelleted in PBS with centrifugation at 100g for 5 minutes. Pellets were resuspended in cryopreservation medium (10% DMSO in FBS), which is used to prevent the formation of ice crystals and cell disruption. Cells were rapidly aliquoted in cryovials and stored at -80 °C in a Mr. Frosty™ Freezing Container (Thermo Scientific, Cat# 5100-0001). The cells were then transferred to a liquid nitrogen tank in the next following days for long-term storage.

#### **2.14. Cell transfection and ubiquitin assay**

Ubiquitinated proteins were detected using the 6xHis-ubiquitin assay for mammalian cell protocol of Tansey laboratory ([www.tanseylab.com](http://www.tanseylab.com)). Cells were seeded at a  $2.5 \times 10^6$  confluency in a P100 dish in the evening, and cells were transfected the morning after for 6 hrs with the desired expression plasmids using polyethylenimine (PEI) in DMEM without FBS. Five  $\mu\text{g}$  of 6xHis-ubiquitin plus 5 additional  $\mu\text{g}$  of Arrestin-1 (plasmid kindly provided by Dr. Vsevolod Gurevich), FAIM-L or FAIM-S, as indicated, were transfected. When needed, empty vector pCDNA3 was co-transfected to reach 15  $\mu\text{g}$  of total DNA in the indicated conditions. After transfection, media was removed, and cells were maintained with supplemented culture media for 48 hrs. To achieve proteasome inhibition, six hrs before cell collection, cell culture media was replaced with supplemented medium containing 10  $\mu\text{M}$  of MG132 (Sigma Aldrich Cat# HY-13259) from a stock solution of 10 mg/ml of MG132 diluted in DMSO.

Before ubiquitin assay was performed, Anti-His affinity resin was washed in buffer A (**Table 8**) three times by shaking the tube in hand for 10 seconds. After

centrifugation for one minute at 1,000g, the resin was pelleted and in the final wash resuspended in A buffer in a 1:1 ratio.

Then, ubiquitin assay was performed as follows. Cells were collected in PBS pH 7.0 and spun down at 1000g for five minutes. Cell pellets were resuspended in PBS and 20 µl of input was stored. Cells were spun down again at 1000g for five minutes and pellets were resuspended in buffer A (6M guanidine pH8, 0.1M Na<sub>2</sub>PO<sub>4</sub> and 10mM Imidazol). Samples were sonicated and homogenised with 24 g insulin syringe and lysates were centrifugated at 16,000g for 15 minutes at 4°C. Supernatant was transferred to a new tube and 50 µl of resuspended Anti-His affinity resin was added.

**Table 6.** List of buffers for ubiquitin assay and its

<i>Buffer</i>	<i>Recipe</i>
<i>Buffer A</i>	6M guanidine-HCl 0.1M Na <sub>2</sub> PO <sub>4</sub> 10mM Imidazol pH=8 (adjust w. NaOH)
<i>Buffer T1</i>	25mM Tris-HCl 20mM Imidazol pH=6.8 (adjust w. HCl)
<i>Buffer A/T1</i>	1:3 ratio

Cell lysates were orbitally rotated for 4h at 4°C at 25 rpm. After a short spin, supernatant was discarded, and resin was washed twice with 800 µl of buffer A, four times in buffer A/T1 (1 volume of buffer A for 3 volumes of buffer T1), and twice in buffer T1 (25mM Tris-HCl, 20 mM Imidazol pH 6.8). After a short spin, a needle was used to aspirate the supernatant and 37.5 µl of T1 buffer supplemented with 25% Imidazol 1M was added to the resin. 12.5 µl of 4x Laemmli buffer (60 mM Tris-HCl pH 6.8, 4 mM EDTA, 10% glycerol, 2% SDS, 100 mM dithiothreitol (DTT) and traces of Bromophenol blue) was

added to IP lysates and stored inputs and boiled at 95°C for 10 minutes for elution. Afterwards, lysates were loaded in SDS-PAGE for western blot analysis.

### **2.15. Statistical analyses**

We performed a pilot study to estimate sample size required for 0.8 power and two-sided 0.05 significance for retinal morphometric analysis. For the rest of analyses, we limited the number of animals to mice availability and preliminary data. Data sets were plotted and analysed using GraphPad Prism v8.0.1, and no data was removed prior to analysis unless only repeated measures were used for analyses. Data was graphed before statistical test to check whether the data met the assumptions of the statistical approach. Statistical comparisons were made using a two-way ANOVA test followed by Sidak's post hoc test when analysing two or more ages between WT and Faim KO. Three-way ANOVA was used to assess three factors in electroretinogram analyses: light intensity, light damage, and genotype. Unpaired two-tailed Student's t test was used for parametric data when assessing only one factor. All p values lower than 0.05 were considered statistically significant. The ROUT method (with Q set to 1%) was used to detect outliers.

### 3. Results

#### 3.1. Loss of FAIM leads to age-related rod photoreceptor and RGC defect

To assess whether the absence of FAIM in the retina leads to functional deficits, we performed dark-adapted (scotopic) and light-adapted (photopic) ERG assays. In previous studies we observed that neurodegeneration in Faim KO retinas occurred gradually and peaked at 18 months, when photoreceptor cell death was detected. In sight of this, we first analysed the responses of 18-month-old Faim KO mice.

Upon a light stimulus, the retinal cells produce electrical activity that can be captured through ERG (explained in detail in Methods Section, *page 6*). Responses from photoreceptors and bipolar cells elicit an electrical activity called a-wave and b-wave, respectively. Rod photoreceptors and rod-associated bipolar cells respond both in scotopic and mixed conditions, while cone photoreceptors and cone-associated bipolar cells only respond to photopic conditions. Scotopic and mixed ERG analyses revealed reduced amplitudes in both a-wave and b-wave (**Figure 42A**), suggesting that FAIM is important for maintenance of rod function during ageing. To detect a clean and unambiguous response of RGCs electrical activity after light stimulation, a low light intensity ( $-4.0 \log(\text{cd}\cdot\text{s}\cdot\text{m}^{-2})$ ) was used, which gives a positive scotopic threshold response (pSTR). At 18 months, the pSTR peak amplitude of Faim KO mice was reduced in comparison with its WT counterparts, suggesting that RGCs are compromised (**Figure 42A**).

Oscillatory potentials are ERG waveforms of high frequency and low amplitude that stem from the b-wave. They are obtained by bandpass filtering at 100 Hz the ERG responses at  $1.5 \log \text{cd}\cdot\text{s}\cdot\text{m}^{-2}$  of light intensity. At 18 months, neither OP1, OP2 or OP3 amplitudes were altered in Faim KO mice,

## Scotopic and photopic ERG at 18 months

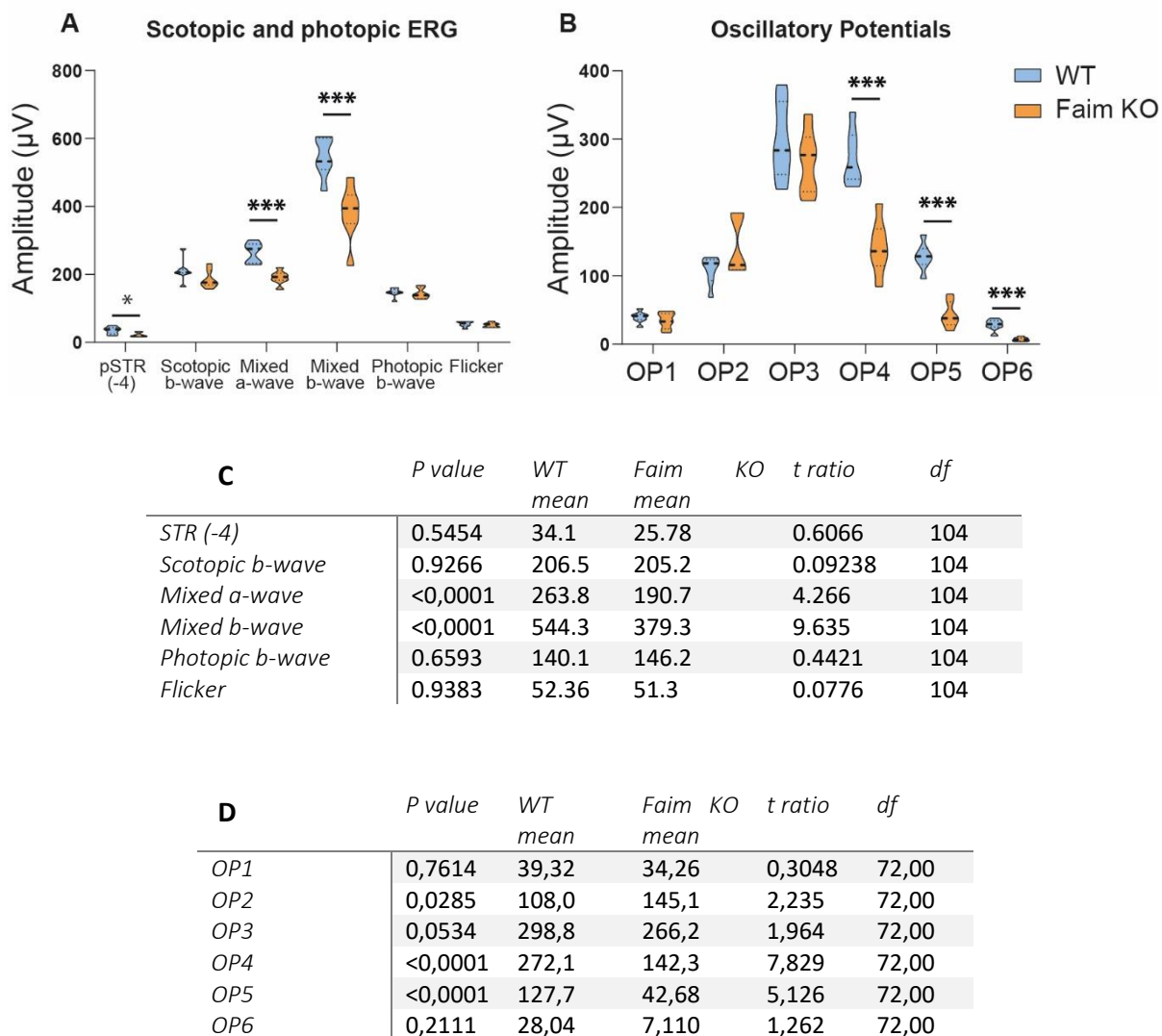


**Figure 6. Photoreceptors, bipolar cells and RGCs are altered in Faim KO mice at 18 months. (A)** Summary of ERG analysis of pSTR (-4) representing RGCs, scotopic b-wave, mixed a-wave, mixed b-wave, photopic b-wave and flicker (20 Hz). **(B)** Summary of the amplitudes recorded on ERG of the oscillatory potentials. OP1 corresponds to photoreceptors, OP2 and OP3 to bipolar and horizontal cells and OP4-6 to amacrine and RGCs (n = 7-14 mice/group). Each violin plot extends from the min to max values, the median is represented by a thick dashed line, and quartiles are represented by thin dotted lines. **(C)** Table with the results of statistical analysis using Student's t test of summary graphs. **(D)** Table with the results of statistical analysis using Student's t test of the oscillatory potentials. To summarize, data were plotted together \* p < 0.05, \*\* p < 0.01, \*\*\* p < 0.005.

but there was a significant decrease in OP4, OP5 and OP6 (see **Figure 42B**). OP4 to OP6 are thought to be linked to amacrine and RGCs, as they are the only neurons in the retina able to fire action potentials. These results suggest that the ganglion cell layer (GCL) may be also altered in Faim KO mice.

However, under photopic conditions, which are used to study cone photoreceptor pathways, b-wave amplitudes remained unchanged. Similarly, the rod-saturating flicker ERG recorded no alterations in Faim KO mice (see **Figure 42A**), indicating cone photoreceptors are not impaired.

We also checked the b:a ratio in scotopic conditions, which is used to assess electronegative ERGs and whether system dysfunction is found post-phototransduction, and found no alterations (**Figure 43**), indicating alterations stem from phototransduction.

Given that neurodegeneration in Faim KO retinas occurs progressively, we wondered whether retinal function could be already impaired at younger ages, when Faim KO mice already present a gliotic phenotype. As shown in **Figure 44**, retinal function was examined at 2 months but no alterations in amplitudes were found in either scotopic, photopic, pSTR, flicker or oscillatory potentials ERG analysis, suggesting that retinal functional alterations in Faim KO mice, just as photoreceptor cell death, is associated to aged retinas.

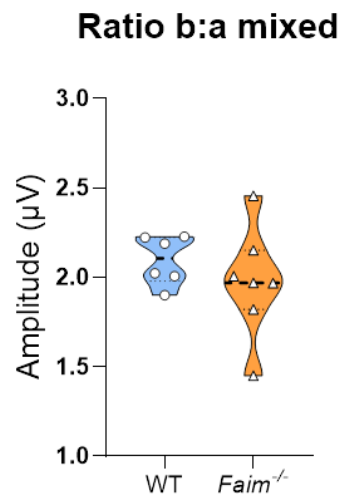


**Figure 7. b:a ratio is normal in Faim KO mice.** Ratio of mixed b-wave and mixed a-wave graphed as amplitude. Data are represented as violin plots. Each dot corresponds to a retina, the median is represented by a thick dashed line, and quartiles are represented by thin dotted lines. Below is shown a table with Student's t test statistical analysis, p value = 0.3949.



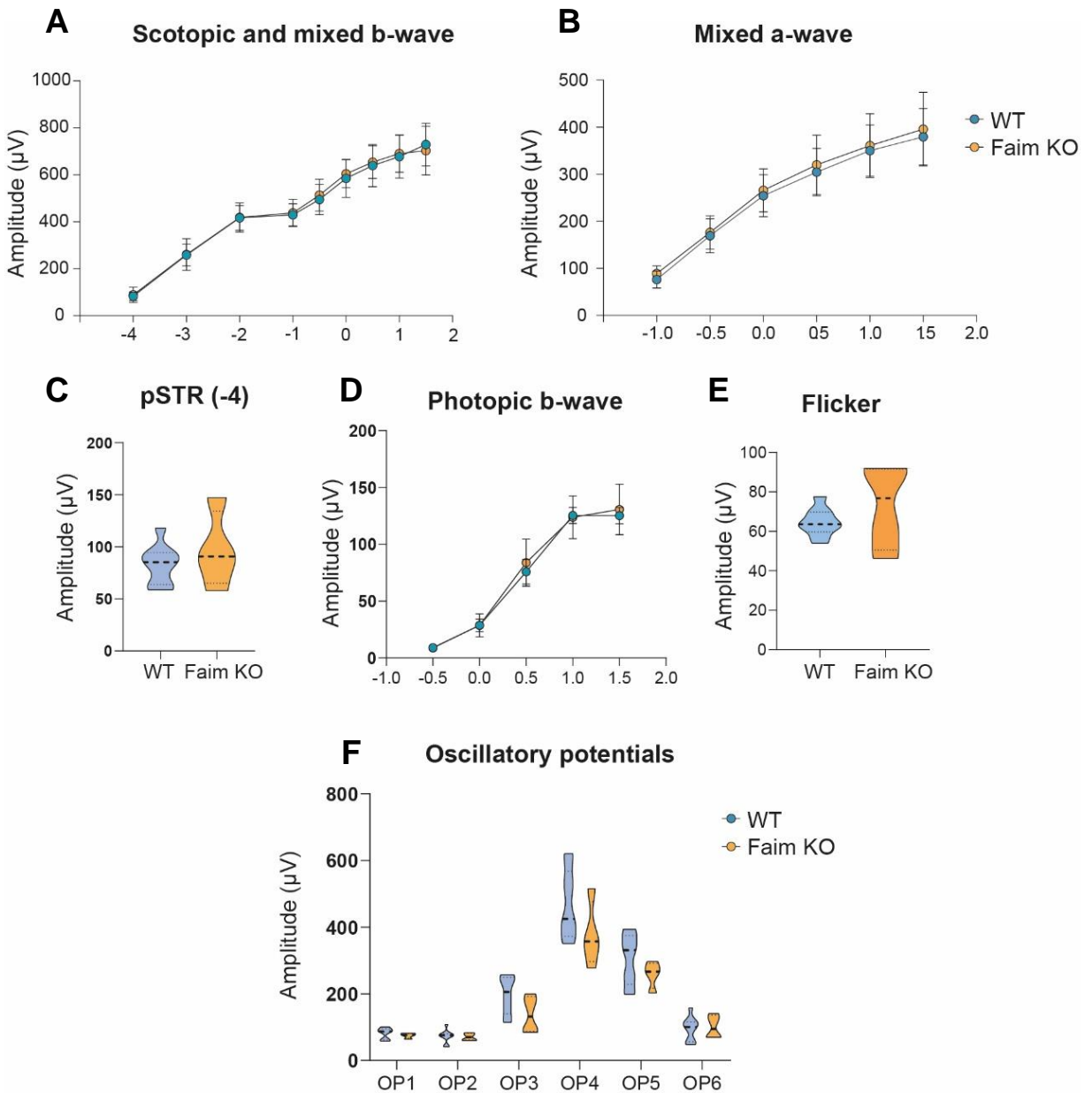


**Figure 8** Faim KO mice ERG analyses are not altered at 2 months of age. ERG analyses of 2-month-old Faim KO mice. **(A)** Amplitudes of scotopic and mixed b-wave representing bipolar cells, ranging from -4 to 2 log cd·s·m<sup>-2</sup>. **(B)** Amplitudes of mixed a-wave representing photoreceptor cells, ranging from -1 to 1.5 log cd·s·m<sup>-2</sup>. **(C)** Amplitudes of pSTR at -4 log cdsm2 representing RGCs. **(D)** Amplitudes from photopic b-wave responses ranging from -0.5 to 2 log cd·s·m<sup>-2</sup>, representing cone photoreceptors. **(E)** Flicker responses at Hz, representing cone photoreceptors. **(F)** Oscillatory potentials obtained from XXXX. Each violin plot extends from the min to max values, the median is represented by a thick dashed line, and quartiles are represented by thin dotted lines. Statistical analysis was used performing Two-way ANOVA.

Besides being associated with ageing processes, retinal degeneration can also be caused or influenced by extrinsic environmental conditions such as light damaging conditions (Hao et al. 2002; Christian Grimm and Remé 2013). Light stress induces the expression of endogenous molecular factors that confer protection to the retina and the eye (Pearson and Ali 2018; Liu et al. 1998). We previously showed that Endothelin-2 and FGF2 are upregulated in Faim KO mice without any additional stress. Interestingly, these proteins have been proposed to act as retinal neuroprotective factors after light damage exposure (Ueki et al. 2009; Joly et al. 2008; Liu et al. 1998). In sight of this, we decided to study whether Faim KO mice show increased sensitivity to light damage than its WT counterparts. To test whether we could emulate this impairment through an environmental stress, we exposed 2-month-old mice to light damage (LD). After applying 8h of continuous light exposure at 10,000 lux, we did not find any decrease in ERG amplitudes in scotopic ERG nor photopic ERG or OP (**Figure 45**).

Nonetheless, even though amplitudes under scotopic and photopic conditions were not significantly different, we observed unusual ERG shapes in Faim KO mice after light stimuli (**Figure 45A**).

For proper retinal function, photoresponse needs to terminate, and electrical activity must return to its resting state after light levels drop. ERG recordings showed that electrical activity decay differed between Faim KO and WT mice (**Figure 46A**). Hence, we analysed Faim KO and WT amplitudes at 200 ms after flash exposure of different intensities. Analysis revealed that Faim KO retinas are still firing electrical responses (**Figure 46B**) when WT have already returned to resting state. These results suggest that Faim KO mice could have a defective photoreceptor deactivation after stimulation, indicating alterations in adequate photoresponse termination.

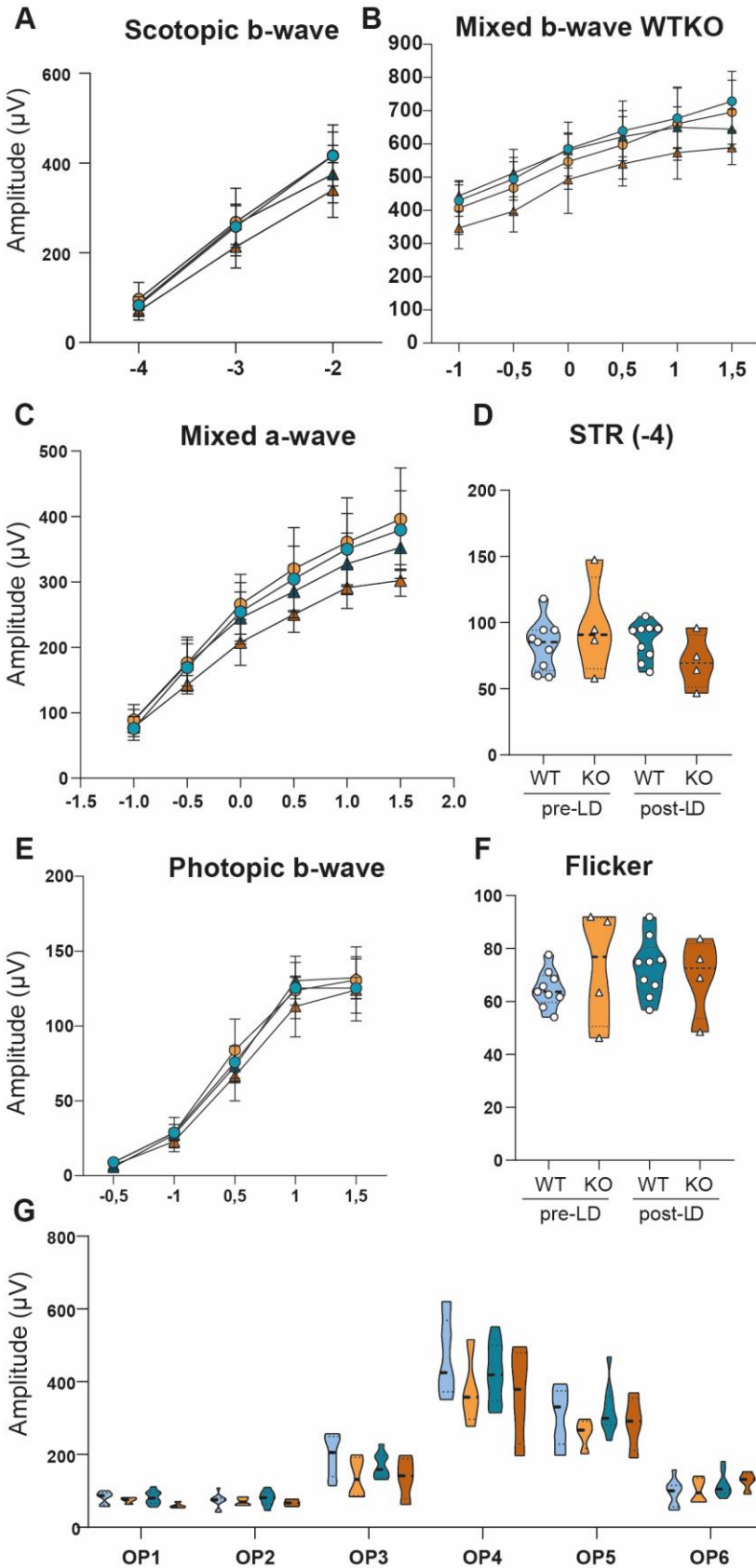


**Figure 9. No changes were found in ERG analysis in 2-month-old Faim KO mice after light damage.** ERG was performed at the indicated light intensities, corresponding to scotopic (A), mixed (B, C) and photopic (E) conditions. pSTR was performed at  $-4 \log \text{cd}\cdot\text{s}\cdot\text{m}^{-2}$  (D), and flicker recordings at 20 Hz (F). Oscillatory potentials are represented in (G). At least 4 animals were analysed per each group. Data are represented as XY or violin plots. In violin plots, each animal is represented as a dot. Each violin plot extends from the min to max values, the median is represented by a thick dashed line, and quartiles are represented by thin dotted lines. Statistical analysis was used performing Two-way ANOVA. Statistical analysis was performed using repeated measures three-way ANOVA, in which genotype, light intensity and light damage were used as factors. \*  $p < 0.05$ .



**B** Recovery amplitude 200ms after flash

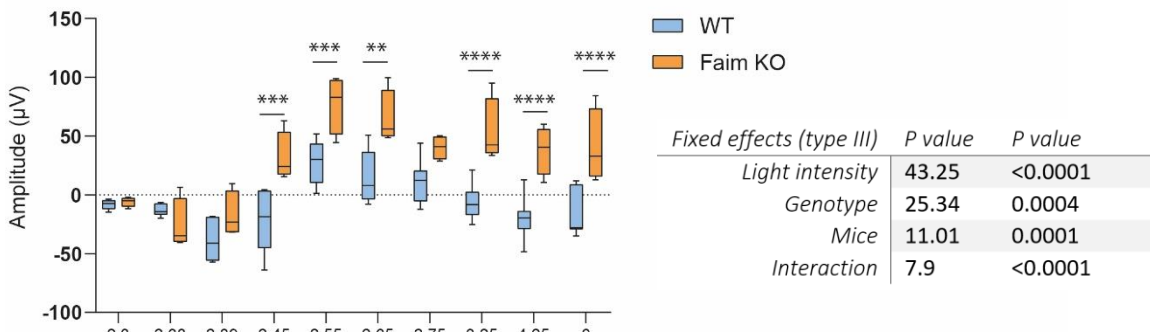


**Figure 10. Recovery amplitude in Faim KO mice is higher at 200 ms after light flash.**

**(A)** From top to bottom and left to right, ERG responses from different light intensities are represented from WT and Faim KO mice before and after light damage. It can be observed how the shape in the recovery time of Faim KO differs from WT mice. **(B)** Recovery amplitude of WT and Faim KO mice pre-light damage 200 ms after the flash was evoked. The source of variation (light intensity, genotype, its interaction, and mice) and the total % of variation that accounts for the results and its p value are represented. Three-way ANOVA with repeated measures was performed. \*\*  $p < 0.01$ , \*\*\*  $p < 0.005$ , #  $p < 0.001$ .

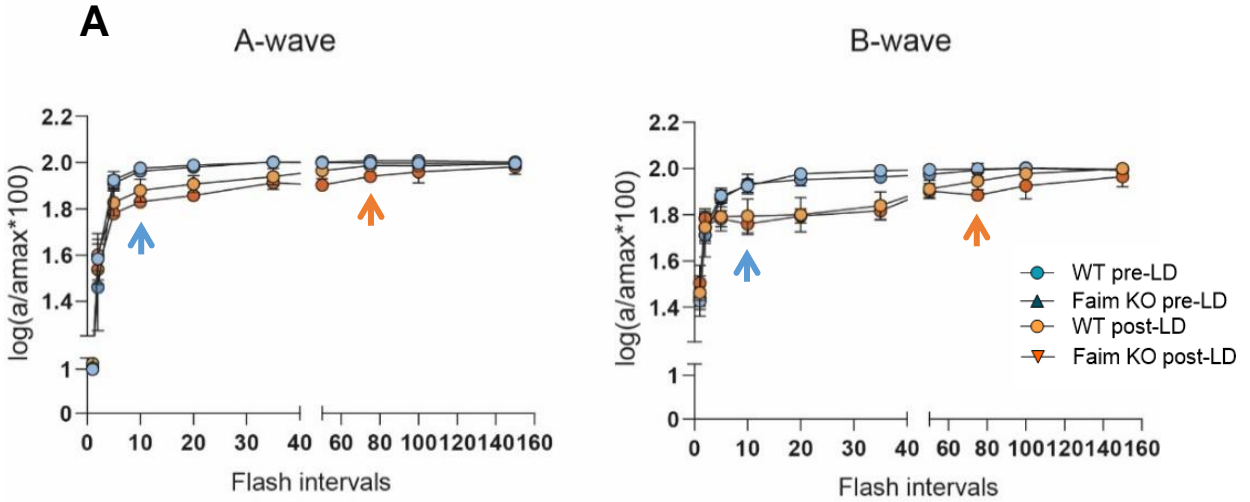
### 3.2.Faim depletion causes a delayed dark adaptation

The difference in amplitude shapes in scotopic ERG of Faim KO in comparison to WT mice (**Figure 46**) prompted us to study whether dark adaptation in Faim KO retinas was hindered, as this could be the consequence of a delayed photoresponse deactivation. To assess this, a double-flash protocol was performed to measure the photoresponse recovery at both 2 (**Figure 47**) and 18 months of age (**Figure 48**). We used ten different time intervals in between the two flashes to assess the rod recovery time.

The following full-field ERG resolved that Faim KO mice present a severe delay in dark-adaptation at both ages in comparison to WT mice (**Figure 47**, **Figure 48**). By 10 seconds, 2-month-old WT mice were able to recover and elicit the same amplitudes as the first flash (**Figure 47**, blue arrows), while it took approximately 75 seconds for Faim KO mice to achieve full photoreceptor and bipolar cell recovery (**Figure 47**, orange arrows).

We also studied whether light damage exacerbated this delay at 2 months of age given the reported effects of this stress specifically in photoreceptors and photoreceptor light and dark adaptation. Although the power size of the light damage effect may not be evident (**Figure 47A**), it is significant in photoreceptor response (**Figure 47B**, a-wave, light damage,  $p=0.0014^{**}$ ), but not at the bipolar response level (**Figure 47C**, b-wave, light damage,  $p=0,2409$ ). Moreover, the interaction between genotype and light damage in the a-wave is significant too (**Figure 47B**, a-wave, genotype \* light damage,  $p=0.013^{*}$ ), and thus observing our results **Figure 47A**, this indicates that light damage effect is more determinant in Faim KO dark adaptation than in WT mice.

## Dark adaptation at 2 months pre-LD and post-LD



### B

Three-way ANOVA, A-wave at 2 months old

Fixed effects (type III)	P value	P value	F (DFn, DFd)
Light intensity	<0,0001	****	F (9, 126) = 664,4
Genotype	<0,0001	****	F (1, 42) = 34,72
Light damage	0.0014	**	F (1, 14) = 15,73
Light intensity x Genotype	<0,0001	****	F (9, 42) = 7,364
Light intensity x Light damage	0.361	ns	F (9, 42) = 1,134
Genotype x Light damage	0.013	*	F (1, 42) = 6,736
Light intensity x Genotype x LD	0.4218	ns	F (9, 42) = 1,045

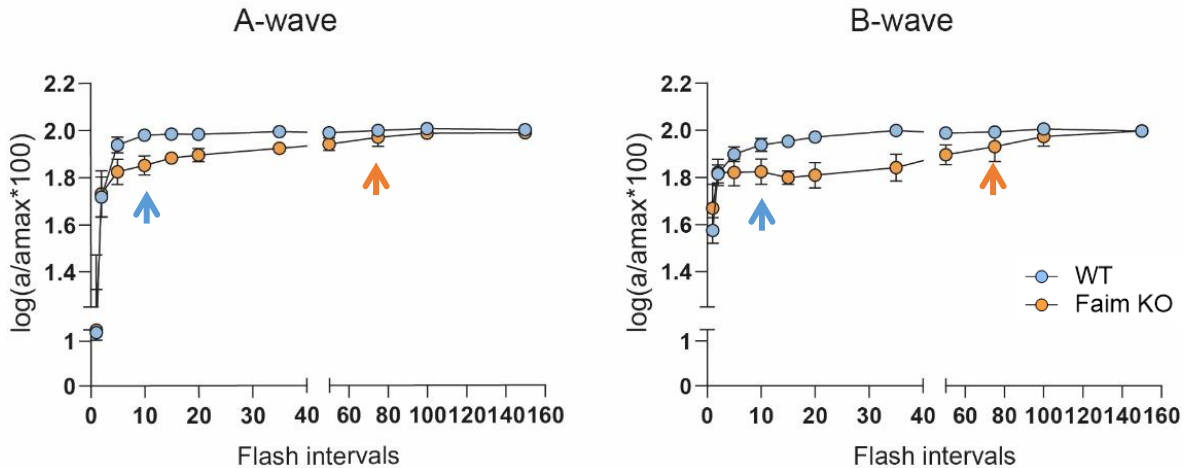
### C

Three-way ANOVA, B-wave at 2 months old

Fixed effects (type III)	P value	P value	F (DFn, DFd)
Light intensity	<0,0001	****	F (9, 126) = 357,7
Genotype	<0,0001	****	F (1, 42) = 45,60
Light damage	0.2409	ns	F (1, 14) = 1,500
Light intensity x Genotype	<0,0001	****	F (9, 42) = 20,90
Light intensity x Light damage	0.3724	ns	F (9, 42) = 1,117
Genotype x Light damage	0.8513	ns	F (1, 42) = 0,03559
Light intensity x Genotype x LD	0.1949	ns	F (9, 42) = 1,459

**Figure 11. Faim KO mice show a great delay in dark adaptation in comparison to WT mice at 2 months, but no differences are found after LD. (A)** Dark adaptation of WT and Faim KO mice at 2 months of age before and after light damage. Mice were dark-adapted overnight, and after anaesthesia double flash protocol was used to study a delay in dark adaptation using the following time intervals (s): 1, 2, 5, 10, 20, 35, 50, 75, 100, 150. Amax corresponds to the ERG responses after the first flash, and A corresponds to the second response after the second flash. Data are represented as  $\log(a/a_{max}) \cdot 100$  in XY table, and statistical analysis was performed using three-way ANOVA. Results are depicted in **(B)** for the a-wave and in **(C)** for the b-wave. 6-7 mice were for pre-LD analyses, and 4 mice were used for post-LD analyses.

## Dark adaptation at 18 months



### Two-way ANOVA, A-wave at 18 months

Fixed effects (type III)	P value	P value	F (DFn, DFd)
Interval time	<0,0001	****	F (1,516, 17,43) = 186,8
Genotype	0.0189	*	F (1, 12) = 7,353
Interval time x Genotype	0.0033	**	F (10, 115) = 2,849

### Two-way ANOVA, B-wave at 18 months

Fixed effects (type III)	P value	P value	F (DFn, DFd)
Interval time	<0,0001	****	F (3,714, 42,71) = 110,3
Genotype	0.0007	***	F (1, 12) = 20,62
Interval time x Genotype	<0,0001	****	F (10, 115) = 16,51

**Figure 12. Faim KO mice show a great delay in dark adaptation in comparison to WT mice at 18 months.** Dark adaptation of WT and Faim KO mice at 18 months of age. Mice were dark-adapted overnight, and after anaesthesia double flash protocol was used to study a delay in dark adaptation using the following time intervals (s): 1, 2, 5, 10, 20, 35, 50, 75, 100, 150. Amax corresponds to the ERG responses after the first flash, and A corresponds to the second response after the second flash. Arrowheads point towards the timepoint in which amax response was recovered (blue: WT, orange: Faim KO). Data are represented as  $\log(a/amax)*100$  in XY table, and statistical analysis was performed using two-way ANOVA (depicted below) (n=6-7 mice/group).

### **3.3.Light-dependent Arrestin-1 translocation is delayed in Faim KO mice**

To study the mechanism that could be lying beneath the delay in dark adaptation in Faim KO mice, we aimed to study the photoreceptor desensitizing process.

After dark-adaptation and upon light reception, Arrestin-1 and Transducin- $\alpha$  are translocated between the inner segment (IS) and the outer segment (OS) of photoreceptors in opposite directions (Mendez et al. 2003; Nair et al. 2005) (**Figure 49A**).

To assess whether this translocation is altered in Faim KO mice, Arrestin-1 (**Figure 49B**) and Transducin- $\alpha$  (**Figure 49C**) immunolocalization were examined in retinal sections. To this end, mice were dark-adapted overnight and exposed to 2,500 lux of white LED light for different periods of time.

Arrestin-1 in dark-adapted mice that were not exposed to light was completely localized in the IS both in WT and Faim KO mice. However, after 15 minutes of light exposure, 70% of Arrestin-1 was translocated to the OS in WT mice, while Faim KO mice roughly exhibited 20% of Arrestin-1 to the OS (**Figure 49D**). However, Transducin- $\alpha$  translocation levels from the OS to the IS upon light exposure were similar between Faim KO and WT mice (**Figure 49F**).



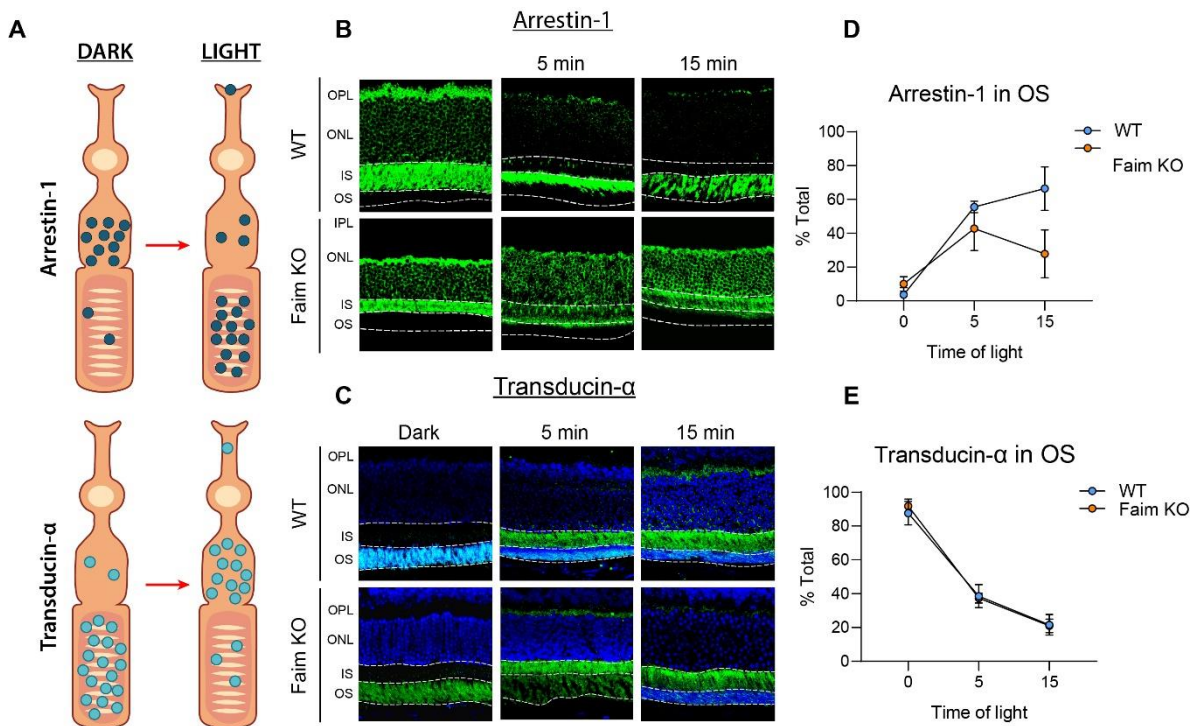


**Figure 13. Light dependent arrestin-1 and Transducin-1 localization at dark and translocation upon light reception for 5 and 15 minutes. (A)** Diagram representing the translocation of Arrestin-1 and Transducin- $\alpha$  in dark-adapted retinas that are exposed to light. **(B, C)** Retinal sections (4  $\mu$ m) were obtained from 2-month-old WT and Faim KO mice and immunofluorescence was performed with Arrestin-1 **(B)** or Transducin- $\alpha$  **(C)**. Mice were dark-adapted overnight, and pupils were dilated with tropicamide 1%. Mice were either euthanised in the dark or exposed to light for the indicated times. **(D)** Arrestin-1 translocation in Faim KO mice was delayed in comparison to WT mice, but Transducin- $\alpha$  translocation **(E)** remained normal. (n=4 mice/group). Data are represented as XY graphs, X= total % of protein translocated in the OS, Y= time of light exposure.

Moreover, we also checked Arrestin-1 and Transducin- $\alpha$  protein levels at 2 and 18 months of age and found a reduction of both Arrestin-1 and Transducin- $\alpha$  protein levels at 18 months **(Figure 50)**.

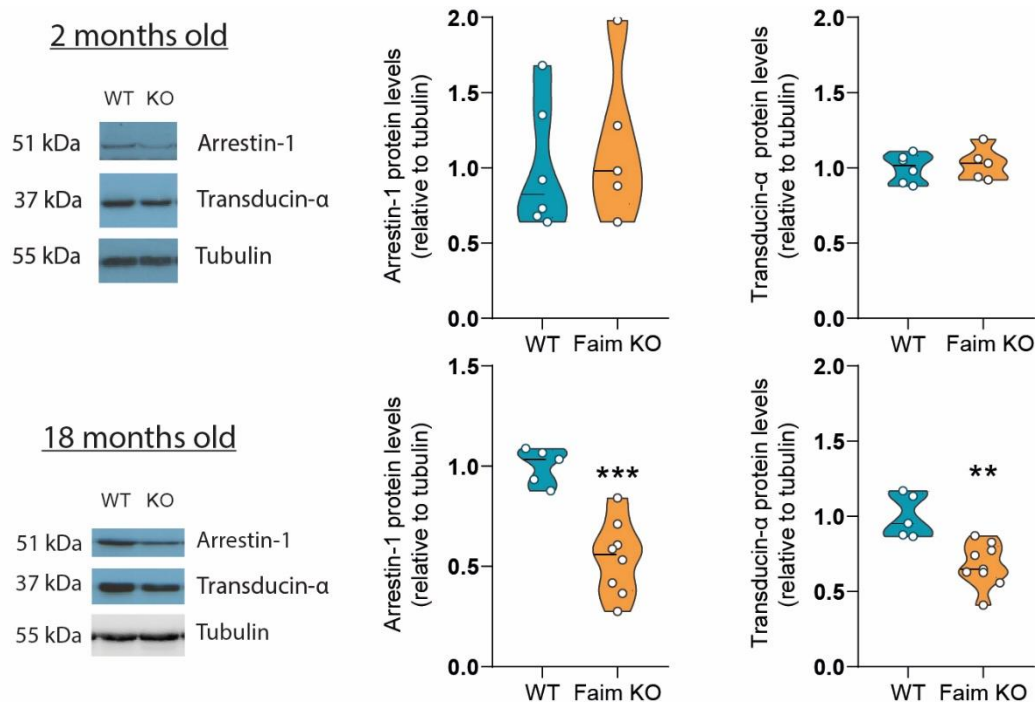


**Figure 14. Protein levels of Arrestin-1 and Transducin- $\alpha$  are reduced at 18 months in Faim KO mice, but not at 2 months.** Expression of Arrestin-1 and Transducin- $\alpha$  at 2 and 18 months of age in WT and Faim KO mice. Protein levels were normalized with tubulin- $\alpha$  and quantified in ImageJ. Data are plotted relative to WT values. Data are represented in violin plots. Each violin plot extends from the min to max values, the median is represented by a thick dashed line, and quartiles are represented by thin dotted lines. Statistical analysis was performed using Student's t test. \*\*  $p < 0.01$ , \*\*\*  $p < 0.005$ .

### 3.4.Both FAIM isoforms prevent Arrestin-1 ubiquitination *in vitro*

To perform its anti-apoptotic function, FAIM regulates XIAP autoubiquitination by blocking its E3 ligase domain (Weissman, Shabek, and Ciechanover 2011; Martínez-Mármol et al. 2016; Moubarak et al. 2013). This affinity binding stabilizes the levels of XIAP and allows its ultimate function:

the inhibition of caspase-3 (Moubarak et al. 2013). Members of the Arrestin-1 family have also been found as a target of ubiquitination for signalling purposes, and E3 ubiquitin ligase proteins have been found to act as Transducin- $\alpha$  translocation modulators during light/dark adaptation (Taro Chaya, Ryotaro Tsutsumi, Leah Rie Varner, Yamato Maeda, 2019).

Since ubiquitination has been reported as a regulator of light and dark-dependent translocation of proteins involved in phototransduction in rod photoreceptors, and FAIM is a regulator of XIAP by ubiquitination, we tested whether FAIM could be associated to Arrestin-1 ubiquitination events. On that account, HEK293T cells were transfected with 6xHis-Ubiquitin encoding plasmid together with Arrestin-1-HA alone or Arrestin-1-HA with either FAIM-L-FLAG or FAIM-S-FLAG (**Figure 51**).

After ubiquitin immunoprecipitation and in the condition in which neither FAIM-L or FAIM-S were co-expressed, Arrestin-1-HA ubiquitination was abundant. However, FAIM-L and FAIM-S co-expression almost completely abrogated Arrestin-1-HA ubiquitination (**Figure 51**). Same ubiquitination assay was performed under the effects of inhibitor of proteasome MG132. As shown in the right panel, this condition increased the levels of ubiquitinated Arrestin-1 co-expressed with FAIM-L and FAIM-S, indicating that at least some of this ubiquitination is degradative via the proteasome.

Altogether, this result suggests that that both FAIM isoforms can negatively regulate Arrestin-1 ubiquitination and therefore play a role on the retinal phototransduction signalling.

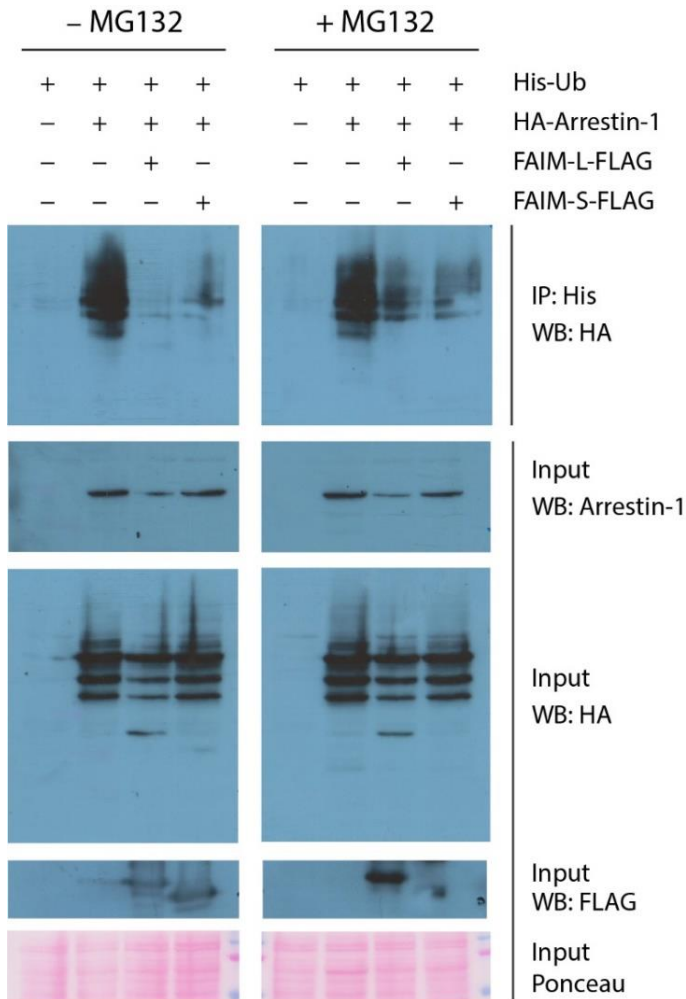


**Figure 15. FAIM-S and FAIM-L block Arrestin-1 ubiquitination *in vitro*.** HEK293T cells were transfected with the described plasmids, in the presence or absence of MG132 treatment as indicated. Successful transfection was confirmed by immunoblotting for HA and FLAG for Arrestin-1 and both FAIM-L and FAIM-S expression, respectively. Ponceau staining was used to check protein loading. Ubiquitin-His pull-down membrane was immunoblotted with HA. Evident ubiquitination is observed in the condition where Arrestin-1 is expressed alone with ubiquitin, and a significant decrease of ubiquitin is found both in FAIM-L and FAIM-S conditions.

### 3.5. Photoreceptors in Faim KO mice are more sensitive after light damage

As mentioned above, functional alterations on standard scotopic and mixed ERG analyses were only observed in aged Faim KO mice, and 8h of light damage did not induce significant functional alterations in young mice. Retinal neurodegeneration and a decrease in its functionality are commonly associated to ageing processes. We previously described that aged retinas with FAIM deficiency show increased retinal gliosis, accumulation of ubiquitinated

aggregates, breakdown of the blood-retinal barrier and photoreceptor cell death (Sirés et al. 2021), so we hypothesized that Faim KO mice may be more susceptible to these alterations at early ages after stress induction.

There are several models that mimic degenerative retinal diseases, such as light-induced retinal damage (LIRD). These LIRD models have been used to study natural ageing processes, retinal pathologies like age-related macular disease (AMD) and retinitis pigmentosa (RP) (Christian Grimm and Remé 2019; 2013; Krigel et al. 2016; Yang et al. 2022), which are characterised by photoreceptor cell death.

To evaluate whether light stress renders Faim KO mice more sensible to neurodegenerative mechanisms, we exposed mice to cool LED light at 10,000 Lux for 8h and 24h and after two weeks we analysed the effects. As shown in **Figure 52A** after 8h of LIRD, Faim KO mice already exhibited accumulation of ubiquitinated proteins. We also studied retinal gliosis and found an increase in GFAP immunoreactivity (**Figure 52B**).

To determine the effect of LIRD in cell death we performed TUNEL assay, and a significant number of TUNEL-positive cells was found at both LIRD condition, with a significant increase in the more severe LIRD (8,000 lux for 24h) (**Figure 53**).

These results indicate that lack of FAIM renders the retina more sensible to light stress, suggesting that FAIM could confer protection to photoreceptors against light damage.

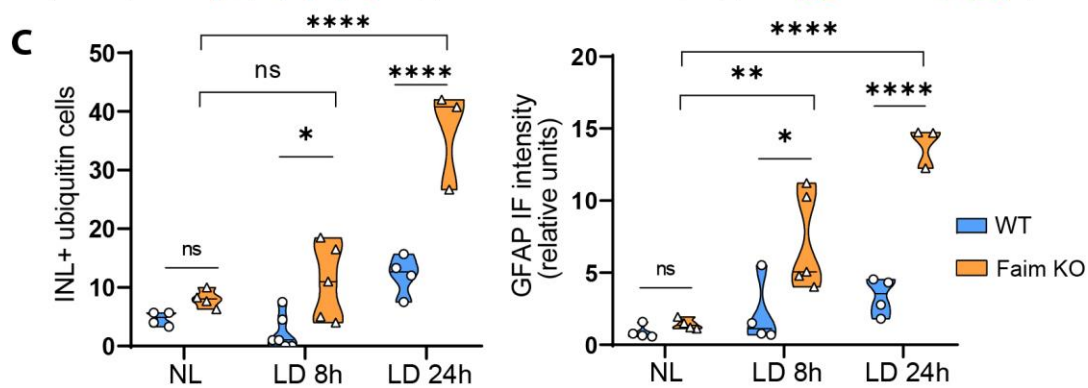
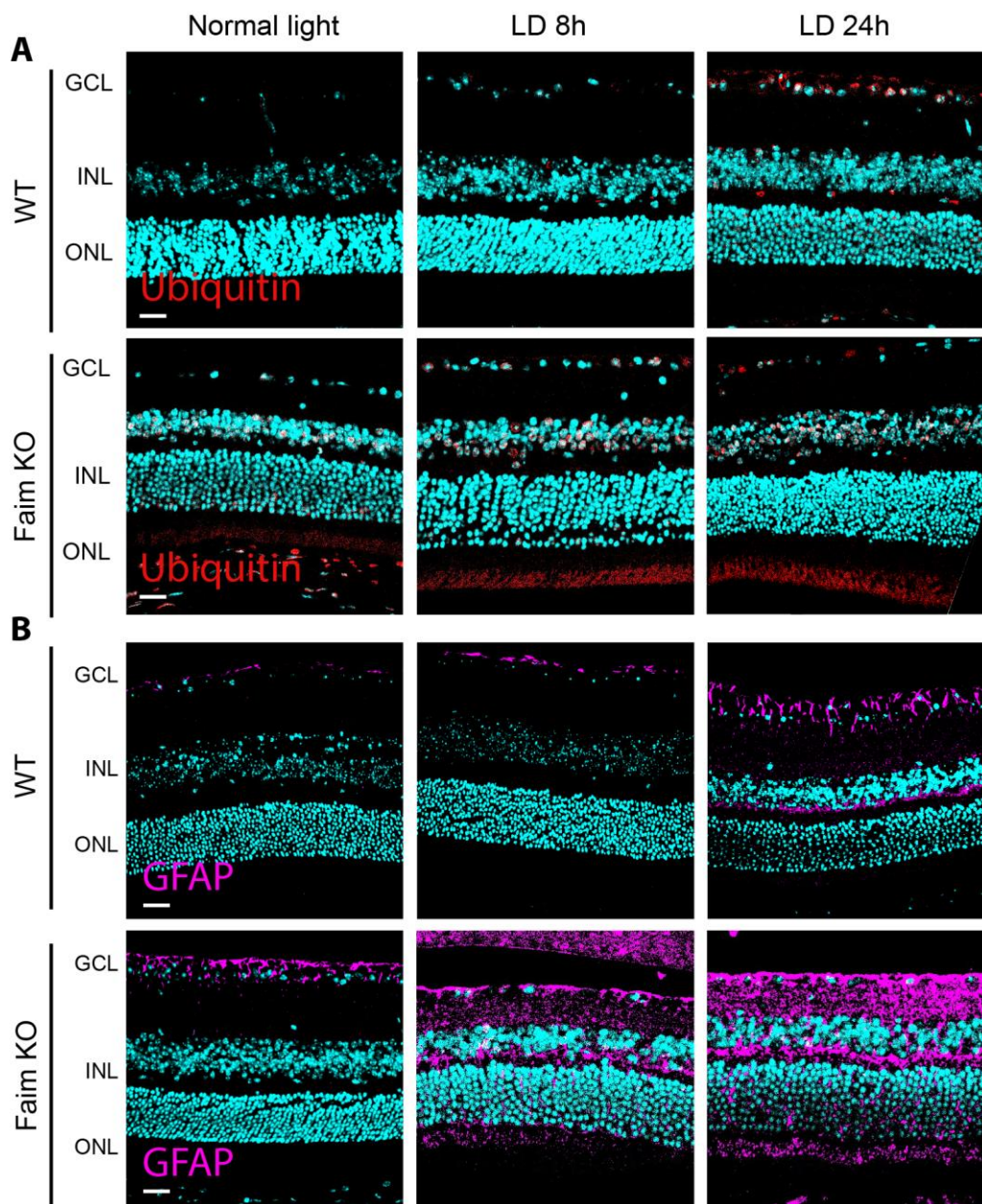


**Figure 16. Faim KO retinas are more prone to accumulate ubiquitin aggregates and express more GFAP than WT mice after light damage.** Representative images of 4  $\mu\text{m}$  paraffin sections of retinas taken from 2-month-old mice exposed normal light and to light damage for 8h (LD 8h) or light damage for 24h (LD 24h). **(A)** Ubiquitin-positive cells in the INL were counted, and at least 5 images per mice were used and averaged. **(B)** Total GFAP intensity was quantified with ImageJ, at least 5 images per mice were used and averaged. **(C)** Each violin plot extends from the min to max values, the median is represented by a thick dashed line, and quartiles are represented by thin dotted lines (n=4-6 mice/group). Statistical analysis was performed using Two-way ANOVA \* p<0.05, \*\* p<0.01 \*\*\*\* p<0.001.

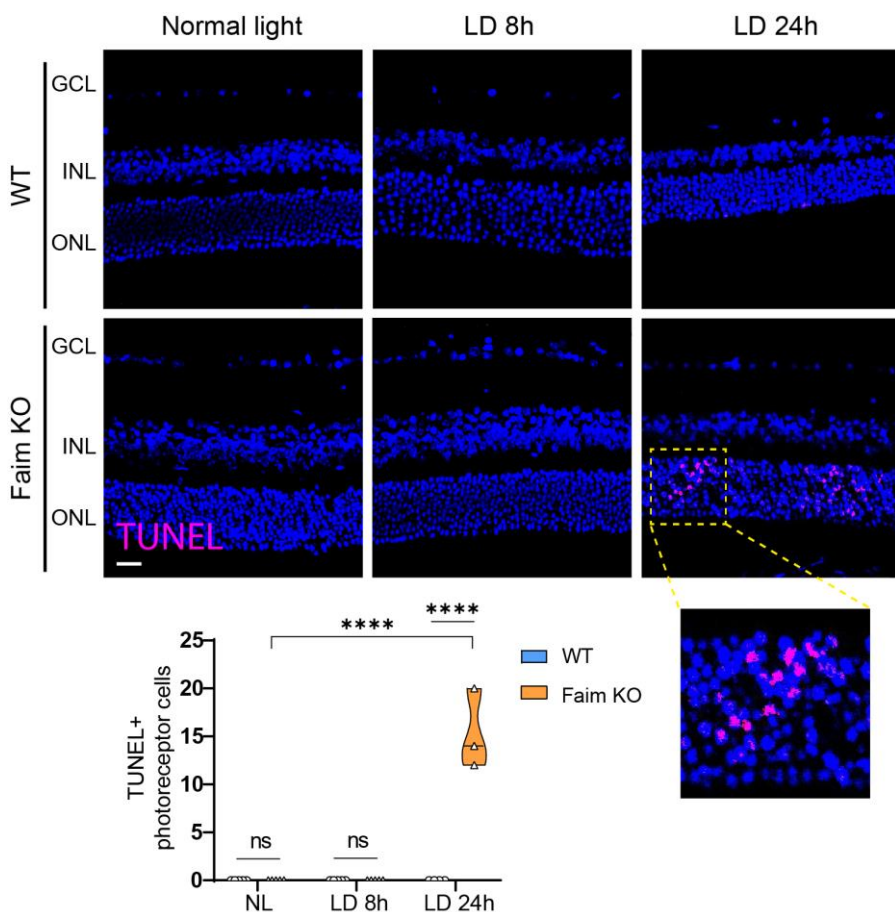


**Figure 17. Light-induced retinal degeneration (LIRD) in Faim KO mice after 24h of light exposure at 8,000 lux.** Representative images of 4  $\mu\text{m}$  paraffin sections of retinas taken from 2-month-old mice exposed normal light and to light damage for 8h (LD 8h) or light damage for 24h (LD 24h). Total number of TUNEL+ cells (*arrowheads*) per section were counted. Each violin plot extends from the min to max values, the median is represented by a thick dashed line, and quartiles are represented by thin dotted lines (n=4-6 mice/group). Statistical analysis was performed using Two-way ANOVA. \*\*\*\* p < 0.001.

Additionally, we recently performed bulk RNA-seq with mice exposed to LIRD for 24h at 8,000 lux to study whether Faim KO retinas countered light damage by overexpressing or downregulating a different set of genes in comparison to WT mice (**Figure 54**).

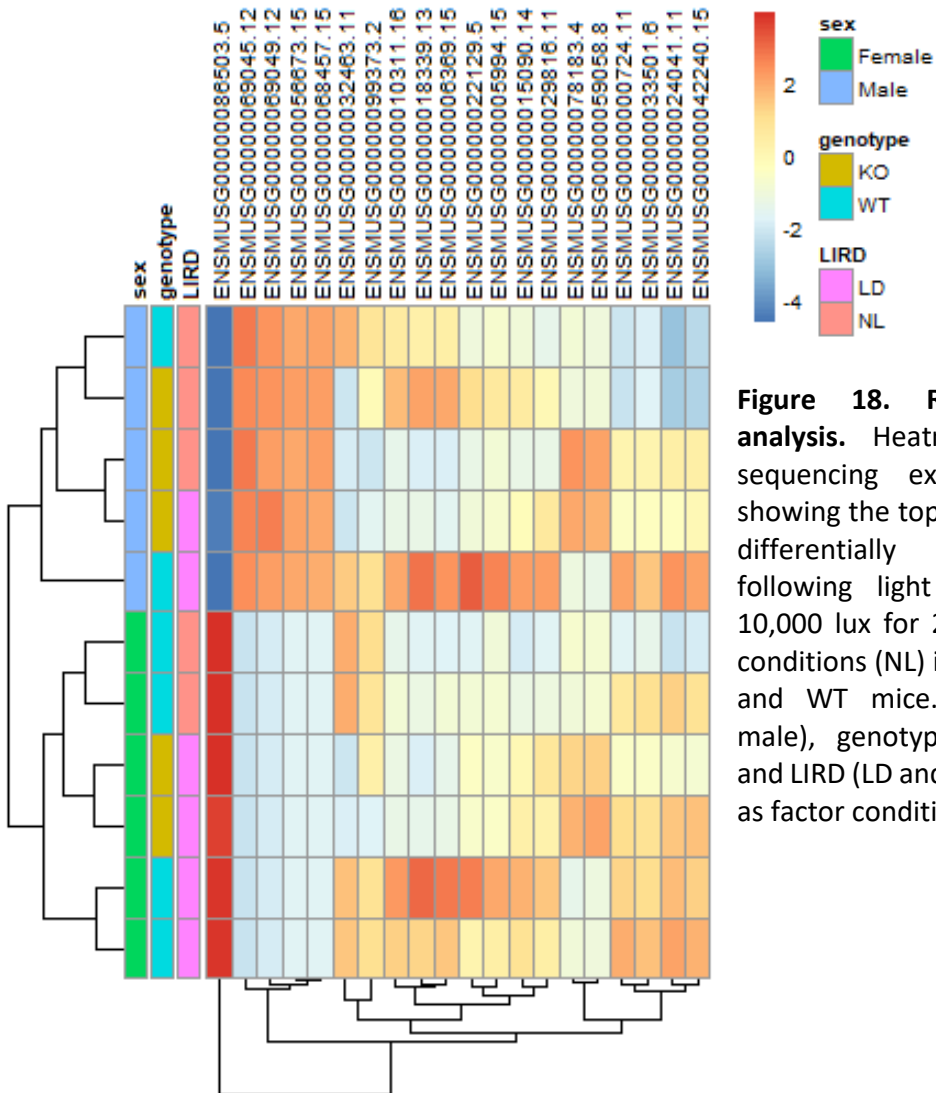


**Figure 18. RNA-seq data analysis.** Heatmap of RNA-sequencing expression data showing the top genes that are differentially regulated following light damage (LD, 10,000 lux for 24h) or normal conditions (NL) in Faim KO (KO) and WT mice. Sex (female, male), genotype (KO, WWT) and LIRD (LD and NL) are shown as factor conditions.



We used Gene Ontology (GO) terms for gene-enrichment analysis (Carbon et al. 2009; 2021) in order to identify potential associations. We found in preliminary results that Faim KO mice present a different response to WT against light damage and upregulate the expression of genes linked to inflammatory responses and cell death, and downregulate gene pathways linked to eye, retinal and neuronal development (**Table 7**).

**Table 7.** List of gene pathways upregulated or downregulated in Faim KO mice after light damage in comparison to WT mice.

<i>UPREGULATED GO pathway terms</i>	<i>DOWNREGULATED GO pathway terms</i>
GO:0006925 inflammatory cell apoptotic process	GO:0007423 sensory organ development
GO:0071346 cellular response to interferon-gamma	GO:0043010 camera-type eye development
GO:0006959 humoral immune response	GO:0002088 lens development in camera-type eye
GO:0002922 positive regulation of humoral immune response	GO:0045165 cell fate commitment
GO:0010939 regulation of necrotic cell death	GO:0048663 neuron fate commitment
GO:0070265 necrotic cell death	GO:0048568 embryonic organ

Therefore, this supports the notion that Faim KO mice behaves differently to WT mice in the presence of light damage, and that the consequences of the absence of FAIM are detrimental to the retina in response to light stress.

## 4. Discussion

In the present work we report for the first time how the mouse retina is functionally impaired in the absence of FAIM, following our previous results in which we showed how *Faim* KO mice present a neurodegenerative phenotype. Remarkably, this is also the first time that the lack of FAIM has been reported to cause a functional deficit in the CNS *in vivo*, specifically in the retina.

After assessing the retinal function through ERG analyses, we found a rod-driven retinal malfunction in photoreceptor (a-wave) and bipolar cells (b-wave) at 18 months, while cone pathways remained unaltered. This is consistent with previous single-cell RNA-seq analyses, in which we found that *Faim* expression was heavily enriched in rod photoreceptor cells in comparison to other neuronal cell types, including cone photoreceptors. This photoreceptor malfunction could be a result of the cell death that we previously reported at this age, though the relatively low number of TUNEL-positive cells that we encountered may not be enough to explain such retinal malfunction.

RGCs responses were also reduced in aged *Faim* KO mice, although not severely. This decrease in RGC electrical activity could be explained by the chronic pro-inflammatory phenotype and blood-brain barrier (BRB) breakdown that was previously found in these mice, which progressively worsened with age. Similarly, the retinal neurodegeneration in a tauopathy mouse model (P301S) (Yoshiyama et al. 2007; Xia et al. 2021), presents a progression timeline that resembles the one in *Faim* KO retinas. In the P301S model, impairment of the BRB (which is caused by abnormal tau accumulation) is observed from early ages and increases progressively, but RGC dysfunction only appears in aged mice (Xia et al. 2021), just like in *Faim*

KO mice. Likewise, in glaucoma, a disease characterized by progressive damage of the optic nerve produced by RGCs death, it has been reported how glial activation and neurovascular alterations are associated to RGC degeneration, and that Müller cell gliosis may exacerbate RGC apoptosis (Munemasa and Kitaoka 2012; Fernández-Albarral et al. 2021; Li et al. 2021).

Having observed at this point that a lack of Faim led to a neurodegenerative phenotype at late ages, we wanted to assess whether stress induction would trigger the same neurodegenerative phenotype at early ages. Hence, we used a protocol of mild light damage (10,000 lux for 8h) in 2 months-old mice. However, this light exposure was not enough to evoke the decrease in amplitude in the electrical responses of photoreceptors, bipolar cells or RGCs that we did observe at 18 months. Interestingly, although this protocol did not seem to alter retinal function, it was enough to elicit an increase in gliotic marker GFAP, ubiquitin aggregates and TUNEL-positive photoreceptor cells in Faim KO mice, both in respect to the WT mice exposed to the same conditions and to Faim KO mice without light damage. Although this phenotype could be predictive of a future retinal malfunction, our results were not conclusive on this end and additional light damage protocols with different light intensities and latency periods might be needed. This would allow us to ascertain whether Faim KO retinal function is sensible to light damage and whether FAIM confers protection against it, aside from a histopathological level.

Interestingly, it was described how after loss of half rod photoreceptors in murine retinas, rod bipolar cells were able to mitigate the deleterious effect by preserving their own voltage output and presenting normal b-wave responses (Care et al. 2020). These compensating mechanisms could be another plausible explanation as to why mild (10,000 lux for 8h) LIRD did not alter electrical

responses in Faim KO mice but did cause histopathological alterations in the form of ubiquitin aggregates and retinal gliosis.

In this regard, the effect of the substrain in which Faim KO mice were bred must be taken into account, as C57BL/6J mice are notoriously known in the ophthalmologic field for its light damage resistance (Bravo-Nuevo, Walsh, and Stone 2004). Hence, we cannot dismiss the possible limitations of this study, in which the specific conditions of light intensity and duration of light exposure may not have been enough to induce a significant LIRD.

Incidentally, a stronger LIRD protocol (10,000 lux for 24h) increased the accumulation of ubiquitin aggregates, the severity of retinal gliosis, and caused photoreceptor cell death, which was not present with milder conditions. To this end, it would be very useful to assess the retinal function of Faim KO and WT mice exposed to the more severe LIRD protocol, given these conditions may be enough to cause a deficit in retinal activity.

The use of LIRD protocols and mouse models allows to replicate the damage caused by environmental exposure to high levels of light in retinal diseases like AMD or inherited retinal dystrophies, which accelerate loss of vision (Remé et al. 1998; Wenzel et al. 2005). After light damage, a persistent bleaching of rhodopsin caused by excessive photon absorption follows, increasing the rate of rhodopsin deactivation and regeneration in photoreceptors in order to adapt to these conditions. This leads to the deleterious production of phototoxic products (Wenzel et al. 2005; C Grimm et al. 2000) that accumulate in photoreceptors, which are particularly sensible to this kind of stress, ultimately causing photoreceptor death (Saari et al. 1998). In view of this, it could be interesting to explore whether Faim KO retinas exhibit accumulation of oxidative species in photoreceptors, which could be measured by normal phase

HPLC (T. Maeda, Golczak, and Maeda 2012; A. Maeda et al. 2009; Różanowska and Sarna 2005). This would provide us great insight of the possible mechanisms by which the absence of Faim leads to photoreceptor cell death.

To avoid the phototoxic effects of a persistent rhodopsin signalling it is essential to maintain an adequate photoresponse termination, which is also a key process for dark adaptation (Weiss 2020). To this end, transgenic mice that present functional alterations in proteins involved in rhodopsin deactivation, like Arrestin-1 and GRK1, have been studied (Coleman and Semple-Rowland 2005; Frederiksen et al. 2016; Aryan et al. 2020; Bayburt et al. 2011; Sokolov et al. 2004). For instance, in mouse models in which the SAG gene (which encodes Arrestin-1) is mutated or Arrestin-1 function is compromised, photoresponse is not properly inhibited and the retina is incapable of adequate dark adaptation, which can lead to night blindness (Gurevich and Gurevich 2019). Intriguingly, when we studied retinal function in Faim KO mice we found a severe delay in dark adaptation in young and aged mice, implying that FAIM could be involved in this mechanism.

Dark adaptation allows the retina to increase its sensitivity in the dark after bright light exposure, and it relies in adequate photoresponse termination (Kalloniatis and Luu 2007; J. Chen et al. 1995; Xu et al. 1997; C. K. Chen et al. 1999). Following disruption of dark adaptation, temporal resolution of vision is impaired, and it can lead to suboptimal eyesight and night blindness. This symptomatology is characteristic of congenital stationary night blindness (CSNB) (Singhal et al. 2013), Oguchi disease (Fuchs et al. 1995; Yamamoto et al. 1997) or Retinitis Pigmentosa (RP), diseases that are directly linked to Arrestin-1 and GRK1 (J. Chen et al. 1999; Fuchs et al. 1995; Dai and Sun 2021; Aryan et al. 2020) and Rhodopsin and Transducin- $\alpha$  (Singhal et al. 2013; Zeitz,

Robson, and Audo 2015; Kim 2019). This type of retinopathologies are rare, and there is no cure or treatment to date (Dai and Sun 2021; Singhal et al. 2013; Das et al. 2019). To explore a possible role of FAIM, it would be interesting to quantify the levels of FAIM-L and FAIM-S in retinas of mouse models or patients of these diseases.

To study the mechanism by which the absence of FAIM causes a dark adaptation delay, we focused on Arrestin-1 function, which is crucial for photoresponse termination. Hence, we assessed its process of translocation within photoreceptor segments, given this is a key event in phototransduction signalling (Sokolov et al. 2002; Majumder et al. 2013). We observed how Arrestin-1 translocation was delayed in Faim KO in comparison to WT mice, which suggests that FAIM could be important for adequate dark adaptation through the modulation of Arrestin-1 translocation.

The mechanism underlying the kinetics of this translocation is unknown, and different hypotheses have been enunciated (Sokolov et al. 2002; Nair et al. 2005). Protein-protein interactions in phototransduction are under a strict control for adaptational responses to light exposure and photoreceptor cell viability (Campello et al. 2013), and it has been described that ubiquitin holds a role in protein trafficking. For instance, a ubiquitin-dependent regulation of Transducin- $\alpha$  translocation has been proposed. In this model, Cul3-RetUbE3, an E3 ligase, modulates Transducin- $\alpha$  translocation through the ubiquitination and degradation of Unc119, an interacting partner of Transducin- $\alpha$ . Thus, alterations in Cul3-RetUbE3 or Unc119 protein levels or function results in a delay in light and dark-dependent Transducin- $\alpha$  translocation (Chaya et al. 2019). Although we did not find alterations in Transducin- $\alpha$  translocation in Faim KO mice, its protein levels were reduced at 18 months of age. A significant reduction in Transducin- $\alpha$  could hinder phototransduction and even

cause a decrease in a-wave amplitudes, which we observed in our Faim KO at the same age. Therefore, the study of possible alterations in the ubiquitination of Transducin-  $\alpha$  or its partner Unc119 would be interesting.

Curiously, there is not much available information regarding visual Arrestin-1 ubiquitination. Ubiquitination of the Arrestin family was first demonstrated for the mammalian and nonvisual  $\beta$ -Arrestin-2. After agonist stimulation,  $\beta$ -Arrestin-2 immunoprecipitates were accompanied by a smear of ubiquitination (Kommaddi and Shenoy 2013).

Previous results describe how FAIM has a role in modulating ubiquitination. For instance, we have shown FAIM-L blocks XIAP auto-ubiquitination (Moubarak et al. 2013), and Rothstein and colleagues established how in the absence of FAIM-S there was an accumulation of ubiquitin aggregates after oxidative stress (Kaku and Rothstein 2020). Upon seeing the roles of ubiquitin in protein translocation and after we found a specific delay in Arrestin-1 translocation in FAIM KO retinas, we studied Arrestin-1 ubiquitination and showed that 1) Arrestin-1 is susceptible to ubiquitination *in vitro*, and 2) its ubiquitination is greatly reduced after overexpressing FAIM-S or FAIM-L. Thus, in the presence of FAIM, Arrestin-1 ubiquitination is decreased and almost abrogated.

Interestingly, it has been reported how oxidative stress causes the aggregation of Rhodopsin and Transducin- $\alpha$ , and how this aggregation targets them for ubiquitin-mediated degradation (Illing et al. 2002; Schmidt et al. 2021; Shang and Taylor 2011). This field has not been extensively studied, and to the best of our knowledge, this is the first time that a visual Arrestin-1 has been shown to be susceptible of ubiquitination. To further explore this, it would be interesting to study whether oxidative stress generated by light damage causes

Arrestin-1 ubiquitination and its consequent aggregation in WT mice, and whether the absence of Faim exacerbates this mechanism.

Moreover, it would be valuable to discern what type of Arrestin-1 ubiquitination is FAIM blocking. In this regard, performing ubiquitin assays in the presence of proteasome inhibitor MG132 provided valuable information, since we found that at least a fraction of the ubiquitination that FAIM is blocking is degradative. Agreeing with these results, we found a decrease in Arrestin-1 protein levels in Faim KO mice, meaning that Arrestin-1 is excessively being targeted for degradation via the UPS in the absence of FAIM. Given the mechanism of ubiquitin chain elongation, we could perform additional ubiquitin assays with mutated lysines to discern the type of ubiquitination that FAIM is blocking, namely polyubiquitination (which usually leads to proteasomal degradation), mono or multiubiquitination (linked to signalling properties or receptor endocytosis) (Haglund and Dikic 2005; Thrower et al. 2000).

In summary, we have observed that Faim KO mice present retinal malfunction at late ages and a delay in dark adaptation from two months, and we believe the latter could be linked to alterations in Arrestin-1 translocation upon light reception. Hence, it is possible that the ultimate goal of FAIM is to assist Arrestin-1 translocation through the modulation of its ubiquitination, similarly to the process that regulates this movement in Transducin- $\alpha$  (Chaya et al. 2019). Therefore, in the absence of Faim, Arrestin-1 ubiquitination would be increased, hampering its translocation and causing a delay in dark adaptation. The obstruction of the role of Arrestin-1 in rhodopsin deactivation by a lack of FAIM could lead to impaired rhodopsin degradation, rendering photoreceptors more sensitive to age-related neurodegenerative events and to light damage, ultimately causing functional alterations in rod photoreceptor and bipolar cells.



Hereby, we propose that FAIM has a role in phototransduction termination through its ability to promote Arrestin-1 translocation, and as a result of this, Faim KO retinas present a symptomatology that is typically found in night blindness disorders. In view of this, we believe that research in proteins involved in the mechanisms underlying these diseases, such as FAIM, is of utmost importance.

## 5. References

- Anderson, Peter Jb, Hr Watts, Cj Hille, Kl Philpott, P Clark, M Croucher S Gentleman, and Ling-Sun Jen. 2008. "Glial and Endothelial Blood-Retinal Barrier Responses to Amyloid-Beta in the Neural Retina of the Rat." *Clinical Ophthalmology (Auckland, N.Z.)* 2 (4): 801–16. <https://doi.org/10.2147/oph.s3967>.
- Aryan, Hajar, Atekeh Bahadori, Dariush D. Farhud, Marjan Zarif Yeganeh, and Haniyeh Pourkalthor. 2020. "A Homozygote Mutation in S-Antigen Visual Arrestin SAG Gene in an Iranian Patient with Oguchi Type One: A Case Report." *Iranian Journal of Public Health* 49 (5). <https://doi.org/10.18502/ijph.v49i5.3219>.
- Bayburt, Timothy H., Sergey A. Vishnivetskiy, Mark A. McLean, Takefumi Morizumi, Chih Chin Huang, John J.G. Tesmer, Oliver P. Ernst, Stephen G. Sligar, and Vsevolod V. Gurevich. 2011. "Monomeric Rhodopsin Is Sufficient for Normal Rhodopsin Kinase (GRK1) Phosphorylation and Arrestin-1 Binding." *Journal of Biological Chemistry* 286 (2): 1420–28. <https://doi.org/10.1074/JBC.M110.151043>.
- Berger, Adeline, Sophie Cavallero, Elisa Dominguez, Peggy Barbe, Manuel Simonutti, José Alain Sahel, Florian Sennlaub, William Raoul, Michel Paques, and Alexis Pierre Bemelmans. 2014. "Spectral-Domain Optical Coherence Tomography of the Rodent Eye: Highlighting Layers of the Outer Retina Using Signal Averaging and Comparison with Histology." *PLoS ONE* 9 (5).
- Bourne, Rupert R.A., Jaimie D. Steinmetz, Seth Flaxman, Paul Svitil Briant, Hugh R. Taylor, Serge Resnikoff, Robert James Casson, et al. 2021. "Trends in Prevalence of Blindness and Distance and near Vision Impairment over 30 Years: An Analysis for the Global Burden of Disease Study." *The Lancet Global Health* 9 (2): e130–43. [https://doi.org/10.1016/S2214-109X\(20\)30425-3](https://doi.org/10.1016/S2214-109X(20)30425-3).
- Bravo-Nuevo, Arturo, Natalie Walsh, and Jonathan Stone. 2004. "Photoreceptor Degeneration and Loss of Retinal Function in the C57BL/6-C2J Mouse." *Investigative Ophthalmology and Visual Science* 45 (6): 2005–12. <https://doi.org/10.1167/iovs.03-0842>.
- Campello, Laura, Julián Esteve-Rudd, Nicolás Cuenca, and José Martín-Nieto. 2013. "The

Ubiquitin-Proteasome System in Retinal Health and Disease.” *Molecular Neurobiology* 47 (2): 790–810. <https://doi.org/10.1007/s12035-012-8391-5>.

Carbon, Seth, Eric Douglass, Benjamin M. Good, Deepak R. Unni, Nomi L. Harris, Christopher J. Mungall, Siddhartha Basu, et al. 2021. “The Gene Ontology Resource: Enriching a Gold Mine.” *Nucleic Acids Research* 49 (D1): D325–34. <https://doi.org/10.1093/NAR/GKAA1113>.

Carbon, Seth, Amelia Ireland, Christopher J. Mungall, Shengqiang Shu, Brad Marshall, Suzanna Lewis, Jane Lomax, et al. 2009. “AmiGO: Online Access to Ontology and Annotation Data.” *Bioinformatics* 25 (2): 288–89. <https://doi.org/10.1093/BIOINFORMATICS/BTN615>.

Care, Rachel A., Ivan A. Anastassov, David B. Kastner, Yien Ming Kuo, Luca Della Santina, and Felice A. Dunn. 2020. “Mature Retina Compensates Functionally for Partial Loss of Rod Photoreceptors.” *Cell Reports* 31 (10): 107730. <https://doi.org/10.1016/j.celrep.2020.107730>.

Carriba, P, S Jimenez, V Navarro, and R S Moubarak. 2015. “Amyloid- $\beta$  Reduces the Expression of Neuronal FAIM-L , Thereby Shifting the Inflammatory Response Mediated by TNF  $\alpha$  from Neuronal Protection to Death.” *Cell Death and Disease* 6 (2): e1639-13. <https://doi.org/10.1038/cddis.2015.6>.

Chaya, Taro, Ryotaro Tsutsumi, Leah Rie Varner, Yamato Maeda, Satoyo Yoshida, and Takahisa Furukawa. 2019. “Cul3-Klhl18 Ubiquitin Ligase Modulates Rod Transducin Translocation during Light-dark Adaptation.” *The EMBO Journal* 38 (23). <https://doi.org/10.15252/embj.2018101409>.

Chen, Ching Kang, Marie E. Burns, Maribeth Spencer, Gregory A. Niemi, Jeannie Chen, James B. Hurley, Denis A. Baylor, and Melvin I. Simon. 1999. “Abnormal Photoresponses and Light-Induced Apoptosis in Rods Lacking Rhodopsin Kinase.” *Proceedings of the National Academy of Sciences of the United States of America* 96 (7): 3718–22. <https://doi.org/10.1073/pnas.96.7.3718>.

Chen, Jeannie, Clint L. Makino, Neal S. Peachey, Denis A. Baylor, and Melvin I. Simon. 1995. “Mechanisms of Rhodopsin Inactivation in Vivo as Revealed by a COOH-

Terminal Truncation Mutant.” *Science* 267 (5196): 374–77.

<https://doi.org/10.1126/SCIENCE.7824934>.

Chen, Jeannie, Melvin I. Simon, Michael T. Matthes, Douglas Yasumura, and Matthew M. LaVail. 1999. “Increased Susceptibility to Light Damage in an Arrestin Knockout Mouse Model of Oguchi Disease (Stationary Night Blindness).” *Investigative Ophthalmology and Visual Science* 40 (12): 2978–82.

Coleman, Jason E., and Susan L. Semple-Rowland. 2005. “GC1 Deletion Prevents Light-Dependent Arrestin Translocation in Mouse Cone Photoreceptor Cells.” *Investigative Ophthalmology and Visual Science* 46 (1): 12–16. <https://doi.org/10.1167/iovs.04-0691>.

Dai, Ying, and Tao Sun. 2021. “Oguchi’s Disease: Two Cases and Literature Review.” *The Journal of International Medical Research* 49 (5). <https://doi.org/10.1177/03000605211019921>.

Das, Rueben G., Doreen Becker, Vidhya Jagannathan, Orly Goldstein, Evelyn Santana, Kendall Carlin, Raghavi Sudharsan, et al. 2019. “Genome-Wide Association Study and Whole-Genome Sequencing Identify a Deletion in LRIT3 Associated with Canine Congenital Stationary Night Blindness.” *Scientific Reports* 2019 9:19 (1): 1–12. <https://doi.org/10.1038/s41598-019-50573-7>.

Dobin, Alexander, Carrie A. Davis, Felix Schlesinger, Jorg Drenkow, Chris Zaleski, Sonali Jha, Philippe Batut, Mark Chaisson, and Thomas R. Gingeras. 2013. “STAR: Ultrafast Universal RNA-Seq Aligner.” *Bioinformatics (Oxford, England)* 29 (1): 15–21. <https://doi.org/10.1093/BIOINFORMATICS/BTS635>.

Fernández-Albarral, José A., Juan J. Salazar, Rosa de Hoz, Eva M. Marco, Beatriz Martín-Sánchez, Elena Flores-Salguero, Elena Salobar-García, et al. 2021. “Retinal Molecular Changes Are Associated with Neuroinflammation and Loss of RGCs in an Experimental Model of Glaucoma.” *International Journal of Molecular Sciences* 22 (4): 1–29. <https://doi.org/10.3390/IJMS22042066>.

Fernández-Sánchez, Laura, Pedro Lax, Carolina Isiegas, Eduard Ayuso, José M. Ruiz, Pedro De La Villa, Fatima Bosch, Enrique J. De La Rosa, and Nicolás Cuenca. 2012.

- “Proinsulin Slows Retinal Degeneration and Vision Loss in the P23H Rat Model of Retinitis Pigmentosa.” *Human Gene Therapy* 23 (12): 1290–1300.  
<https://doi.org/10.1089/hum.2012.067>.
- Flick, Karin, and Peter Kaiser. 2012. “Protein Degradation and the Stress Response.” *Semin Cell Dev Biol.* 23 (5): 515–22. <https://doi.org/10.1016/j.semcdb.2012.01.019>.
- Frederiksen, Rikard, Soile Nymark, Alexander V. Kolesnikov, Justin D. Berry, Leopold Adler, Yiannis Koutalos, Vladimir J. Kefalov, and M. Carter Cornwall. 2016. “Rhodopsin Kinase and Arrestin Binding Control the Decay of Photoactivated Rhodopsin and Dark Adaptation of Mouse Rods.” *The Journal of General Physiology* 148 (1): 1–11. <https://doi.org/10.1085/JGP.201511538>.
- Fu, Zhongjie, Shen Nian, Suk Yee Li, David Wong, Sookja K. Chung, and Amy C.Y. Lo. 2015. “Deficiency of Aldose Reductase Attenuates Inner Retinal Neuronal Changes in a Mouse Model of Retinopathy of Prematurity.” *Graefe’s Archive for Clinical and Experimental Ophthalmology* 253 (9): 1503–13. <https://doi.org/10.1007/S00417-015-3024-0>.
- Fuchs, Sigrid, Mitsuru Nakazawa, Marion Maw, Makoto Tamai, Yoshihisa Oguchi, and Andreas Gal. 1995. “Oguchi Disease in Japanese” 10 (july): 360–62.
- Gosbell, Andrew D., Nada Stefanovic, Lyndee L. Scurr, Josefa Pete, Ismail Kola, Ian Favilla, and Judy B. De Haan. 2006. “Retinal Light Damage: Structural and Functional Effects of the Antioxidant Glutathione Peroxidase-1.” *Investigative Ophthalmology and Visual Science* 47 (6): 2613–22. <https://doi.org/10.1167/iovs.05-0962>.
- Grimm, C, A Wenzel, F Hafezi, S Yu, T M Redmond, and C E Remé. 2000. “Protection of Rpe65-Deficient Mice Identifies Rhodopsin as a Mediator of Light-Induced Retinal Degeneration.” *Nature Genetics* 25 (1): 63–66. <https://doi.org/10.1038/75614>.
- Grimm, Christian, and Charlotte E. Remé. 2013. “Light Damage as a Model of Retinal Degeneration.” *Methods in Molecular Biology* 935: 87–97.  
<https://doi.org/10.1007/978-1-62703-080-9-6>.
- . 2019. “Light Damage Models of Retinal Degeneration.” *Methods in Molecular*

*Biology* 1834: 167–78. [https://doi.org/10.1007/978-1-4939-8669-9\\_12](https://doi.org/10.1007/978-1-4939-8669-9_12).

- Gurevich, Vsevolod V, and Eugenia V Gurevich. 2019. “Arrestin Mutations: Some Cause Diseases, Others Promise Cure.” *Progress in Molecular Biology and Translational Science* 161: 29–45. <https://doi.org/10.1016/bs.pmbts.2018.09.004>.
- Haglund, Kaisa, and Ivan Dikic. 2005. “Ubiquitylation and Cell Signaling.” *EMBO Journal* 24 (19): 3353–59. <https://doi.org/10.1038/SJ.EMBOJ.7600808>.
- Hao, Wenshan, Andreas Wenzel, Martin S. Obin, Ching Kang Chen, Elliott Brill, Nataliia V. Krasnoperova, Pamela Eversole-Cire, et al. 2002. “Evidence for Two Apoptotic Pathways in Light-Induced Retinal Degeneration.” *Nature Genetics* 32 (2): 254–60. <https://doi.org/10.1038/ng984>.
- Huo, J, S Xu, K Guo, Q Zeng, and K-p Lam. 2009. “Genetic Deletion of Faim Reveals Its Role in Modulating C-FLIP Expression during CD95-Mediated Apoptosis of Lymphocytes and Hepatocytes.” *Cell Death and Differentiation*, 1062–70. <https://doi.org/10.1038/cdd.2009.26>.
- Illing, Michelle E., Rahul S. Rajan, Neil F. Bence, and Ron R. Kopito. 2002. “A Rhodopsin Mutant Linked to Autosomal Dominant Retinitis Pigmentosa Is Prone to Aggregate and Interacts with the Ubiquitin Proteasome System.” *The Journal of Biological Chemistry* 277 (37): 34150–60. <https://doi.org/10.1074/jbc.M204955200>.
- Joly, S., C. Lange, M. Thiersch, M. Samardzija, and C. Grimm. 2008. “Leukemia Inhibitory Factor Extends the Lifespan of Injured Photoreceptors In Vivo.” *Journal of Neuroscience* 28 (51): 13765–74. <https://doi.org/10.1523/jneurosci.5114-08.2008>.
- Kaku, Hiroaki, and Thomas L. Rothstein. 2020. “FAIM Is a Non-Redundant Defender of Cellular Viability in the Face of Heat and Oxidative Stress and Interferes With Accumulation of Stress-Induced Protein Aggregates.” *Frontiers in Molecular Biosciences* 7 (February): 1–10. <https://doi.org/10.3389/fmolb.2020.00032>.
- Kalloniatas, Michael, and Charles Luu. 2007. “Light and Dark Adaptation.” *The Australasian Journal of Optometry* 18 (8): 384–85. <https://doi.org/10.1111/j.1444-0938.1935.tb05750.x>.

- Kim, Leo. 2019. "Congenital Stationary Night Blindness (CSNB)," 2019.  
[https://eyewiki.aao.org/Congenital\\_Stationary\\_Night\\_Blindness\\_\(CSNB\)](https://eyewiki.aao.org/Congenital_Stationary_Night_Blindness_(CSNB)).
- Kommaddi, Reddy Peera, and Sudha K. Shenoy. 2013. *Arrestins and Protein Ubiquitination. Progress in Molecular Biology and Translational Science*. 1st ed. Vol. 118. Elsevier Inc. <https://doi.org/10.1016/B978-0-12-394440-5.00007-3>.
- Krigel, A., M. Berdugo, E. Picard, R. Levy-Boukris, I. Jaadane, L. Jonet, M. Dernigoghossian, C. Andrieu-Soler, A. Torriglia, and F. Behar-Cohen. 2016. "Light-Induced Retinal Damage Using Different Light Sources, Protocols and Rat Strains Reveals LED Phototoxicity." *Neuroscience* 339 (October): 296–307.  
<https://doi.org/10.1016/j.neuroscience.2016.10.015>.
- Li, Qian, Yun Cheng, Shenghai Zhang, Xinghuai Sun, and Jihong Wu. 2021. "TRPV4-Induced Müller Cell Gliosis and TNF- $\alpha$  Elevation-Mediated Retinal Ganglion Cell Apoptosis in Glaucomatous Rats via JAK2/STAT3/NF-KB Pathway." *Journal of Neuroinflammation* 2021 18:1 18 (1): 1–22. <https://doi.org/10.1186/S12974-021-02315-8>.
- Liu, Changdong, Min Peng, Alan M Laties, and Rong Wen. 1998. "Preconditioning with Bright Light Evokes a Protective Response against Light Damage in the Rat Retina." *The Journal of Neuroscience* 18 (4): 1337 LP – 1344.  
<https://doi.org/10.1523/JNEUROSCI.18-04-01337.1998>.
- London, Anat, Inbal Benhar, and Michal Schwartz. 2013. "The Retina as a Window to the Brain - From Eye Research to CNS Disorders." *Nature Reviews Neurology* 9 (1): 44–53. <https://doi.org/10.1038/nrneurol.2012.227>.
- Love, Michael I., Wolfgang Huber, and Simon Anders. 2014. "Moderated Estimation of Fold Change and Dispersion for RNA-Seq Data with DESeq2." *Genome Biology* 15 (12): 1–21. <https://doi.org/10.1186/S13059-014-0550-8/FIGURES/9>.
- Lyubarsky, A., S. Nikonov, and E. N. Pugh. 1996. "The Kinetics of Inactivation of the Rod Phototransduction Cascade with Constant Ca<sup>2+</sup>." *Journal of General Physiology* 107 (1): 19–34. <https://doi.org/10.1085/jgp.107.1.19>.

- Maeda, Akiko, Tadao Maeda, Marcin Golczak, Steven Chou, Amal Desai, Charles L. Hoppel, Shigemi Matsuyama, and Krzysztof Palczewski. 2009. "Involvement of All-Trans-Retinal in Acute Light-Induced Retinopathy of Mice." *Journal of Biological Chemistry* 284 (22): 15173–83. <https://doi.org/10.1074/JBC.M900322200>.
- Maeda, Tadao, Marcin Golczak, and Akiko Maeda. 2012. "Retinal Photodamage Mediated by All-Trans-Retinal." *Photochemistry and Photobiology* 88 (6): 1309–19. <https://doi.org/10.1111/j.1751-1097.2012.01143.x>.
- Majumder, Anurima, Johan Pahlberg, Kimberly K. Boyd, Vasily Kerov, Saravanan Kolandaivelu, Visvanathan Ramamurthy, Alapakkam P. Sampath, and Nikolai O. Artemyev. 2013. "Transducin Translocation Contributes to Rod Survival and Enhances Synaptic Transmission from Rods to Rod Bipolar Cells." *Proceedings of the National Academy of Sciences of the United States of America* 110 (30): 12468–73. <https://doi.org/10.1073/pnas.1222666110>.
- Martínez-Mármol, Ramón, Bruna Barneda-Zahonero, David Soto, Rosa Maria Andrés, Elena Coccia, Xavier Gasull, Laura Planells-Ferrer, Rana S. Moubarak, Eduardo Soriano, and Joan X. Comella. 2016. "FAIM-L Regulation of XIAP Degradation Modulates Synaptic Long-Term Depression and Axon Degeneration." *Scientific Reports* 6 (November 2015): 1–16. <https://doi.org/10.1038/srep35775>.
- Mendez, Ana, Janis Lem, Melvin Simon, and Jeannie Chen. 2003. "Light-Dependent Translocation of Arrestin in the Absence of Rhodopsin Phosphorylation and Transducin Signaling." *Journal of Neuroscience* 23 (8): 3124–29. <https://doi.org/10.1523/jneurosci.23-08-03124.2003>.
- Moubarak, R. S., L. Planells-Ferrer, J. Urresti, S. Reix, M. F. Segura, P. Carriba, F. Marques-Fernandez, et al. 2013. "FAIM-L Is an IAP-Binding Protein That Inhibits XIAP Ubiquitinylation and Protects from Fas-Induced Apoptosis." *Journal of Neuroscience* 33 (49): 19262–75. <https://doi.org/10.1523/JNEUROSCI.2479-13.2013>.
- Mukhopadhyay, Debdyuti, and Howard Riezman. 2007. "Proteasome-Independent Functions of Ubiquitin in Endocytosis and Signaling." *Science* 315 (5809): 201–5. <https://doi.org/10.1126/SCIENCE.1127085>.



- Munemasa, Yasunari, and Yasushi Kitaoka. 2012. "Molecular Mechanisms of Retinal Ganglion Cell Degeneration in Glaucoma and Future Prospects for Cell Body and Axonal Protection." *Frontiers in Cellular Neuroscience* 6 (DEC).  
<https://doi.org/10.3389/FNCEL.2012.00060>.
- Nair, K. Saidas, Susan M. Hanson, Ana Mendez, Eugenia V. Gurevich, Matthew J. Kennedy, Valery I. Shestopalov, Sergey A. Vishnivetskiy, et al. 2005. "Light-Dependent Redistribution of Arrestin in Vertebrate Rods Is an Energy-Independent Process Governed by Protein-Protein Interactions." *Neuron* 46 (4): 555–67.  
<https://doi.org/10.1016/j.neuron.2005.03.023>.
- Obin, Martin S., Jessica Jahngen-Hodge, Thomas Nowell, and Allen Taylor. 1996. "Ubiquitinylation and Ubiquitin-Dependent Proteolysis in Vertebrate Photoreceptors (Rod Outer Segments): EVIDENCE FOR UBIQUITINYLATION OF Gt AND RHODOPSIN." *Journal of Biological Chemistry* 271 (24): 14473–84.  
<https://doi.org/10.1074/JBC.271.24.14473>.
- Pearson, Rachael A, and Robin R Ali. 2018. "Unlocking the Potential for Endogenous Repair to Restore Sight." *Neuron* 100 (3): 524–26.  
<https://doi.org/10.1016/j.neuron.2018.10.035>.
- Remé, C E, C Grimm, F Hafezi, A Marti, and A Wenzel. 1998. "Apoptotic Cell Death in Retinal Degenerations." *Progress in Retinal and Eye Research* 17 (4): 443–64.  
[https://doi.org/10.1016/s1350-9462\(98\)00009-3](https://doi.org/10.1016/s1350-9462(98)00009-3).
- Różanowska, Małgorzata, and Tadeusz Sarna. 2005. "Light-Induced Damage to the Retina: Role of Rhodopsin Chromophore Revisited." *Photochemistry and Photobiology* 81 (6): 1305. <https://doi.org/10.1562/2004-11-13-ir-371>.
- RStudio Team. 2015. "RStudio: Integrated Development Environment for R." Boston, MA.  
<http://www.rstudio.com/>.
- Saari, John C., Gregory G. Garwin, J. Preston Van Hooser, and Krzysztof Palczewski. 1998. "Reduction of All-Trans-Retinal Limits Regeneration of Visual Pigment in Mice." *Vision Research* 38 (10): 1325–33. [https://doi.org/10.1016/S0042-6989\(97\)00198-3](https://doi.org/10.1016/S0042-6989(97)00198-3).

- Samaranayake, Srimal, Sergey A. Vishnivetskiy, Camilla R. Shores, Kimberly C. Thibeault, Seunghyi Kook, Jeannie Chen, Marie E. Burns, Eugenia V. Gurevich, and Vsevolod V. Gurevich. 2020. "Biological Role of Arrestin-1 Oligomerization." *Journal of Neuroscience* 40 (42): 8055–69. <https://doi.org/10.1523/JNEUROSCI.0749-20.2020>.
- Sánchez-Cruz, Alonso, Andrea C. Méndez, Ignacio Lizasoain, Pedro de la Villa, Enrique J. de la Rosa, and Catalina Hernández-Sánchez. 2021. "Tlr2 Gene Deletion Delays Retinal Degeneration in Two Genetically Distinct Mouse Models of Retinitis Pigmentosa." *International Journal of Molecular Sciences* 22 (15). <https://doi.org/10.3390/ijms22157815>.
- Schmidt, Marlene F., Zhong Yan Gan, David Komander, and Grant Dewson. 2021. "Ubiquitin Signalling in Neurodegeneration: Mechanisms and Therapeutic Opportunities." *Cell Death and Differentiation* 28 (2): 570–90. <https://doi.org/10.1038/s41418-020-00706-7>.
- Schneider, Caroline A, Wayne S Rasband, and Kevin W Eliceiri. 2012. "NIH Image to ImageJ: 25 Years of Image Analysis." *Nature Methods* 9 (7): 671–75. <https://doi.org/10.1038/nmeth.2089>.
- Segura, M. F., C. Sole, M. Pascual, R. S. Moubarak, M. Jose Perez-Garcia, R. Gozzelino, V. Iglesias, et al. 2007. "The Long Form of Fas Apoptotic Inhibitory Molecule Is Expressed Specifically in Neurons and Protects Them against Death Receptor-Triggered Apoptosis." *Journal of Neuroscience* 27 (42): 11228–41. <https://doi.org/10.1523/JNEUROSCI.3462-07.2007>.
- Shang, Fu, and Allen Taylor. 2011. "Ubiquitin-Proteasome Pathway and Cellular Responses to Oxidative Stress." *Free Radical Biology & Medicine* 51 (1): 5. <https://doi.org/10.1016/J.FREERADBIOMED.2011.03.031>.
- Singhal, Ankita, Martin K. Ostermaier, Sergey A. Vishnivetskiy, Valérie Panneels, Kristoff T. Homan, John J.G. Tesmer, Dmitry Veprintsev, et al. 2013. "Insights into Congenital Stationary Night Blindness Based on the Structure of G90D Rhodopsin." *EMBO Reports* 14 (6): 520–26. <https://doi.org/10.1038/embor.2013.44>.
- Sirés, Anna, Mireia Turch-Anguera, Patricia Bogdanov, Joel Sampedro, Hugo Ramos,

- Agustín Ruíz Lasa, J. Huo, et al. 2021. “Faim Knockout Leads to Gliosis and Late-onset Neurodegeneration of Photoreceptors.” *Journal of Neuroscience Research* 99: 3103–20. <https://doi.org/https://doi.org/10.1002/jnr.24978>.
- Sokolov, Maxim, Arkady L Lyubarsky, Katherine J Strissel, Andrey B Savchenko, Viktor I Govardovskii, Edward N Pugh, and Vadim Y Arshavsky. 2002. “Massive Light-Driven Translocation of Transducin between the Two Major Compartments of Rod Cells: A Novel Mechanism of Light Adaptation.” *Neuron* 33: 1–12.
- Sokolov, Maxim, Katherine J. Strissel, Ilya B. Leskov, Norman A. Michaud, Viktor I. Govardovskii, and Vadim Y. Arshavsky. 2004. “Phosducin Facilitates Light-Driven Transducin Translocation in Rod Photoreceptors: Evidence from the Phosducin Knockout Mouse.” *Journal of Biological Chemistry* 279 (18): 19149–56. <https://doi.org/10.1074/jbc.M311058200>.
- Sole, Carme, Xavier Dolcet, Miguel F. Segura, Humberto Gutierrez, Maria Teresa Diaz-Meco, Raffaella Gozzelino, Daniel Sanchis, et al. 2004. “The Death Receptor Antagonist FAIM Promotes Neurite Outgrowth by a Mechanism That Depends on ERK and NF-KB Signaling.” *Journal of Cell Biology* 167 (3): 479–92. <https://doi.org/10.1083/jcb.200403093>.
- Thrower, Julia S., Laura Hoffman, Martin Rechsteiner, and Cecile M. Pickart. 2000. “Recognition of the Polyubiquitin Proteolytic Signal.” *The EMBO Journal* 19 (1): 94–102. <https://doi.org/10.1093/EMBOJ/19.1.94>.
- Trachsel-Moncho, Laura, Soledad Benlloch-Navarro, Ángel Fernández-Carbonell, Dolores Tania Ramírez-Lamelas, Teresa Olivar, Dolores Silvestre, Enric Poch, and María Miranda. 2018. “Oxidative Stress and Autophagy-Related Changes during Retinal Degeneration and Development.” *Cell Death & Disease* 2018 9:8 9 (8): 1–12. <https://doi.org/10.1038/s41419-018-0855-8>.
- Ueki, Yumi, Yun Zheng Le, Srinivas Chollangi, Werner Muller, and John D. Ash. 2009. “Preconditioning-Induced Protection of Photoreceptors Requires Activation of the Signal-Transducing Receptor Gp130 in Photoreceptors.” *Proceedings of the National Academy of Sciences of the United States of America* 106 (50): 21389–94. <https://doi.org/10.1073/pnas.0906156106>.

- Wang, Gui-Qin Qin, Zong-Xi Xi Bai, Jing Shi, Sang Luo, Hong-Fa Fa Chang, and Xiao-Yong Yong Sai. 2013. "Prevalence and Risk Factors for Eye Diseases, Blindness, and Low Vision in Lhasa, Tibet." *International Journal of Ophthalmology* 6 (2): 237–41. <https://doi.org/10.3980/j.issn.2222-3959.2013.02.24>.
- Weiss, Ellen. 2020. "Shedding Light on Dark Adaptation." *Biochemist* 42 (5): 44–50. <https://doi.org/10.1042/BIO20200067>.
- Weissman, Allan M, Nitzan Shabek, and Aaron Ciechanover. 2011. "The Predator Becomes the Prey: Regulating the Ubiquitin System by Ubiquitylation and Degradation." *Nature Reviews Molecular Cell Biology* 12 (9): 605–20. <https://doi.org/10.1038/nrm3173>.
- Wenzel, Andreas, Christian Grimm, Marijana Samardzija, and Charlotte E. Remé. 2005. "Molecular Mechanisms of Light-Induced Photoreceptor Apoptosis and Neuroprotection for Retinal Degeneration." *Progress in Retinal and Eye Research* 24 (2): 275–306. <https://doi.org/10.1016/j.preteyeres.2004.08.002>.
- Xia, Fan, Yonju Ha, Shuizhen Shi, Yi Li, Shengguo Li, Jonathan Luisi, Rakez Kayed, Massoud Motamedi, Hua Liu, and Wenbo Zhang. 2021. "Early Alterations of Neurovascular Unit in the Retina in Mouse Models of Tauopathy." *Acta Neuropathologica Communications* 9 (1): 1–16. <https://doi.org/10.1186/s40478-021-01149-y>.
- Xu, Jun, Robert L. Dodd, Clint L. Makino, Melvin I. Simon, Denis A. Baylor, and Jeannle Chen. 1997. "Prolonged Photoresponses in Transgenic Mouse Rods Lacking Arrestin." *Nature* 389 (6650): 505–9. <https://doi.org/10.1038/39068>.
- Yamamoto, Shuichi, Masanori Hayashi, Shinobu Takeuchi, Yutaka Shirao, Katsutoshi Kita, and Kazuo Kawasaki. 1997. "Normal S Cone Electroretinogram B-Wave in Oguchi's Disease." *The British Journal of Ophthalmology* 81 (12): 1043–45. <https://doi.org/10.1136/BJO.81.12.1043>.
- Yang, Jun, Yujian Song, Alexander D. Law, Conner J. Rogan, Kelsey Shimoda, Danijel Djukovic, Jeffrey C. Anderson, Doris Kretzschmar, David A. Hendrix, and Jadwiga M. Giebuttowicz. 2022. "Chronic Blue Light Leads to Accelerated Aging in Drosophila by Impairing Energy Metabolism and Neurotransmitter Levels." *Frontiers in Aging* 0

(August): 94. <https://doi.org/10.3389/FRAGI.2022.983373>.

Yoshiyama, Yasumasa, Makoto Higuchi, Bin Zhang, Shu Ming Huang, Nobuhisa Iwata, Takaomi C C. Saido, Jun Maeda, Tetsuya Suhara, John Q. Trojanowski, and Virginia M.Y. Lee. 2007. "Synapse Loss and Microglial Activation Precede Tangles in a P301S Tauopathy Mouse Model." *Neuron* 53 (3): 337–51.  
<https://doi.org/10.1016/j.neuron.2007.01.010>.

Zeitz, Christina, Anthony G. Robson, and Isabelle Audo. 2015. "Congenital Stationary Night Blindness: An Analysis and Update of Genotype-Phenotype Correlations and Pathogenic Mechanisms." *Progress in Retinal and Eye Research* 45: 58–110.  
<https://doi.org/10.1016/j.preteyeres.2014.09.001>.

